FEDERAL UNIVERSITY OF SÃO CARLOS
Exact and Technology Sciences Center
Chemical Engineering Graduate Program

Cássia Maria de Oliveira

Energy Integration of Sugarcane Biorefineries with Multiperiod Operation

São Carlos
2018

FEDERAL UNIVERSITY OF SÃO CARLOS

Exact and Technology Sciences Center

Chemical Engineering Graduate Program

Cássia Maria de Oliveira

Energy Integration of Sugarcane Biorefineries with Multiperiod Operation

Thesis presented to the Chemical Engineering Graduate Program of the Federal University of São Carlos in partial fulfillment of the requirements for the Degree of Doctor in Chemical Engineering.

Supervisor: Prof. Dr. Antonio José Gonçalves Cruz

Co-supervisor: Prof.ª Dr.ª Caliane Bastos Borba Costa

São Carlos

2018

MEMBROS DA BANCA EXAMINADORA DA DEFESA DE TESE DE CÁSSIA MARIA DE OLIVEIRA APRESENTADA AO PROGRAMA DE PÓS-GRADUAÇÃO EM ENGENHARIA QUÍMICA DA UNIVERSIDADE FEDERAL DE SÃO CARLOS, EM 16 DE JANEIRO DE 2018.

BANCA EXAMINADORA:

Antonio José Gonçalves da Cruz
Orientador, UFSCar

Caliane Bastos Borba Costa
Coorientadora, UEM

André Luiz Hemerly Costa
UERJ

Mauro Antônio da Silva Sá Ravagnani
UEM

Alice Medeiros de Lima

Alice Medeiros de Lima
UFSCar

Wu Hong Kwong

Wu Hong Kwong
UFSCar

A quem se dedicou inteiramente a minha felicidade
minha mãe, Wilma

In memoriam
meu pai, Paulo

Agradecimentos

Agradeço a Deus, por ter me guiado e protegido ao longo das minhas decisões. Agradeço a Ele também por manter as pessoas que amo ao meu lado.

À minha mãe e minha irmã Fernanda, pelo apoio, carinho e paciência. Sou infinitamente grata por ter vocês ao meu lado. Vocês representam o meu porto seguro.

À minha vó Cida, pelo amor e dedicação que sempre teve por mim.

Aos meus tios e tias, pelo incentivo e confiança ao longo de toda a caminhada. Não foi fácil, mas teria sido ainda mais difícil sem vocês.

Aos meus orientadores, Caliane e Antonio, pelos ensinamentos, sabedoria e dedicação que me ofereceram durante todo o mestrado e doutorado, assim como a amizade. Obrigada pela paciência que tiveram nos meus momentos de dificuldades. Sou muito grata pela oportunidade que me ofereceram. Você são exemplos pra mim e sempre terei um carinho imenso.

Ao Charles, pela oportunidade de aprender e pelos sábios conselhos, mesmo durante anos após o estágio. Obrigada pelo apoio e por me apresentar, aqueles que seriam após algum tempo, meus orientadores em uma nova etapa da vida.

Ao professor Alberto, pelos ensinamentos e pela oportunidade de aprender um pouquinho sobre outra área de trabalho.

Ao professor Mauro da UEM, por compartilhar seus conhecimentos e pela dedicação.

Ao Leandro, também da UEM, por ter me auxiliado com as inúmeras dificuldades que tive na execução do trabalho.

Aos membros da banca, pela dedicação e contribuição nesse processo de aprendizagem.

Aos meus amigos de infância e adolescência, Daiana, Lidiane, Bruna, Gabriela, Juliane, Mariana, Natália, Rafael, Luiz e Allan, pelo apoio e amizade, a qual é fundamental na minha vida. Vocês fazem de simples momentos, os melhores.

Às minha amigas da FZEA, Ivana, Geisa, Priscila e Danielle, que mesmo em distância são pessoas muito especiais. A cada conversa, percebo o quão bom é ter vocês na minha vida.

Aos meus amigos do Laboratório Kyatera, Gabriel, Karina, Felipe, Eric, Anderson, Andreza e Guilhermina, por partilharem seus conhecimentos, pela amizade e bons momentos de convivência. Obrigada, vocês fizeram desses anos de estudo um momento muito especial na minha vida. Um agradecimento especial ao Felipe, atualmente professor do Departamento, e ao Anderson, pela disponibilidade, dedicação e paciência em me ajudar em várias etapas do trabalho.

À minha amiga Paula, quem tive a feliz oportunidade de conhecer no primeiro dia de mestrado, pelo carinho, amizade e incentivo. Obrigada por fazer parte da minha vida e fazê-la mais leve e alegre.

Aos meus amigos do IFSP, pela amizade, paciência e boas risadas. Agradeço também por me ensinaram o que é ser docente e o que isso representa na vida dos alunos.

Ao Programa de Pós-Graduação de Engenharia Química da UFSCar, pela oportunidade.

Ao Instituto Federal de São Paulo, pela oportunidade em me tornar professora e pelo investimento na minha carreira.

À FAPESP (Processo 2013/21343-3) e CAPES, pelo suporte financeiro.

A todas as demais pessoas que contribuíram, direta ou indiretamente, para que o presente trabalho fosse concluído. Esta, sem dúvidas, não é apenas uma conquista profissional, mas uma grande conquista pessoal.

"Quando você conseguir superar graves problemas de relacionamentos, não se detenha na lembrança dos momentos difíceis, mas na alegria de haver atravessado mais essa prova em sua vida.
Quando sair de um longo tratamento de saúde, não pense no sofrimento que foi necessário enfrentar, mas na benção de DEUS que permitiu a cura.

Leve na sua memória, para o resto da vida, as coisas boas que surgiram nas dificuldades.
Elas serão uma prova de sua capacidade e lhe darão confiança diante de qualquer obstáculo.

Uns queriam um emprego melhor; outros só um emprego.
Uns queriam uma refeição mais farta; outros, só uma refeição.
Uns queriam uma vida mais amena; outros, apenas viver.
Uns queriam pais mais esclarecidos; outros, apenas ter pais.
Uns queriam ter olhos claros; outro, enxergar.
Uns queriam ter voz bonita; outros, falar.
Uns queriam silêncio; outros, ouvir.
Uns queriam sapatos novos; outros, ter pés.
Uns queriam um carro; outros, andar.
Uns queriam o supérfluo, outros, apenas o necessário."

(Chico Xavier)

Integração Energética de Biorrefinarias de Cana-de-açúcar com Operação Multiperiódica

Resumo

O Brasil tem uma grande importância como produtor de biocombustíveis, especialmente na produção de etanol a partir de cana-de-açúcar. O bagaço, um subproduto das biorrefinarias de cana-de-açúcar, pode ser usado para gerar energia elétrica e produzir etanol de segunda geração. No entanto, as variações nos preços da energia elétrica e do etanol podem motivar variações nas condições operacionais do processo integrado da biorrefinaria, a qual produz etanol de primeira e segunda geração e energia elétrica. A rede de trocador de calor (RTC) de tal processo deve ser capaz de atender a essas variações. Este trabalho teve como objetivo a síntese de RTC multiperiódica em biorrefinarias de cana-de-açúcar. Nesta abordagem, cada período indica uma condição de processo e a RTC sintetizada é capaz de atender a essas diferentes condições de operação. Três estudos de caso industriais são considerados. O Estudo de Caso 1 (EC1) é uma biorrefinaria que produz etanol 1G/2G e energia elétrica, descartando a fração de pentoses. Nos Estudos de Caso 2 e 3, EC2 e EC3, o processo é semelhante, mas a fração de pentoses é usada para produzir etanol (EC2) ou biogás (EC3). Para cada biorrefinaria, foram considerados três períodos, que diferem na fração do bagaço desviada para a produção de etanol 2G. Em cada período, um problema de Programação Não Linear Inteira Mista (PNLIM) foi resolvido para minimizar o Custo Total Anualizado (CTA) e mecanismos de compartilhamento de tempo foram utilizados para integrar as RTCs de todos os períodos em uma RTC multiperiódica. Os problemas de otimização foram resolvidos em dois níveis usando três estratégias diferentes. Na primeira estratégia, uma adaptação do algoritmo Otimização por Enxame de Partículas foi usada em ambos os níveis. No entanto, as soluções por este método apresentaram pequenas melhorias de CTA em comparação com o processo comumente encontrado nas plantas brasileiras, onde já existe integração de energia entre algumas correntes de processo (chamado neste trabalho de processo com integração de projeto). Para lidar com esse problema, duas estratégias foram empregadas com metaheurísticas híbridas: Recozimento Simulado e Otimização por Fogos de Artificio; e Busca Tabu e Otimização por Enxame de Partículas. Para os processos com as RTCs multiperiódicas, estas duas últimas estratégias apresentaram reduções acima de 58% e 54% no CTA e na demanda de vapor, respectivamente, em comparação com processos sem integração de energia. Além disso, usando os métodos acima mencionados, as melhorias no CTA e na demanda de vapor para o processo com as RTCs multiperiódicas atingem valores acima de 44% e 41%, respectivamente, em relação aos processos com integração de projeto. Tais reduções na demanda de vapor permitem desviar mais bagaço para a produção de etanol de segunda geração. Além disso, a integração energética em biorrefinarias oferece melhor gerenciamento da energia e redução nos custos de operação e de capital. Assim, todas essas melhorias contribuem para o processo de produção de etanol 1G/2G e energia elétrica.

Palavras-chave: Etanol 1G/2G. Síntese de Rede de Trocador de Calor. Otimização por Exame de Partículas. Recozimento Simulado. Otimização por Fogos de Artifício. Busca Tabu.

Energy Integration of Sugarcane Biorefineries with Multiperiod Operation

Abstract

Brazil has a great importance as biofuels producer, especially of ethanol from sugarcane. The bagasse, a by-product of sugarcane biorefineries, can be used to generate electricity and produce second generation ethanol. However, variations in prices of electricity and ethanol may motivate variations in the operating conditions of the integrated biorefinery process, which produces first and second generation ethanol and bioelectricity. The heat exchanger network (HEN) of such a process must be able to meet these variations. This work aimed the synthesis of multiperiod HEN in sugarcane biorefineries. In this approach, each period indicates a process condition and the HEN synthesized is able to meet these different operating conditions. Three industrial case studies are considered. Case Study 1 (CS1) is a biorefinery that produces 1G/2G ethanol and electricity, disposing the pentoses fraction. In Case Studies 2 and 3, CS2 and CS3, the process is similar, but the pentoses fraction is used to produce ethanol (CS2) or biogas (CS3). For each biorefinery, three periods were considered, which differ in the bagasse fraction diverted to 2G ethanol production. In each period, a Mixed Integer Nonlinear Programming (MINLP) problem was solved to minimize the total annualized cost (TAC) and timesharing mechanisms were used to integrate the HENs of all periods into a multiperiod HEN. Optimization problems were solved at two levels using three different strategies. In the first strategy, an adapted Particle Swarm Optimization algorithm was used in both levels. However, the solutions by this method presented small TAC improvements compared to the process commonly found in Brazilian plants, where there is already energy integration among some process streams (called in this work of the process with project integration). To deal with this problem, two strategies were employed with hybrid metaheuristics: Simulated Annealing and Rocket Fireworks Optimization; and Tabu Search and Particle Swarm Optimization. For processes with the multiperiod HENs, these latter two strategies presented reductions above 58% and 54% in TAC and steam demand, respectively, compared to processes without energy integration. Also, using the aforementioned methods, improvements in TAC and steam demand for process with the multiperiod HENs reach values above 44% and 41%, respectively, in relation to processes with project integration. Such reductions in steam demand allow diverting more bagasse to produce second generation ethanol. In addition, energy integration in biorefineries provides improved energy management and reduced operating and capital costs. Thus, all these improvements contribute to 1G/2G ethanol and electricity production process.

Keywords: Ethanol 1G/2G. Synthesis of Heat Exchanger Network. Particle Swarm Optimization. Simulated Annealing. Rocket Firework Optimization. Tabu Search.

Summary

Figures list

Tables list

Chapter 1

Introduction and Justification

Concern with better use of energy began during the 1970s-1980s oil crises. During that period, actions aiming diversification of energy matrix, conservation and better use of natural resources were performed. Brazil is the second largest producer of ethanol in the world, behind only the United States of America. In Brazil, ethanol is mostly produced from sugarcane juice, in a process known as first generation ethanol (1G) production process. In sugarcane plants, the bagasse is used to produce electricity and steam in order to ensure the energy self-sufficiency of the process and, sometimes, sell the electricity surplus. Sugarcane bagasse can also be used in second generation ethanol (2G) production. However, it is not yet a consolidated technology and requires studies to propose improvements, which allow making the integrated production of 1G/2G ethanol more sustainable and economical.

In chemical processes, an efficient alternative to save energy is the exchange of thermal energy among process streams by synthesis of heat exchanger networks (HENs). However, prices of electricity and ethanol vary according to market demand, which implies changing operating conditions of the plant, as well as utilities consumption. Thus, the HEN synthesized should be able to meet different operating conditions. To deal with this problem, a common practice is to synthesize a HEN with multiple periods. In a multiperiod HEN, each period represents a different process condition and the HEN synthesized is able to operate in these established conditions. In this sense, Chapter 2 presents a brief literature review about multiperiod HENs and mathematical methods for solving such problems.

This work includes industrial case studies of energy integration in sugarcane biorefineries by HEN synthesis with multiple operation periods. The case studies differ in the disposal of pentose fraction or in the use of this fraction to produce ethanol or biogas. For each biorefinery case study, three periods were considered. In each period, a different bagasse fraction is diverted to second generation ethanol section. This fraction determines the number of streams involved in energy integration and the flow rates of some streams. A Mixed Integer Nonlinear Programming (MINLP) problem formulation was solved for each period, separately. To integrate the HENs of all periods into a single HEN, timesharing mechanisms were employed. This approach suits to requirements of biorefineries, since it does not require the duration of periods and the number of transitions from one operating condition to another in order to synthetize the multiperiod HEN, which may be difficult to specify. MINLP problems were solved at two levels of optimization using meta-heuristic methods. This approach consists in solving the problem at the upper level for integer variables and at the lower level for continuous variables. Different strategies were used to solve the optimization problems. In Chapter 3, an adapted Particle Swarm Optimization (PSO) algorithm was used for integer and continuous variables in a case study of energy integration in a sugarcane biorefinery. However, marginal improvements were achieved using that method compared to the process already existing in Brazilian plants. Two other strategies applying hybrid meta-heuristic methods were employed. In Chapter 4, a case study of energy integration in a biorefinery was solved by the hybridization of Simulated Annealing (SA) and Rocket Fireworks Optimization (RFO). The latter combines two algorithms, SA and PSO. In Chapter 5, three case studies of energy integration in biorefineries using the hybridization of Tabu Search (TS) and Particle Swarm Optimization (PSO) were presented. The hybrid approaches, SA-RFO and TS-PSO, are recent strategies that can be used for problems of large-scale HEN synthesis. Chapters 3, 4 and 5 are chapters structured each as full (*i.e.*, each chapter has abstract, introduction, methodology, results and discussion and conclusion sections).Finally, in Chapter 6, the conclusions of this study and the suggestions for future works are presented, respectively. It is important to highlight that the synthesis of HENs in biorefineries has as one of the main goals to reduce steam consumption by the process. Thus, less bagasse needs to be burned to generate steam and the surplus can be diverted to 2G ethanol or electricity production, depending on the demand. However, other goals associated to energy integration, such as energy security and reduced consumption of environmental resources and waste generation, are very important. Therefore, all improvements provided by energy integration contribute to catalyze the viability of second generation ethanol production.

Chapter 2

Literature Review

2.1 Introduction

Energy integration is a process integration technique that matches hot and cold streams, by heat exchanger network (HEN) synthesis. For a given set of hot and cold streams, energy integration techniques find the best combination among these streams aiming at the lowest cost for the process. Depending on the method employed for energy integration, the cost includes only operating cost or operating and capital costs, as well as other costs (*e.g.*, piping costs). For energy integration, it is necessary to know thermal loads (or heat capacity), the inlet and outlet temperatures and heat transfer convective coefficients of all streams, cost of heat exchanger units, cost of utilities and their heat transfer convective coefficients. In the literature, important review papers of the state of the art for HEN synthesis can be cited, such as Gundersen and Naess (1988), Grossmann, Caballero and Yeomans (2000), Furman and Sahinidis (2002), Morar and Agachi (2010), Klemeš and Kravanja (2013) and Klemeš, Varbanova and Kravanja (2013), as well as books ‘Chemical Process Design and Integration’ (SMITH, 2014), ‘Redes de cambiadores de calor’ (RAVAGNANI; CABALLERO SUÁREZ, 2012), ‘Energy Optimization in Process Systems and Fuel Cells’ (SIENIUTYCZ; JEŻOWSKI, 2013) and ‘Handbook of Process Integration (PI)’ (PARDALOS; DU, 1998). In general, the methods for HEN synthesis can be classified into two groups: sequential and simultaneous.

Sequential techniques subdivide the problem into subproblems to reduce complexity and include methods that use thermodynamic concepts (*e.g.*, Pinch Analysis) and mathematical programming methods. Pinch Analysis is a well-known methodology for energy integration, which is simply and easy to apply. However, HEN should be synthesized manually by the designer or with the help of some available pieces of software, which can be an advantage or disadvantage, depending on the knowledge level of the designer. Although the Pinch Analysis is easy to apply, the HEN synthesized does not guarantee the minimization of the total annualized cost (TAC), since the minimization of the energy demand is not performed simultaneously to the investment cost of HEN. That technique provides tools that allow verifying the energy flow inside the process and identifying the more economical way to recover energy by means of concepts such as determination of the minimum utility demand, Pinch temperature, the minimum number of units for HEN and the minimum average area of heat transfer. For applying the technique, the minimum temperature difference between a hot and a cold stream should be specified. It has influence on operating and capital costs. In other words, for a given minimum temperature difference, a minimum utility demand is achieved and the HEN synthesized should meet this energy demand.

Sequential techniques for energy integration also include mathematical programming methods. Papoulias and Grossmann (1983) introduced concepts of the sequential approach for the HEN synthesis using mathematical programming. The methodology consists in separately solving three optimization problems: the minimization of operating cost (giving rise to a Linear Programming, LP, formulation), the minimization of the number of units of heat transfer (formulated as a Mixed Integer Linear Programming, MILP) and the minimization of the investment cost (formulated as a Non-Linear Programming, NLP). This strategy decreases the complexity of the problem and relatively large problems can be solved with minor computational effort. However, since different costs associated to HEN synthesis are not optimized simultaneously, suboptimal solutions can be obtained. Studies on sequential techniques have produced great advances for energy integration area.

In simultaneous techniques all variables of the problem are optimized in a single step. For this approach, the problem is usually formulated using a superstructure that contains different possible combinations for heat transfer among streams. Thus, a Mixed Integer Nonlinear Programming (MINLP) problem is solved, where operating and capital costs are minimized simultaneously. Such strategy makes it possible to find better solutions, but it requires more computational effort given the nonlinearities and non-convexities present in its mathematical formulation.

This chapter is organized as follows. Section 2.2 provides a literature review on multiperiod HENs. Section 2.3 presents mathematical methods for solving optimization problems in HEN synthesis area. It is important to mention that this chapter aims to provide a brief review on applications of the multiperiod HEN. Concepts and more detailed description of sequential and simultaneous techniques, as well as advances on these approaches, can be found in the references cited previously.

2.2 Multiperiod HEN

The synthesis of networks of heat exchanger is an area that has been explored since the 1970s. However, many of the contributions presented do not consider oscillations in the process, which may occur due to changes in environmental conditions, quality of raw materials or the products, market demand and disturbances in the process. To circumvent this problem, methodologies for the flexible HEN synthesis have been developed, which allow changes in some parameters of the process. One of the more common approaches to deal with variations in the process is to design a multiperiod HEN, which can operate under various established conditions. These operating conditions are denominated periods and can present changes in temperature, heat capacity, heat transfer convective coefficient or/and number of streams. It is important to mention that the flexibility concept is broader, since this concept involves other approaches for the HEN synthesis under uncertainty, such as identification of critical values of uncertain parameters (PINTARIČ; KRAVANJA, 2008), sensitivity analysis for identification of uncertain parameters (PINTARIČ; KASAŠ; KRAVANJA, 2013) and measurement of flexibility degree by resilient (SABOO; MORARI; WOODCOCK, 1985) and flexibility indexes (SWANEY; GROSSMANN, 1985). Sequential or simultaneous techniques can be used to solve problems of the multiperiod HEN synthesis.

The synthesis of a multiperiod HEN using the Pinch Analysis, a sequential approach, was performed by Ravagnani and Modenes (1996). In this study, a procedure was proposed to evaluate the flexibility of HENs that operate with multiple conditions. Silva (1995) also presented a sequential methodology for the multiperiod HEN synthesis using the Pinch Analysis. In the first step, a HEN is designed for each period. After, all HENs are analyzed and a new configuration that meets those established conditions is proposed.

The sequential approach using mathematical programming for the multiperiod HEN synthesis was presented by Floudas and Grossmann (1986). These authors proposed an extension of the single-period model of Papoulias and Grossmann (1983), aiming to obtain the minimum cost of utility and the minimum number of heat transfer units in each period. Later, the automatic generation of the minimum HEN cost for a multiperiod model was developed by Floudas and Grossmann (1987), based on the single-period NLP model of Floudas, Ciric and Grossmann (1986).

Konukman, Çamurdan and Akman (2002) performed the synthesis of HEN configurations, which remains viable to changes in inlet temperatures of streams, ensuring a minimum total utility consumption. The objective function minimizes the total utility cost, which is solved for different flexibility levels. Thus, for each flexibility level, a total minimum utility demand and one or more HEN structures are obtained. Since that work is restricted to determining the HEN configuration, the designer should choose the best HEN according to investment cost, controllability and/or operability.

In order to reduce costs in the plant, many processes use more than one hot and cold utility. In this context, a MILP formulation was presented by Marechal and Kalitventzeff (2003) for solving the multiperiod HEN problem with a utility system. The proposed methodology incorporates models to select and to guide the choice of the best strategy for the utility system. Later, El-Temtamy and Gabr (2012) used the MILP model of Floudas and Grossmann (1986) for the multiperiod HEN synthesis and applied it to a case study of the literature in order to discuss alternatives for the HEN configuration achieved by random iteration runs.

Recently, Mian, Martelli and Maréchal (2016a) proposed a multiperiod HEN approach including selection, design and scheduling of multiple utilities. The problem was solved by a sequential procedure. In the first step the optimal selection of utilities, the installation capacity and the installed capacity required for each period are established. In the second stage, the number of heat transfer units is calculated for that given utility demand. In the third step, the investment cost is minimized. The same authors (2016b) extended that approach to utility systems including storages.

More lately, Miranda et al. (2017) presented a strategy for the multiperiod HEN synthesis via sequential mathematical programming based on models of Floudas and Grossmann (1986 and 1987). This strategy includes new bypass streams and an improvement in the model, which allowed better solution than those achieved in the literature.

The multiperiod HEN synthesis can also be treated as an MINLP problem, in which utility and capital costs for all periods are minimized simultaneously. Aaltola (2002) introduced the simultaneous approach to the multiperiod HEN problems from extension of single-period MINLP model of Yee and Grossmann (1990). This model has some simplifications, such as elimination of bypasses and assumptions of average areas required by the units of all periods and isothermal mixing. These simplifications reduce the complexity of the optimization problem, but capital costs would be slightly underestimated. To deal partially with those limitations, a search algorithm involving LP and NLP models was applied by those authors.

Chen and Hung (2004) proposed a methodology of three stages for HENs under uncertainty: simultaneous HEN synthesis, flexibility analysis and removal of infeasible HENs. The approach is based on the model presented by Aaltola (2002). Those authors introduced the concept of the maximum area from a discontinuous maximization function. Although this approach allows better solutions, the maximization function added to the problem can result in higher computational cost and problems of convergence.

Verheyen and Zhang (2006) modified the model of Aaltola (2002) by removing assumptions of isothermal mixture and average area. In this strategy, the term of average area is replaced by a term of maximum area (*i.e.*, maximum areas required by heat transfer units that involve the same streams in more than one period) and nonlinear constraints are enabled. This approach allows more realistic solutions. However, since nonlinear terms are present in the set of constraints, the problem is more complex and difficult to solve.

The previous works reported for the multiperiod HEN synthesis via simultaneous techniques used deterministic algorithms. Recently, stochastic optimization algorithms have been used in the HEN synthesis with multiple operating conditions. Ma et al. (2008) presented a new strategy in two steps. In the first step, a diagram of temperature and enthalpy is used for the HEN synthesis of each operation period. So, a multiperiod HEN that includes all matches among periods found in the previous step is synthesized. After, a subsequent optimization in the heat transfer area of that HEN is performed. For the multiperiod HEN synthesis, Genetic Algorithm (GA) and Simulated Annealing (SA) were used. Perhaps, that work was one of the first to use a hybrid meta-heuristic method for the multiperiod HEN synthesis. According to the authors, the proposed method allows reducing the size and the complexity of the problem compared to formulations of Aaltola (2002) and Verheyen and Zhang (2006). More recently, Ahmad et al. (2012) performed the synthesis of the multiperiod HEN in an industrial case study using the meta-heuristic Simulated Annealing (SA).

The duration of periods influences the design of the multiperiod HEN, which can be unviable due to unexpected changes in operating conditions (*i.e.*, the energy demand cannot be met by the HEN design). However, it is difficult to define the duration of periods. To circumvent the issue of the unequal durations of periods, Isafiade and Fraser (2010) used the concept of maximum area in the model and compared a case study for HEN synthesis with equal and unequal duration of periods.

Isafiade et al. (2015) proposed a procedure in two stages to reduce the computational cost of the multiperiod HEN problems. In the first stage, the best matches of hot and cold streams are identified varying the minimum temperature approximation in heat exchangers and the number of stages in the superstructure. In the second stage, a reduced MINLP model is formulated from the previous matches for a fixed number of stages. This strategy facilitates the search for good solutions.

Recently, Kang, Liu and Wu (2016) presented two approaches for solving the HEN synthesis problem using the features of periods. In the first approach, the single-period problem that has the longest duration is solved and the HEN configuration achieved for that problem is used to solve the multiperiod HEN problem. For cases with similar duration of periods, the devices commonly found among single-period HENs are used in the multiperiod HEN synthesis.

Isafiade and Short (2016a) presented a procedure to deal with duration of periods and number of transitions from one operating condition to another. In this procedure, single-period MINLP problems are solved separately and used to initialize the multiperiod HEN configuration. So, the HEN provided in the previous step is redesigned and evaluated to meet unexpected changes in operating conditions and their transitions among periods. After, Pavão et al. (2018a) adapted meta-heuristic method of Simulated Annealing (SA) and Rocket Fireworks Optimization (RFO) for the HEN synthesis in single-period problems to deal with multiple periods. The authors included a post-stage of stochastic optimization to improve the results.

Studies about the HEN retrofit have been mainly focused on the adaptation of single-period HENs (*i.e.*, HENs with fixed process conditions). In this sense, Kang and Liu (2014) presented a methodology of matching heat transfer areas for the HEN retrofit. This purpose aims to avoid idle area in existing devices through the reverse order procedure (*i.e.*, procedure for rematching the existing device areas with the required device areas). Afterwards, based on that method, Kang and Liu (2015) proposed three correspondence strategies to minimize the investment cost for the retrofit of the multiperiod HEN. In these strategies, substitution and addition of heat exchangers and addition of heat transfer area are performed.

Short et al. (2016) approached the synthesis of multiperiod HEN including details of heat exchangers, based on the model of Verheyen and Zhang (2006). Correction factors are included into the objective function, which consider features of the real design. However, that approach uses heuristics, and so it requires experience of the designer to synthesize devices that operate under all periods. When this is not possible, extra heat exchangers are designed for periods that cannot be satisfied.

Lately, Isafiade and Short (2016b) studied the use of alternative energy sources as utilities. The authors evaluated renewable and non-renewable sources of utilities, such as biomass, coal, solar and wind power, for the multiperiod HEN problems evaluating economics and environmental impacts.

Traditional multiperiod HEN designs can be improved with timesharing schemes (*i.e.*, a heat exchanger can be used for different pairs of streams among periods). This strategy avoids overestimating the capital costs, a common problem when the maximum area approach is used in the objective function. Using this approach, Sadeli and Chang (2012) extended the model of Verheyen and Zhang (2006) by adding a set of timesharing heuristics. Recently, Jiang and Chang (2013) presented an approach for the multiperiod HEN, which involves solving the problem for each period separately and using the timesharing mechanisms to integrate all HENs of individual periods into one. This strategy allows designing a multiperiod HEN without defining the duration of periods and the number of transitions from one operating condition to another. Since the problems of each period are solved individually, the computational cost is reduced. Note that although the capital and investment costs are minimized simultaneously in the objective function, the approach presented by Jiang and Chang (2013) is a sequential technique, since the optimization problems are solved individually. Later, Jiang and Chang (2015) compared two strategies for the multiperiod HEN using timesharing scheme, which allowed saving capital costs. That scheme was also applied by Miranda et al. (2016) in three case studies. The authors corrected inconsistences of the literature and obtained better results. More recently, Pavão et al. (2018b) presented an approach to synthesize HENs with multiple operating cycles using those timesharing mechanisms and a post-stage of stochastic optimization to reduce costs. In that work, two strategies to achieve solutions for HEN problems were used before applying such switching mechanisms.

2.3 Mathematical methods

This section is restricted to mathematical methods used to solve HEN problems via MINLP models, since these problems are often non-convex, nonlinear and complex. Grossmann and Kravanja (1997), Grossmann (2002), Behera, Sahoo and Pati (2015), and Boukouvala, Misener and Floudas (2016) presented important reviews on techniques that can be used for these problems.

Many advances have been achieved in the optimization area to deal with large-scale MINLP problems. The most common deterministic algorithms used in HEN problems are Generalized Benders Decomposition (GEOFFRION, 1972), Branch and Bound (LAND; DOIG, 1960), Outer-Approximation/Equality-Relaxation (DURAN; GROSSMANN, 1986) and Extended Cutting Plane (WESTERLUND; PETTERSSON, 1995). Some of these methods are found in solvers available in commercial computational pieces of software (*e.g.*, CPLEX, BARON and DICOPT ++ are solvers that include those methods and are integrated to the commercial program ‘GAMS modelling environment’). However, the computational burden to solve HEN problems by deterministic methods increases considerably with the size of the problem and the solution can be stuck to local minima.

To attack the problems mentioned, meta-heuristic methods have been widely used for the HEN synthesis. Examples of meta-heuristic algorithms applied to these problems are Particle Swarm Optimization (SILVA; RAVAGNANI; BISCAIA, 2008), Genetic Algorithm (BOCHENEK; JEŻOWSKI, 2006), Simulated Annealing (AHMAD et al., 2012) and Tabu Search (LIN; MILLER, 2004). These methods are important approaches for solving large-scale HEN problems. In general, they avoid getting stuck in local minima and obtain better results to complex problems when compared to purely deterministic methods (RAVAGNANI; CABALLERO SUÁREZ, 2012). However, meta-heuristic algorithms require a large number of evaluations of the objective function, and so a long processing time until termination criterion is met. A recent review about meta-heuristic techniques applied to the HEN synthesis was performed by Toimil and Gómez (2017).

An alternative approach to solve HEN synthesis is using hybrid methods, in which the problem is divided into two levels. The problem is solved for integer variables at the upper level and for continuous variables at the lower level. Since the problem is divided in two levels, promising results can be achieved with less computational effort. Hybrid strategies using the same algorithm to both levels were employed in the HEN synthesis with Genetic Algorithm (GA) (LEWIN, 1998), Differential Evolution (DE) (YERRAMSETTY; MURTY, 2008) and Chaotic Ant Swarm (CAS) (ZHANG; CUI; PENG, 2016) algorithms. The hybridization between a meta-heuristic and a deterministic method was applied combining Harmonic Search (HS) and Sequential Quadratic Programming (SQP) (KHORASANY; FESANGHARY, 2009), Tabu Search (TS) and Sequential Quadratic Programming (SQP) (CHEN et al., 2008), Variable Neighborhood Search (VNS) and Sequential Quadratic Programming (SQP) (MARTELLI; MIAN; MARÉCHAL, 2015). Hybrid approaches using meta-heuristic methods in both levels were performed with Genetic Algorithm (GA) and Particle Swarm Optimization (PSO) (PAVÃO; COSTA; RAVAGNANI, 2016), Simulated Annealing (SA) and Particle Swarm Optimization (PSO) (PAVÃO; COSTA; RAVAGNANI, 2017) and Simulated Annealing (SA) and Rocket Fireworks Optimization (RFO) (PAVÃO et al., 2017). It is important to mention that large-scale HEN synthesis problems are more complex due to number of variables of the problem, so hybrid meta-heuristic methods are good options for these problems.

2.4 Conclusion

In order to reduce impacts of renewable and non-renewable energy consumption, the development of process integration techniques that bring economic and environmental benefits is performed. Process integration by HEN synthesis allows reducing energy consumption, as well as their associated costs. Thus, studies about models and mathematical methods allow advances in research area and improvements to industrial processes. Regarding multiperiod HEN synthesis, one of the first approaches was the use of Pinch Analysis. Although Pinch technique allows good results, the investment costs are not minimized simultaneously. Besides, the procedure for HEN synthesis can be exhaustive when the number of streams is large, since the HEN is designed manually for each operation period and, later, for the multiperiod HEN. Sequential techniques via mathematical programing are an interesting strategy for large problems of multiperiod HEN synthesis, because they allow obtaining good solutions with minor computational effort. In those techniques, the problems are solved separately (*i.e.,* the complexity of the problem is reduced), but different costs associated to HENs are not optimized simultaneously. In simultaneous methods, operating and capital costs of all operation periods are minimized in a single step. For this reason, the larger the HEN synthesis problem, the larger is the complexity of the problem. Consequently, robust mathematical methods are required. Thus, the best option to solve HEN synthesis problems depends on several factors, such as the purpose of study, the size of the problem and the mathematical methods available. Moreover, few applications of HEN synthesis in real problems are found in the literature. In most cases, methodologies are proposed and applied in small-scale benchmark problems, which do not represent real plants. In addition, the literature demonstrates success in applications of multiperiod HEN synthesis for small-scale problems, but few applications of multiperiod HEN synthesis for large-scale problems are known.

References

AALTOLA, J. Simultaneous synthesis of flexible heat exchanger network. Applied Thermal Engineering, v. 22, n. 8, p. 907–918, 2002.

AHMAD, M. I.; ZHANG, N.; JOBSON, M.; CHEN, L. Multi-period design of heat exchanger networks. Chemical Engineering Research and Design, v. 90, n. 11, p. 1883–1895, 2012.

BEHERA, S.; SAHOO, S.; PATI, B. B. A review on optimization algorithms and application to wind energy integration to grid. Renewable and Sustainable Energy Reviews, v. 48, p. 214–227, 2015.

BOCHENEK, R.; JEŻOWSKI, J. M. Genetic algorithms approach for retrofitting heat exchanger network with standard heat exchangers. v. 21, p. 871–876, 2006.

BOUKOUVALA, F.; MISENER, R.; FLOUDAS, C. A. Global optimization advances in Mixed-Integer Nonlinear Programming, MINLP, and Constrained Derivative-Free Optimization, CDFO. European Journal of Operational Research, v. 252, n. 3, p. 701–727, 2016.

CHEN, C.-L.; HUNG, P.-S. Simultaneous Synthesis of Flexible Heat-Exchange Networks with Uncertain Source-Stream Temperatures and Flow Rates. 2004.

CHEN, X.; ZHAOHUA, L.; YANG, J.; SHAO, Z.; ZHU, L. Nested Tabu Search (TS) and Sequential Quadratic Programming (SQP) Method, Combined with Adaptive Model Reformulation for Heat Exchanger Network Synthesis (HENS). 2008.

DURAN, M. A.; GROSSMANN, I. E. An outer-approximation algorithm for a class of mixed-integer nonlinear programs. Mathematical Programming, v. 36, n. 3, p. 307–339, 1986.

EL-TEMTAMY, S. A.; GABR, E. M. Design of optimum flexible heat exchanger networks for multiperiod process. Egyptian Journal of Petroleum, v. 21, n. 2, p. 109–117, 2012.

FLOUDAS, C. A.; CIRIC, A. R.; GROSSMANN, I. E. Automatic synthesis of optimum heat exchanger network configurations. AIChE Journal, v. 32, n. 2, p. 276–290, 1986.

FLOUDAS, C. A.; GROSSMANN, I. E. Synthesis of flexible heat exchanger networks for multiperiod operation. Computers & Chemical Engineering, v. 10, n. 2, p. 153–168, 1986.

FLOUDAS, C. A.; GROSSMANN, I. E. Automatic generation of multiperiod heat exchanger network configurations. Computers & Chemical Engineering, v. 11, n. 2, p. 123–142, 1987.

FURMAN, K. C.; SAHINIDIS, N. V. A Critical Review and Annotated Bibliography for Heat Exchanger Network Synthesis in the 20th Century. 2002.

GEOFFRION, A. M. Generalized Benders decomposition. Journal of Optimization Theory and Applications, v. 10, n. 4, p. 237–260, 1972.

GROSSMANN, I. E. Review of Nonlinear Mixed-Integer and Disjunctive Programming Techniques. Optimization and Engineering, v. 3, n. 3, p. 227–252, 2002.

GROSSMANN, I. E.; CABALLERO, J. A.; YEOMANS, H. Advances in mathematical programming for the synthesis of process systems. Latin American Applied Research, v. 30, n. 4, p. 263–284, 2000.

GROSSMANN, I. E.; KRAVANJA, Z. Mixed-Integer Nonlinear Programming: A Survey of Algorithms and Applications. In: [s.l.] Springer New York, 1997. p. 73–100.

GUNDEPSEN, T.; NAESS, L. The synthesis of cost optimal heat exchanger networks: An industrial review of the state of the art. Computers & Chemical Engineering, v. 12, n. 6, p. 503–530, 1988.

ISAFIADE, A.; BOGATAJ, M.; FRASER, D.; KRAVANJA, Z. Optimal synthesis of heat exchanger networks for multi-period operations involving single and multiple utilities. Chemical Engineering Science, v. 127, p. 175–188, 2015.

ISAFIADE, A. J.; FRASER, D. M. Interval based MINLP superstructure synthesis of heat exchanger networks for multi-period operations. Chemical Engineering Research and Design, v. 88, n. 10, p. 1329–1341, 2010.

ISAFIADE, A. J.; SHORT, M. Simultaneous synthesis of flexible heat exchanger networks for unequal multi-period operations. Process Safety and Environmental Protection, v. 103, p. 377–390, 2016a.

ISAFIADE, A. J.; SHORT, M. Multi-Period Heat Exchanger Network Synthesis Involving Multiple Sources of Utilities and Environmental Impact. Computer Aided Chemical Engineering, v. 38, p. 2067–2072, 2016b.

JIANG, D.; CHANG, C.-T. A New Approach to Generate Flexible Multiperiod Heat Exchanger Network Designs with Timesharing Mechanisms. Industrial & Engineering Chemistry Research, v. 52, n. 10, p. 3794–3804, 2013.

JIANG, D.; CHANG, C.-T. An algorithmic approach to generate timesharing schemes for multi-period HEN designs. Chemical Engineering Research and Design, v. 93, p. 402–410, 2015.

KANG, L.; LIU, Y. Retrofit of Heat Exchanger Networks for Multiperiod Operations by Matching Heat Transfer Areas in Reverse Order. Industrial & Engineering Chemistry Research, v. 53, n. 12, p. 4792–4804, 2014.

KANG, L.; LIU, Y. Minimizing investment cost for multi-period heat exchanger network retrofit by matching heat transfer areas with different strategies. Chinese Journal of Chemical Engineering, v. 23, n. 7, p. 1153–1160, 2015.

KANG, L.; LIU, Y.; WU, L. Synthesis of multi-period heat exchanger networks based on features of sub-period durations. Energy, v. 116, p. 1302–1311, 2016.

KHORASANY, R. M.; FESANGHARY, M. A novel approach for synthesis of cost-optimal heat exchanger networks. Computers & Chemical Engineering, v. 33, n. 8, p. 1363–1370, 2009.

KLEMEŠ, J. J.; KRAVANJA, Z. Forty years of Heat Integration: Pinch Analysis (PA) and Mathematical Programming (MP). Current Opinion in Chemical Engineering, v. 2, n. 4, p. 461–474, 2013.

KLEMEŠ, J. J.; VARBANOVA, P. S.; KRAVANJA, Z. Recent developments in Process Integration. Chemical Engineering Research and Design, v. 91, n. 10, p. 2037–2053, 2013.

KONUKMAN, A. E. S.; ÇAMURDAN, M. C.; AKMAN, U. Simultaneous flexibility targeting and synthesis of minimum-utility heat-exchanger networks with superstructure-based MILP formulation. Chemical Engineering and Processing: Process Intensification, v. 41, n. 6, p. 501–518, 2002.

LAND, A. H.; DOIG, A. G. An Automatic Method of Solving Discrete Programming Problems. Econometrica, v. 28, n. 3, p. 497, 1960.

LEWIN, D. R. A generalized method for HEN synthesis using stochastic optimization — II.: The synthesis of cost-optimal networks. Computers & Chemical Engineering, v. 22, n. 10, p. 1387–1405, 1998.

LIN, B.; MILLER, D. C. Solving heat exchanger network synthesis problems with Tabu Search. Computers & Chemical Engineering, v. 28, n. 8, p. 1451–1464, 2004.

MA, X.; YAO, P.; LUO, X.; ROETZEL, W. Synthesis of multi-stream heat exchanger network for multi-period operation with genetic/simulated annealing algorithms. Applied Thermal Engineering, v. 28, n. 8, p. 809–823, 2008.

MARECHAL, F.; KALITVENTZEFF, B. Targeting the integration of multi-period utility systems for site scale process integration. Applied Thermal Engineering, v. 23, n. 14, p. 1763–1784, 1 out. 2003.

MARTELLI, E.; MIAN, A.; MARÉCHAL, F. MINLP Model and two-level Algorithm for the Simultaneous Synthesis of Heat Exchanger Networks and Utility Systems. Computer Aided Chemical Engineering, v. 37, p. 1979–1984, 2015.

MIAN, A.; MARTELLI, E.; MARÉCHAL, F. Framework for the Multiperiod Sequential Synthesis of Heat Exchanger Networks with Selection, Design, and Scheduling of Multiple Utilities. Industrial & Engineering Chemistry Research, v. 55, n. 1, p. 168–186, 2016a.

MIAN, A.; MARTELLI, E.; MARÉCHAL, F. Multiperiod Sequential Synthesis of Heat Exchanger Networks and Utility Systems including storages. Computer Aided Process Engineering, v. 38, p. 967–972, 2016b.

MIRANDA, C. B.; COSTA, C. B. B.; CABALLERO, J. A.; RAVAGNANI, .A.S.S. Optimal synthesis of multiperiod heat exchanger networks: A sequential approach. Applied Thermal Engineering, v. 115, p. 1187–1202, 2017.

MIRANDA, C. B.; COSTA, C. B. B.; CABALLERO, J. A.; RAVAGNANI, M. A. S. S. Heat Exchanger Network Optimization for Multiple Period Operations. Industrial & Engineering Chemistry Research, v. 55, n. 39, p. 10301–10315, 2016.

MORAR, M.; AGACHI, P. S. Review: Important contributions in development and improvement of the heat integration techniques. Computers & Chemical Engineering, v. 34, n. 8, p. 1171–1179, 2010.

PAPOULIAS, S. A.; GROSSMANN, I. E. A structural optimization approach in process synthesis—II. Computers & Chemical Engineering, v. 7, n. 6, p. 707–721, 1983.

PARDALOS, P. M.; DU, D.-Z. Handbook of combinatorial optimization. 1. ed. [s.l.] Kluwer Academic Publishers, 1998.

PAVÃO, L. V.; COSTA, C. B. B.; RAVAGNANI, M. A. da S. S. Automated heat exchanger network synthesis by using hybrid natural algorithms and parallel processing. Computers & Chemical Engineering, v. 94, p. 370–386, 2016.

PAVÃO, L. V.; COSTA, C. B. B.; RAVAGNANI, M. A. S. S. Heat Exchanger Network Synthesis without stream splits using parallelized and simplified Simulated Annealing and Particle Swarm Optimization. Chemical Engineering Science, v. 158, p. 96–107, 2017.

PAVÃO, L. V.; COSTA, C. B. B.; RAVAGNANI, M. A. da S. S.; JIMÉNEZ, L. Large-scale heat exchanger networks synthesis using simulated annealing and the novel rocket fireworks optimization.

AIChE Journal, v. 63, n. 5, p. 1582–1601, 2017.

PAVÃO, L. V.; MIRANDA, C. B.; COSTA, C. B. B.; RAVAGNANI, M. A. S. S. Efficient multiperiod heat exchanger network synthesis using a meta-heuristic approach. Energy, v. 142, p. 356–372, 2018a.

PAVÃO, L. V; MIRANDA, C. B.; COSTA, C. B. B.; RAVAGNANI, M. A. S. S. Synthesis of multiperiod heat exchanger networks with timesharing mechanisms using meta-heuristics. Applied Thermal Engineering, v. 128, p. 637–652, 2018b.

PINTARIČ, Z. N.; KASAŠ, M.; KRAVANJA, Z. Sensitivity analyses for scenario reduction in flexible flow sheet design with a large number of uncertain parameters. AIChE Journal, v. 59, n. 8, p. 2862–2871, 2013.

PINTARIČ, Z. N.; KRAVANJA, Z. Identification of critical points for the design and synthesis of flexible processes. Computers & Chemical Engineering, v. 32, n. 7, p. 1603–1624, 2008.

RAVAGNANI, M. A. S. S.; CABALLERO SUÁREZ, J. A. Redes de cambiadores de calor. [s.l.] Publicaciones de la Universidad de Alicante, 2012.

RAVAGNANI, M. A. S. S.; MÓDENES, A. N. Heat exchanger networks with multiple periods of operation. Brazilian Journal of Chemical Engineering, v. 13, n. 2, p. 71–84, 1996.

SABOO, A. K.; MORARI, M.; WOODCOCK, D. C. Design of resilient processing plants—VIII. A resilience index for heat exchanger networks. Chemical Engineering Science, v. 40, n. 8, p. 1553–1565, 1985.

SADELI, E.; CHANG, C.-T. Heuristic Approach to Incorporate Timesharing Schemes in Multiperiod Heat Exchanger Network Designs. Industrial & Engineering Chemistry Research, v. 51, n. 23, p. 7967–7987, 2012.

SHORT, M.; ISAFIADE, A. J.; FRASER, D. M.; KRAVANJA, Z. Two-step hybrid approach for the synthesis of multi-period heat exchanger networks with detailed exchanger design. Applied Thermal Engineering, v. 105, p. 807–821, 2016.

SIENIUTYCZ, S.; JEŻOWSKI, J. Energy optimization in process systems and fuel cells. [s.l.] Elsevier Science, 2013.

SILVA, A. P.; RAVAGNANI, M. A. S. S.; BISCAIA, E. C. Particle Swarm Optimisation in heat exchanger network synthesis including detailed equipment design. Computer Aided Chemical Engineering, v. 25, p. 713–718, 2008.

SILVA, A. P.; RAVAGNANI, M. A. S. S.; BISCAIA, E. C.; CABALLERO, J. A. Optimal heat exchanger network synthesis using particle swarm optimization. Optimization and Engineering, v. 11, n. 3, p. 459–470, 2010.

SILVA, M. L. Descrição: Aplicação da analise pinch na sintese de redes de trocadores de calor flexiveis. 1995. State University of Campinas, 1995.

SMITH, R. Chemical Process: Design and Integration. [s.l.] Wiley, 2014.

SWANEY, R. E.; GROSSMANN, I. E. An index for operational flexibility in chemical process design. Part I: Formulation and theory. AIChE Journal, v. 31, n. 4, p. 621–630, 1985.

TOIMIL, D.; GÓMEZ, A. Review of metaheuristics applied to heat exchanger network design. International Transactions in Operational Research, v. 24, n. 1–2, p. 7–26, 2017.

VERHEYEN, N.; ZHANG, W. Design of flexible heat exchanger network for multi-period operation. Chemical Engineering Science, v. 61, n. 23, p. 7730–7753, 2006.

WESTERLUND, T.; PETTERSSON, F. An extended cutting plane method for solving convex MINLP problems. Computers & Chemical Engineering, v. 19, p. 131–136, 1995.

YEE, T. F.; GROSSMANN, I. E. Simultaneous optimization models for heat integration—II. Heat exchanger network synthesis. Computers & Chemical Engineering, v. 14, n. 10, p. 1165–1184, 1990.

YERRAMSETTY, K. M.; MURTY, C. V. S. Synthesis of cost-optimal heat exchanger networks using differential evolution. Computers & Chemical Engineering, v. 32, n. 8, p. 1861–1876, 2008.

ZHANG, C.; CUI, G.; PENG, F. A novel hybrid chaotic ant swarm algorithm for heat exchanger networks synthesis. Applied Thermal Engineering, v. 104, p. 707–719, 2016.

Chapter 3

Energy Integration of a Sugarcane Biorefinery using Particle Swarm Optimization

This chapter presents the synthesis of heat exchanger network (HEN) for one industrial case study of biorefinery using an adapted Particle Swarm Optimization (PSO) algorithm. The Particle Swarm Optimization method has been already used in other works of HEN synthesis and presented good results (SILVA; RAVAGNANI; BISCAIA, 2008; SILVA et al., 2010). For this reason, the meta-heuristic method PSO was chosen in this study as the first mathematical approach to solve HEN problems in the case study of biorefinery. The equations of the model and the mathematical method were written in C ++ language. Preliminary tests were performed using literature examples for the validation of this approach. Although those examples have achieved solutions with quality equivalent to the literature, they are not showed in this thesis, since similar studies have already demonstrated the success of PSO (SILVA; RAVAGNANI; BISCAIA, 2008; SILVA et al., 2010). The results of this approach are presented in the following text entitled “Energy Integration of a Sugarcane Biorefinery using Particle Swarm Optimization”. It was structured into five main topics: introduction; approach for solving the multiperiod HEN problem; biorefinery description and data of case study; results and discussions; and conclusion.

Energy Integration of a Sugarcane Biorefinery using Particle Swarm Optimization

Oliveira, C. M.[a]; Cruz, A. J. G.[a]; Costa, C. B. B.[b]

[a] Chemical Engineering Department, Federal University of São Carlos, Rodovia Washington Luís, km 235, 13565-905 São Carlos, São Paulo, Brazil

[b] Chemical Engineering Department, State University of Maringá, Av. Colombo 5790, Bloco D-90, 87020-900 Maringá, Paraná, Brazil

Abstract

Energy integration in a sugarcane biorefinery allows reducing the steam consumption in the plant and, consequently, more bagasse is available to be processed into second generation ethanol. However, sugarcane plants can vary the production of ethanol and electricity depending on the demand. This study presents the energy integration of a sugarcane biorefinery by multiperiod Mixed Integer Nonlinear Programming (MINLP). The periods indicate different process conditions and differ in the bagasse fractions diverted to the second generation ethanol section and to the cogeneration system. To reduce the complexity of heat exchanger network (HEN) synthesis for all periods, an MINLP model was solved for each period, separately. Later, a timesharing scheme was used for the automatic integration of heat exchanger networks obtained in each period. For solving the MINLP problem, an adapted Particle Swarm Optimization (PSO) algorithm was used. The results demonstrated reductions in TAC (Total Annualized Cost) of HEN proposed in this work compared to the process without any energy integration. However, that saving is small when compared to the process with project energy integration (*i.e.*, process commonly found in Brazilian plants).

Keyword: Sugarcane Biorefinery, Second generation ethanol, Multiperiod Heat Exchanger Network, Mixed Integer Nonlinear Programming, Particle Swarm Optimization.

3.1 Introduction

Sugarcane plants in Brazil have great importance in world market of ethanol production, as well in sugar production. So, large amounts of bagasse are generated in those industries. In the last decades studies have presented the use of sugarcane bagasse in second generation (2G) ethanol production, such as evaluation of pretreatments for bagasse (CARDONA; QUINTERO; PAZ, 2010; ZHOU et al., 2016); bagasse hydrolysis using acid (RODRÍGUEZ-CHONG et al., 2004; KUMAR et al., 2015) and enzymes (SANTOS et al., 2017); fermentation of bagasse hydrolyzed by *Mucor* e *Fusarium* (UENG; GONG, 1982), *Pichia stipites* (ROBERTO et al., 1991) and *Saccharomyces cerevisiae* (MARTÍN et al., 2002; SINGH et al., 2013); simulations of first and second generation ethanol process (DIAS et al., 2013a,b); evaluation of technical configurations for bioenergy production with sugarcane bagasse (DANTAS; LEGEY; MAZZONE, 2013); and studies about process flexibility in second generation ethanol and electricity production (FURLAN et al., 2013). In this context, the sugarcane biorefinery concept is introduced, which refers to the production of different products and by-products (sugar, 1G/2G ethanol and electricity) from the main raw material (sugarcane). The current efforts to turn 2G ethanol viable have, among other goals, the increase in energy security and the decrease in environmental resources consumption, since 2G ethanol turns possible increasing the production of this biofuel without increasing the cultivated land area. However, 2G ethanol technology is still not consolidated and requires studies to allow the integrated first and second generation ethanol production to be more sustainable and economic.

Process integration techniques provide increased productivity, improved energy management and reduced operating and capital costs. Energy integration is one of the process integration techniques and one of its fundamental tasks is the synthesis of the heat exchanger network (HEN). In general, the methods for HEN synthesis can be classified into two groups: sequential and simultaneous.

The first group subdivides the problem into subproblems to reduce complexity and include methods that use thermodynamic concepts and mathematical programming. The methods that uses thermodynamic principles and heuristic rules allowed the development of Pinch Analysis in 1970s (FLOWER; LINNHOFF, 1979; CERDA et al., 1983; LINNHOFF; HINDMARSH, 1983). Pinch Analysis uses thermodynamic concepts to improve energy efficiency through the minimization of utilities demand to a given minimum temperature difference between a hot and a cold stream. The HEN is synthesized by the designer to meet that energy demand. In methods that use sequential mathematical programming, three optimization problems are solved separately: minimization of operating cost (Linear Programming formulation, LP), number of units of heat transfer (Mixed Integer Linear Programming, MILP) and investment cost (Non-Linear Programming, NLP). This strategy decreases the complexity of the entire task, so that relatively large problems can be solved with less effort and good solutions can be achieved. However, since different costs associated to HEN synthesis are not optimized simultaneously, suboptimal solutions can be obtained. The second group, simultaneous methods, considers all constraints and costs (both operating and capital costs) simultaneously through a Mixed Integer Nonlinear Programming (MINLP) problem. This strategy makes it possible to find better solutions, but it requires more computational effort.

Energy integration in the sugarcane biorefinery has as one of main goals the minimization the utility consumption. However, in a flexible plant, ethanol and electricity production can vary, according to variations in the prices of such products. Thus, the HEN synthetized should be able to meet different operating conditions.

Energy integration studies have been performed with processes of 1G ethanol and sugar production from sugarcane (PINA et al., 2014, 2015); 1G ethanol production from corn (BRUNET et al., 2015); 2G ethanol production from the straw (KRAVANJA; MODARRESI; FRIEDL, 2013); and 1G/2G ethanol production from sugarcane (OLIVEIRA; CRUZ; COSTA, 2016). However, these studies used the sequential technique Pinch Analysis and considered one single-period of operation (*i.e.*, HEN is rigid and cannot operate under more than one operating condition).

Collaborations under flexible HENs include methodologies to design HENs that operate in more than one operating condition, which are called the multiperiod HEN. Techniques applied to HEN synthesis with multiple operations can be sequential or simultaneous. Floudas and Grossmann (1986) presented an MILP formulation for HEN synthesis with multiperiod operations. Afterwards, the automatic HEN costs for a multiperiod model was developed by Floudas and Grossmann (1987), based on the NLP model for single-period of Floudas, Ciric and Grossmann (1986). The simultaneous approach of the multiperiod HEN synthesis was introduced by Aaltola (2002) from the extension of the MINLP model of Yee and Grossmann (1990).

In this work, a multiperiod approach was used for the HEN synthesis in a sugarcane biorefinery that produces 1G/2G anhydrous ethanol and electricity. The periods differ essentially in the bagasse fraction diverted to second generation ethanol production. This fraction is responsible for changing the flow rates of many streams in the integrated process. This paper is organized as follows. Section 3.2 presents the approach for solving the multiperiod HEN problem, including superstructure, HEN model equations, mathematical algorithm, timesharing mechanisms to integrate the HENs of all periods and procedure for solving the multiperiod HEN problem. Section 3.3 describes the process of 1G/2G anhydrous ethanol and electricity production process in the sugarcane biorefinery, as well as the streams data in each period for the case study and the costs of utilities and of HEN applied to the Brazilian sugarcane industry. Sections 3.4 and 3.5 present results and discussion and main conclusions of this study, respectively.

3.2 Approach for solving the multiperiod HEN problem

In order to reduce the complexity of HEN synthesis for all periods, an MINLP model is solved for each period, separately. In addition, the presence of process streams with phase change makes the HEN synthesis problems even more difficult to solve since it requires extra constraints. A usual approach in HEN synthesis problems in which latent heat is present is to consider latent heat as equivalent to a large heat capacity over a small temperature difference (usually equal to 1.0 K). More assumptions includes constant specific heat capacities, constant heat transfer convective coefficients, counter-flow heat exchangers, nonisothermal mixing, non-consideration of fouling and pressure drop effects and non-inclusion of piping costs in the TAC function. These approaches were used in this study to simplify the calculations. In each period, an adapted Particle Swarm Optimization algorithm is used to solve the MINLP optimization model. To integrate the HENs of all periods into one, timesharing mechanisms presented by Jiang and Chang (2013) were used.

3.2.1 Superstructure

The superstructure used in this study is based on the superstructure of Yee and Grossmann (1990), but the original assumption of isothermal mixing is not here adopted. A superstructure with two hot streams, two cold streams and two stages is shown in Fig. 3.1.

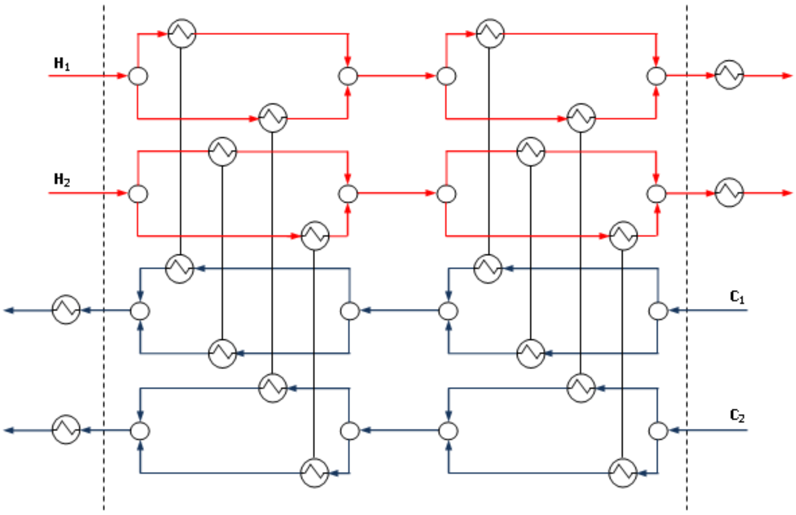

Figure 3.1. Superstructure of Yee and Grossmann (YEE; GROSSMANN, 1990) with two stages, two hot and two cold streams.

3.2.2 Model equations

Objective function

$$min{:}\ C_{\text{total}} = \sum_i Qcu_i\,.ccu + \sum_j Qhu_j\,.chu + \sum_i \sum_j \sum_k z_{i,j,k} \cdot (a + b \cdot A_{i,j,k}{}^c) + \sum_i zcu_i \cdot (a + b \cdot Acu_i{}^c) + \sum_j zhu_j \cdot (a + b \cdot Ahu_j{}^c), \qquad i \in N_H, j \in N_C, k \in N_S \tag{3.1}$$

Energy balance in mixers

$$Thmix_{i,1} = Th_i^0, \qquad i \in N_H \tag{3.2}$$

$$Tcmix_{j,K+1} = Tc_i^0, \qquad j \in N_C \tag{3.3}$$

$$Thmix_{i,k+1} = Thmix_{i,k} - \frac{\sum_{j \in N_C} z_{i,j,k} Q_{i,j,k}}{CPh_i}, \qquad i \in N_H, j \in N_C, k \in N_S \tag{3.4}$$

$$Tcmix_{j,k} = Tcmix_{j,k+1} + \frac{\sum_{i \in N_H} z_{i,j,k} Q_{i,j,k}}{CPc_j}, \qquad i \in N_H, j \in N_C, k \in N_S \tag{3.5}$$

Energy balance in heat exchangers

$$Thin_{i,j,k} = Thmix_{i,k}, \qquad i \in N_H, j \in N_C, k \in N_S \tag{3.6}$$

$$Tcin_{i,j,k} = Tcmix_{j,k+1}, \qquad i \in N_H, j \in N_C, k \in N_S \tag{3.7}$$

$$Thout_{i,j,k} = Thmix_{i,k} - \frac{z_{i,j,k} Q_{i,j,k}}{Fh_{i,j,k}\, CPh_i}, \qquad i \in N_H, j \in N_C, k \in N_S \tag{3.8}$$

$$Tcout_{i,j,k} = Tcmix_{j,k+1} + \frac{z_{i,j,k} Q_{i,j,k}}{Fc_{i,j,k}\, CPc_j}, \qquad i \in N_H, j \in N_C, k \in N_S \tag{3.9}$$

Energy balance for utilities

$$Qcu_i = CPh_i \left(Th_i^0 - Th_i^{final}\right) - \sum_k \sum_j z_{i,j,k} Q_{i,j,k}, \qquad i \in N_H, j \in N_C, k \in N_S \tag{3.10}$$

$$Qhu_j = CPc_j \left(Tc_j^{final} - Tc_j^0\right) - \sum_k \sum_i z_{i,j,k} Q_{i,j,k}, \qquad i \in N_H, j \in N_C, k \in N_S \tag{3.11}$$

If Qcu_i is different from zero, then $ycu_i = 1$, otherwise $ycu_i = 0$. If Qhu_j is different from zero, then $yhu_j = 1$, otherwise $yhu_j = 0$.

$$Thcuin_i = Thmix_{i,K+1}, \qquad i \in N_H \tag{3.12}$$

$$Tchuin_j = Tcmix_{j,1}, \qquad j \in N_C \tag{3.13}$$

LMTD

For process streams

$$\theta_{i,j,k}^{(1)} = Thin_{i,j,k} - Tcout_{i,j,k}, \qquad i \in N_H, j \in N_C, k \in N_S \tag{3.14}$$

$$\theta_{i,j,k}^{(2)} = Thout_{i,j,k} - Tcin_{i,j,k}, \qquad i \in N_H, j \in N_C, k \in N_S \tag{3.15}$$

$$LMTD_{i,j,k} = \frac{\theta_{i,j,k}^{(1)} - \theta_{i,j,k}^{(2)}}{\ln\left(\frac{\theta_{i,j,k}^{(1)}}{\theta_{i,j,k}^{(2)}}\right)}, \qquad i \in N_H, j \in N_C, k \in N_S \tag{3.16}$$

If $\theta_{i,j,k}^{(1)}$ is equal to $\theta_{i,j,k}^{(2)}$, then $\theta_{i,j,k}^{(1)} = LMTD_{i,j,k}$.

For cold utility

$$\theta_{i,cu}^{(1)} = Thcuin_{i,} - Twout, \qquad i \in N_H \tag{3.17}$$

$$\theta_{i,cu}^{(2)} = Th_i^{final} - Twin, \qquad i \in N_H, j \in N_C, k \in N_S \tag{3.18}$$

$$LMTD_{i,cu} = \frac{\theta_{i,cu}^{(1)} - \theta_{i,cu}^{(2)}}{\ln\left(\frac{\theta_{i,cu}^{(1)}}{\theta_{i,cu}^{(2)}}\right)}, \qquad i \in N_H \tag{3.19}$$

If $\theta_{i,cu}^{(1)}$ is equal to $\theta_{i,cu}^{(2)}$, then $LMTD_{i,cu} = \theta_{i,cu}^{(1)}$.

For hot utility

$$\theta_{j,hu}^{(1)} = Tsout - Tchuin_j, \qquad j \in N_C \tag{3.20}$$

$$\theta_{j,hu}^{(2)} = Tsin - Tc_j^{final}, \qquad j \in N_C \tag{3.21}$$

$$LMTD_{j,hu} = \frac{\theta_{j,hu}^{(1)} - \theta_{j,hu}^{(2)}}{\ln\left(\frac{\theta_{j,hu}^{(1)}}{\theta_{j,hu}^{(2)}}\right)}, \qquad i \in N_H, j \in N_C, k \in N_S \tag{3.22}$$

If $\theta_{j,hu}^{(1)}$ is equal to $\theta_{j,hu}^{(2)}$, then $LMTD_{j,hu} = \theta_{j,hu}^{(1)}$.

Overall heat transfer coefficient

For process streams

$$U_{i,j} = \frac{1}{\frac{1}{hh_i} + \frac{1}{hc_j}}, \qquad i \in N_H, j \in N_C \tag{3.23}$$

For cold utility

$$U_{i,cu} = \frac{1}{\frac{1}{hh_i} + \frac{1}{hcu}}, \qquad i \in N_H \tag{3.24}$$

For hot utility

$$U_{j,hu} = \frac{1}{\frac{1}{hc_j} + \frac{1}{hhu}}, \qquad j \in N_C \tag{3.25}$$

Area

For process streams

$$A_{i,j,k} = \frac{z_{i,j,k} Q_{i,j,k}}{U_{i,j,k}\, LMTD_{i,j,k}}, \qquad i \in N_H, j \in N_C, k \in N_S \tag{3.26}$$

For cold utility

$$A_{i,cu} = \frac{zcu_i Qcu_i}{U_{i,cu}\, LMTD_{i,cu}}, \qquad i \in N_H \tag{3.27}$$

For hot utility

$$A_{j,hu} = \frac{zhu_j Qhu_j}{U_{j,hu}\, LMTD_{j,hu}}, \qquad j \in N_C \tag{3.28}$$

Constraints

$$\sum_j Fh_{i,j,k} = 1, \qquad i \in N_H, j \in N_C, k \in N_S \tag{3.29}$$

$$\sum_i Fc_{i,j,k} = 1, \qquad i \in N_H, j \in N_C, k \in N_S \tag{3.30}$$

$$0 \le Qcu_i \le CPh_i \cdot \left(Th_i^0 - Th_i^{final} \right), \qquad i \in N_H \tag{3.31}$$

$$0 \le Qhu_j \le CPc_j \cdot \left(Th_j^{final} - Th_j^0 \right), \qquad j \in N_C \tag{3.32}$$

$$Thmix_{i,k} \ge Thmix_{i,k+1}, \qquad i \in N_H, k \in N_S \tag{3.33}$$

$$Thmix_{i,K+1} \ge Th_i^{final}, \qquad i \in N_H, k \in N_S \tag{3.34}$$

$$Tcmix_{j,k} \ge Tcmix_{j,k+1}, \qquad j \in N_C, k \in N_S \tag{3.35}$$

$$Tc_j^{final} \ge Tcmix_{j,1}, \qquad j \in N_C, k \in N_S \tag{3.36}$$

$$\theta_{i,j,k}^{(1)} \ge EMAT, \qquad i \in N_H, j \in N_C, k \in N_S \tag{3.37}$$

$$\theta_{i,j}^{(2)} \ge EMAT, \qquad i \in N_H, j \in N_C, k \in N_S \tag{3.38}$$

$$\theta_{i,cu}^{(1)} \ge EMAT, \qquad i \in N_H \tag{3.39}$$

$$\theta_{i,cu}^{(2)} \ge EMAT, \qquad i \in N_H \tag{3.40}$$

$$\theta_{j,hu}^{(1)} \ge EMAT, \qquad j \in N_C \tag{3.41}$$

$$\theta_{j,hu}^{(2)} \geq EMAT, \qquad j \in N_C \tag{3.42}$$

$$Thout_{i,j,k} \geq Th_i^{final}, \qquad i \in N_H, j \in N_C, k \in N_S \tag{3.43}$$

$$Tc_j^{final} \geq Tcout_{i,j,k}, \qquad i \in N_H, j \in N_C, k \in N_S \tag{3.44}$$

$$CPh_i \left(Th_i^0 - Th_i^{final}\right) \geq \sum_k \sum_j z_{i,j,k} Q_{i,j,k}, \qquad i \in N_H, j \in N_C, k \in N_S \tag{3.45}$$

$$CPc_j \left(Tc_j^{final} - Tc_j^0\right) \geq \sum_k \sum_i z_{i,j,k} Q_{i,j,k}, \qquad i \in N_H, j \in N_C, k \in N_S \tag{3.46}$$

The objective function is penalized by the constraints, which are multiplied by a weight and added to the objective function. The weight can vary from problem to problem, but it should be of an order of magnitude consistent with investment and operating costs. Constraints (3.37)-(3.44) are only activated when the heat exchanger exists for the indicated match. In other words, they are only accounted if there is that heat exchanger in a given position of the superstructure. The strategy used in this study does not penalize the equality constraints of adding fractions, indicated by Eqs. (3.29) and (3.30). Meeting these constraints make it difficult to solve the MINLP problem and can lead to a poor solution search scheme. For this reason, constraints of adding fractions, when violated, are modified with the strategy described in Section 3.2.5.

Variables

The variables estimated by PSO algorithm are $Q_{i,j,k}$, $z_{i,j,k}$, $Fh_{i,j,k}$ and $Fc_{i,j,k}$. In this model, the number of continuous variables can be calculated by:

$$n_{continuous} = n_Q + n_{Fh} + n_{Fc} \tag{3.47}$$

$$n_Q = n_{Fh} = n_{Fc} = N_H \cdot N_C \cdot N_S \tag{3.48}$$

where n_Q is the number of variables of heat load for each potential heat exchanger in the network, n_{Fh} is the number of fraction variables for hot streams, n_{Fc} is the number of fraction variables for cold streams, N_H and N_C are the numbers of hot and cold streams, respectively, and N_S is the number of stages.

The number of estimated binary variables, n_z, is calculated by Eq. (3.49).

$$n_z = N_H \cdot N_C \cdot N_S \tag{3.49}$$

So, the total number of independent variables is:

$$n_{total} = n_z + n_Q + n_{Fh} + n_{Fc} = 4\,.\,N_H \cdot N_C \cdot N_S \tag{3.50}$$

Bounds

Eqs. (3.51)-(3.55) present the bounds of the variables estimated by PSO algorithm. Note that *zcont* is a continuous variable that indicates the existence of a heat exchanger. It is converted to binary variable, $z_{i,j,k}$, according to the strategy of PSO for dealing with binary variables (please, see the topic 3.2.3).

$$Qmax_{i,j,k} = min\left(CP_i\left(Th_i^0 - Th_i^{final}\right), CP_j\left(Tc_j^{final} - Tc_j^0\right)\right), i \in N_H, j \in N_C, k \in N_S \tag{3.51}$$

$$0 \leq Q_{i,j,k} \leq Qmax_{i,j,k}, \qquad i \in N_H, j \in N_C, k \in N_S \tag{3.52}$$

$$0 \leq zcont_{i,j,k} \leq 1, \qquad i \in N_H, j \in N_C, k \in N_S \tag{3.53}$$

$$0 \leq Fh_{i,j,k} \leq 1, \qquad i \in N_H, j \in N_C, k \in N_S \tag{3.54}$$

$$0 \leq Fc_{i,j,k} \leq 1, \qquad i \in N_H, j \in N_C, k \in N_S \tag{3.55}$$

3.2.3 Particle Swarm Optimization algorithm

Particle Swarm Optimization (PSO) belongs to the group of Evolutionary Computation algorithms. It is employed in nonlinear optimization problems, which have solutions difficult to find using the traditional approaches with deterministic methods. The Evolutionary Computation algorithms are based on populations and meta-heuristics. Fundamental principles are a constructive method to obtain the initial population and a local search technique to improve the solution of the population (BOUSSAÏD; LEPAGNOT; SIARRY, 2013). The evolutionary approach can be subdivided into two subgroups: Evolutionary algorithms and Swarm Intelligence algorithms.

Evolutionary algorithms are based on biological evolution by means of genetic operators such as selection, mutation and crossover, while the Swarm algorithms, also known as Natural Computing algorithms, are based on populations of individuals able to interact. The Particle Swarm method, proposed by Kennedy and Eberhart (1995), belongs to the Swarm algorithms. According to the authors, the method for nonlinear problems was discovered through experiments with simplified social models of bird species and schools of fish and paradigms, and can be implemented in few lines of code (KENNEDY; EBERHART, 1995).

The Particle Swarm Optimization algorithm is based on a population of individuals (particles) able to interact with others, that is, each particle is influenced by its own experience and the experience of the entire swarm. Mathematically, each individual or particle of the swarm is a candidate for solution and indicates a point in the search space. The particle has associated a velocity term, which is determined by weighting the distance between the actual position and the best own position, the distance between the actual position and the best position of the swarm, and the previous own velocity. Thus, each particle modifies its velocity according to the individual and group experience, aiming to achieve, over iterations, better solutions.

Eqs. (3.56) and (3.57) show the vectors of velocity ($\boldsymbol{v}_p$) and position ($\boldsymbol{x}_p$) of particle p. The inertia weight (w) controls the impact of previous velocity in the current velocity. A high inertia weight value favors global exploration, while a small inertia weight value favors local exploration. Thus, the satisfactory selection of inertia weight provides a balance between global and local exploration. The inertia weight can be a constant or a value adjusted dynamically by a linear function. In this study, the inertia weight is adjusted dynamically.

$$\boldsymbol{v}_p^{k+1} = w \, . \, \boldsymbol{v}_p^k + c_1 \, . \, r_{1\,.} \left(\boldsymbol{f}_{Bp} - \boldsymbol{x}_p^k\right) + c_2 \, . \, r_{2\,.} \, (\boldsymbol{g}_{Bp} - \boldsymbol{x}_p^k) \tag{3.56}$$

$$\boldsymbol{x}_p^{k+1} = \boldsymbol{x}_p^k + \boldsymbol{v}_p^{k+1} \tag{3.57}$$

After the original proposal, Kennedy and Eberhart (1997) reformulated the Particle Swarm algorithm, allowing it to operate with binary variables. In this version, a particle moves in the space restricted to zero and one. The velocity term represents the probability of the particle assuming the value one or zero. In other words, if the velocity of a particle is equal to 0.30 then there is 30% probability of the particle assuming the value one and 70% probability of the particle assuming the value zero. In this work, a rounding function is used to adapt PSO algorithm to binary variables.

PSO is a simple method to be implemented and has low computational cost in terms of memory, because it uses only basic mathematical operators. Studies of energy integration using only PSO were performed by Silva, Ravagnani and Biscaia Jr (2008) and Silva et al. (2010). Other studies also employed the PSO, but combined two algorithms to solve HENs problems, such as Genetic Algorithm and Particle Swarm Optimization (ZHAOYI et al., 2013; PAVÃO; COSTA, RAVAGNANI, 2016), and Simulated Annealing and Particle Swarm Optimization (PAVÃO; COSTA; RAVAGNANI, 2017). Stochastic techniques are important approaches to solve large-scale problems. In general, they avoid to get stuck in local minima and have better results in complex problems when compared to purely deterministic methods (RAVAGNANI; CABALLERO SUÁREZ, 2012). However, since it is a population-based method, the number of objective function evaluations may be too large. A more specific review on meta-heuristic techniques applied to HEN synthesis was performed by Toimil e Gómez (2017).

The implementation of the PSO method used in this study was performed by Furlan et al. (2012). The stopping criterion is the number of iterations. The logic of the algorithm is presented in the following steps.

Step 1: Specify the number of particles in the swarm.

Step 2: Initialize initial position of each particle.

Step 3: Allocate an initial velocity equal to zero for all particles.

Step 4: For each particle:

i. Calculate objective function.

ii. Identify if actual position is better than recorded best position, *i.e.*, identify if actual position corresponds to a better objective function value. If yes, update $\mathbf{f}_{Bp}$ vector.

Step 5: Identify if actual best position in the swarm is better than recorded swarm best position. If yes, update $\mathbf{g}_{Bp}$ vector.

Step 6: For each particle, update:

i. Particle velocity by Eq. (3.56).

ii. Particle position by Equation (3.57).

Step 7: Verify if algorithm termination condition is satisfied. If condition is satisfied, end the procedure. Otherwise, return to step 4.

3.2.4 Timesharing mechanisms

In order to integrate heat exchanger networks of all periods, the strategy of Jiang and Chang (2013) was used, which involves solving the MINLP model separately for each period and applying timesharing mechanisms to integrate all HENs into a single one. This approach allows dealing with periods of unequal durations without defining their duration, using the same heat exchanger for different pair of streams matched in different periods, as well as reducing capital cost. In addition, the solution is not limited to a fixed duration of period, which may need to be adjusted due to unexpected changes in supplies, demand, prices and/or process conditions. This strategy is presented below.

Step 1: Classify heat exchanger areas of all periods in descending order (list);

Step 2: In the previous list, select the first device and allocate it in the multiperiod HEN;

Step 3: For each period, identify the device with the largest area. For the device allocated in the multiperiod HEN, assign the streams and the superstructure stage identified in this step;

Step 4: Remove from the list produced in Step 1 the areas identified in Steps 2 and 3;

Step 5: Perform this procedure until the list is empty.

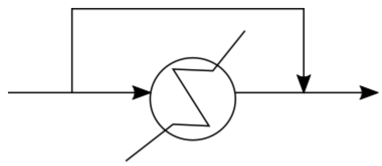

Figure 3.2. By-pass in heat exchanger.

To exemplify the strategy, suppose a problem with three periods. Suppose that, during the HEN synthesis for Period 1, the device with the largest area had 420 m^2 and it combined streams H1 and C4 in the second stage of superstructure. Also suppose, when the HEN synthesis for Period 2 was performed, the largest device had 500 m^2, combining streams H3 and C2 in the third stage of the superstructure. Finally, suppose that the largest area found for Period 3 was 475 m^2, corresponding to the match of streams H4 and C2 in the first stage of the superstructure. Therefore, the first device of the ordered list has 500 m^2 (*i.e.*, it is the largest area among devices of all periods). In Step 2 this device will be allocated in the multiperiod HEN. In Step 3, streams H1 and C4, matched in the second stage of the superstructure, will be assigned to the multiperiod HEN when operated under the conditions of Period 1. Then, there will be an area oversize of 19% for that device in Period 1. The same procedure is performed to Periods 2 and 3 (assignment, to this device, respectively of streams H3 and C2 in the third stage of the superstructure in Period 2, without any area oversize, and streams H1 and C2 in the first stage of the superstructure, leading to an area oversize of 5.3%). In step 4 the areas identified (*i.e.*, devices with area of 500 m^2, 475 m^2 and 420 m^2) are removed from the list. This procedure is performed until the list is empty.

A cleaning step among the periods may be necessary to prevent contamination inside the heat exchangers. Moreover, in order to allocate the correct matching of streams in a given period to a device, a set of bypasses must be designed (Fig. 3.2). However, capital cost due to the use of valves and pipes for the design of the bypasses is not considered in the objective function of this study.

3.2.5 Procedure for solving the multiperiod HEN problem

For the multiperiod HEN synthesis, the mathematical model and the procedure for integration of HENs of all periods were written in C++ language. Dev C ++ Integrated Development Environment (IDE) and GCC compiler were used. In this work, some strategies were applied to enable solving the optimization problems more easily.

The first strategy modifies the value of the variables estimated by the algorithm when one of them is equal to zero in a given position of the superstructure (i, j, k). For example, if there is no heat exchanger in position 1,1,1 (*i.e.*, if $z_{1,1,1} = 0$), all other variables corresponding to position 1,1,1 ($Q_{1,1,1}$, $Fh_{1,1,1}$ and $Fc_{1,1,1)}$ are modified to zero, no matter the value estimated for them by the algorithm.

The second strategy changes the values of fractions of hot and cold streams so that the constraints of adding fractions (Eqs. 3.29 and 3.30) are met without penalizing them. This strategy can be easily explained with an example. Suppose that in the first stage of a superstructure of a problem with two hot streams and two cold streams, the fractions of hot stream number 1 estimated by the algorithm are equal to 0.6 ($Fh_{1,1,1}$) and 0.5 ($Fh_{1,2,\ 1}$). These fractions violate Eq. (3.29), because their sum exceeds by 0.1 the value of 1.0. The strategy applied randomly modifies one of these fractions so that the sum is equal to 1.0; in other words, $Fh_{1,1,1}$ is changed to 0.5 or $Fh_{1,2,1}$ is changed to 0.4.

The last strategy introduces a good solution previously obtained (*e.g.*, the best particle of the swarm so far, a solution from the literature or a solution derived from Pinch Analysis), named "guess solution", into the swarm, so that the algorithm can improve it. This strategy showed, in the previous tests conducted, to be of prime importance for solving more complex problems, since the greater the number of streams involved in energy integration, the greater the number of possible combinations among the variables of the problem. Without the help of an initial good particle, PSO method was not able to, alone, find promising solutions. The execution procedure for energy integration in each period is described in the following steps. The procedure of Step 2 was executed more than twenty times for some periods.

Step 1: Use the parameters of Table 3.1 (column value identified by 1) for the first execution of the program. In this step no "guess solution" is provided.

Step 2: Use the parameters of Table 3.1 (column value identified by 2) for the second execution of the program. Add to the swarm the best particle obtained in the previous execution.

Step 3: Repeat Step 2 until the solution does not vary.

Step 4: Execute the program more five times using parameters of Table 3.1 (column value identified by 2) and adding to the swarm the best solution obtained in previous execution. If a better solution is found, restart this step.

Step 5: Execute the program more fifteen times using the parameters of Table 3.1 (column value identified by 3) and adding to the swarm the best solution obtained in previous execution (refining step). If a better solution is found, return to Step 4. Otherwise, stop executions.

Table 3.1 PSO tuning parameters.

Parameter	**Value (see footnote)**		
	1	**2**	**3**
Number of particles	200	500	500
Inertia weight (maximum and minimum)	0.9-0.4	0.9-0.4	0.9-0.4
Constant of Particle Swarm algorithm (c1)	1.1	1.1	1.1
Constant of Particle Swarm algorithm (c2)	1.1	1.1	1.1
Number of iterations	5,000	5,000	1,000
Weight for penalty functions	10,000	1,000	1,000

[1] When no "guess solution" is provided; [2] when a "guess solution" is provided; [3] in the refining step.

Sugarcane biorefineries with some degree of energy integration are commonly found (referred to in this study as process "with project energy integration"). Since the problems solved in this study are large, the solutions obtained from PSO algorithm can be poor when compared to these biorefineries. In this situation, the following procedure is used (solutions combination procedure).

Step 1: Add a new particle to the swarm, which incorporates the matches of the solution obtained by the PSO algorithm and the matches of the process with project energy integration, and execute the program using parameters of Table 3.1 (column value identified by 2);

Step 2: Execute the program more five times with the best solution using parameters of Table 3.1 (column value identified by 2). If a better solution is found, restart this step;

Step 3: Execute the program more fifteen times using the parameters of Table 3.1 (column value identified by 3) (refining step). If a better solution is found, return to Step 2. Otherwise, stop executions.

It is important to mention that the selection of PSO tuning parameters requires previous studies, especially the selection weights for function penalties. In this work, previous tests were performed to solve the HEN synthesis problem using data of Period 1. After the selection of PSO tuning parameters for Period 1, the same values were used to other periods and case studies.

3.3 Sugarcane biorefinery

3.3.1 Process description

In this study, a virtual biorefinery modeled in EMSO simulator (Environment for Modeling, Simulation, and Optimization) was used (FURLAN et al., 2012, 2013). Fig. 3.3 shows the diagram of this 1G/2G anhydrous ethanol and electricity production process (autonomous distillery). Topics 3.3.1 to 3.3.7 present a description of the process. Tables 3.2 and 3.3 present parameters of composition of sugarcane, which represent an average of these parameters throughout the harvest period. Tables 3.4 and 3.5 provide main parameters for biorefinery simulation.

Brazilian sugarcane plants often integrate energetically some streams. In this study, for comparison, energy integration between wine and vapor from Column B top (device indicated in Fig. 3.3 by E301), between streams of wine and vinasse (E302), and between pretreated bagasse and soaking water (E506) were considered. This process was named in this work as “with project energy integration". The process without any energy integration was named in this study as "without energy integration".

Table 3.2. Composition of sugarcane.

Component	Mass composition (%)
Water	69.864
Sucrose	14.033
Glucose	1.303
Fibers	13.653
Ash	1.147

Table 3.3. Composition of fiber and straw of sugarcane.

Component	Mass composition (%)	
	Fiber	Straw
Cellulose	45.57	46.05
Hemicellulose	26.93	27.20
Lignin	24.41	24.67
Ash	3.09	2.08

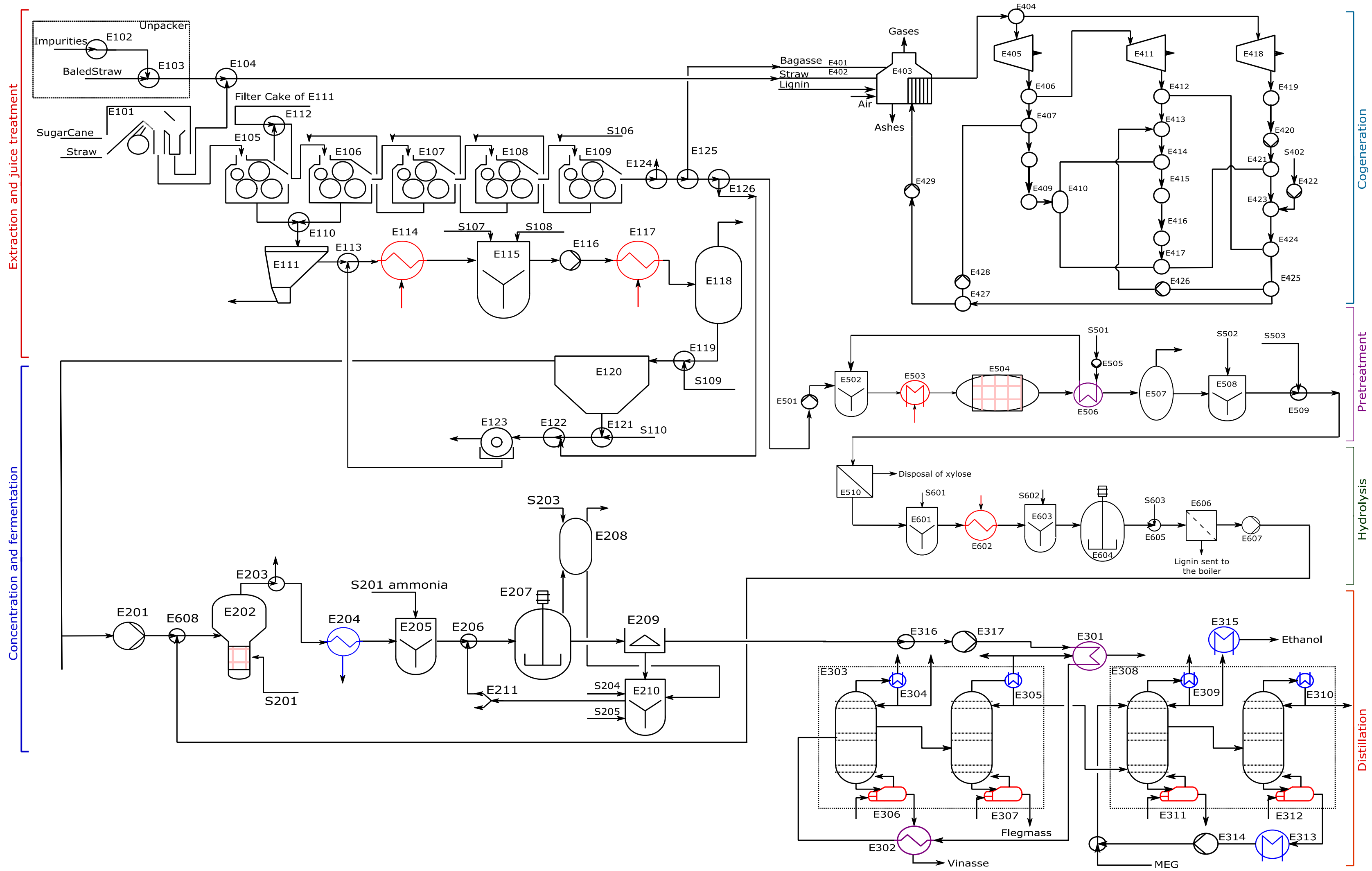

Figure 3.3. Diagram of the sugarcane biorefinery.

Table 3.4. Main data for 1G ethanol production.

Input	**Parameter**	**Unit**
Sugarcane flow	833	tonne/h
Straw flow	75	tonne/h
Fraction of bagasse reserved for start-ups of the plant	5	%
Cleaning section		
Removal efficiency of vegetal and mineral impurities	65	%
Sugar extraction section		
Sugarcane bagasse humidity	50	% w/w
Sugar recovery (total)	96	%
Duty	16	kWh/tonne of fiber
Water flow	30	% w/w
Sugarcane juice treatment section		
CaO flow	0.5-0.8	kg/tonne of sugarcane
H_3PO_4 concentration	85	% w/w
Heating final temperature	105	°C
Global coefficient heat transfer	0.69	$kW/m^2.K$
Solids concentration in the sludge (soluble and insoluble solids)	9	%
Decantation of insoluble solids efficiency	99.7	%
Sugar losses (filter)	1.5-2.0	%
Filter cake humidity	75-80	% w/w
Filter efficiency	70-90	%
Water flow (filter)	30	kg/tonne of sugarcane
Sugarcane bagasse pith flow	7	kg/ tonne of sugarcane
Sugarcane juice concentration section		
Outlet sugar concentration	20	°Brix
Pressure of steam	2.5	bar
Pressure of steam produced	1.6	bar
Fermentation section (include 1G+2G)		
Fermentation yield	90.48	%

Space-time	1	h
Recuperation of ethanol (absorption column)	99.96	% w/w
Ethanol purification section (include 1G+2G)		
Ethanol recovery	99.3	% w/w
Cogeneration system		
65 bar steam temperature	485	°C
Turbines isentropic efficiency	80	%
Turbines mechanic efficiency	95.8	%
Steam pressure – process	2.5	bar
Steam pressure – dehydration column	6	bar
Steam pressure – pretreatment	17.4	bar

Table 3.5. Main data for 2G ethanol production.

	Value	**Unit**
Pretreatment		
Pressure	1	bar
Temperature	195	°C
Cellulose to glucose yield	8.12	%, w/w
Hemicellulose to xylose yield	46.53	% w/w
Solid/liquid ratio	10	%
Space-time	10	min
Hydrolysis		
Cellulose to glucose yield	75	%, w/w
Solid/liquid ratio	15	%
Enzyme/Cellulose ratio	15	FPU/g
Space-time	48	h
Temperature	50	°C

3.3.1.1 Extraction and juice treatment

Ethanol production begins with the dry cleaning of sugarcane (E101). Straw can be maintained in the plantation area to preserve the soil and can be brought to the biorefinery to be used in the cogeneration system to produce steam and electricity. The clean sugarcane is sent to extraction system, which consists in separating bagasse from sugarcane juice by mills or diffusers. In industry, the milling system is more commonly used, since it is often a pre-existing infrastructure in the plant, and there is no need for new investments at this stage. Besides, bagasse with less moisture content is obtained with milling system (NAZATO et al., 2011). In this study an extraction system by mills is considered (E105, E106, E107, E108 and E109). Also straw is considered to be kept part in plantation area and the remaining is sent to the cogeneration system.

Bagasse from the extraction section is destined for the boiler, the pretreatment and a safety reserve. The extracted juice is carried to the strainer (E111). Subsequently, it is heated (E114) before entering into the liming tank (E115). The resulting mixture of the liming tank is heated (E117) and carried to the flash tank (E118). Next, the juice is introduced into the decanter (E120), where polymers are added to the juice. Then, clarified juice is obtained. Bagasse and water are added to the slurry leaving the decanter to increase the filtration efficiency on the rotary drum (E123). The resulting fraction of juice from the rotary drum is mixed with the filtered juice of the strainer.

3.3.1.2 Concentration

The clarified juice from the decanter is mixed with the hexose sugar liquor from the hydrolysis process, producing a mixture of sugars containing, mainly, glucose and sucrose. The mixture of sugars is concentrated in a pre-evaporator (E202) to 20°Brix. Commonly, a multi-effect evaporator is used in ethanol and sugar production process, which allows reaching greater concentrations with lower consumption of turbine extraction steam. Since the process here considered comprises only ethanol production and requires sugarcane juice to be concentrated up to 20°Brix, a single effect evaporator (pre-evaporator) was considered. However, the implementation of a multi-effect evaporator promotes saving of turbine extraction steam and, consequently, diverting the surplus bagasse for cogeneration system or 2G ethanol production.

3.3.1.3 Fermentation

Concentrated juice is cooled (E204) and mixed with ammonia (E205). Afterwards, *Saccharomyces cerevisae* yeast is added to the juice (E206), which is sent to the fermenter (E207). During fermentation, ethanol, CO_2 and, in minor proportions, other products such as glycerol, organic acids and higher alcohols are produced. Carbon dioxide containing ethanol is sent to the absorption column (E208) to recover ethanol in water solvent, which returns to the yeast treatment vessel (E210). The wine from the fermenter is centrifuged (E209) and carried to the distillation column (block E303 indicates the distillation unit). Yeasts are treated (E210) and mixed with ethanol recovered in the absorption column by recycle (E211). The most common configurations in fermentation are fed batch with cells recycle, known as Melle-Boinot process, and continuous multistage with cells recycle. Melle-Boinot process is more common in Brazil. For this reason, it is the configuration chosen for this study.

3.3.1.4 Distillation

Wine coming from the concentration and the fermentation section is heated (E301) and sent to the distillation unit (E303), where hydrous ethanol is produced. After the first distillation unit, anhydrous ethanol can be produced by extractive distillation, azeotropic distillation or molecular sieves. In this work, anhydrous ethanol is produced by extractive distillation (block E308 indicates the extractive distillation unit) and cooled to 308 K (E315). Solvent monoethyleneglycol is added to the extractive distillation column and subsequently recovered. Before returning to the extractive distillation column, the solvent monoethyleneglycol is cooled (E313).

3.3.1.5 Cogeneration system

In the present study, three fuel sources are considered: bagasse, lignin and straw. Energy cogeneration system can operate with or without condensation turbine, depending on the purpose of the plant. The simulations of this study allow choosing not to use the condensation turbine when the objective is producing ethanol, and using the condensation turbine when the objective is to increase the surplus of electricity. When the proposal is to guarantee the energy demand of the process and to produce 2G ethanol, the first option is chosen. The second option is used when all the bagasse is diverted to the cogeneration system, aiming to sell surplus of electricity.

In cogeneration system, steam is produced at 17.4 bar, 6.0 bar and 2.5 bar. Steam at 17.4 bar (outlet of E405) is used in the pretreatment stage (E503). Steam at 6 bar (outlet of E411) is used in the dehydration columns (reboilers indicated by E311 and E312) and for heating soaking water (E506), while steam at 2.5 bar (outlet of E418) is used in the pre-evaporator (E202), distillation columns (reboilers indicated by E306 and E307) and for heating the solids stream from the pretreatment (E602). Note that there is already energy integration between pretreated bagasse and soaking water, but soaking water has a an energy demand higher than the energy available in pretreated bagasse and, for this reason, it is necessary surplus steam at 6.0 bar to meet the energy demand of soaking water. In addition, in the biorefinery that does not produce 2G ethanol (process represented by Period 1), steam at 17.4 bar is not generated, since the bagasse pretreatment step is not required.

3.3.1.6 Bagasse pretreatment

Sugarcane bagasse is mainly composed of cellulose, hemicellulose and lignin. To use it in 2G ethanol production, the cellulose, hemicellulose and lignin complex must be broken down. For this reason, pretreatment is an important step, since it makes cellulose more accessible to enzymes that convert carbohydrate polymers to fermentable sugars (MOSIER et al., 2005).

In this work, the hydrothermal pretreatment was chosen because it presents promising results in laboratory scale and, at the same time, does not use any raw material besides water (COSTA et al., 2014). In addition, the hydrothermal pretreatment, if performed in continuous operation as it is assumed in this study, allows the reuse of the thermal energy contained in the pretreated bagasse for heating soaking water, reducing the consumption of high pressure steam (FURLAN et al., 2012, 2013).

In the hydrothermal pretreatment, bagasse is pressurized (E501) and then mixed to soaking water (E502), which is preheated (E506). The mixture is heated (E503) to the pretreatment temperature and sent to the pretreatment reactor (E504). After pretreatment, the mixture is cooled (E506) and carried to the flash tank (E507), where pressure drops to 1 atm. The mixture is neutralized using ammonia (E508) and sent to a filter (E510). The resulting liquid fraction, rich in hydrolysis products from hemicellulose (xylose) is discarded, but its pentose sugars could be fermented or biodigested. The solid fraction is sent to the cellulose hydrolysis step.

3.3.1.7 Cellulose hydrolysis

Hydrolysis of lignocellulosic materials is the conversion of cellulose and hemicellulose into fermentable sugars. This operation can be performed by hydrolysis with dilute acid, hydrolysis with concentrated acid or enzymatic hydrolysis. If the hydrolysis is enzymatic, a pretreatment, as mentioned above, is required. Enzymatic hydrolysis using cellulases does not generate inhibitors to subsequent fermentation step. In addition, the enzymes are specific for cellulose. For these reasons, enzymatic hydrolysis was chosen for biorefinery. Lignin is not converted into ethanol, but it is used in the cogeneration system.

In this step, in a mixing tank (E601), water is added to the solid fraction coming from the filter (E510), the mixture is heated (E602) and enzymes are added (E603). The mixture is sent to the hydrolysis reactor (E604) to convert cellulose into glucose. Finally, the resulting mixture is filtered (E606). The liquid fraction is sent to the concentration step, along with the sugarcane juice, while the solid fraction, consisting mainly of lignin, is sent to the boiler (E403).

3.3.2 Energy integration case study

Period 1 represents the simulation of 1G ethanol and electricity production process and Periods 2 and 3 represent the simulation of 1G/2G ethanol and electricity production process with different fractions of bagasse. In Period 3, 66% of all bagasse is destined for the 2G ethanol production. This value is the maximum fraction of bagasse that could be destined for the 2G ethanol production without compromising the energy self-sufficiency of the process. In Period 2, 33% of all bagasse is destined for the 2G ethanol production. The remainder is used for safety reserve, steam generation and electricity production. Therefore, the number of streams involved in energy integration differs among periods and, consequently, also does the number of variables. In this study, 3 stages were used in the superstructure. Thus, Period 1 has 672 variables and Periods 2 and 3 have 1080 variables.

Table 3.6 shows streams data for the three periods. The heat transfer convective coefficient was considered the same for all streams and estimated from the overall heat transfer coefficient given by Ensinas (2008). EMAT is 1 K.

Table 3.6. Input data for energy integration.

	Stream	**Corresponding HE in Fig. 3.3**	**T^0 (K)**	**T^{final} (K)**	**CP (kW/K)**	**h (kW/m^2 K)**
	Period 1					
H1	Concentrated juice	E204	388	306	638	1.38
H2	Vapor from Column D top (Condenser D)	E304	358	357	11,661	1.38
H3	Vapor from Column B top (Condenser B)	E305/E301	355	354	60,307	1.38
H4	Vapor from extractive column top (Condenser DEH1)	E309	351	350	24,592	1.38
H5	Vapor from recovery column top (Condenser DEH2)	E310	333	332	2,074	1.38
H6	Vinasse	E302	385	363	747	1.38
H7	Monoethylene glycol	E313	421	353	33	1.38
H8	Anhydrous ethanol	E315	351	308	43	1.38
C1	Juice	E114	321	343	1,256	1.38
C2	Juice	E117	343	378	1,288	1.38
C3	Wine	E301/E302	303	362	867	1.38
C4	Liquid from Column A bottom (Reboiler A)	E306	384	385	67,968	1.38
C5	Liquid from Column B1 bottom (Reboiler B)	E307	381	382	22,466	1.38
C6	Liquid from extractive column bottom (Reboiler DEH1)	E311	379	407	352	1.38
C7	Liquid from recovery column bottom (Reboiler DEH2)	E312	411	421	335	1.38
	Period 2					
H1	Concentrated juice	E204	388	306	713	1.38
H2	Vapor from Column D top (Condenser D)	E304	358	357	13,086	1.38
H3	Vapor from Column B top (Condenser B)	E305/E301	355	354	66,136	1.38
H4	Vapor from extractive column top (Condenser DEH1)	E309	351	350	26,942	1.38
H5	Vapor from recovery column top (Condenser DEH2)	E310	333	332	2,272	1.38

H6	Vinasse	E302	385	363	862	1.38
H7	Monoethylene glycol	E313	421	353	37	1.38
H8	Anhydrous ethanol	E315	351	308	47	1.38
H9	Pretreated bagasse	E506	468	353	525	1.38
C1	Juice	E114	321	343	1,256	1.38
C2	Juice	E117	343	378	1,288	1.38
C3	Wine	E301/E302	303	362	995	1.38
C4	Liquid from Column A bottom (Reboiler A)	E306	384	385	76,914	1.38
C5	Liquid from Column B1 bottom (Reboiler B)	E307	381	382	23,510	1.38
C6	Liquid from extractive column bottom (Reboiler DEH1)	E311	379	407	386	1.38
C7	Liquid from recovery column bottom (Reboiler DEH2)	E312	411	421	367	1.38
C8	Bagasse + soaking water	E503	439	468	523	1.38
C9	Soaking water	E506	303	458	418	1.38
C10	Solid fraction (cellulose + lignin)	E602	315	323	206	1.38
	Period 3					
H1	Concentrated juice	E204	388	306	788	1.38
H2	Vapor from Column D top (Condenser D)	E304	358	357	14,532	1.38
H3	Vapor from Column B top (Condenser B)	E305/E301	355	354	71,935	1.38
H4	Vapor from extractive column top (Condenser DEH1)	E309	351	350	29,277	1.38
H5	Vapor from recovery column top (Condenser DEH2)	E310	333	332	2,469	1.38
H6	Vinasse	E302	385	363	981	1.38
H7	Monoethylene glycol	E313	421	353	40	1.38
H8	Anhydrous ethanol	E315	351	308	51	1.38
H9	Pretreated bagasse	E506	468	353	1,047	1.38
C1	Juice	E114	321	343	1,256	1.38
C2	Juice	E117	343	378	1,288	1.38
C3	Wine	E301/E302	303	362	1,129	1.38
C4	Liquid from Column A bottom (Reboiler A)	E306	384	385	86,036	1.38
C5	Liquid from Column B1 bottom (Reboiler B)	E307	381	382	24,443	1.38
C6	Liquid from extractive column bottom (Reboiler DEH1)	E311	379	407	419	1.38
C7	Liquid from recovery column bottom (Reboiler DEH2)	E312	411	421	398	1.38
C8	Bagasse + soaking water	E503	439	468	1,042	1.38
C9	Soaking water	E506	303	458	834	1.38
C10	Solid fraction (cellulose + lignin)	E602	315	323	410	1.38

In this study, one hot utility and one cold utility were considered. Saturated steam at 17.4 bar is the hot utility, since it meets the temperature constraints for all cold stream. For cold utility, cooling water at 298 K was selected (*i.e.,* water is cooled from 305 K to 298 K in the cooling tower).

Although cost of generating steam from the boiler (C_G) includes several components, the fuel cost is usually the most important (US, 2003). Equations for estimating the cost of utility are presented as follows. Eq. (3.58) calculates fuel cost (C_F), where a_F is fuel cost per unit of energy, η is boiler efficiency in relation to *LHV* (Lower Heating Value), H_S is enthalpy of steam at 65 bar and 758 K (*i.e.*, condition of steam generated in the boiler) and h_W is enthalpy of boiler feed water at 298 K.

$$C_F = \frac{a_F \, . \, (H_S - h_W)}{\eta} \tag{3.58}$$

Eq. (3.59) calculates fuel cost per unity of energy (a_F), where C_b is bagasse cost and *LHV* is Lower Heating Value. In order to simplify the calculations, two assumptions were performed: only bagasse is considered in fuel cost per unit of energy and cost of steam from the backpressure turbine is considered equal to cost of generating steam from the boiler. Eq. (3.60) is used to calculate the cost of generating steam from the boiler (C_G), where C_F is fuel cost.

$$a_F = \frac{C_b}{LHV} \tag{3.59}$$

$$C_G = 1.3 \, . \, C_F \tag{3.60}$$

Cost of cooling water was estimated based on Ensinas (2008), who evaluated this cost in 0.02 USD/m^3. All prices were calculated in Brazilian reais (BRL, Brazil's currency). For the conversion of such costs to US dollars, the exchange rate value of 3.4885 BRL/USD (average exchange rate from January to December 2016) was adopted. The values were also updated to December 2016 based on the IGPM index (Market Prices General Index), which is a Brazilian index calculated that reflects price fluctuations (FGV, 2017).

Eqs. (3.61) and (3.62) are used to annualize and convert the cost of utilities from mass and volume unit (C_G and C_W) to energy unit (*chu* and *ccu*). The terms h_{COND} and τ in Eq. (3.61) refer to condensation enthalpy of saturated steam at 17.4 bar and operation time, respectively. Inlet and outlet temperature of steam was considered 479 K and 478 K, respectively. In Eq. (3.62), C_W is cost of cooling water, $\hat{v}$ is specific volume, τ is operation time, h_{OUT} and h_{IN} are enthalpy of water at 305 K and 298 K, respectively. Table 3.7 shows the parameters used in estimating the costs of steam and cooling water and Table 3.8 presents the costs of steam (*chu*) and cooling water (*ccu*) per energy unit.

$$chu = \frac{C_G}{h_{COND}} \,.\, \tau \quad (3.61)$$

$$ccu = \frac{C_W}{(h_{OUT} - h_{IN})} \,.\, \hat{v} \,.\, \tau \quad (3.62)$$

$$HE\ cost = a + b \,.\, A^c \quad (3.63)$$

Table 3.7. Parameters for HEN operating calculations.

Parameter	Value	Unit
C_G [1]	15.0	USD/ton
LHV	7,121.3	kJ/kg
η	88	%
τ	5760	h/year

[1] Information about cost of bagasse from Brazilian mills. The value described is the average between 2015 and 2016.

Table 3.8. Costs of utilities and parameters for calculation of annualized cost of heat exchanger.

Cost	Value	Unit
chu	96	USD/kW year
ccu	50	USD/kW year
a	4,897	USD/year
b	33	USD/m$^{1.56}$ year
c	0.78	[-]

Eq. (3.63) indicates the annualized cost of heat exchangers. Coefficients *a*, *b* were estimated from cost and area data of heat exchangers used in biorefineries, which were described by Bohórquez (2014). Coefficient *c* for plate heat exchanger was obtained by Hall, Ahmad and Smith (1990). In order to obtain the annualized HEN cost, 10% of annual capital interest and 15 years of plant life were adopted. The coefficients for annual costs of investment on heat exchanger network are shown in Table 3.8.

3.4 Results and discussion

In this section main results and discussions of energy integration in an industrial case study of the biorefinery presented in the previous section are described. The TAC of processes with project energy integration for Periods 1, 2 and 3 is 23.0, 26.8 and 30.5 million USD/year, respectively. A HEN was synthesized for each period. For Period 1, at each execution, the average processing time using parameters of Tables 3.1, 3.2 and 3.3 was 5, 65 and 14 minutes, respectively (2.50 GHz Intel® Core™ i5-3210 processor with 6.00 GB of RAM). For Periods 2 and 3, at each execution, the average processing time using the same parameters was 12, 108 and 20 minutes (2.50 GHz Intel® Core™ i5-3210 processor with 6.00 GB of RAM). Note that these times refer to one execution of problem, but the procedure was executed until the stop criterion is met (*i.e.*, according to the methodology previously presented in Section 3.2.5). Single-period solutions for Periods 2 and 3 presented a value of TAC greater (19% and 26% respectively) than the TAC for the process with project energy integration, as commonly found in Brazilian industrial plants. For this reason, the solutions combination procedure (please, see Section 3.2.6) was used. After applying that procedure, the TAC for Periods 1, 2 and 3 was 19.6, 25.5 and 27.8 million USD/year, respectively. Figs. 3.4, 3.5, and 3.6 present the HENs for each period, where the values next to and below the heat exchangers are temperature, in Kelvin, and heat load, in kW, respectively. Tables 3.9, 3.10 and 3.11 show the configurations of these networks. More information on heat exchanger area, number of heat transfer units and costs is presented in Table 3.12.

In order to integrate the heat exchanger networks of all periods, the timesharing strategy was used. For the integrated HEN, the capital cost estimated is 236,570 USD/year with total area of 20,906.5 m^2 and 21 heat exchangers. It represents an area overdesign of 33% for Period 1, 15% for Period 2 and 3% for Period 3. Supposing that each period operates 1/3 of the total operation time, the operating cost and the TAC of the multiperiod HEN are 24,106,206 USD/year and 24,342,777 USD/year, respectively. Tables 3.9, 3.10 and 3.11 show the assigned area by the procedure for periods integration (A_s) and the ratio between required area and assigned area ($A_{i,j,k}/A_s$). Table 3.13 presents the integrated HEN with assigned areas for each of heat transfer device and matches in each period.

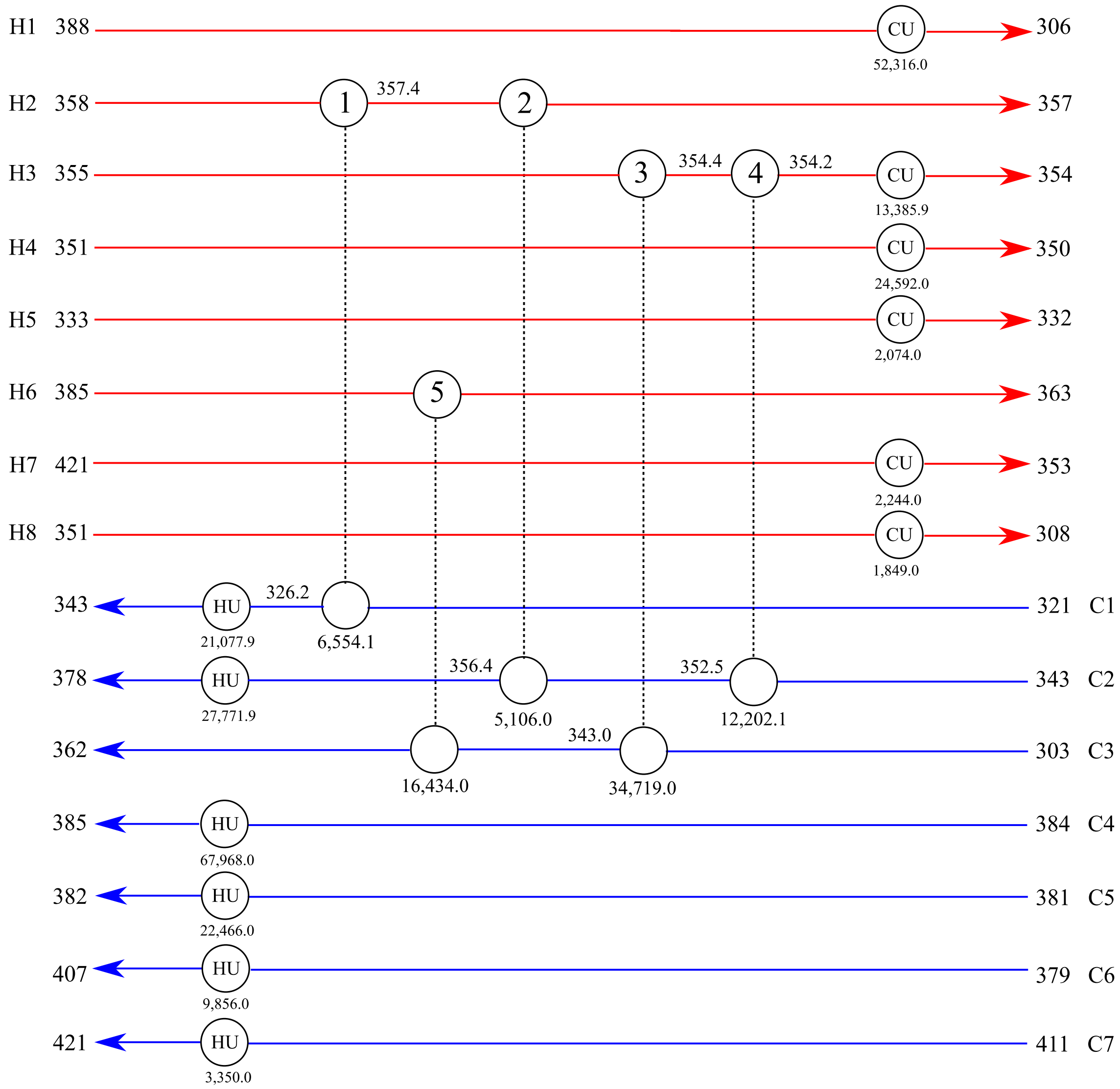

Figure 3.4. Diagram of HEN for Period 1 using PSO.

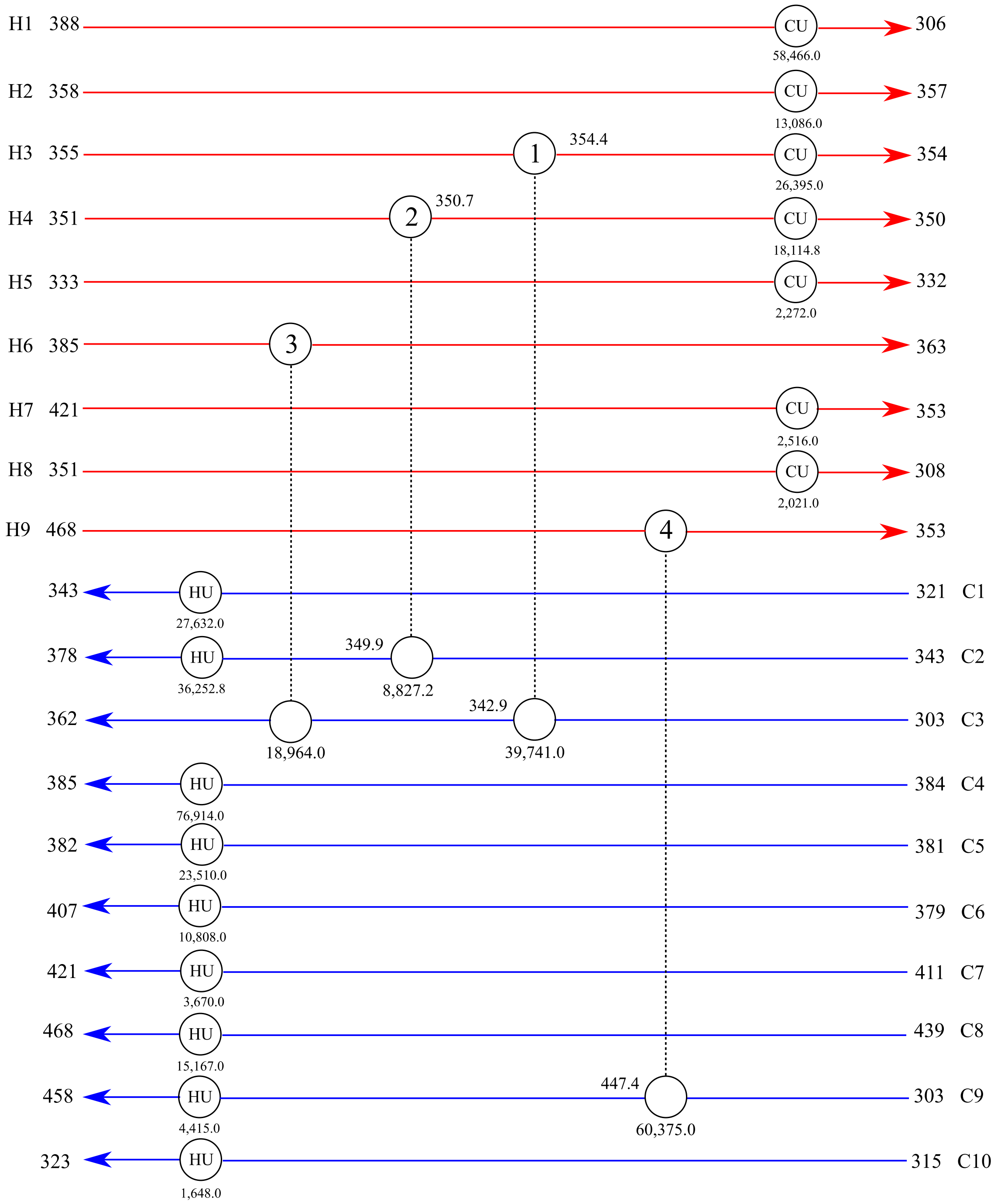

Figure 3.5. Diagram of HEN for Period 2 using PSO.

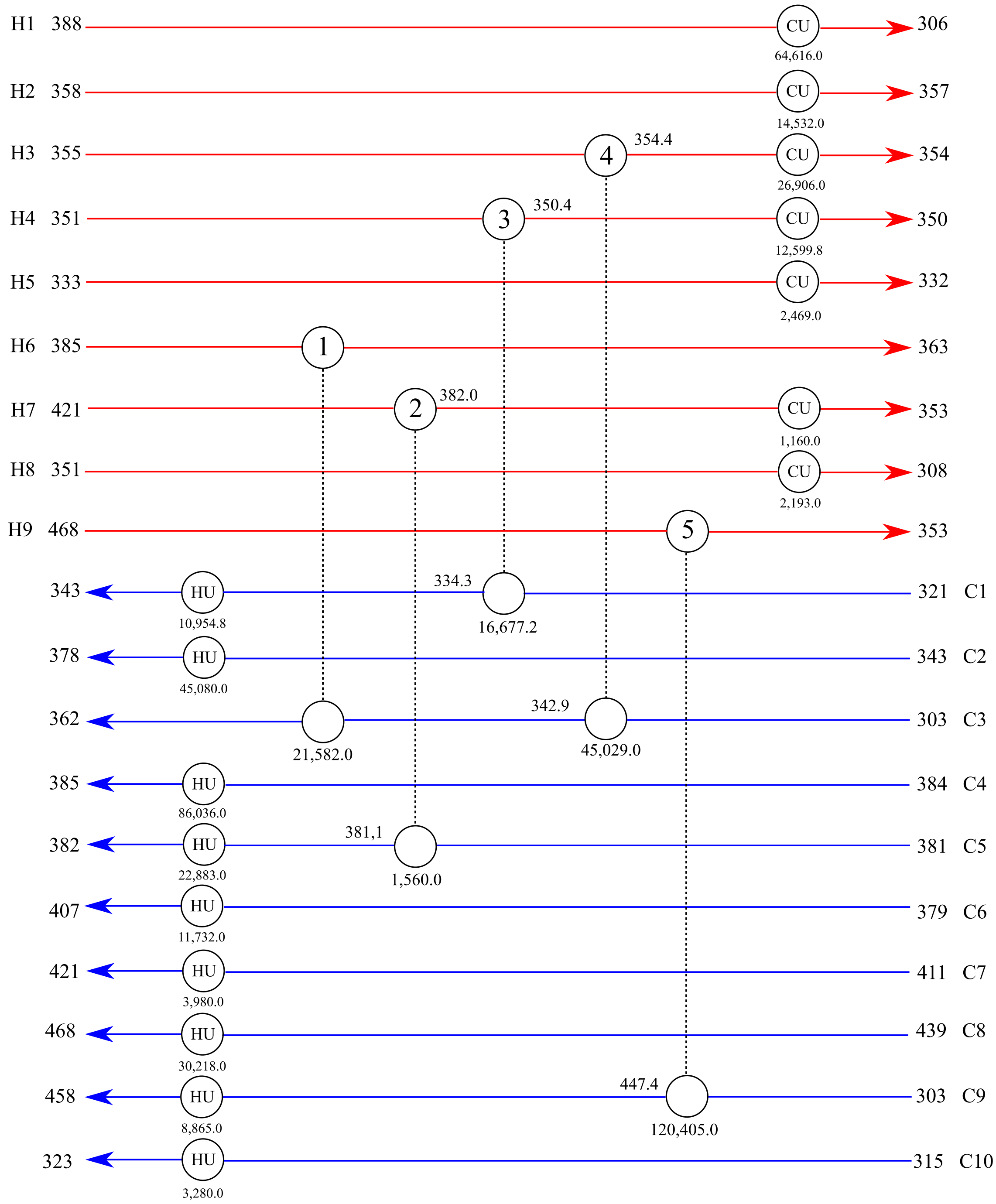

Figure 3.6. Diagram of HEN for Period 3 using PSO.

Table 3.9. Data for HEN in Periods 1, 2 and 3 using PSO (Part 1).

Match	$(\boldsymbol{i}, \boldsymbol{j}, \boldsymbol{k})$	**(2,1,1)**	**(2,2,2)**	**(3,2,3)**	**(3,3,2)**	**(4,1,2)**	**(4,2,3)**	**(6,3,1)**	**(7,5,3)**	**(9,9,1)**
Period 1										
A_s	m^2	376.4	3,168.5	5,259.9	2,122.6	-	-	1,453.1	-	
$A_{i,j,k}$	m^2	278.9	3,168.5	3,337.4	1,860.0	-	-	1,110.8	-	
$A_{i,j,k}/A_s$	%	74.1	100.0	63.5	87.6	-	-	76.4	-	
$Q_{i,j,k}$	kW	6,554.1	5,106.0	12,202.1	34,719.0	-	-	16,434.0	-	
$Fh_{i,j,k}$		1.0	1.0	1.0	1.0	-	-	1.0	-	
$Fc_{i,j,k}$		1.0	1.0	1.0	1.0	-	-	1.0	-	
$Thmix_{i,k}$	K	358.0	357.4	355.4	355.0	-	-	385.0	-	
$Thmix_{i,k+1}$	K	357.4	357.0	354.2	354.4	-	-	363.0	-	
$Thout_{i,j,k}$	K	357.4	357.0	354.2	354.4	-	-	363.0	-	
$Tcmix_{j,k+1}$	K	321.0	352.5	343.0	303.0	-	-	343.0	-	
$Tcmix_{j,k}$	K	326.2	356.4	352.5	343.0	-	-	362.0	-	
$Tcout_{i,j,k}$	K	326.2	356.4	352.5	343.0	-	-	362.0	-	
Period 2										
A_s	m^2	-	-	-	2,122.6	-	5,259.9	1,453.1	-	2,641.2
$A_{i,j,k}$	m^2	-	-	-	2,122.6	-	3,726.4	1,278.6	-	2,641.2
$A_{i,j,k}/A_s$	%	-	-	-	100.0	-	70.8	88.0	-	100.0
$Q_{i,j,k}$	kW	-	-	-	39,741.0	-	8,827.2	18,964.0	-	60,375.0
$Fh_{i,j,k}$		-	-	-	1.0	-	1.0	1.0	-	1.0
$Fc_{i,j,k}$		-	-	-	1.0	-	1.0	1.0	-	1.0
$Thmix_{i,k}$	K	-	-	-	355.0	-	351.0	385.0	-	468.0
$Thmix_{i,k+1}$	K	-	-	-	354.4	-	350.7	363.0	-	353.0
$Thout_{i,j,k}$	K	-	-	-	354.4	-	350.7	363.0	-	353.0
$Tcmix_{j,k+1}$	K	-	-	-	303.0	-	343.0	342.9	-	303.0
$Tcmix_{j,k}$	K	-	-	-	342.9	-	349.9	362.0	-	447.4
$Tcout_{i,j,k}$	K	-	-	-	342.9	-	349.9	362.0	-	447.4
Period 3										
A_s	m^2	-	-	-	2,641.2	1,075.1	-	1,453.1	251.1	5,259.9
$A_{i,j,k}$	m^2	-	-	-	2,401.4	1,075.1	-	1,453.1	214.1	5,259.9
$A_{i,j,k}/A_s$	%	-	-	-	90.9	100.0	-	100.0	85.3	100.0
$Q_{i,j,k}$	kW	-	-	-	45,029.0	16,677.2	-	21,582.0	1,560.0	120,405.0
$Fh_{i,j,k}$		-	-	-	1.0	1.0	-	1.0	1.0	1.0
$Fc_{i,j,k}$		-	-	-	1.0	1.0	-	1.0	1.0	1.0
$Thmix_{i,k}$	K	-	-	-	355.0	351.0	-	385.0	421.0	468.0
$Thmix_{i,k+1}$	K	-	-	-	354.4	350.4	-	363.0	382.0	353.0
$Thout_{i,j,k}$	K	-	-	-	354.4	350.4	-	363.0	382.0	353.0
$Tcmix_{j,k+1}$	K	-	-	-	303.0	321.0	-	342.9	381.0	303.0
$Tcmix_{j,k}$	K	-	-	-	342.9	334.3	-	362.0	381.1	447.4
$Tcout_{i,j,k}$	K	-	-	-	342.9	334.3	-	362.0	381.1	447.4

Table 3.10. Data for HEN in Periods 1, 2 and 3 using PSO (Part 2).

Match	(i,j,k)	(1,CU,4)	(2,CU,4)	(3,CU,4)	(4,CU,4)	(5,CU,4)	(6,CU,4)	(7,CU,4)	(8,CU,4)	(9,CU,4)
Period 1										
A_s	m^2	2,641.2	-	741.1	1,075.1	200.5		134.7	251.1	-
$A_{i,j,k}$	m^2	2,365.0	-	369.3	728.3	97.3	-	39.8	113.6	-
$A_{i,j,k}/A_s$	%	89.5	-	49.8	67.7	48.5	-	29.5	45.2	-
$Q_{i,j,k}$	kW	52,316.0	-	13,385.9	24,592.0	2,074.0	-	2,244.0	1,849.0	-
$Fh_{i,j,k}$		1.0	-	1.0	1.0	1.0	-	1.0	1.0	-
$Fc_{i,j,k}$		1.0	-	1.0	1.0	1.0	-	1.0	1.0	-
$Thmix_{i,k}$	K	388.0	-	354.2	351.0	333.0	-	421.0	351.0	-
$Thmix_{i,k+1}$	K	306.0	-	354.0	350.0	332.0	-	353.0	308.0	-
$Thout_{i,j,k}$	K	306.0	-	354.0	350.0	332.0	-	353.0	308.0	-
$Tcmix_{j,k+1}$	K	298.0	-	298.0	298.0	298.0	-	298.0	298.0	-
$Tcmix_{j,k}$	K	305.0	-	305.0	305.0	305.0	-	305.0	305.0	-
$Tcout_{i,j,k}$	K	305.0	-	305.0	305.0	305.0	-	305.0	305.0	-
Period 2										
A_s	m^2	3,168.5	375.4	741.1	557.6	115.8		92.4	134.7	
$A_{i,j,k}$	m^2	2,643.0	339.0	726.8	538.3	106.6	-	44.6	124.2	-
$A_{i,j,k}/A_s$	%	83.4	90.3	98.1	96.5	92.0	-	48.3	92.2	-
$Q_{i,j,k}$	kW	58,466.0	13,086.0	26,395.0	18,114.8	2,272.0	-	2,516.0	2,021.0	-
$Fh_{i,j,k}$		1.0	1.0	1.0	1.0	1.0	-	1.0	1.0	-
$Fc_{i,j,k}$		1.0	1.0	1.0	1.0	1.0	-	1.0	1.0	-
$Thmix_{i,k}$	K	388.0	358.0	354.4	350.7	333.0	-	421.0	351.0	-
$Thmix_{i,k+1}$	K	306.0	357.0	354.0	350.0	332.0	-	353.0	308.0	-
$Thout_{i,j,k}$	K	306.0	357.0	354.0	350.0	332.0	-	353.0	308.0	-
$Tcmix_{j,k+1}$	K	298.0	298.0	298.0	298.0	298.0	-	298.0	298.0	-
$Tcmix_{j,k}$	K	305.0	305.0	305.0	305.0	305.0	-	305.0	305.0	-
$Tcout_{i,j,k}$	K	305.0	305.0	305.0	305.0	305.0	-	305.0	305.0	-
Period 3										
A_s	m^2	3,168.5	376.4	741.1	375.4	115.8		25.7	134.7	
$A_{i,j,k}$	m^2	2,921.0	376.4	741.1	375.4	115.8	-	25.7	134.7	-
$A_{i,j,k}/A_s$	%	92.2	100.0	100.0	100.0	100.0	-	100.0	100.0	-
$Q_{i,j,k}$	kW	64,616.0	14,532.0	26,906.0	12,599.8	2,469.0	-	1,160.0	2,193.0	-
$Fh_{i,j,k}$		1.0	1.0	1.0	1.0	1.0	-	1.0	1.0	-
$Fc_{i,j,k}$		1.0	1.0	1.0	1.0	1.0	-	1.0	1.0	-
$Thmix_{i,k}$	K	388.0	358.0	354.4	350.4	333.0	-	382.0	351.0	-
$Thmix_{i,k+1}$	K	306.0	357.0	354.0	350.0	332.0	-	353.0	308.0	-
$Thout_{i,j,k}$	K	306.0	357.0	354.0	350.0	332.0	-	353.0	308.0	-
$Tcmix_{j,k+1}$	K	298.0	298.0	298.0	298.0	298.0	-	298.0	298.0	-
$Tcmix_{j,k}$	K	305.0	305.0	305.0	305.0	305.0	-	305.0	305.0	-
$Tcout_{i,j,k}$	K	305.0	305.0	305.0	305.0	305.0	-	305.0	305.0	-

Table 3.11. Data for HEN in Periods 1, 2 and 3 using PSO (Part 3).

Match	(i, j, k)	**(HU,1,0)**	**(HU,2,0)**	**(HU,3,0)**	**(HU,4,0)**	**(HU,5,0)**	**(HU,6,0)**	**(HU,7,0)**	**(HU,8,0)**	**(HU,9,0)**	**(HU,10,0)**
Period 1											
A_s	m^2	375.4	557.6		1,326.5	503.6	342.0	115.8	-	-	-
$A_{i,j,k}$	m^2	212.5	362.7	-	1,047.9	335.7	168.5	77.8	-	-	-
$A_{i,j,k}/A_s$	%	56.6	65.1	-	79.0	66.7	49.3	67.2	-		
$Q_{i,j,k}$	kW	21,077.9	27,771.9	-	67,968.0	22,466.0	9,856.0	3,350.0	-	-	-
$Fh_{i,j,k}$		1.0	1.0	-	1.0	1.0	1.0	1.0	-	-	-
$Fc_{i,j,k}$		1.0	1.0	-	1.0	1.0	1.0	1.0	-	-	-
$Thmix_{i,k}$	K	479.0	479.0	-	479.0	479.0	479.0	479.0	-	-	-
$Thmix_{i,k+1}$	K	478.0	478.0	-	478.0	478.0	478.0	478.0	-	-	-
$Thout_{i,j,k}$	K	478.0	478.0	-	478.0	478.0	478.0	478.0	-	-	-
$Tcmix_{j,k+1}$	K	326.2	356.4	-	384.0	381.0	379.0	411.0	-	-	-
$Tcmix_{j,k}$	K	343.0	378.0	-	385.0	382.0	407.0	421.0	-	-	-
$Tcout_{i,j,k}$	K	343.0	378.0	-	385.0	382.0	407.0	421.0	-	-	-
Period 2											
A_s	m^2	342.0	503.6		1,326.5	376.4	200.5	113.5	1,075.1	251.1	29.8
$A_{i,j,k}$	m^2	273.8	460.7	-	1,185.9	351.3	184.7	85.2	993.6	251.1	15.0
$A_{i,j,k}/A_s$	%	80.1	91.5	-	89.4	93.3	92.1	75.1	92.4	100.0	50.3
$Q_{i,j,k}$	kW	27,632.0	36,252.8	-	76,914.0	23,510.0	10,808.0	3,670.0	15,167.0	4,415.0	1,648.0
$Fh_{i,j,k}$		1.0	1.0	-	1.0	1.0	1.0	1.0	1.0	1.0	1.0
$Fc_{i,j,k}$		1.0	1.0	-	1.0	1.0	1.0	1.0	1.0	1.0	1.0
$Thmix_{i,k}$	K	479.0	479.0	-	479.0	479.0	479.0	479.0	479.0	479.0	479.0
$Thmix_{i,k+1}$	K	478.0	478.0	-	478.0	478.0	478.0	478.0	478.0	478.0	478.0
$Thout_{i,j,k}$	K	478.0	478.0	-	478.0	478.0	478.0	478.0	478.0	478.0	478.0
$Tcmix_{j,k+1}$	K	321.0	349.9	-	384.0	381.0	379.0	411.0	439.0	447.4	315.0
$Tcmix_{j,k}$	K	343.0	378.0	-	385.0	382.0	407.0	421.0	468.0	458.0	323.0
$Tcout_{i,j,k}$	K	343.0	378.0	-	385.0	382.0	407.0	421.0	468.0	458.0	323.0
Period 3											
A_s	m^2	113.5	557.6		1,326.5	342.0	200.5	92.4	2,122.6	503.6	29.8
$A_{i,j,k}$	m^2	113.5	557.6	-	1,326.5	342.0	200.5	92.4	1,979.6	503.6	29.8
$A_{i,j,k}/A_s$	%	100.0	100.0	-	100.0	100.0	100.0	100.0	93.3	100.0	100.0
$Q_{i,j,k}$	kW	10,954.8	45,080.0	-	86,036.0	22,883.0	11,732.0	3,980.0	30,218.0	8,865.0	3,280.0
$Fh_{i,j,k}$		1.0	1.0	-	1.0	1.0	1.0	1.0	1.0	1.0	1.0
$Fc_{i,j,k}$		1.0	1.0	-	1.0	1.0	1.0	1.0	1.0	1.0	1.0
$Thmix_{i,k}$	K	479.0	479.0	-	479.0	479.0	479.0	479.0	479.0	479.0	479.0
$Thmix_{i,k+1}$	K	478.0	478.0	-	478.0	478.0	478.0	478.0	478.0	478.0	478.0
$Thout_{i,j,k}$	K	478.0	478.0	-	478.0	478.0	478.0	478.0	478.0	478.0	478.0
$Tcmix_{j,k+1}$	K	334.3	343.0	-	384.0	381.1	379.0	411.0	439.0	447.4	315.0
$Tcmix_{j,k}$	K	343.0	378.0	-	385.0	382.0	407.0	421.0	468.0	458.0	323.0
$Tcout_{i,j,k}$	K	343.0	378.0	-	385.0	382.0	407.0	421.0	468.0	458.0	323.0

Table 3.12. Number of HE, HEN area, capital cost (CC), operating cost (OC), and total annualized cost (TAC) for each period of operation of HEN using PSO.

	No. of heat transfer units	Total area (m^2)	CC (USD/year)	OC (USD/year)	TAC (USD/year)
Period 1	17	15,673.9	186,540	19,427,278	19,613,818
Period 2	20	18,092.4	217,915	25,300,954	25,518,869
Period 3	21	20,239.3	233,407	27,590,386	27,823,794

Table 3.13. Data for the integrated HEN using PSO.

Exchanger label	Assigned area (m^2)	Period	Match (i, j, k)	Exchanger label	Assigned area (m^2)	Period	Match (i, j, k)
		1	3,2,3			1	HU,1,0
A	5,259.90	2	4,2,3	L	375.4	2	2,CU,4
		3	9,9,1			3	4,CU,4
		1	2,2,2			1	HU,6,0
B	3,168.50	2	1,CU,4	M	342	2	HU,1,0
		3	1,CU,4			3	HU,5,0
		1	1,CU,4			1	8,CU,4
C	2,641.20	2	9,9,1	N	251.1	2	HU,9,0
		3	3,3,2			3	7,5,3
		1	3,3,2			1	5,CU,4
D	2,122.60	2	3,3,2	O	200.5	2	HU,6,0
		3	HU,8,0			3	HU,6,0
		1	6,3,1			1	7,CU,4
E	1,453.10	2	6,3,1	P	134.7	2	8,CU,4
		3	6,3,1			3	8,CU,4
		1	HU,4,0			1	HU,7,0
F	1,326.50	2	HU,4,0	Q	115.8	2	5,CU,4
		3	HU,4,0			3	5,CU,4
		1	4,CU,0			1	-
G	1,075.10	2	HU,8,0	R	113.5	2	HU,7,0
		3	4,1,2			3	HU,1,0
		1	3,CU,4			1	-
H	741.1	2	3,CU,4	S	92.4	2	7,CU,4
		3	3,CU,4			3	HU,7,0
		1	HU,2,0			1	-
I	557.6	2	4,CU,4	T	29.8	2	HU,10,0
		3	HU,2,0			3	HU,10,0
		1	HU,5,0			1	-
J	503.6	2	HU,2,0	U	25.7	2	-
		3	HU,9,0			3	7,CU,4

		1	2,1,1
K	376.4	2	HU,5,0
		3	2,CU,4

Tables 3.14, 3.15 and 3.16 compare the utility demand, area and costs between processes without any energy integration, with project energy integration, with energy integration proposed in this study for each period and with the integrated HEN (that is, HEN that integrates all periods and assumes the utility demand of proposed HEN for each period). The operating cost has an order of magnitude of 10^2 greater than the investment cost. Thus, the TAC is more influenced by the operating cost. This information is important when comparing the TAC of processes with energy integration proposed in this study for each period with the integrated HEN. For Periods 1, 2 and 3, the TAC for the process with the integrated HEN is 0.26%, 0.07% and 0.01% higher than the TAC for the process with energy integration proposed for each period, respectively. Since the variations in TAC are small among these two processes (*i.e.*, with energy integration proposed for each period and with integrated HEN), a small additional investment allows the process to be more flexible. Note that the HENs synthesized have few heat exchanger units (that is, a large amount of energy of cold streams is supplied by hot utility and of hot streams is withdrawn by cold utility). This inference also contributes to utility cost being more representative than capital cost.

Table 3.14. Comparison among the processes without energy integration (S1), with project energy integration (S2), with energy integration proposed in this work (S3) and with the integrated HEN (S4) using PSO for Period 1.

Parameter	Period 1			
	S1	**S2**	**S3**	**S4**
CU (kW)	171,477	120,324	96,462	96,462
HU (kW)	227,505	176,352	152,490	152,490
Area (m^2)	8,602.4	9,782.4	15,673.9	20,906.5
Cost of utility(USD/year)	30,351,067	22,902,099	19,427,278	19,427,278
Cost of HEN (USD/year)	137,644	144,668	186,540	236,570
TAC (USD/year)	30,488,710	23,046,767	19,613,818	19,663,848

Table 3.15. Comparison among the processes without energy integration (S1), with project energy integration (S2), with energy integration proposed in this work (S3) and with the integrated HEN (S4) using PSO for Period 2.

Parameter	Period 2			
	S1	S2	S3	S4
CU (kW)	250,778	131,698	122,871	122,871
HU (kW)	327,924	208,844	200,017	200,017
Area (m^2)	12,656.7	14,722.4	18,092.4	20,906.5
Cost of utility(USD/year)	43,926,941	26,586,353	25,300,954	25,300,954
Cost of HEN (USD/year)	184,932	195,126	217,915	236,570
TAC (USD/year)	44,111,874	26,781,480	25,518,869	25,537,524

Table 3.16. Comparison among the processes without energy integration (S1), with project energy integration (S2), with energy integration proposed in this work (S3) and with the integrated HEN (S4) using PSO for Period 3.

Parameter	Period 3			
	S1	S2	S3	S4
CU (kW)	329,729	142,713	124,476	124,476
HU (kW)	428,282	241,266	223,029	223,029
Area (m^2)	14,623.6	19,647.7	20,239.3	20,906.5
Cost of utility(USD/year)	57,479,601	30,246,083	27,590,386	27,590,386
Cost of HEN (USD/year)	205,998	218,640	233,407	236,570
TAC (USD/year)	57,685,599	30,464,722	27,823,794	27,826,957

Table 3.17 shows saving of utility cost, steam demand and TAC of processes without and with energy integration. Special attention is given to the process with the integrated HEN, because a multiperiod HEN design allows the biorefinery to operate with different bagasse fractions diverted to second generation ethanol production. Process with the integrated HEN presents reduction in TAC of 36%, 42% and 52% when compared to the process without energy integration for Periods 1, 2 and 3,

respectively. Process with the integrated HEN presents reduction in TAC of 15%, 5% and 9% when compared to the process with project energy integration for Periods 1, 2 and 3, respectively. As the HEN that integrates all periods has the same utility demand of proposed HEN for each period, the saving in steam will be equal. For these processes, reductions in steam consumption reach 33%, 39% and 48% when compared to the process without energy integration for Periods 1, 2 and 3, respectively, and 14%, 4% and 8% when compared to the process with project energy integration for Periods 1, 2 and 3, respectively. Such values indicate energy integration turn possible that more bagasse (compared to the same process without any energy integration) can be deviated to second generation ethanol production or the cogeneration system. However, only a fraction of the bagasse saved can be deviated to 2G ethanol section, since the surplus 2G ethanol will imply greater steam demand. Note that these improvements will be marginal in processes with the HEN synthesized for each period and with the integrated HEN when compared to the process existing in Brazilian plants (*i.e.*, the process with project integration), since reductions in TAC and steam demand are small and only a fraction of that bagasse saved can be used to produce 2G ethanol. In order to extend the analysis of the magnitude of these improvements, Pinch Analysis was performed to each period with ΔT_{min} = 1 K. For all periods, the energy demand of the integrated HEN is higher than the Pinch Analysis solution (*i.e.*, the hot utility demand of solutions using PSO method is two times greater than hot utility demand using Pinch Analysis and the cold utility demand of solutions using PSO method is six times greater than cold utility demand using Pinch Analysis). Since the operating cost has more influence on the TAC, the solutions obtained by PSO algorithm are poor. Such results are due to the difficulty of the PSO algorithm when dealing, mainly, with integer variables in large-scale problems. Thus, strategies, such as other mathematical algorithms or modifications in the model, should be proposed for solving the multiperiod HEN problem in order to find better solutions.

As previously discussed, bypasses must be installed in heat exchangers with greater assigned area than required area in order to meet the designed stage temperatures and the designed streams target temperatures. Table 3.18 shows bypasses for cold streams in heat exchangers with surplus area.

Table 3.17. Saving of utility cost, hot utility (HU) and total annualized cost (TAC) of processes with energy integration proposed in this study for each period (S3) and with the integrated HEN (S4) using PSO in relation to the processes without energy integration (S1) and with project energy integration (S2).

Saving (%)	Period 1				Period 2				Period 3			
	S3/S1	S3/S2	S4/S1	S4/S2	S3/S1	S3/S2	S4/S1	S4/S2	S3/S1	S3/S2	S4/S1	S4/S2
Cost of utility	35.99	15.17	35.99	15.17	42.40	4.83	42.40	4.83	52.00	8.78	52.00	8.78
HU	32.97	13.53	32.97	13.53	39.01	4.23	39.01	4.23	47.92	7.56	47.92	7.56
TAC	35.67	14.90	35.50	14.68	42.15	4.71	42.11	4.64	51.77	8.67	51.76	8.66

Table 3.18. Bypass for cold streams in heat exchangers.

Bypass (%)	Match					
	(2,1,1)	(3,2,3)	(3,3,2)	(4,2,3)	(6,3,1)	(7,5,3)
Period 1	74.4	20.5	8.3		33.8	
Period 2				9.8	21.1	
Period 3			6.4			99.1

3.5 Conclusion

Energy integration is a process integration technique that enables to reduce energy consumption by means of a heat exchanger network. For sugarcane biorefineries, energy integration allows to increase energy security, decrease environmental resources consumption and, consequently, contributes to making viability of 2G ethanol a reality. However, sugarcane industry can vary the production of ethanol and electricity depending on the demand, which influences the HEN design. To attack this problem, the methodology for the multiperiod HEN synthesis was used. For each period, an MINLP problem was solved and then an automatic integration of HENs obtained in each period was performed. The results demonstrated a reduction in TAC of HEN proposed in this work compared with processes without any energy integration and with project energy integration. In process with the integrated HEN, the saving in TAC can reach 52% when compared to the process without energy integration and 15% when compared to the process with project energy integration. Furthermore, the process with the integrated HEN can save up to 48% and up to 14% of steam in relation to processes without energy integration and with project energy integration, respectively. Note that these results are marginal improvements when compared to the process with project integration (*i.e.*, the process commonly found in Brazilian plants), since only a fraction that bagasse saved can be diverted to 2G ethanol section. Thus, more studies, such as solving the problems with other mathematical strategies, are required in order to obtain better results.

Nomenclature

Variables

A	[m^2]	Heat exchanger area
Acu	[m^2]	Cooler area
Ahu	[m^2]	Heater area
C_{total}	[USD/year]	Annualized total cost
Fc	[-]	Fraction of cold stream
Fh	[-]	Fraction of hot stream
LMTD	[K]	Logarithmic mean temperature difference
Q	[kW]	Heat load in a heat exchanger
Qcu	[kW]	Heat load in a cooler
Qhu	[kW]	Heat load in a heater
Qmax	[kW]	Maximum heat load
TAC	[USD/year]	Total annualized cost
Tchuin	[K]	Inlet temperature of the cold stream in a heater
Thcuin	[K]	Inlet temperature of the hot stream in a cooler
Tcin	[K]	Inlet temperature of the cold stream in a heat exchanger
Thin	[K]	Inlet temperature of the hot stream in a heat exchanger
Tcout	[K]	Outlet temperature of the cold stream in a heat exchanger
Thout	[K]	Outlet temperature of the hot stream in a heat exchanger

Tcmix	[K]	Mixture temperature of the cold stream after mixer
Thmix	[K]	Mixture temperature of the hot stream after mixer
U	[kW/(m^2 K)]	Overall coefficient of heat transfer
z	[-]	Binary variable representing existence of a heat exchanger
zcont	[-]	Continuous variable representing existence of a heat exchanger
zcu	[-]	Binary variable representing existence of a cooler
zhu	[-]	Binary variable representing existence of a heater
$\theta^{(1)}$	[K]	Temperature approximation at the hot end of a heat exchanger
$\theta^{(2)}$	[K]	Temperature approximation at the cold end of a heat exchanger
ΔT	[K]	Temperature Difference

Parameters

a	[USD/year]	Annual fixed cost coefficient for heat exchangers
a_F	[USD/kJ]	Fuel cost per unit of energy
b	[USD/(m^2 year)]	Annual variable cost coefficient for heat exchangers
c	[-]	Area cost exponent
C_B	[USD/tonne]	Cost of bagasse
ccu	[USD/(kW year)]	Cost of cold utility
C_F	[USD/kg]	Fuel cost for steam generation
C_G	[USD/kg]	Total cost for steam generation
chu	[USD/(kW year)]	Cost of hot utility
CPc	[kW/K]	Heat capacity of the cold stream
CPh	[kW/K]	Heat capacity of the hot stream
C_W	[USD/m^3]	Cost of cooling water
EMAT	[K]	Minimum temperature approximation in the heat exchanger
hc	[kW/(m^2 K)]	Heat transfer convective coefficient of the cold stream
hh	[kW/(m^2 K)]	Heat transfer convective coefficient of the hot stream

h_{IN}	[kJ/kg]	Enthalpy of cooling water at inlet cooler
h_{OUT}	[kJ/kg]	Enthalpy of cooling water at outlet cooler
h_{COND}	[kJ/kg]	Enthalpy of condensation
H_S	[kJ/kg]	Enthalpy of steam
h_W	[kJ/kg]	Enthalpy of boiler feedwater
k	[-]	Number of the stage
LHV	[kJ/kg]	Lower heating value
Tc^0	[K]	Initial temperature of the cold stream
Tc^{final}	[K]	Final (target) temperature of the cold stream
Th^0	[K]	Initial temperature of the hot stream
Th^{final}	[K]	Final (target) temperature of the hot stream
$\hat{v}$	[m^3/kg]	Specific volume
η	[%]	Boiler efficiency in relation to LHV
τ	[h/year]	Operation time

Data set

N_C	[-]	Cold streams
N_H	[-]	Hot streams
N_S	[-]	Stages

Subscripts

i	Cold streams
j	Hot streams
k	Stage superstructure

Text

HE	Heat exchanger

HEN	Heat exchanger network
HENs	Heat exchanger networks
LP	Linear Programming
MILP	Mixed Integer Linear Programming
MINLP	Mixed Integer Nonlinear Programming
NL	Nonlinear Programming
PSO	Particle Swarm Optimization

Particle Swarm

c_1	Constant of Particle Swarm algorithm
c_2	Constant of Particle Swarm algorithm
$\boldsymbol{f}_{Bp}$	Position with the best value of the objective function already obtained by the particle p (the best local solution)
$\boldsymbol{g}_{Bp}$	Position with the best value of the objective function already obtained by the swarm (the best global solution)
r_1	Random number with uniform distribution in the interval [0 , 1]
r_2	Random number with uniform distribution in the interval [0 , 1]
$\boldsymbol{v}_p$	Particle velocity
w	Inertia weight
$\boldsymbol{x}_p$	Particle position

References

AALTOLA, J. Simultaneous synthesis of flexible heat exchanger network. Applied Thermal Engineering, v. 22, n. 8, p. 907–918, 2002.

BOHÓRQUEZ, J. F. C. Modelagem dos custos de unidades industriais de processamento de cana-de-açúcar. Campinas, 2014.

BOUSSAÏD, I.; LEPAGNOT, J.; SIARRY, P. A survey on optimization metaheuristics. Information Sciences, v. 237, p. 82–117, 2013.

BRUNET, R.; BOER, D.; GUILLÉN-GOSÁLBEZ, G.; JIMÉNEZ, L. Reducing the cost, environmental impact and energy consumption of biofuel processes through heat integration. Chemical Engineering Research and Design, v. 93, p. 203–212, 2015.

CARDONA, C. A.; QUINTERO, J. A.; PAZ, I. C. Production of bioethanol from sugarcane bagasse: Status and perspectives. Bioresource Technology, v. 101, n. 13, p. 4754–4766, 2010.

CERDA, J.; WESTERBERG, A. W.; MASON, D.; LINNHOFF, B. Minimum utility usage in heat exchanger network synthesis A transportation problem. Chemical Engineering Science, v. 38, n. 3, p. 373–387, 1983.

COSTA, C. B. B.; FURLAN, F. F.; CRUZ, A. J. G.; DE LIMA CAMARGO GIORDANO, R.; DE CAMPOS GIORDANO, R. Integrated Production of 1G–2G Bioethanol and Bioelectricity from Sugarcane: Impact of Bagasse Pretreatment Processes. In: Biofuels in Brazil. Cham: Springer International Publishing, 2014. p. 85–95.

DANTAS, G. A.; LEGEY, L. F. L.; MAZZONE, A. Energy from sugarcane bagasse in Brazil: An assessment of the productivity and cost of different technological routes. Renewable and Sustainable Energy Reviews, v. 21, p. 356–364, 2013.

DIAS, M. O. S.; JUNQUEIRA, T. L.; CAVALETT, O.; CUNHA, M. P.; JESUS, C. D. F.; MANTELATTO, P. E.; ROSSELL, C. E. V.; MACIEL FILHO, R.; BONOMI, A. Cogeneration in integrated first and second generation ethanol from sugarcane. Chemical Engineering Research and Design, v. 91, n. 8, p. 1411–1417, 2013a.

DIAS, M. O. S.; JUNQUEIRA, T. L.; CAVALETT, O.; PAVANELLO, L. G.; CUNHA, M. P.; JESUS, C. D. F.; MACIEL FILHO, R.; BONOMI, A. Biorefineries for the production of first and second generation ethanol and electricity from sugarcane. Applied Energy, v. 109, p. 72–78, 2013b.

ENSINAS, A. V. Energy integration and thermo-economic optimization applied to the industrial process of sugar and ethanol production from sugarcane. 2008. PhD Thesis (Chemical Engineering), State University of Campinas, 2008.

FGV. IGPM index. Disponível em: <http://portalibre.fgv.br/>. Acesso em: 31 jan. 2017.

FLOUDAS, C. A.; CIRIC, A. R.; GROSSMANN, I. E. Automatic synthesis of optimum heat exchanger network configurations. AIChE Journal, v. 32, n. 2, p. 276–290, 1986.

FLOUDAS, C. A.; GROSSMANN, I. E. Synthesis of flexible heat exchanger networks for multiperiod operation. Computers & Chemical Engineering, v. 10, n. 2, p. 153–168, 1986.

FLOUDAS, C. A.; GROSSMANN, I. E. Automatic generation of multiperiod heat exchanger network configurations. Computers & Chemical Engineering, v. 11, n. 2, p. 123–142, 1987.

FLOWER, J. R.; LINNHOFF, B. Thermodynamic analysis in the design of process networks. Computers & Chemical Engineering, v. 3, n. 1–4, p. 283–291, 1979.

FURLAN, F. F.; COSTA, C. B. B.; CRUZ, A. J. G.; SECCHI, A. R.; SOARES, R. P.; GIORDANO,

R. C. Integrated tool for simulation and optimization of a first and second generation ethanol-from-sugarcane production plant. Computer Aided Chemical Engineering, v. 30, p. 81–85, 2012.

FURLAN, F. F.; FILHO, R.; PINTO, F. H.; COSTA, C. B.; CRUZ, A. J.; GIORDANO, R. L.; GIORDANO, R. C. Bioelectricity versus bioethanol from sugarcane bagasse: is it worth being flexible? Biotechnology for Biofuels, v. 6, n. 1, p. 142, 2013.

HALL, S. G.; AHMAD, S.; SMITH, R. Capital cost targets for heat exchanger networks comprising mixed materials of construction, pressure ratings and exchanger types. Computers & Chemical Engineering, v. 14, n. 3, p. 319–335, 1990.

JIANG, D.; CHANG, C.-T. A New Approach to Generate Flexible Multiperiod Heat Exchanger Network Designs with Timesharing Mechanisms. Industrial & Engineering Chemistry Research, v. 52, p. 3794–3804, 2013.

KENNEDY, J.; EBERHART, R. Particle Swarm Optimization. Proceedings of IEEE International Conference on Neural Networks, p. 1942–1948, 1995.

KENNEDY, J.; EBERHART, R. C. A discrete binary version of the particle swarm algorithm. In: 1997 IEEE International Conference on Systems, Man, and Cybernetics. Computational Cybernetics and Simulation, Anais...IEEE, 1997.

KRAVANJA, P.; MODARRESI, A.; FRIEDL, A. Heat integration of biochemical ethanol production from straw – A case study. Applied Energy, v. 102, p. 32–43, 2013.

KUMAR, S.; DHEERAN, P.; SINGH, S. P.; MISHRA, I. M.; ADHIKARI, D. K. Kinetic studies of two-stage sulphuric acid hydrolysis of sugarcane bagasse. Renewable Energy, v. 83, p. 850–858, 2015.

LINNHOFF, B.; HINDMARSH, E. The pinch design method for heat exchanger networks. Chemical Engineering Science, v. 38, n. 5, p. 745–763, 1983.

MARTÍN, C.; GALBE, M.; WAHLBOM, C. F.; HAHN-HÄGERDAL, B.; JÖNSSON, L. J. Ethanol production from enzymatic hydrolysates of sugarcane bagasse using recombinant xylose-utilising Saccharomyces cerevisiae. Enzyme and Microbial Technology, v. 31, n. 3, p. 274–282, 2002.

MOSIER, N.; WYMAN, C.; DALE, B.; ELANDER, R.; LEE, Y. Y.; HOLTZAPPLE, M.; LADISCH, M. Features of promising technologies for pretreatment of lignocellulosic biomass. Bioresource Technology, v. 96, n. 6, p. 673–686, 2005.

NAZATO, C.; SILVA, D. F. C.; FERRAZ, S. C. U.; HARDER, M. N. C. Moenda x Difusor: diferentes pontos de vista sobre assunto. Bioenergia em revista: Diálogos, v. 1, n. 1, p. 129–139, 2011.

OLIVEIRA, C. M.; CRUZ, A. J. G.; COSTA, C. B. B. Improving second generation bioethanol production in sugarcane biorefineries through energy integration. Applied Thermal Engineering, v. 109, p. 819–827, 2016.

PAVÃO, L. V.; COSTA, C. B. B.; RAVAGNANI, M. A. da S. S. Automated heat exchanger network synthesis by using hybrid natural algorithms and parallel processing. Computers & Chemical

Engineering, v. 94, p. 370–386, 2016.

PAVÃO, L. V.; COSTA, C. B. B.; RAVAGNANI, M. A. S. S. Heat Exchanger Network Synthesis without stream splits using parallelized and simplified Simulated Annealing and Particle Swarm Optimization. Chemical Engineering Science, v. 158, p. 96–107, 2017.

PINA, E. A.; PALACIOS-BERECHE, R.; CHAVEZ-RODRIGUES, M. F.; ENSINAS, A. V.; MODESTO, M.; NEBRA, S. A. Thermal integration of different plant configurations of sugar and ethanol production from sugarcane. Chemical Engineering Transactions, v. 39, p. 1147–1152, 2014.

PINA, E. A.; PALACIOS-BERECHE, R.; CHAVEZ-RODRIGUEZ, M. F.; ENSINAS, A. V.; MODESTO, M.; NEBRA, S. A. Reduction of process steam demand and water-usage through heat integration in sugar and ethanol production from sugarcane – Evaluation of different plant configurations. Energy, 2015.

RAVAGNANI, M. A. S. S.; CABALLERO SUÁREZ, J. A. Redes de cambiadores de calor. [s.l.] Publicaciones de la Universidad de Alicante, 2012.

ROBERTO, I. C.; LACIS, L. S.; BARBOSA, M. F. S.; DE MANCILHA, I. M. Utilization of sugar cane bagasse hemicellulosic hydrolysate by pichia stipitis for the production of ethanol. Process Biochemistry, v. 26, n. 1, p. 15–21, 1991.

RODRÍGUEZ-CHONG, A.; ALBERTO RAMÍREZ, J.; GARROTE, G.; VÁZQUEZ, M. Hydrolysis of sugar cane bagasse using nitric acid: a kinetic assessment. Journal of Food Engineering, v. 61, n. 2, p. 143–152, 2004.

SANTOS, D. A.; OLIVEIRA, M. M.; CURVELO, A. A. S.; FONSECA, L. P.; PORTO, A. L. M. Hydrolysis of cellulose from sugarcane bagasse by cellulases from marine-derived fungi strains. International Biodeterioration & Biodegradation, v. 121, p. 66–78, 2017.

SILVA, A. P.; RAVAGNANI, M. A. S. S.; BISCAIA, E. C. Particle Swarm Optimisation in heat exchanger network synthesis including detailed equipment design. Most, p. 713–718, 2008.

SILVA, A. P.; RAVAGNANI, M. A. S. S.; BISCAIA, E. C.; CABALLERO, J. A. Optimal heat exchanger network synthesis using particle swarm optimization. Optimization and Engineering, v. 11, n. 3, p. 459–470, 2010.

SINGH, A.; SHARMA, P.; SARAN, A. K.; SINGH, N.; BISHNOI, N. R. Comparative study on ethanol production from pretreated sugarcane bagasse using immobilized Saccharomyces cerevisiae on various matrices. Renewable Energy, v. 50, p. 488–493, 2013.

TOIMIL, D.; GÓMEZ, A. Review of metaheuristics applied to heat exchanger network design. International Transactions in Operational Research, v. 24, n. 1–2, p. 7–26, 2017.

UENG, P. P.; GONG, C. Ethanol production from pentoses and sugar-cane bagasse hemicellulose hydrolysate by Mucor and Fusarium species. Enzyme and Microbial Technology, v. 4, n. 3, p. 169–171, 1982.

US. A Best practices steam technical brief: How to calculate the true cost of steam. Washington: Department of Energy, 2003.

YEE, T. F.; GROSSMANN, I. E. Simultaneous optimization models for heat integration—II. Heat exchanger network synthesis. Computers & Chemical Engineering, v. 14, n. 10, p. 1165–1184, 1990.

ZHAOYI, H.; LIANG, Z.; HONGCHAO, Y.; JIANXIONG, Y. Simultaneous synthesis of structural-constrained heat exchanger networks with and without stream splits. The Canadian Journal of Chemical Engineering, v. 91, n. 5, p. 830–842, 2013.

ZHOU, Z.; XUE, W.; LEI, F.; CHENG, Y.; JIANG, J.; SUN, D. Kraft GL-ethanol pretreatment on sugarcane bagasse for effective enzymatic hydrolysis. Industrial Crops and Products, v. 90, p. 100–109, 2016.

Chapter 4

Energy Integration of a Sugarcane Biorefinery using Simulated Annealing and Rocket Fireworks Optimization

As presented in the previous chapter, the problem of heat exchanger network (HEN) synthesis in a biorefinery, solved by Particle Swarm Optimization (PSO), showed only marginal improvements in the process compared to the process already existing in Brazilian plants. The PSO algorithm is a method originally developed for continuous optimization and adaptations are performed to deal with binary optimization. In the previous chapter, a rounding function was used to adapt the PSO to binary variables. This strategy is commonly good for small-scale problems. However, in large-scale problems, as HENs synthesis in biorefineries, challenges in mathematical optimization using that algorithm were expected. To circumvent this problem, a hybrid method composed by Simulated Annealing (SA) and Rocket Fireworks Optimization (RFO) was used to solve Mixed Integer Nonlinear Programming problems. This approach was developed by Pavão et al. (2017) and presented good results for large-scale HEN problems of single-period (PAVÃO et al., 2017) and multiple periods (PAVÃO et al., 2018a,b). The results of energy integration applied to one biorefinery case study using SA-RFO are better than solutions with PSO algorithm presented in the previous chapter and it is able to achieve significant savings. These results are presented in the following text, "Process Integration of a Multiperiod Sugarcane Biorefinery", which was published in Applied Energy (v.213, p.520-539, 2018). It was structured into five main topics: introduction; approach for solving the multiperiod HEN problem; sugarcane biorefinery; results and discussions; and conclusion.

Applied Energy 213 (2018) 520–539

Contents lists available at ScienceDirect

Applied Energy

journal homepage: www.elsevier.com/locate/apenergy

Process integration of a multiperiod sugarcane biorefinery

Cássia M. Oliveira[a], Leandro V. Pavão[b], Mauro A.S.S. Ravagnani[b], Antonio J.G. Cruz[a], Caliane B.B. Costa[b,*]

[a] Chemical Engineering Department, Federal University of São Carlos, Rodovia Washington Luís, km 235, 13565-905 São Carlos, São Paulo, Brazil
[b] Chemical Engineering Department, State University of Maringá, Av. Colombo 5790, Bloco D-90, 87020-900 Maringá, Paraná, Brazil

HIGHLIGHTS

- A Multiperiod Heat Exchanger Network is proposed for a sugarcane biorefinery.
- The energy integration is able to increase energy security.
- More bagasse becomes available to produce second generation ethanol or electricity.
- The solution scheme is based on an efficient meta-heuristic method.
- Total Annualized Cost and energy demand reduction are obtained.

ARTICLE INFO

Keywords:
Sugarcane biorefinery
1G/2G ethanol
Multiperiod Heat Exchanger Network
Mixed integer nonlinear programming
Simulated annealing
Rocket Fireworks Optimization

ABSTRACT

Process integration in sugarcane biorefineries allows reducing steam consumption. As a consequence, the bagasse surplus can be diverted to second generation ethanol production. Furthermore, sugarcane plants can vary the production of ethanol and electricity, depending on the demand. For those reasons, equipment present in the plant might be required to operate under different conditions. This study presents the energy integration of a sugarcane biorefinery. A Mixed Integer Nonlinear Programming (MINLP) optimization model is proposed to solve the problem of synthesizing a Heat Exchanger Network (HEN) able to periodically operate under the distinct conditions required in the biorefinery, *i.e.*, a multiperiod HEN. For solving the MINLP problem, a hybrid metaheuristic approach was used, which combines Simulated Annealing and Rocket Fireworks Optimization. The proposed strategy achieved lower HEN total annualized cost (TAC) when compared with the project energy integration that is commonly found in Brazilian plants. This reduction in TAC, in particular in utilities demand, allows the surplus bagasse to be available for the most suitable application: produce 2G ethanol or more electricity.

1. Introduction

Sugarcane mills present economic importance not only in ethanol and sugar production, but also in the generation of electricity from sugarcane biomass. Sugarcane bagasse is burned in the boiler and the steam produced moves the turbines and generates energy. Cogeneration process reduces energy costs in the plant, supplies internal energy demand and, in many cases, allows selling the surplus.

A sugarcane biorefinery can be defined as an industrial process able to produce different products and by-products (sugar, 1G/2G ethanol and electricity) from the main raw material (sugarcane). The current efforts to turn 2G ethanol production process viable aim, among other goals, at increasing energy security and decreasing environmental resources consumption, since 2G ethanol turns possible the increase of production of this biofuel without the increase of cultivated land area. However, 2G ethanol technology is still not consolidated and requires studies to allow the integrated first and second generation ethanol production process to be more sustainable and economic.

* Corresponding author.
E-mail address: cbbcosta@uem.br (C.B.B. Costa).

https://doi.org/10.1016/j.apenergy.2017.11.020
Received 10 July 2017; Received in revised form 12 October 2017; Accepted 2 November 2017
Available online 10 November 2017

Nomenclature

Variables

A	heat exchanger area [m^2]
Acu	cooler area [m^2]
Ahu	heater area [m^2]
C_{total}	annualized total cost [USD/year]
Fc	fraction of cold stream [–]
Fh	fraction of hot stream [–]
$LMTD$	logarithmic mean temperature difference [K]
Q	heat load in a heat exchanger [kW]
Qcu	heat load in a cooler [kW]
Qhu	heat load in a heater [kW]
$Qmax$	maximum heat load [kW]
TAC	total annualized cost [USD/year]
$Tchuin$	inlet temperature of the cold stream in a heater [K]
$Thcuin$	inlet temperature of the hot stream in a cooler [K]
$Tcin$	inlet temperature of the cold stream in a heat exchanger [K]
$Thin$	inlet temperature of the hot stream in a heat exchanger [K]
$Tcout$	outlet temperature of the cold stream in a heat exchanger [K]
$Thout$	outlet temperature of the hot stream in a heat exchanger [K]
$Tcmix$	mixture temperature of the cold stream after mixer [K]
$Thmix$	mixture temperature of the hot stream after mixer [K]
U	overall coefficient of heat transfer [kW/(m^2 K)]
z	binary variable representing existence of a heat exchanger [–]
zcu	binary variable representing existence of a cooler [–]
zhu	binary variable representing existence of a heater [–]
$\theta^{(1)}$	temperature approximation at the hot end of a heat exchanger [K]
$\theta^{(2)}$	temperature approximation at the cold end of a heat exchanger [K]
ΔT	temperature difference [K]

Parameters

a	annual fixed cost coefficient for heat exchangers [USD/year]
a'	fixed cost coefficient for heat exchangers [USD]
a_F	fuel cost per unit of energy [USD/kJ]
b	annual variable cost coefficient for heat exchangers [USD/(m^2 year)]
b'	variable cost coefficient for heat exchangers [USD/m^2]
c	area cost exponent [–]
c'	area cost exponent [–]
C_B	cost of bagasse [USD/tonne]
ccu	cost of cold utility [USD/(kW year)]
C_F	fuel cost for steam generation [USD/kg]
C_G	total cost for steam generation [USD/kg]
chu	cost of hot utility [USD/(kW year)]
CPc	heat capacity of the cold stream [kW/K]
CPh	heat capacity of the hot stream [kW/K]
C_W	cost of cooling water [USD/m^3]
$EMAT$	minimum temperature approximation in the heat exchanger [K]
hc	heat transfer convective coefficient of the cold stream [kW/(m^2 K)]
hh	heat transfer convective coefficient of the hot stream [kW/(m^2 K)]
h_{IN}	enthalpy of cooling water at inlet cooler [kJ/kg]
h_{OUT}	enthalpy of cooling water at outlet cooler [kJ/kg]
h_{COND}	enthalpy of condensation [kJ/kg]
H_S	enthalpy of steam [kJ/kg]
h_W	enthalpy of boiler feedwater [kJ/kg]
k	number of the stage [–]
LHV	lower heating value [kJ/kg]
t	plant life [h/year]
Tc^0	initial temperature of the cold stream [K]
Tc^{final}	final (target) temperature of the cold stream [K]
Th^0	initial temperature of the hot stream [K]
Th^{final}	final (target) temperature of the hot stream [K]
u	annual capital interest [–]
$\hat{v}$	specific volume [m^3/kg]
η	boiler efficiency in relation to LHV [%]
θ	annualization factor [1/year]
τ	operation time [h/year]

Data set

N_C	cold streams [–]
N_H	hot streams [–]
N_S	stages [–]

Subscripts

i	cold streams
j	hot streams
k	stage superstructure

Text

CSA	Continuous Simulated Annealing
GA	Genetic Algorithm
HS	Harmonic Search
HEN	Heat Exchanger Network
HENs	Heat Exchanger Networks
LP	Linear Programming
MILP	Mixed Integer Linear Programming
MINLP	Mixed Integer Non-Linear Programming
NL	Non-Linear Programming
NIM-SWS	Nonisothermal Mixing Stage-wise Superstructure
SA	Simulated Annealing
SQP	Sequential Quadratic Programming
SWS	Stage-wise Superstructure
PSO	Particle Swarm Optimization
RFO	Rocket Fireworks Optimization
TS	Tabu Search

Some important computational studies in sugarcane biorefineries were published, considering the simulation of first and second ethanol generation process [1], the evaluation of technical configurations for bioenergy production with sugarcane bagasse [2], the process flexibility in second generation ethanol and electricity production [3], an economic perspective of ethanol production costs in Brazil [4], and the optimization and comparison of processes for 1G/2G ethanol and electricity production [5]. Recently, studies applied to biorefineries include the process optimization involving process and environmental criteria [6], the evaluation of potential of CO_2 as a carbon source for synthetic methane production [7] and the evaluation of impact of sugarcane hybrids in ethanol, sugar, and electricity production [8].

Process integration techniques provide increased efficiency of the process productivity, improved profitability, and, at the same time, reduced use of environmental resources and generation of residues. Energy integration is one of the process integration techniques and one of its fundamental tasks is the synthesis of the Heat Exchanger Network (HEN). Former methods were based on heuristic rules and thermodynamic insights, such as the well-known Pinch Analysis. Aiming for an automated HEN synthesis, mathematical optimization models to tackle the problem have been developed. Given the problem complexity, some models required a sequential approach for achieving solutions, such as Papoulias and Grossmann's [9]. A simultaneous one-step approach requires a superstructure-based MINLP formulation [10], such as the model of Yee and Grossmann [11], which is well accepted and used as basis to other models in HEN synthesis literature. Simultaneous strategies make it possible to find better solutions, but require more computational effort and well-elaborated solution schemes given the non-linearities and non-convexities present in the mathematical formulations for this type of problem.

In recent years, many studies to help solving these problems via hybrid metaheuristic approaches have been proposed. These approaches rely on randomness to find better solutions and are attractive since they require no advanced mathematical concepts, as in deterministic methods. Lewin [12] introduced a two-level optimization model. The approach consists in solving the problem at the upper level for integer variables and at the lower level for continuous variables. The partition of the problem into two levels allows solving large problems with reasonable computational effort and very promising results can be achieved. In the mentioned work [12], the Genetic Algorithm (GA) was used at both levels of the problem. Recently, Martelli et al. [13] used Variable Neighborhood Search (VNS) in the upper level and the Sequential Quadratic Programming (SQP) in the lower level optimization. Note that SQP is a deterministic approach, thus this method is a hybridization between a stochastic and a deterministic method. Pavão et al. [14] used Simulated Annealing (SA) and Rocket Fireworks Optimization (RFO) in the upper and lower level, respectively. This sort of strategy was also used with Differential Evolution (DE) at both levels by Yerramsetty and Murty [15], combining Harmonic Search (HS) and Sequential Quadratic Programming (SQP) by Khorasany and Fesanghary [16], Tabu Search (TS) and Sequential Quadratic Programming (SQP) by Chen et al. [17], Genetic Algorithm (GA) and Simulated Annealing (SA) by Luo et al. [18], Genetic Algorithm (GA) and Particle Swarm Optimization (PSO) by Pavão et al. [19] and Simulated Annealing (SA) and Particle Swarm Optimization (PSO) by Pavão et al. [20].

Energy integration of sugarcane biorefinery aims at minimizing total annual cost, taking into account the utilities consumption by means of a HEN and its corresponding investment cost. An important parameter for energy integration of biorefineries is the steam consumption, since lower steam consumption in the plant requires less bagasse to be destined to the cogeneration system, and then the surplus bagasse can be made available for second generation ethanol production. Therefore, energy integration enables improvements in the biorefinery, such as increased ethanol production, reduced costs and better use of environmental resources. However, in a flexible plant, sugarcane bagasse fractions diverted to 2G ethanol production and to the cogeneration system can vary, according to variations in the prices of ethanol and electricity, which, ultimately, determines 2G ethanol and surplus electricity production, as well as internal process utilities demands. The heat exchanger network synthesized should, therefore, be able to meet the different process conditions.

Studies in this regard include methodologies for the design of flexible heat exchanger networks, which allow fluctuations in some process parameters, such as flow rates and temperatures. Among the approaches used to tackle this problem, a common practice is to synthesize multiperiod networks, which can operate under different established conditions. The optimization problem formulated to the synthesis of HEN for multiperiod operations can be solved using sequential or simultaneous approaches. Pinch Analysis was used in early multiperiod HEN studies, *e.g.*, those by Tjoe and Linnhoff [21] and Ravagnani and Módenes [22]. Floudas and Grossmann [23] presented a Mixed Integer Linear Programming (MILP) formulation for heat exchanger networks synthesis for multiperiod operations as an extension of the Papoulias and Grossmann's [9] model, aiming at obtaining the minimum utilities cost and the minimum number of units in the heat exchanger network, in each period. Afterwards, the automatic generation of minimum investment cost for a multiperiod model was developed by Floudas and Grossmann [24], based on the NLP model for single-period of Floudas et al. [25]. Miranda et al. [26] proposed an approach similar to the previous work [24], finding better results. The simultaneous approach for flexible networks synthesis for multiperiod operations was introduced by Aaltola [27], extending the MINLP model of Yee and Grossmann [11]. The author, however, assumed the average of the areas required by the units in each period to calculate their costs. That would yield slightly underestimated capital costs. Verheyen and Zhang [28] were able to tailor a model where the larger area required by a unit among all periods was considered in capital costs calculation. The superstructure model of Yee and Grossmann [11] and the maximal area consideration were used as basis in the work of Pavão et al. [29], who employed a metaheuristic method to solve the model and achieve multiperiod HENs. Recently, Jiang and Chang [30,31] demonstrated a timesharing mechanism for multiperiod HEN. This concept differs from that employed in works cited so far, where solutions comprised a set of heat exchangers sized to perform feasibly the same service in all operating periods. Under Jiang and Chang's timesharing concept [30,31], a heat exchanger (HE) can perform different stream pairing depending on the period, overcoming overdesign and periods' duration uncertainty issues. That concept was further adopted by Miranda et al. [32], who improved the HEN synthesis model of Jiang and Chang [30], being able to achieve better results; and by Pavão et al. [33], who presented significant improvements to multiperiod HEN synthesis with timesharing mechanisms via employment of a stochastic optimization approach. That approach consists in applying the scheme of Jiang and Chang [30] followed by an areas re-optimization stage, which allows more efficient use of the area available in devices.

Energy integration studies were performed with sugarcane biorefineries for 1G ethanol and sugar production [34] and 1G/2G ethanol production [35]. However, these studies used Pinch Analysis and did not consider process flexibility to operate under different conditions. These assumptions and the adopted approach allow obtaining good solutions, but when different process conditions are considered and optimization methods for the minimization of total annual costs are applied, better and more realistic solutions can be attained.

In that sense, this work aims to explore the identified gaps in the study of sugarcane biorefinery heat integration: to solve the problem with an energy integration technique different from Pinch Analysis and to consider the possibility of operating the process under different conditions. For filling the gaps, a multiperiod MINLP approach was used for the HEN synthesis in a biorefinery that produces 1G/2G anhydrous ethanol and electricity. The periods differ essentially in the bagasse fraction diverted to second generation ethanol production. This fraction is responsible for changing the flow rates of many streams in the integrated process. However, it is difficult to estimate the durations of the periods, because they depend on a series of factors such as market prices for ethanol and electricity. In that manner, the concepts of timesharing mechanisms proposed by Jiang and Chang [30] are suitable for the multiperiod HEN synthesis here proposed. For each period, the MINLP problem was solved using the hybridized method of SA and RFO presented by Pavão et al. [14]. SA-RFO was able to achieve promising solutions to industrial-scale HEN synthesis cases, being also recently adapted to handle a multi-objective formulation [36].

The synthesis of HEN in biorefineries has as one of the main goals to reduce the steam consumption in the process so that more bagasse can be diverted to 2G ethanol or electricity production. Besides that, it can help increasing energy security and decreasing environmental resources consumption. In that manner, it is expected that it can help making 2G ethanol production process viable. In this work, assumptions made for deriving the HEN model and that are commonly employed in the literature are presented in Section 2.1. It is worth noting that the HEN synthesized in this study can operate under multiple operation conditions, which provides flexibility to the biorefinery.

2. Approach for solving the multiperiod HEN problem

2.1. HEN mathematical model

In this work, a MINLP model is solved for each period separately. The superstructure used is based on stage-wise superstructure (SWS) of Yee and Grossmann [11], but the original assumption of isothermal mixing is not here adopted (nonisothermal mixing stage-wise superstructure, NIM-SWS). To make the HEN more practical from a design perspective, a minimal value of 1.0 m^2 for heat exchanger areas is assumed, as well as a maximum value of 5500 m^2 for heat exchanger areas. In addition, process streams with phase change are present. A rigorous modeling of such streams would make the HEN synthesis problems even more difficult to solve since it would require extra constraints. A common approach in HEN synthesis problems in which latent heat is present is to consider latent heat as equivalent to a large heat capacity over a small temperature difference (usually equal to 1.0 K). Other usual assumptions are constant film heat transfer coefficients and non-consideration of fouling and pressure drop effects. Piping costs are also not included in the model. These assumptions were used in this study to simplify the calculations. Since the equations of the MINLP model are well known in the literature, those are provided in Appendix A. The calculation of the number of variables of MINLP model is detailed in Supplementary Material.

2.2. Simulated Annealing and Rocket Fireworks Optimization

In this study, a hybrid stochastic method was used to solve a single MINLP problem for the conditions of each period. The hybrid approach was developed by Pavão et al. [14]. It is based on Simulated Annealing (SA) and a newly developed approach so-called Rocket Fireworks

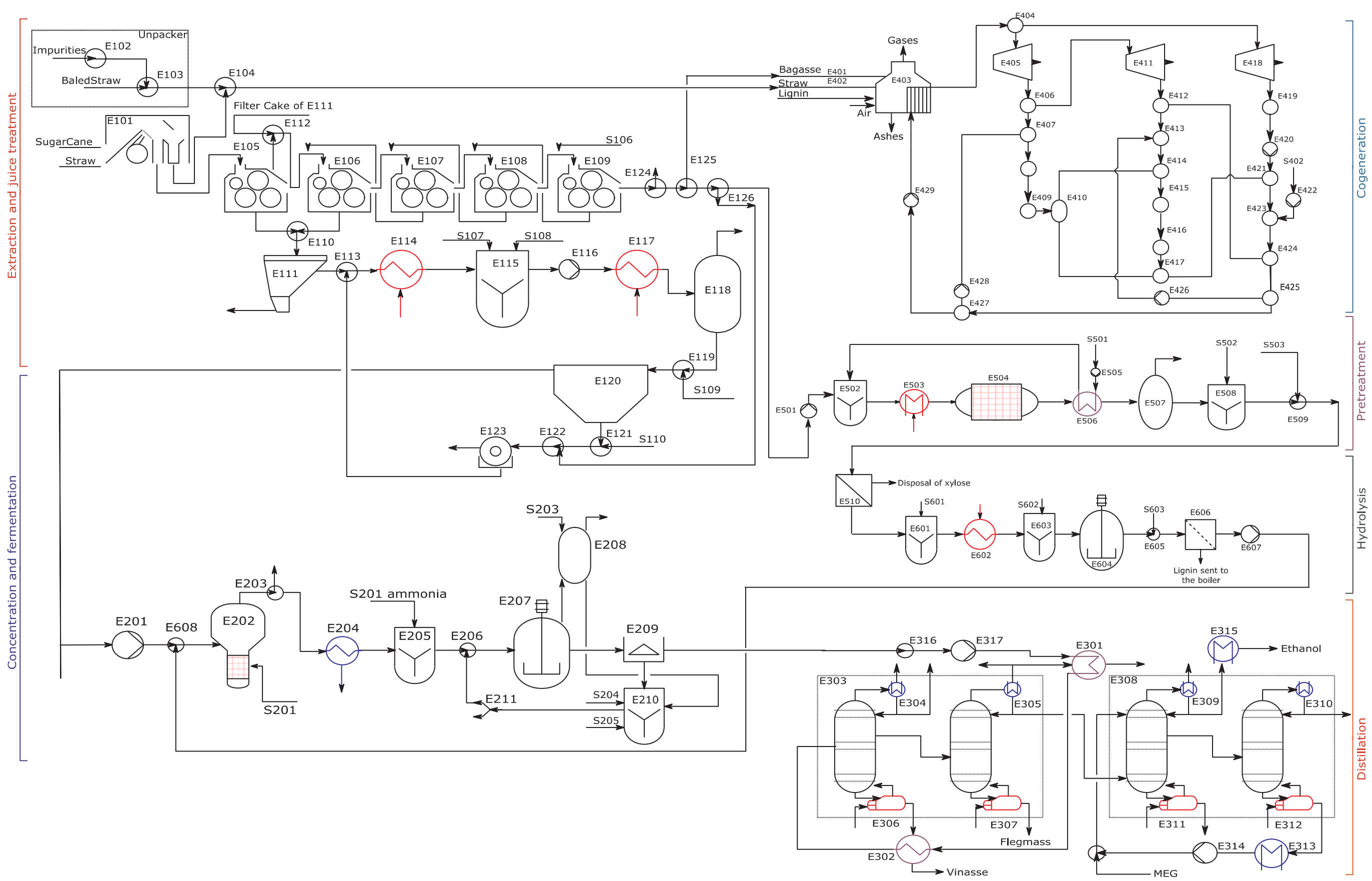

Fig. 1. Diagram of 1G/2G anhydrous ethanol and electricity production.

Optimization (RFO). SA is used in upper level for combinatorial optimization ($z_{i,j,k}$) and RFO is used in lower level for continuous variables optimization ($Q_{i,j,k}$, $Fh_{i,j,k}$ and $Fc_{i,j,k}$). The method is written in C++ language, which can yield fast optimization CPU times and whose compilers and development environments can be easily obtained free of charges.

SA is a local search method of easy implementation to solve large-scale combinatorial problems proposed by Kirkpatrick et al. [37]. Pavão et al. [14,20] adapted SA to tackle HEN synthesis problem through a rather simple exploration move, where a random HE is added to the HEN structure at a time.

Continuous level optimization uses the Rocket Fireworks Optimization [14], which combines a modified SA (Continuous Simulated Annealing, CSA) with the Particle Swarm Optimization (PSO) algorithm [38]. This method mimics both the "firework tail" (single CSA solution) and the explosion (randomly generated PSO solutions) of a firework.

CSA is employed to find solutions in a promising region. It is based on random movements (*i.e.*, random quantities are added/removed from continuous variables). The random moves are applied to continuous variables selected by a trivial roulette method. The final CSA solution is maintained and becomes a member of the PSO scheme. With such promising solution included in its initial population, PSO is then able to "refine" that result, finding a better HEN configuration. The interested reader is referred to Pavão et al. [14] for a more detailed explanation on the strategies used to maintain solutions feasibility. Other computational aspects of SA-RFO, such as parameters tuning, are also found therein.

It is important to mention that the HEN synthesis problem, when mathematically formulated as an optimization problem, is sensitive to the solution method. For instance, preliminary tests carried out to the biorefinery case study by the present authors with PSO algorithm led to results with marginal improvement only. For this reason, a hybrid meta-heuristic method (SA-RFO) was chosen, which was efficiently used for HEN synthesis in previous works [14,29,33].

2.3. Procedure for periods integration

In order to integrate heat exchanger networks of all periods, the strategy of Jiang and Chang [30] is used, which involves solving the MINLP model separately for each period and applying a timesharing strategy to integrate all HENs into a single one. This approach allows dealing with periods of durations that cannot be easily estimated, using the same heat exchanger for different pairs of streams matched in different periods. Given that the solution is not limited to a fixed duration of periods, the methodology suits perfectly well to the sugarcane biorefinery case, which may need to be adjusted due to unexpected changes in supplies, demand, prices and/or process conditions. After solving the problem for each period, the procedure to integrate all HENs is applied. This procedure is briefly described in Appendix B. More details about the procedure are provided in the work of Jiang and Chang [30].

A cleaning step among the periods may be necessary to prevent contamination inside the heat exchangers. Moreover, in order to allocate the correct matching of streams in a certain period to a device, a set of bypasses must be designed. However, the capital costs due to the use of valves and pipes for the design of the bypasses are not considered in the objective function of this study, similarly to the works conducted by Jiang and Chang [30,31] and Miranda et al. [32]. Those authors also assumed as negligible the dead times required for shutdown, cleaning, and starting up the plant between each operation condition change, since their duration is typically of hours or days, which is rather small when compared to steady plant operation times (months). In that manner, no costs associated to such idle plant periods are included in the models. Moreover, the duration and costs of such plant inactivity periods, and the number of times those transitions might apply is difficult to accurately estimate. Some additional information is needed for performing those predictions, such as cleaning and startup schedules. If such data is available, dead times and their associated costs might as well be included in a more thorough mathematical model. Furthermore, it is worth stressing that the timesharing approach applied in this work is employed to circumvent the uncertainty associated with predicting durations of each period of plant operation condition. With that methodology, it is possible to use efficient multiperiod HEN that performs well in all predicted conditions regardless of the period duration. The works of Jiang and Chang [30,31] and Miranda et al. [32] demonstrated that this strategy leads to costs reduction when compared to the typical approach of using a fixed set of equipment designed to perform heat integration in all possible operating conditions of a given plant. The usual multiperiod approach takes periods' duration into account, which may lead to a HEN more fit to conditions of periods that are expected to last longer. If those period durations are much uncertain, as in the biorefinery case, a fixed-services HEN might perform poorly, which justifies the use of a strategy that does not rely on periods' duration, as is Jiang and Chang's [30,31] methodology.

In this work, the biorefinery with HEN synthesized for each period is named "with energy integration proposed in this study for each period" and the biorefinery with the multiperiod HEN is named "with integrated HEN".

3. Sugarcane biorefinery

3.1. Process description

In this study, a virtual biorefinery modeled in EMSO simulator (Environment for Modeling, Simulation, and Optimization) was used [3,39]. Fig. 1 shows the diagram of this 1G/2G anhydrous ethanol and electricity production process (autonomous distillery). Tables S.1 and S.2 of the Supplementary Material provide main parameters for biorefinery simulation. More information on the simulations can be found in the cited works of Furlan et al. [3,39].

Brazilian sugarcane biorefineries often present some degree of energy integration, which depends on the design of each plant. The simulated biorefinery has energy integration between wine and vapor from the top of Column B (Condenser B), between streams of wine and vinasse, and between pretreated bagasse and soaking water (these heat exchangers are indicated in Fig. 1 by E301, E302 and E506). The first two instances of energy integration are commonly found in Brazilian mills, while the third is a suggestion of energy integration made by developers of virtual biorefinery [3,39]. In the present work, the process with such degree of energy integration is named as biorefinery "with project energy integration". When no energy integration is present, every heating and cooling of streams is provided by hot and cold utilities. The biorefinery process with this feature is then named in this work as "without energy integration". A sugarcane biorefinery process without any energy integration is in fact not a realistic hypothesis, since the first generation ethanol production process is a consolidated process and improvement studies have already been made. Therefore, the 1G/2G ethanol production process has, leastwise, energy integration among the streams of first generation ethanol process. However, the comparison with the process without energy integration is valid, since the energy integration instance can vary from a plant to another. Moreover, this comparison denotes the energy recovery achieved by the model, which can be used as an efficiency parameter for other energy integration proposals in biorefineries. In Fig. 1, heat exchangers named E114, E117, E306, E307, E311, E312, E503 and E602 indicate the supply of energy with hot utility and heat exchangers named E204, E304, E305, E309, E310, E313 and E315 indicate the withdrawal of energy by cold utility.

Ethanol production begins with the dry cleaning of sugarcane (E101). In this study, a fraction of straw is maintained in the plantation area to preserve the soil and the other fraction is used in the cogeneration system to produce steam and electricity. The clean sugarcane is sent to the extraction system (E105-E109), which consists in separating the bagasse from sugarcane juice by mills. The juice is chemically and physically treated (E110-E123) to remove impurities. The clarified juice is concentrated (E202) in a pre-evaporator to 20° Brix (*i.e.*, 20 g of sugar per 100 g of solution). After that, the concentrated juice is fed to bioreactor (E207) for sugar fermentation by *Saccharomyces cerevisiae*. The wine from the fermenter is centrifuged (E209) and sent to the distillation unit (E303 and E308), where anhydrous ethanol is produced by extractive distillation (E308).

To produce 2G ethanol, bagasse from the extraction section is split into three fractions: one for the boiler (stream E125), another for the pretreatment stage (stream E126) and an amount to be kept as a safety reserve (stream E124). In this work, hydrothermal pretreatment was

Table 1
Stream data for sugarcane biorefinery energy integration.

Stream		Corresponding HE in Fig. 1	T^0 (K)	T^{final} (K)	CP (kW/K)	h (kW/m^2 K)
Period 1						
H1	Concentrated juice	E204	388	306	638	1.38
H2	Vapor from Column D top (Condenser D)	E304	358	357	11,661	1.38
H3	Vapor from Column B top (Condenser B)	E305/E301	355	354	60,307	1.38
H4	Vapor from extractive column top (Condenser DEH1)	E309	351	350	24,592	1.38
H5	Vapor from recovery column top (Condenser DEH2)	E310	333	332	2074	1.38
H6	Vinasse	E302	385	363	747	1.38
H7	Monoethylene glycol	E313	421	353	33	1.38
H8	Anhydrous ethanol	E315	351	308	43	1.38
C1	Juice	E114	321	343	1256	1.38
C2	Juice	E117	343	378	1288	1.38
C3	Wine	E301/E302	303	362	867	1.38
C4	Liquid from Column A bottom (Reboiler A)	E306	384	385	67,968	1.38
C5	Liquid from Column B1 bottom (Reboiler B)	E307	381	382	22,466	1.38
C6	Liquid from extractive column bottom (Reboiler DEH1)	E311	379	407	352	1.38
C7	Liquid from recovery column bottom (Reboiler DEH2)	E312	411	421	335	1.38
Period 2						
H1	Concentrated juice	E204	388	306	713	1.38
H2	Vapor from Column D top (Condenser D)	E304	358	357	13,086	1.38
H3	Vapor from Column B top (Condenser B)	E305/E301	355	354	66,136	1.38
H4	Vapor from extractive column top (Condenser DEH1)	E309	351	350	26,942	1.38
H5	Vapor from recovery column top (Condenser DEH2)	E310	333	332	2272	1.38
H6	Vinasse	E302	385	363	862	1.38
H7	Monoethylene glycol	E313	421	353	37	1.38
H8	Anhydrous ethanol	E315	351	308	47	1.38
H9	Pretreated bagasse	E506	468	353	525	1.38
C1	Juice	E114	321	343	1256	1.38
C2	Juice	E117	343	378	1288	1.38
C3	Wine	E301/E302	303	362	995	1.38
C4	Liquid from Column A bottom (Reboiler A)	E306	384	385	76,914	1.38
C5	Liquid from Column B1 bottom (Reboiler B)	E307	381	382	23,510	1.38
C6	Liquid from extractive column bottom (Reboiler DEH1)	E311	379	407	386	1.38
C7	Liquid from recovery column bottom (Reboiler DEH2)	E312	411	421	367	1.38
C8	Bagasse + soaking water	E503	439	468	523	1.38
C9	Soaking water	E506	303	458	418	1.38
C10	Solid fraction (cellulose + lignin)	E602	315	323	206	1.38
Period 3						
H1	Concentrated juice	E204	388	306	788	1.38
H2	Vapor from Column D top (Condenser D)	E304	358	357	14,532	1.38
H3	Vapor from Column B top (Condenser B)	E305/E301	355	354	71,935	1.38
H4	Vapor from extractive column top (Condenser DEH1)	E309	351	350	29,277	1.38
H5	Vapor from recovery column top (Condenser DEH2)	E310	333	332	2469	1.38
H6	Vinasse	E302	385	363	981	1.38
H7	Monoethylene glycol	E313	421	353	40	1.38
H8	Anhydrous ethanol	E315	351	308	51	1.38
H9	Pretreated bagasse	E506	468	353	1047	1.38
C1	Juice	E114	321	343	1256	1.38
C2	Juice	E117	343	378	1288	1.38
C3	Wine	E301/E302	303	362	1129	1.38
C4	Liquid from Column A bottom (Reboiler A)	E306	384	385	86,036	1.38
C5	Liquid from Column B1 bottom (Reboiler B)	E307	381	382	24,443	1.38
C6	Liquid from extractive column bottom (Reboiler DEH1)	E311	379	407	419	1.38
C7	Liquid from recovery column bottom (Reboiler DEH2)	E312	411	421	398	1.38
C8	Bagasse + soaking water	E503	439	468	1042	1.38
C9	Soaking water	E506	303	458	834	1.38
C10	Solid fraction (cellulose + lignin)	E602	315	323	410	1.38

chosen because it presents promising results in laboratory scale and, at the same time, does not use any raw material besides water [40]. In hydrothermal pretreatment, bagasse is pressurized (E501), mixed to the soaking water (E502) and then sent to the pretreatment reactor (E504). After the pretreatment, two fractions are obtained (and separated in filter E510), one enriched with sugars from hemicellulose (liquid fraction) and the other enriched with cellulose and lignin (solid fraction). The resulting liquid fraction, rich in hydrolysis products from hemicellulose (xylose), is discarded. The solid fraction is sent to the enzymatic cellulose hydrolysis (E604) to convert cellulose into glucose. Finally, the resulting mixture is filtered (E606). The liquid fraction is sent to the concentration step (E202), along with the sugarcane juice, while the solid fraction, consisting mainly of lignin, is sent to the boiler (E403).

Energy cogeneration system can operate with or without condensation turbine, depending on the purpose of the plant. The simulations present in this study allow choosing not to use the condensation turbine, when the objective is to produce ethanol, and using the condensation turbine, when the objective is to increase the surplus of electricity. In the cogeneration system without the condensation turbine, the steam generated in the boiler (E403) is sent to three back pressure turbines (E405, E411 and E418), where turbine extraction steam is produced at 17.4 bar, 6.0 bar and 2.5 bar. The turbine extraction steam at 17.4 bar (outlet of E405) is used in the pretreatment stage (E503), while the turbine extraction steam at 6 bar (outlet of E411) is used in the dehydration columns (reboilers indicated by E311 and E312). The turbine extraction steam at 2.5 bar (outlet of E418) is used in the pre-evaporator (E202), the reboiler of Column B1 (E307) and for heating the solids stream (cellulose + lignin) from the pretreatment stage (E602). As previously mentioned, in processes with project energy integration, the thermal energy contained in the pretreated bagasse is used to heat the soaking water. However, the soaking water stream has an energy demand higher than the energy available in pretreated bagasse. For this reason, the remaining energy required by the soaking water stream is also supplied with turbine extraction steam at 6 bar. In the cogeneration system with condensation turbine, steam generated in the boiler is sent to two back pressure turbines (E405 and E411), where turbine extraction steam is produced at 6.0 bar and 2.5 bar, and to a condensation turbine (E418), where surplus electricity is generated. Main results for 1G/2G anhydrous ethanol and electricity production process are presented in Table S3 of the Supporting Information.

3.2. Energy integration case study

Table 1 shows streams data for the three periods. In this table, column 1 identifies hot and cold streams and their numbers. Column 2 denotes their corresponding heat exchanger presented in Fig. 1. For example, H2 is the hot stream from the top of Column D. This stream is condensed in device called Condenser D, indicated by E304 in Fig. 1. The convective heat transfer coefficient was considered the same for all streams and estimated from the overall heat transfer coefficient given by Ensinas [41]. EMAT is 1 K.

Period 1 represents the simulation of 1G ethanol and electricity production process and Periods 2 and 3 represent the simulation of 1G/2G ethanol and electricity production process with different fractions of bagasse diverted to 2G ethanol production. In Period 3, 66% of all bagasse is destined for the 2G ethanol production. This value is the maximum fraction of bagasse that could be destined for this purpose without compromising the energy self-sufficiency of the process. In Period 2, 33% of all bagasse is destined for the 2G ethanol production. The remainder is used for safety reserve, steam generation and electricity production. Therefore, the number of streams involved in energy integration differs among periods and, consequently, the number of variables also varies among periods. In this study, four stages were used in the superstructure. Thus, Period 1 has 896 variables and Periods 2 and 3 have 1440 variables.

The model used in this study considers only one hot utility and one cold utility. Steam at 65 bar generated in the boiler is sent to the backpressure turbine to produce an extraction steam at 17.4 bar. Then, it is desuperheated to saturation and selected as hot utility, since it meets the temperature constraints for all cold streams. It is important to mention that simple calculations are used to estimate the cost of hot utility, as is shown from Eq. (1) to Eq. (4). Thus, there is no significant difference in estimated cost of steam at different pressures. However, in common plants, steam is used at different pressures for heating streams and has a slightly different cost at each pressure. As cold utility, cooling water at 298 K is selected. This cold utility is produced in the cooling tower, which cools water from 305 K to 298 K. The water temperature of 298 K (i.e., the temperature of water produced in the cooling tower) was defined based on the usual climatic conditions found in Brazilian plants. It is worth noting that in real plants there are uncertainties in the temperature of utilities, which can vary. This variation is more important for cold utility, since the temperature of cooling water produced in the cooling tower can be more affected by climatic conditions. However, the variation in temperature of cooling water, when it occurs, is small. Thus, such small utility temperature variations would represent no significant deviations in the total annualized cost.

The cost of generating steam from the boiler (C_G) includes several components, such as fuel, raw water supply, boiler feed water treatment, water pumping power, combustion air fan power, environmental emissions control, maintenance materials and labor. However, fuel cost is usually the most important, responsible for as much as 90% of the total steam cost [42]. Eqs. (1)–(3) were extracted from US Department of Energy [42]. Eq. (1) calculates fuel cost (C_F), where a_F is fuel cost per unit of energy, η is boiler efficiency in relation to LHV (Lower Heating Value), H_S is enthalpy of steam at 65 bar and 758 K and h_W is enthalpy of boiler feed water at 298 K.

$$C_F = \frac{a_F \cdot (H_S - h_W)}{\eta} \tag{1}$$

In the biorefinery process, bagasse, straw and lignin are used as fuels in the boiler. For simplicity, only bagasse is considered in the fuel cost per unit of energy. Eq. (2) calculates fuel cost per unity of energy (a_F), where C_b is bagasse cost and LHV is Lower Heating Value.

$$a_F = \frac{C_b}{LHV} \tag{2}$$

Strictly, the individual costs components must be used in estimating the total cost of generating steam. In practice, the approximation described in Eq. (3) can be used, where C_F is the fuel cost. To reduce the complexity of calculations, the cost of steam from the backpressure turbine was considered equal to the cost of generating steam in the boiler (C_G).

$$C_G = 1.3 \cdot C_F \tag{3}$$

Cost of cooling water includes components as electricity, chemicals

Table 2
Parameters for HEN operating and capital costs calculations.

Parameter	Value	Unit
C_G[a]	15.0	USD/tonne
LHV	7121.3	kJ/kg
η	88	%
a'	37,247	USD
b'	251	USD/m$^{1.56}$
c'	0.78	[–]
t	15	year
u	10	%
τ	5760	h/year

[a] Information about cost of bagasse from Brazilian mills. The value described is the average between 2015 and 2016.

Table 3
Costs of utilities and parameters for calculation of annualized cost of heat exchangers.

Cost	Value	Unit
chu	96	USD/kW year
ccu	50	USD/kW year
a	4897	USD/year
b	33	USD/m$^{1.56}$ year
c	0.78	[–]

for water treatment and water treatment. Ensinas [41] estimated the cost of cooling water as 0.02 USD/m^3. In this study, all prices were calculated in Brazilian reais (BRL, Brazil's currency), updated to December/2016 value and converted to US dollars using the exchange rate value of 3.4885 BRL/USD (average exchange rate from January to December 2016). The values were updated based on the IGPM index (Market Prices General Index). It is a Brazilian index calculated by FGV (Getulio Vargas Foundation) and reflects price fluctuations [43] .

Utility costs are computed in annual basis, so as to be summed to annualized capital costs in HEN costs calculation. Eqs. (4) and (5) are used to annualize and convert the cost of utilities from mass unit (C_G and C_W) to energy unit (*chu* and *ccu*). The terms h_{COND} and τ in Eq. (4) refer to condensation enthalpy of saturated steam at 17.4 bar and operation time, respectively. In order to simplify the calculations in the mathematical model, inlet and outlet temperatures of steam were considered as 479 K and 478 K, respectively. In Eq. (5), C_W is cost of cooling water, $\hat{v}$ is specific volume, τ is operation time, h_{OUT} and h_{IN} are the enthalpies of water at 305 K and 298 K, respectively. The parameters used in estimating the costs of steam and cooling water are given in Table 2. The costs of steam and cooling water per energy unit are showed in Table 3.

$$chu = \frac{C_G}{h_{COND}} \cdot \tau \quad (4)$$

$$ccu = \frac{C_W}{(h_{OUT} - h_{IN})} \cdot \hat{v} \cdot \tau \quad (5)$$

Eq. (6) indicates the cost of heat exchangers. Coefficients a' and b' were estimated from cost and area data of Brazilian mills and updated to 2016. Coefficient c' for plate heat exchanger was obtained by Hall et al. [44]. Eq. (7) refers to annualized cost of heat exchanger. In Eq. (8), the annualization factor (θ) is calculated using parameters of Table 2, where u is annual capital interest rate and t is plant lifetime.

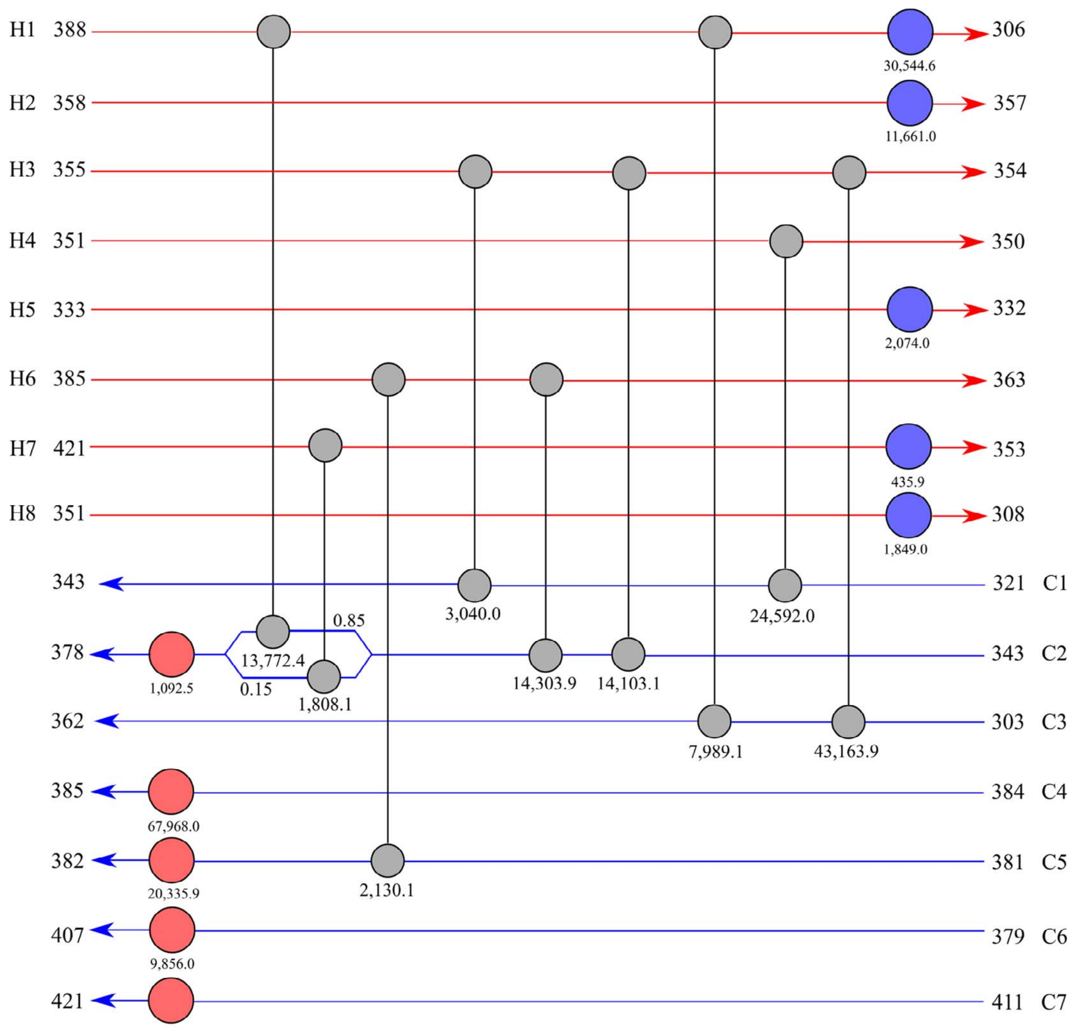

Fig. 2. HEN for Period 1.

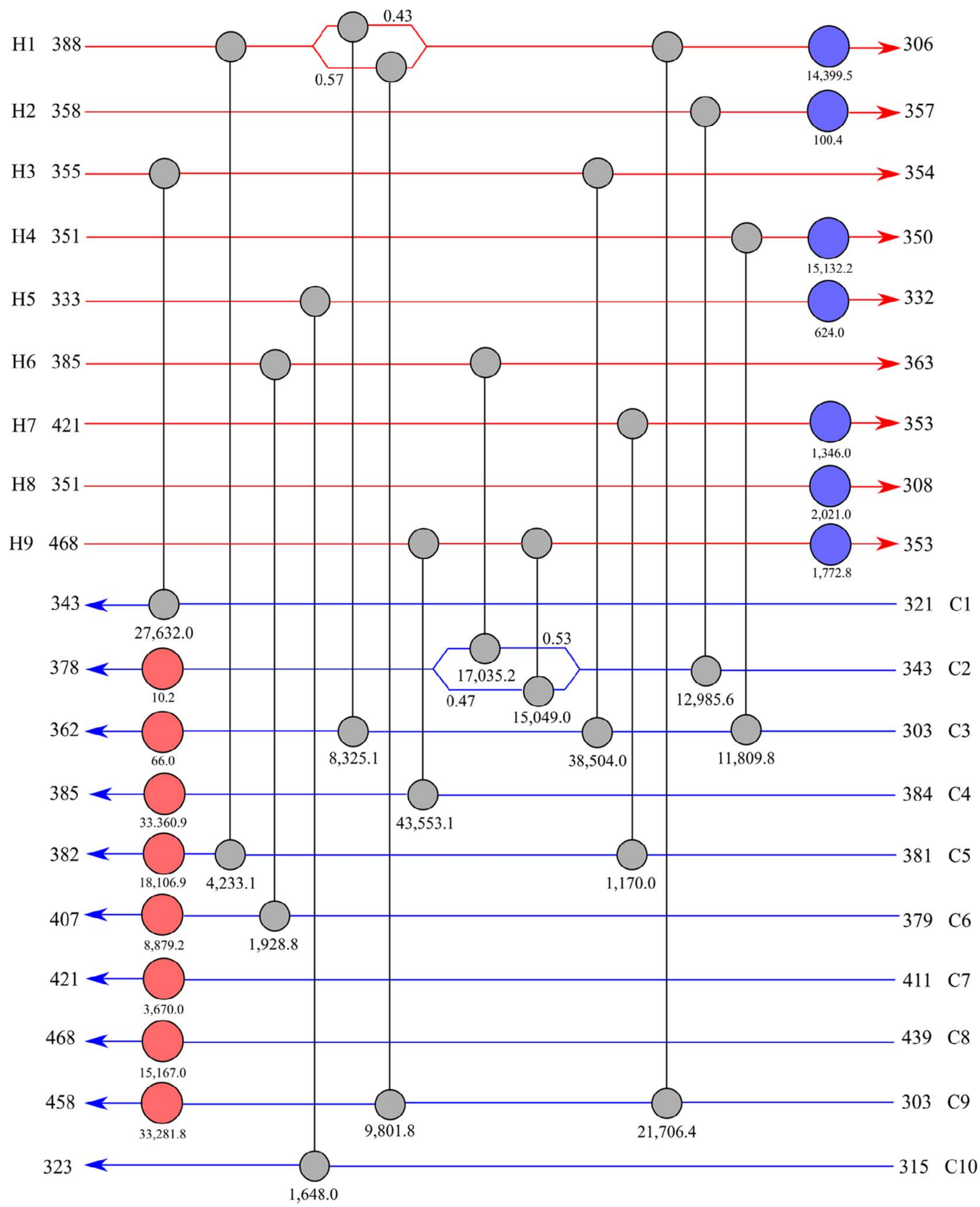

Fig. 3. HEN for Period 2.

The multiplication of Eq. (6) by annualization factor generates Eq. (7). The coefficients for annual costs of investment on heat exchangers are shown in Table 3.

$$HE\ cost = a' + b'{\cdot}A^{c'} \quad (6)$$

$$HE\ cost = a + b{\cdot}A^{c} \quad (7)$$

$$\theta = \frac{u(1+u)^t}{(1+u)^t - 1} \quad (8)$$

4. Results and discussion

The TAC of processes with project energy integration for Periods 1, 2 and 3 are 23.0, 26.8 and 30.5 million USD/year, respectively. Looking for energy integration configuration with lower TAC, a HEN was synthesized for each period. For each period, the method is run until the stop criterion is achieved, according to the methodology previously presented in Section 2.3. For Periods 1, 2 and 3, the total processing time of the algorithm was 10, 16 and 11 min, respectively (3.50 GHz Intel® Core™ i5-4690 processor and 8.00 GB of RAM). Figs. 2–4 present the HENs for each period, where the values below the heat exchangers

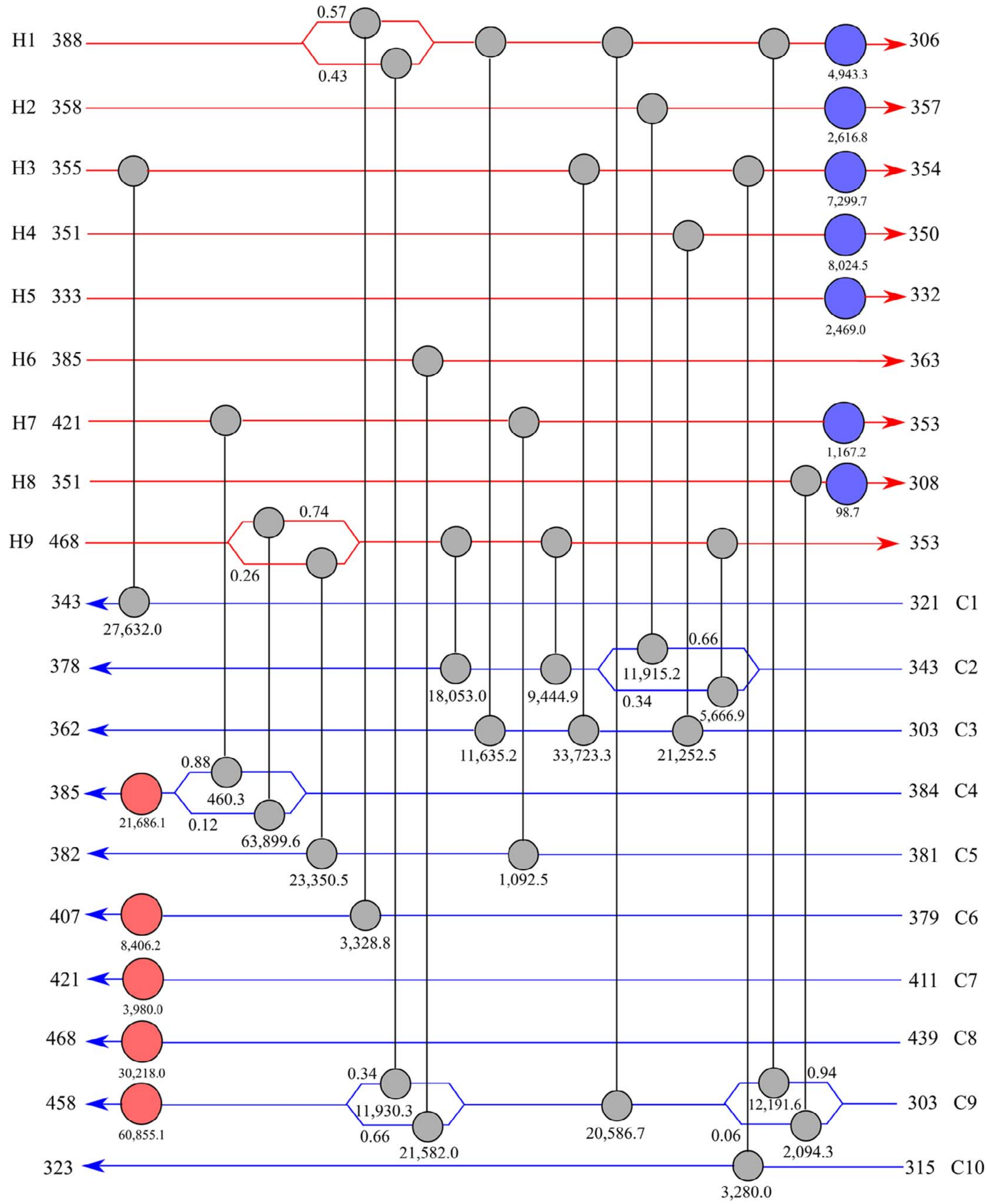

Fig. 4. HEN for Period 3.

are heat load, in kW. The values next to splitters indicate the stream fraction deviated to each heat exchanger. Tables 4–6 show the configurations of these HENs. The TAC for Periods 1, 2 and 3 are 12.4, 12.9 and 13.8 million USD/year, respectively. Note that, in Period 3, three different heat exchangers are assigned to pair H1-C9 (in stages 1, 3 and 4 of the superstructure). The same happens with match H9-C2 (in stages 2, 3 and 4 of the superstructure). This HEN configuration is achieved due to the maximum area constraint of 5500 m^2, which allows designing HENs more feasible from a practical perspective. More information about heat exchangers areas, number of heat transfer units and costs (operating, capital and TAC) for each single-period solution with their required areas are presented in Table 7.

For the integrated HEN, the capital cost estimated is 489,448 USD/year with total area of 60,129.6 m^2 and 31 heat exchangers. It represents an area overdesign of 52% for Period 1, 32% for Period 2 and 0.0% for Period 3. That means the final multiperiod HEN uses the set of devices designed for Period 3, which are, in general, larger, given the great heat exchange potential in that period. Therefore, the area and

Table 4
HEN for periods 1, 2 and 3 (Part 1).

Match	(i,j,k)	(1,2,1)	(1,3,3)	(3,1,2)	(3,2,3)	(3,3,4)	(4,1,3)	(6,2,2)	(6,5,1)	(7,2,1)	-	-	-	-	-	-	-	-	-	-
Period 1																				
A_S	m^2	5309.1	5449.2	3432.1	5354.1	5231.8	4215.9	3995.6	3630.3	1908.4	–	–	–	–	–	–	–	–	–	–
$A_{i,j,k}$	m^2	4492.9	4845.2	335.1	4694.0	4174.0	1963.4	1638.9	1370.6	213.9	–	–	–	–	–	–	–	–	–	–
$A_{i,j,k}/A_s$	m^2	0.85	0.89	0.10	0.88	0.80	0.47	0.41	0.38	0.11	–	–	–	–	–	–	–	–	–	–
$Q_{i,j,k}$	kW	13,772.4	7989.1	3040.0	14,103.1	43,163.9	24,592.0	14,303.9	2130.1	1808.1	–	–	–	–	–	–	–	–	–	–
$Fh_{i,j,k}$	–	1.00	1.00	1.00	1.00	1.00	1.00	1.00	1.00	1.00	–	–	–	–	–	–	–	–	–	–
$Fc_{i,j,k}$	–	0.85	1.00	1.00	1.00	1.00	1.00	1.00	1.00	0.15	–	–	–	–	–	–	–	–	–	–
$Thin_{i,j,k}$	K	388.0	366.4	355.0	354.9	354.7	351.0	382.1	385.0	421.0	–	–	–	–	–	–	–	–	–	–
$Thout_{i,j,k}$	K	366.4	353.9	354.9	354.7	354.0	350.0	363.0	382.1	366.2	–	–	–	–	–	–	–	–	–	–
$Tcin_{i,j,k}$	K	365.1	352.8	340.6	343.0	303.0	321.0	353.9	381.0	365.1	–	–	–	–	–	–	–	–	–	–
$Tcout_{i,j,k}$	K	377.6	362.0	343.0	353.9	352.8	340.6	365.1	381.1	374.6	–	–	–	–	–	–	–	–	–	–
LMTD	K	4.4	2.4	13.1	4.4	15.0	18.2	12.6	2.3	12.2	–	–	–	–	–	–	–	–	–	–
Bypass	%	16.1	7.1	83.2	3.1	2.4	32.5	56.5	97.2	82.4	–	–	–	–	–	–	–	–	–	–
Match	(i,j,k)	(1,3,2)	(1,5,1)	(1,9,2)	(1,9,3)	(2,2,4)	(3,1,1)	(3,3,3)	(4,3,4)	(5,10,1)	(6,2,3)	(6,6,1)	(7,5,3)	(9,2,3)	(9,4,2)	–	–	–	–	–
Period 2																				
A_S	m^2	1979.6	3588.1	5309.1	5231.8	3630.3	3432.1	5449.2	1434.9	412.8	4868.9	1917.8	184.8	5354.1	4215.9	–	–	–	–	–
$A_{i,j,k}$	m^2	1684.3	2024.1	4325.3	3817.6	2167.1	1909.5	5346.0	411.6	179.5	3532.4	1339.2	83.9	4391.7	3358.0	–	–	–	–	–
$A_{i,j,k}/A_s$	m^2	0.85	0.56	0.81	0.73	0.60	0.56	0.98	0.29	0.43	0.73	0.70	0.45	0.82	0.80	–	–	–	–	–
$Q_{i,j,k}$	kW	8325.1	4233.1	9801.8	21,706.4	12,985.6	27,632.0	38,504.0	11,809.8	1648.0	17,035.2	1928.8	1170.0	15,049.0	43,553.1	–	–	–	–	–
$Fh_{i,j,k}$	–	0.43	1.00	0.57	1.00	1.00	1.00	1.00	1.00	1.00	1.00	1.00	1.00	1.00	1.00	–	–	–	–	–
$Fc_{i,j,k}$	–	1.00	1.00	1.00	1.00	1.00	1.00	1.00	1.00	1.00	0.53	1.00	1.00	0.47	1.00	–	–	–	–	–
$Thin_{i,j,k}$	K	382.1	388.0	382.1	356.6	358.0	355.0	354.6	351.0	333.0	382.8	385.0	421.0	385.0	468.0	–	–	–	–	–
$Thout_{i,j,k}$	K	355.1	382.1	357.8	326.2	357.0	354.6	354.0	350.6	332.3	363.0	382.8	389.4	356.4	385.0	–	–	–	–	–
$Tcin_{i,j,k}$	K	353.6	381.0	354.9	303.0	343.0	321.0	314.9	303.0	315.0	353.1	379.0	381.0	353.1	384.0	–	–	–	–	–
$Tcout_{i,j,k}$	K	361.9	381.2	378.4	354.9	353.1	343.0	353.6	314.9	323.0	378.1	384.0	381.0	377.9	384.6	–	–	–	–	–
LMTD	K	7.2	3.0	3.3	8.2	8.7	21.0	10.4	41.6	13.3	7.0	2.1	20.2	5.0	18.8	–	–	–	–	–
Bypass	%	32.7	95.9	5.0	2.2	26.9	30.6	0.2	74.8	52.8	9.2	10.8	99.8	7.7	97.4	–	–	–	–	–
Match		(1,3,2)	(1,6,1)	(1,9,1)	(1,9,3)	(1,9,4)	(2,2,4)	(3,1,1)	(3,3,3)	(3,10,4)	(4,3,4)	(6,9,1)	(7,4,1)	(7,5,2)	(8,9,4)	(9,2,2)	(9,2,3)	(9,2,4)	(9,4,1)	(9,5,1)
Period 3																				
A_S	m^2	4215.9	3630.3	5309.1	3588.1	1917.8	3432.1	1908.4	3995.6	135.9	821.4	5231.8	21.6	184.8	412.8	5354.1	5449.2	1550.4	4868.9	1611.0
$A_{i,j,k}$	m^2	4215.9	3630.3	5309.1	3588.1	1917.8	3432.1	1908.4	3995.6	135.9	821.4	5231.8	21.6	184.8	412.8	5354.1	5449.2	1550.4	4868.9	1611.0
$A_{i,j,k}/A_s$	m^2	1.00	1.00	1.00	1.00	1.00	1.00	1.00	1.00	1.00	1.00	1.00	1.00	1.00	1.00	1.00	1.00	1.00	1.00	1.00
$Q_{i,j,k}$	kW	11,635.2	3328.8	11,930.3	20,586.7	12,191.6	11,915.2	27,632.0	33,723.3	3,280.0	21,252.5	21,582.0	460.3	1092.5	2094.3	18,053.0	9444.9	5666.9	63,889.6	23,350.5
$Fh_{i,j,k}$	–	1.00	0.57	0.43	1.00	1.00	1.00	1.00	1.00	1.00	1.00	1.00	1.00	1.00	1.00	1.00	1.00	1.00	0.74	0.26
$Fc_{i,j,k}$	–	1.00	1.00	0.34	1.00	0.94	0.66	1.00	1.00	1.00	1.00	0.66	0.88	1.00	0.06	1.00	1.00	0.34	0.12	1.00
$Thin_{i,j,k}$	K	368.6	388.0	388.0	353.9	327.7	358.0	355.0	354.6	354.1	351.0	385.0	421.0	409.5	351.0	384.7	367.4	358.4	468.0	468.0
$Thout_{i,j,k}$	K	353.9	380.6	352.4	327.7	312.3	357.2	354.6	354.1	354.1	350.3	363.0	409.5	382.2	309.9	367.4	358.4	353.0	385.4	382.6
$Tcin_{i,j,k}$	K	351.7	379.0	344.8	320.1	303.0	343.0	321.0	321.8	315.0	303.0	344.8	384.0	381.0	303.0	364.0	356.7	343.0	384.0	381.0
$Tcout_{i,j,k}$	K	362.0	386.9	387.0	344.8	318.6	357.0	343.0	351.7	323.0	321.8	384.0	384.0	381.0	343.2	378.0	364.0	356.0	390.4	382.0
LMTD	K	4.0	1.3	3.3	8.3	9.2	5.0	21.0	12.2	35.0	37.5	6.0	30.9	8.6	7.4	4.9	2.5	5.3	19.0	21.0
Bypass	%	–	–	–	–	–	–	–	–	–	–	–	–	–	–	–	–	–	–	–

Table 5
HEN for periods 1, 2 and 3 (Part 2).

Match	(i,j,k)	(1,CU,4)	(2,CU,4)	(3,CU,4)	(4,CU,4)	(5,CU,4)	(6,CU,4)	(7,CU,4)	(8,CU,4)	(9,CU,4)
Period 1										
A_S	m^2	4868.9	1917.8			1550.4		412.8	1611.0	–
$A_{i,j,k}$	m^2	3245.8	302.3	–	–	97.5	–	11.0	153.9	–
$A_{i,j,k}/A_S$	%	0.67	0.16	–	–	0.06	–	0.03	0.10	–
$Q_{i,j,k}$	kW	30,554.6	11,661.0	–	–	2074.0	–	435.9	1849.0	–
$Fh_{i,j,k}$		1.0	1.0	–	–	1.0	–	1.0	1.0	–
$Fc_{i,j,k}$				–	–		–			–
$Thin_{i,j,k}$	K	353.9	358.0	–	–	333.0	–	366.2	351.0	–
$Thout_{i,j,k}$	K	306.0	357.0	–	–	332.0	–	353.0	308.0	–
$Tcin_{i,j,k}$	K	298.0	298.0	–	–	298.0	–	298.0	298.0	–
$Tcout_{i,j,k}$	K	305.0	305.0	–	–	305.0	–	305.0	305.0	–
LMTD	K	13.6	55.9	–	–	30.8	–	57.5	17.4	–
Period 2										
A_S	m^2	3995.6	92.4		1550.4	135.9		116.1	335.7	150.1
$A_{i,j,k}$	m^2	2562.3	2.6	–	450.5	29.7	–	29.0	168.2	48.5
$A_{i,j,k}/A_S$	%	0.6	0.03	–	0.3	0.2	–	0.2	0.5	0.3
$Q_{i,j,k}$	kW	14,399.5	100.4	–	15,132.2	624.0	–	1346.0	2021.0	1772.8
$Fh_{i,j,k}$		1.0	1.0	–	1.0	1.0	–	1.0	1.0	1.0
$Fc_{i,j,k}$				–			–			
$Thin_{i,j,k}$	K	326.2	357.0	–	350.6	332.3	–	389.4	351.0	356.4
$Thout_{i,j,k}$	K	306.0	357.0	–	350.0	332.0	–	353.0	308.0	353.0
$Tcin_{i,j,k}$	K	298.0	298.0	–	298.0	298.0	–	298.0	298.0	298.0
$Tcout_{i,j,k}$	K	305.0	305.0	–	305.0	305.0	–	305.0	305.0	305.0
LMTD	K	8.1	55.4	–	48.7	30.5	–	67.4	17.4	53.0
Period 3										
A_S	m^2	1434.9	68.3	201.6	239.6	116.1		26.3	22.1	–
$A_{i,j,k}$	m^2	1434.9	68.3	201.6	239.6	116.1	–	26.3	22.1	–
$A_{i,j,k}/A_S$	%	1.0	1.0	1.0	1.0	1.0	–	1.0	1.0	–
$Q_{i,j,k}$	kW	4943.3	2616.8	7299.7	8024.5	2469.0	–	1167.2	98.7	–
$Fh_{i,j,k}$		1.0	1.0	1.0	1.0	1.0	–	1.0	1.0	–
$Fc_{i,j,k}$		–	–				–	–		–
$Thin_{i,j,k}$	K	312.3	357.2	354.1	350.3	333.0	–	382.2	309.9	–
$Thout_{i,j,k}$	K	306.0	357.0	354.0	350.0	332.0	–	353.0	308.0	–
$Tcin_{i,j,k}$	K	298.0	298.0	298.0	298.0	298.0	–	298.0	298.0	–
$Tcout_{i,j,k}$	K	305.0	305.0	305.0	305.0	305.0	–	305.0	305.0	–
LMTD	K	5.0	55.5	52.5	48.5	30.8	–	64.4	6.5	–

the capital cost of integrated HEN are equal to corresponding parameters of Period 3. Note that although the units of Period 3 are used in all periods, stream pairing is different in those devices depending on the period. In Tables 4–6 it is possible to observe the assigned area by the procedure for periods integration (A_s), the ratio between required area and assigned area ($A_{i,j,k}/A_s$) and the bypasses for cold streams in heat exchangers with surplus area. Table 8 presents the integrated HEN with assigned areas for each heat transfer device and matches in each period. Note that by using the methodology of Jiang and Chang [30] for obtaining a HEN with timesharing mechanisms, four heat exchangers have bypasses above 50% in Period 1. For Period 2, five cold streams have more than half of its flow rate bypassing heat exchangers. Regarding idleness, 12 and 2 devices, respectively, are not being used during Periods 1 and 2. However, the devices with idle periods present areas lower than 336 m^2, i.e., they entail an also small impact on the economic performance of the HEN. Moreover, when comparing Periods 1 and 2, only three devices have fixed service (i.e., the pair of streams does not change with the period of operation). The same number of heat exchangers with fixed services is observed when comparing Periods 1 and 3. When the comparison is made between Periods 2 and 3, it is observed that ten devices have fixed services. Periods 2 and 3 have more pairs in common. However, in most cases, the areas designed for these heat exchangers are not the same due to the difference in heat load, which implies that, with the change of period of operation, a different fraction of each cold stream should bypass its corresponding heat exchanger.

The procedure used to integrate the heat exchanger networks of all periods [30] does not require their duration, but the operating cost calculation depends on the operation time of the plant for each one of the described conditions. By using the strategy of Jiang and Chang [30] to integrate the HENs synthesized for each period into one multiperiod configuration, estimating such durations of periods is not required. On the other hand, TAC regards one year of operation under (a) given condition(s) with the multiperiod configuration. Thus, for a hypothetical situation where the operation time (5760 h/year) is equally divided among the operating conditions presented (in other words, each period lasts 1/3 of the total operation time), the operating cost of the integrated HEN is 12,688,561 USD/year.

Tables 9–11 compare the values of utilities demand, area and costs among the processes without any energy integration, with project energy integration and with energy integration proposed in this study for each period and with the integrated HEN. The integrated HEN presented in these tables is the HEN that integrates all periods. This HEN assumes the utility demand of proposed HEN for each period (that is,

Table 6
HEN for periods 1, 2 and 3 (Part 3).

Match	(*i,j,k*)	(HU,1,0)	(HU,2,0)	(HU,3,0)	(HU,4,0)	(HU,5,0)	(HU,6,0)	(HU,7,0)	(HU,8,0)	(HU,9,0)	(HU,10,0)
Period 1											
A_S	m^2	–	821.4	–	3588.1	1979.6	1823.7	1434.9	–	–	–
$A_{i,j,k}$	m^2	–	15.7	–	1047.9	304.0	168.5	77.8	–	–	–
$A_{i,j,k}/A_S$	%	–	0.02	–	0.29	0.15	0.09	0.05	–	–	–
$Q_{i,j,k}$	*kW*	–	1092.5	–	67,968.0	20,335.9	9856.0	3350.0	–	–	–
$Fh_{i,j,k}$		–		–					–	–	–
$Fc_{i,j,k}$		–	1.0	–	1.0	1.0	1.0	1.0	–	–	–
$Thin_{i,j,k}$	*K*	–	479.0	–	479.0	479.0	479.0	479.0	–	–	–
$Thout_{i,j,k}$	*K*	–	478.0	–	478.0	478.0	478.0	478.0	–	–	–
$Tcin_{i,j,k}$	*K*	–	377.2	–	384.0	381.1	379.0	411.0	–	–	–
$Tcout_{i,j,k}$	*K*	–	378.0	–	385.0	382.0	407.0	421.0	–	–	–
LMTD	*K*	–	100.9	–	94.0	97.0	84.8	62.4	–	–	–
Period 2											
A_S	m^2	–	68.3	26.3	1611.0	821.4	239.6	201.6	1908.4	1823.7	–
$A_{i,j,k}$	m^2	–	1.0	1.0	515.9	270.9	156.0	85.2	993.6	955.1	–
$A_{i,j,k}/A_S$	%	–	0.01	0.04	0.3	0.3	0.7	0.4	0.5	0.5	–
$Q_{i,j,k}$	*kW*	–	10.2	66.0	33,360.9	18,106.9	8879.2	3670.0	15,167.0	33,281.8	–
$Fh_{i,j,k}$		–	–	–	–	–	–	–	–	–	–
$Fc_{i,j,k}$		–	–	–	1.0	1.0	1.0	1.0	1.0	1.0	–
$Thin_{i,j,k}$	*K*	–	479.0	479.0	479.0	479.0	479.0	479.0	479.0	479.0	–
$Thout_{i,j,k}$	*K*	–	478.0	478.0	478.0	478.0	478.0	478.0	478.0	478.0	–
$Tcin_{i,j,k}$	*K*	–	378.0	361.9	384.6	381.2	384.0	411.0	439.0	378.4	–
$Tcout_{i,j,k}$	*K*	–	378.0	362.0	385.0	382.0	407.0	421.0	468.0	458.0	–
LMTD	*K*	–	100.5	116.5	93.7	96.9	82.5	62.4	22.1	50.5	–
Period 3											
A_S	m^2	–	–	–	335.7	–	150.1	92.4	1979.6	1823.7	–
$A_{i,j,k}$	m^2	–	–	–	335.7	–	150.1	92.4	1979.6	1823.7	–
$A_{i,j,k}/A_S$	%	–	–	–	1.0	–	1.0	1.0	1.0	1.0	–
$Q_{i,j,k}$	*kW*	–	–	–	21,686.1	–	8403.2	3980.0	30,218.0	60,885.1	–
$Fh_{i,j,k}$		–	–	–	–	–					–
$Fc_{i,j,k}$		–	–	–	1.0	–	1.0	1.0	1.0	1.0	–
$Thin_{i,j,k}$	*K*	–	–	–	479.0	–	479.0	479.0	479.0	479.0	–
$Thout_{i,j,k}$	*K*	–	–	–	478.0	–	478.0	478.0	478.0	478.0	–
$Tcin_{i,j,k}$	*K*	–	–	–	384.7	–	386.9	411.0	439.0	385.0	–
$Tcout_{i,j,k}$	*K*	–	–	–	385.0	–	407.0	421.0	468.0	458.0	–
LMTD	*K*	–	–	–	93.6	–	81.2	62.4	22.1	48.4	–

Table 7
Number of heat exchange devices, total area, capital cost (CC), operating cost (OC), and total annualized cost (TAC) for each period of operation.

	Units	Total required area (m^2)	CC (USD/year)	OC (USD/year)	Single-period solution TAC (USD/year)
Period 1	19	29,152.3	261,725	12,162,587	12,424,312
Period 2	29	40,839.7	382,785	12,562,729	12,945,514
Period 3	31	60,129.6	489,448	13,340,368	13,829,816

the biorefinery operates throughout the year under the same process condition) and the capital cost estimated by the final device set from the timesharing procedure. The operating cost has an order of magnitude of 10^2 greater than the investment cost. Thus, the TAC is more influenced by the operating cost. This information is important when comparing the TAC of processes with energy integration proposed in this study for each period with the integrated HEN. For Periods 1 and 2, the TAC for process with the integrated HEN is 2% and 1% higher than the TAC for processes with energy integration proposed for each period, respectively. For Period 3, the TAC for process with energy integration proposed individually is equal to process with the integrated HEN because, as already mentioned, the integrated HEN uses the set of devices designed for Period 3. Since the variations in TAC are small among these two processes (*i.e.*, with energy integration proposed for each period and with integrated HEN), a small additional investment allows the process to be more flexible. Moreover, the uncertainty in values of convective coefficients generated by the assumption that all convective coefficients are equal does not change significantly the optimal solution, since the TAC is little influenced by the investment cost. Other important inference about the HENs costs could be performed. In Period 1, cold stream 7 and, in Periods 2 and 3, cold streams 7 and 8 could not be integrated to other streams, given their high temperatures. Therefore, the TAC already has a built-in cost referring to hot utility consumption and to the area of the heaters that are placed on those

Table 8
Integrated HEN.

Exchanger label	Assigned area (m^2)	Period	Match (i, j, k)	Exchanger label	Assigned area (m^2)	Period	Match (i, j, k)
A	5449.2	1	1,3,3	Q	1434.9	1	HU,7,0
		2	3,3,3			2	4,3,4
		3	9,2,3			3	1,CU,5
B	5354.1	1	3,2,3	R	821.4	1	HU,2,0
		2	9,2,3			2	HU,5,0
		3	9,2,2			3	4,3,4
C	5309.1	1	1,2,1	S	412.8	1	7,CU,5
		2	1,9,2			2	5,10,1
		3	1,9,1			3	8,9,4
D	5231.8	1	3,3,4	T	335.7	1	–
		2	1,9,3			2	8,CU,5
		3	6,9,1			3	HU,4,0
E	4868.9	1	1,CU,5	U	239.6	1	–
		2	6,2,3			2	HU,6,0
		3	9,4,1			3	4,CU,5
F	4215.9	1	4,1,3	V	201.6	1	–
		2	9,4,2			2	HU,7,0
		3	1,3,2			3	3,CU,5
G	3995.6	1	6,2,2	W	184.8	1	–
		2	1,CU,5			2	7,5,3
		3	3,3,3			3	7,5,2
H	3630.3	1	6,5,1	X	150.1	1	–
		2	2,2,4			2	9,CU,5
		3	1,6,1			3	HU,6,0
I	3588.1	1	HU,4,0	Y	135.9	1	–
		2	1,5,1			2	5,CU,5
		3	1,9,3			3	3104
J	3432.1	1	3,1,2	Z	116.1	1	–
		2	3,1,1			2	7,CU,5
		3	2,2,4			3	5,CU,5
K	1979.6	1	HU,5,0	AA	92.4	1	–
		2	1,3,2			2	2,CU,5
		3	HU,8,0			3	HU,7,0
L	1917.8	1	2,CU,5	BB	68.3	1	–
		2	6,6,1			2	HU,2,0
		3	1,9,4			3	2,CU,5
M	1908.4	1	7,2,1	CC	26.3	1	–
		2	HU,8,0			2	HU,3,0
		3	3,1,1			3	7,CU,5
N	1823.7	1	HU,6,0	DD	22.1	1	–
		2	HU,9,0			2	–
		3	HU,9,0			3	8,CU,5
O	1611.0	1	8,CU,5	EE	21.6	1	–
		2	HU,4,0			2	–
		3	9,5,1			3	7,4,1
P	1550.4	1	5,CU,5				
		2	4,CU,5				
		3	9,2,4				

Table 9
Comparison of utility demand, area and costs among the processes without energy integration (S1), with project energy integration (S2), with energy integration proposed in this work (S3) and with the integrated HEN (S4) for Period 1.

Parameter	Period 1			
	S1	S2	S3	S4
CU (kW)	171,477	120,324	46,574	46,574
HU (kW)	227,505	176,352	102,602	102,602
Area (m^2)	8602.4	9782.4	29,152.3	60,129.6
Cost of utility (USD/year)	30,351,067	22,902,099	12,162,587	12,162,587
Cost of HEN (USD/year)	137,644	144,668	261,725	489,448
TAC (USD/year)	30,488,710	23,046,767	12,424,312	12,652,035

Table 10
Comparison of utility demand, area and costs among the processes without energy integration (S1), with project energy integration (S2), with energy integration proposed in this work (S3) and with the integrated HEN (S4) for Period 2.

Parameter	Period 2			
	S1	S2	S3	S4
CU (kW)	250,778	131,698	35,396	35,396
HU (kW)	327,924	208,844	112,542	112,542
Area (m^2)	12,656.7	14,722.4	40,839.7	60,129.6
Cost of utility (USD/year)	43,926,941	26,586,353	12,562,729	12,562,729
Cost of HEN (USD/year)	184,932	195,126	382,785	489,448
TAC (USD/year)	44,111,874	26,781,480	12,945,514	13,052,177

Table 11
Comparison of utility demand, area and costs among the processes without energy integration (S1), with project energy integration (S2), with energy integration proposed in this work (S3) and with the integrated HEN (S4) for Period 3.

Parameter	Period 3			
	S1	S2	S3	S4
CU (kW)	329,729	142,713	26,619	26,619
HU (kW)	428,282	241,266	125,172	125,172
Area (m^2)	14,623.6	19,647.7	60,129.6	60,129.6
Cost of utility (USD/year)	57,479,601	30,246,083	13,340,368	13,340,368
Cost of HEN (USD/year)	205,998	218,640	489,448	489,448
TAC (USD/year)	57,685,599	30,464,722	13,829,816	13,829,816

Table 12
Saving of utility cost, steam demand and TAC of processes with energy integration proposed in this study for each period (S3) and with the integrated HEN (S4) in relation to the processes without energy integration (S1) and with project energy integration (S2).

Saving (%)	Period 1				Period 2				Period 3			
	S3/S1	S3/S2	S4/S1	S4/S2	S3/S1	S3/S2	S4/S1	S4/S2	S3/S1	S3/S2	S4/S1	S4/S2
Cost of utility	59.93	46.89	59.93	46.89	71.40	52.75	71.40	52.75	76.79	55.89	76.79	55.89
HU	54.90	41.82	54.90	41.82	65.68	46.11	65.68	46.11	70.77	48.12	70.77	48.12
TAC	59.25	46.09	58.50	45.10	70.65	51.66	70.41	51.26	76.03	54.60	76.03	54.60

streams. The sum of the operating and capital costs associated to those streams is 0.3, 1.8 and 3.3 million USD/year for Periods 1, 2 and 3, respectively. These values represent 3%, 14% and 24% of TAC for HENs synthesized individually for Periods 1, 2 and 3. Thus, important percentage values of TAC are associated to operating and investment costs of streams that cannot be integrated, notably cold stream 8, due to its heat capacity.

Table 12 shows savings in utility cost, steam demand and TAC of processes without and with energy integration. Special attention is given to the process with the integrated HEN, because a multiperiod HEN design allows the biorefinery to operate with different bagasse fractions diverted to second generation ethanol production. Process with the integrated HEN for all periods presents reduction in TAC of 59%, 70% and 76% when compared to process without energy integration for Periods 1, 2 and 3, respectively. Process with the integrated HEN for all periods presents reduction in TAC of 45%, 51% and 55% when compared to process with project energy integration for Periods 1, 2 and 3, respectively. As the HEN that integrates all periods has the same utilities demand of proposed HEN for each period, the saving in steam will be equal. For these processes, reductions in steam consumption reach 55%, 66% and 71% when compared to process without energy integration for Periods 1, 2 and 3, respectively, and 42%, 46% and 48% when compared to process with project energy integration for Periods 1, 2 and 3, respectively. These values indicate energy integration turn possible that more bagasse (when compared to the same process without any energy integration and with project energy integration) can be deviated to second generation ethanol production or the cogeneration system. However, not all the bagasse saved by energy integration can be used to produce second generation ethanol, since the surplus 2G ethanol will imply greater steam demand. Therefore, only a fraction of the bagasse saved can be used in 2G ethanol production.

Fig. 5 shows the integrated HEN diagram, which includes energy exchanges of all periods. Note that the information above heat exchangers indicates the label of heat exchanger in integrated HEN for each match in Periods 1, 2 and 3, respectively. The symbol '–' refers to the absence of that match in the indicated period. The integrated HEN synthesized is complex and demands control, since the streams should be moved to the heat exchangers indicated on the integrated HEN. However, the multiperiod HEN approach allows changing operating conditions of the plant (that is, the multiperiod HEN is not rigid as a HEN synthesized for a specified period only). The synthesis of multiperiod HEN is very important for biorefineries, since 2G ethanol and electricity production can be vary according to market demand. This study is one of the first reports of energy integration applied to an actual large scale plant, which includes changing operating conditions.

5. Conclusion

Energy integration applied to sugarcane biorefinery showed reductions in TAC of HENs proposed when compared to the process without any energy integration and to the process with the typical energy integration project found in Brazilian plants. In the process with the integrated HEN, the saving in TAC can reach 76% when compared to the process without energy integration and 55% when compared to the process with the typical project energy integration. Furthermore, the process with the integrated HEN can save up to 71% and up to 48% of steam in relation to process without energy integration and with project energy integration, respectively. The reduction in steam demand allows less bagasse to be diverted to the cogeneration system, and then the bagasse surplus can be made available for second generation ethanol production. Moreover, since variations in TAC are small among processes with energy integration proposed for each period and with the integrated HEN, a relatively small additional capital investment provides greater flexibility to a process whose operating conditions regarding throughputs of main products are uncertain, since these are subject to market demands, environmental policies and technological advance.

Funding sources

The authors acknowledge the support from DEQ/UFSCar (Chemical Engineering Department, São Carlos Federal University), DEQ/UEM (Chemical Engineering Department, Maringá State University) and IFSP (Federal Institute of Education, Science and Technology of São Paulo) and the financial support from FAPESP (São Paulo State Research Funding Agency, Process 2013/21343-3), CAPES (Coordination for the Improvement of Higher Education Personnel, Brazil) and CNPq (National Council for Scientific and Technological Development, Brazil).

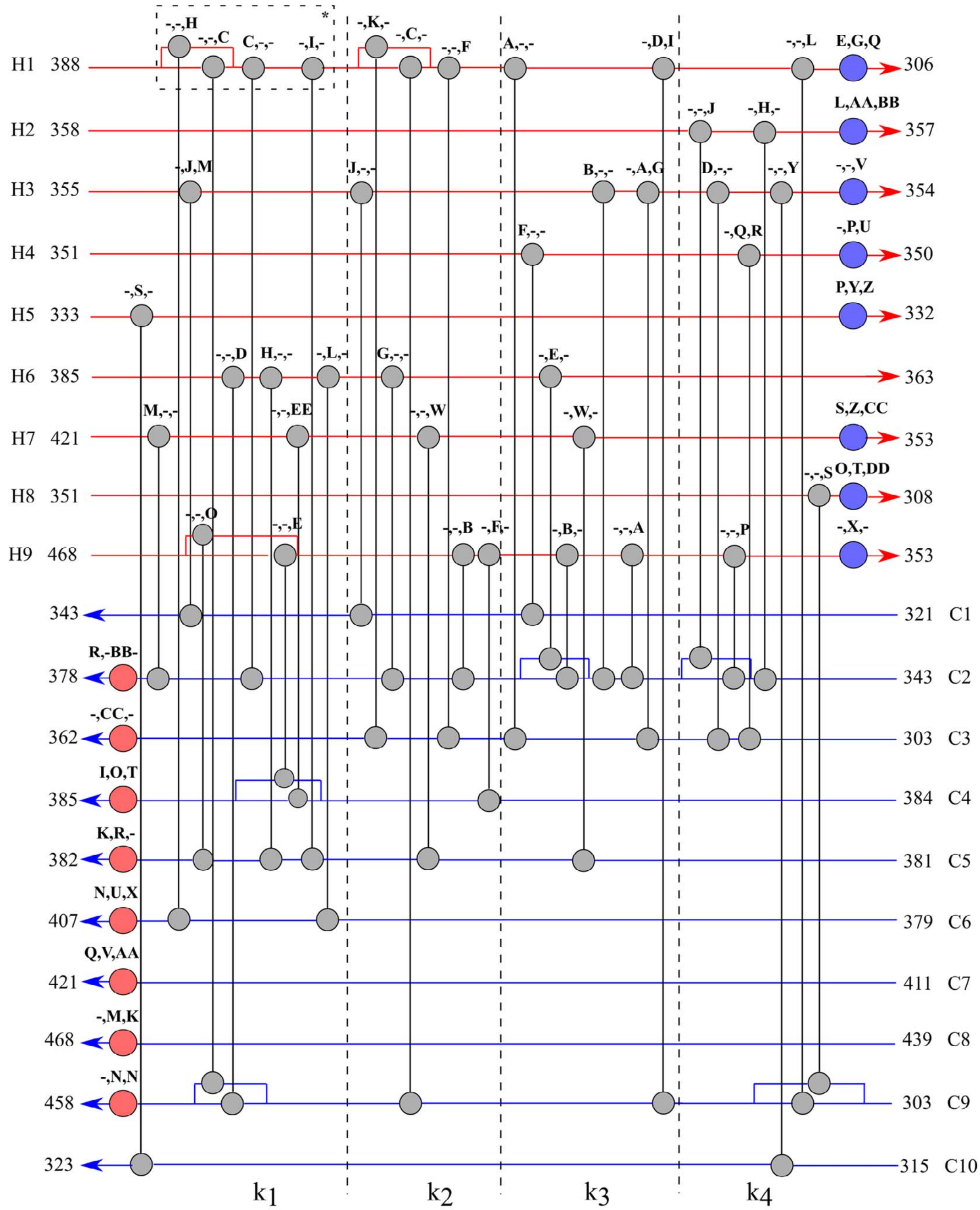

Labels and areas

A	B	C	D	E	F	G	H	I	J	K	L	M	N	O	P
5,449.2 m^2	5,354.1 m^2	5,309.1 m^2	5,231.8 m^2	4,868.9 m^2	4,215.9 m^2	3,995.6 m^2	3,630.3 m^2	3,588.1 m^2	3,432.1 m^2	1,979.6 m^2	1,917.8 m^2	1,908.4 m^2	1,823.7 m^2	1,611.0 m^2	1,550.4 m^2
Q	R	S	T	U	V	W	X	Y	Z	AA	BB	CC	DD	EE	
1,434.9 m^2	821.4 m^2	412.8 m^2	335.7 m^2	239.6 m^2	201.6 m^2	184.8 m^2	150.1 m^2	135.9 m^2	116.1 m^2	92.4 m^2	68.3 m^2	26.3 m^2	22.1 m^2	21.6 m^2	

*Note: No splits are represented because these macthes never take place in the same period simultaneously.

Fig. 5. Integrated HEN for all periods.

Appendix A

This section describes the equations of the MINLP model used in this study.

A.1. Model equations

A.1.1. Objective function to be minimized

$$C_{\text{total}} = \sum_i Ccu_i + \sum_j Chu_j + \sum_i \sum_j \sum_k z_{i,j,k} \cdot (a + b \cdot A^{c}_{i,j,k}) + \sum_i zcu_i \cdot (a + b \cdot Acu_i^{c}) + \sum_j zhu_j \cdot (a + b \cdot Ahu_j^{c}), \quad i \in N_H, j \in N_C, k \in N_S \tag{A.1}$$

A.1.2. Energy balance in the mixers

$$Thmix_{i,1} = Th_i^0, \quad i \in N_H \tag{A.2}$$

$$Tcmix_{j,K+1} = Tc_i^0, \quad j \in N_C \tag{A.3}$$

$$Thmix_{i,k+1} = Thmix_{i,k} - \frac{\sum_{j \in N_C} z_{i,j,k} Q_{i,j,k}}{CPh_i}, \quad i \in N_H, j \in N_C, k \in N_S \tag{A.4}$$

$$Tcmix_{j,k} = Tcmix_{j,k+1} + \frac{\sum_{i \in N_H} z_{i,j,k} Q_{i,j,k}}{CPc_j}, \quad i \in N_H, j \in N_C, k \in N_S \tag{A.5}$$

A.1.3. Energy balance in the heat exchangers

$$Thin_{i,j,k} = Thmix_{i,k}, \quad i \in N_H, j \in N_C, k \in N_S \tag{A.6}$$

$$Tcin_{i,j,k} = Tcmix_{j,k+1}, \quad i \in N_H, j \in N_C, k \in N_S \tag{A.7}$$

$$Thout_{i,j,k} = Thmix_{i,k} - \frac{z_{i,j,k} Q_{i,j,k}}{Fh_{i,j,k} CPh_i}, \quad i \in N_H, j \in N_C, k \in N_S \tag{A.8}$$

$$Tcout_{i,j,k} = Tcmix_{j,k+1} + \frac{z_{i,j,k} Q_{i,j,k}}{Fc_{i,j,k} CPc_j}, \quad i \in N_H, j \in N_C, k \in N_S \tag{A.9}$$

A.1.4. Energy balance for utilities

$$Qcu_i = CPh_i (Th_i^0 - Th_i^{final}) - \sum_k \sum_j z_{i,j,k} Q_{i,j,k}, \quad i \in N_H, j \in N_C, k \in N_S \tag{A.10}$$

$$Qhu_j = CPc_j (Tc_j^{final} - Tc_j^0) - \sum_k \sum_i z_{i,j,k} Q_{i,j,k}, \quad i \in N_H, j \in N_C, k \in N_S \tag{A.11}$$

If Qcu_i is different from zero, then $zcu_i = 1$, otherwise $zcu_i = 0$. If Qhu_j is different from zero, then $zhu_j = 1$, otherwise $zhu_j = 0$.

$$Thcuin_i = Thmix_{i,K+1}, \quad i \in N_H \tag{A.12}$$

$$Tchuin_j = Tcmix_{j,1}, \quad j \in N_C \tag{A.13}$$

A.1.5. LMTDA.1.5.1 For process streams.

$$\theta^{(1)}_{i,j,k} = Thin_{i,j,k} - Tcout_{i,j,k}, \quad i \in N_H, j \in N_C, k \in N_S \tag{A.14}$$

$$\theta^{(2)}_{i,j,k} = Thout_{i,j,k} - Tcin_{i,j,k}, \quad i \in N_H, j \in N_C, k \in N_S \tag{A.15}$$

$$LMTD_{i,j,k} = \frac{\theta_{i,j,k}^{(1)} - \theta_{i,j,k}^{(2)}}{\ln\left(\frac{\theta_{i,j,k}^{(1)}}{\theta_{i,j,k}^{(2)}}\right)}, \quad i \in N_H, j \in N_C, k \in N_S \tag{A.16}$$

If $\theta_{i,j,k}^{(1)}$ is equal to $\theta_{i,j,k}^{(2)}$, then $\theta_{i,j,k}^{(1)} = LMTD_{i,j,k}$.A.1.5.2 For cold utility.

$$\theta_i^{(1)} = Thcuin_{i,} - Twout, \quad i \in N_H \tag{A.17}$$

$$\theta_i^{(2)} = Th_i^{final} - Twin, \quad i \in N_H, j \in N_C, k \in N_S \tag{A.18}$$

$$LMTD_{i,cu} = \frac{\theta_i^{(1)} - \theta_i^{(2)}}{\ln\left(\frac{\theta_i^{(1)}}{\theta_i^{(2)}}\right)}, \quad i \in N_H \tag{A.19}$$

If $\theta_i^{(1)}$ is equal to $\theta_i^{(2)}$, then $\theta_i^{(1)} = LMTD_{i,cu}$.A.1.5.3 For hot utility.

$$\theta_j^{(1)} = Tsout - Tchuin_j, \quad j \in N_C \tag{A.20}$$

$$\theta_j^{(2)} = Tsin - Tc_j^{final}, \quad j \in N_C \tag{A.21}$$

$$LMTD_{j,hu} = \frac{\theta_j^{(1)} - \theta_j^{(2)}}{\ln\left(\frac{\theta_j^{(1)}}{\theta_j^{(2)}}\right)}, \quad i \in N_H, j \in N_C, k \in N_S \tag{A.22}$$

If $\theta_j^{(1)}$ is equal to $\theta_j^{(2)}$, then $\theta_j^{(1)} = LMTD_{j,hu}$.

A.1.6. Overall heat transfer coefficientA.1.6.1 For process streams.

$$U_{i,j} = \frac{1}{\frac{1}{hh_i} + \frac{1}{hc_j}}, \quad i \in N_H, j \in N_C \tag{A.23}$$

A.1.6.2 For cold utility.

$$U_{i,cu} = \frac{1}{\frac{1}{hh_i} + \frac{1}{hcu}}, \quad i \in N_H \tag{A.24}$$

A.1.6.3 For hot utility.

$$U_{j,hu} = \frac{1}{\frac{1}{hc_j} + \frac{1}{hhu}}, \quad j \in N_C \tag{A.25}$$

A.1.7. AreaA.1.7.1 For process streams.

$$A_{i,j,k} = \frac{z_{i,j,k} Q_{i,j,k}}{U_{i,j,k} LMTD_{i,j,k}}, \quad i \in N_H, j \in N_C, k \in N_S \tag{A.26}$$

A.1.7.2 For cold utility.

$$A_{i,cu} = \frac{zcu_i Qcu_i}{U_{i,cu} LMTD_{i,cu}}, \quad i \in N_H \tag{A.27}$$

A.1.7.3 For hot utility.

$$A_{j,hu} = \frac{zhu_j Qhu_j}{U_{j,hu} LMTD_{j,hu}}, \quad j \in N_C \tag{A.28}$$

A.1.8. Constraints

$$\sum_j Fh_{i,j,k} = 1, \quad i \in N_H, j \in N_C, k \in N_S \tag{A.29}$$

$$\sum_i Fc_{i,j,k} = 1, \quad i \in N_H, j \in N_C, k \in N_S \tag{A.30}$$

$$Thin_{i,j,k} \geqslant Tcout_{i,j,k} + EMAT,$$
$$i \in N_H, j \in N_C, k \in N_S \tag{A.31}$$

$$Thout_{i,j,k} \geqslant Tcin_{i,j,k} + EMAT,\quad i \in N_H, j \in N_C, k \in N_S \tag{A.32}$$

$$0 \leqslant Qcu_i \leqslant CPh_i \cdot (Th_i^0 - Th_i^{final}),\quad i \in N_H \tag{A.33}$$

$$0 \leqslant Qhu_j \leqslant CPc_j \cdot (Th_j^{final} - Th_j^0),\quad j \in N_C \tag{A.34}$$

$$Thmix_{i,k} \geqslant Thmix_{i,k+1},\quad i \in N_H, k \in N_S \tag{A.35}$$

$$Thmix_{i,K+1} \geqslant Th_i^{final},\quad i \in N_H, k \in N_S \tag{A.36}$$

$$Tcmix_{j,k} \geqslant Tcmix_{j,k+1},\quad j \in N_C, k \in N_S \tag{A.37}$$

$$Tc_j^{final} \geqslant Tcmix_{j,1},\quad j \in N_C, k \in N_S \tag{A.38}$$

$$\theta^{(1)}_{i,j,k} \geqslant EMAT,\quad i \in N_H, j \in N_C, k \in N_S \tag{A.39}$$

$$\theta^{(2)}_{i,j} \geqslant EMAT,\quad i \in N_H, j \in N_C, k \in N_S \tag{A.40}$$

$$\theta^{(1)}_{i,cu} \geqslant EMAT,\quad i \in N_H \tag{A.41}$$

$$\theta^{(2)}_{i,cu} \geqslant EMAT,\quad i \in N_H \tag{A.42}$$

$$\theta^{(1)}_{i,cu} \geqslant EMAT,\quad j \in N_C \tag{A.43}$$

$$\theta^{(2)}_{i,hu} \geqslant EMAT,\quad j \in N_C \tag{A.44}$$

$$Thout_{i,j,k} \geqslant Th_i^{final},\quad i \in N_H, j \in N_C, k \in N_S \tag{A.45}$$

$$Tc_j^{final} \geqslant Tcout_{i,j,k},\quad i \in N_H, j \in N_C, k \in N_S \tag{A.46}$$

$$CPh_i(Th_i^0 - Th_i^{final}) \geqslant \textstyle\sum_k \sum_j z_{i,j,k} Q_{i,j,k},\quad i \in N_H, j \in N_C, k \in N_S \tag{A.47}$$

$$CPc_j(Tc_j^{final} - Tc_j^0) \geqslant \textstyle\sum_k \sum_i z_{i,j,k} Q_{i,j,k},\quad i \in N_H, j \in N_C, k \in N_S \tag{A.48}$$

A.1.9. Bounds

Eqs. (A.49)–(A.53) present the bounds of the variables estimated by SA-RFO algorithm.

$$Qmax_{i,j,k} = \ min\begin{pmatrix} CP_i(Th_i^0 - Th_i^{final}), \\ CP_j(Tc_j^{final} - Tc_j^0) \end{pmatrix},\quad i \in N_H, j \in N_C, k \in N_S \tag{A.49}$$

$$0 \leqslant Q_{i,j,k} \leqslant Qmax_{i,j,k},\quad i \in N_H, j \in N_C, k \in N_S \tag{A.50}$$

$$0 \leqslant z_{i,j,k} \leqslant 1,\quad i \in N_H, j \in N_C, k \in N_S \tag{A.51}$$

$$0 \leqslant Fh_{i,j,k} \leqslant 1,\quad i \in N_H, j \in N_C, k \in N_S \tag{A.52}$$

$$0 \leqslant Fc_{i,j,k} \leqslant 1,\quad i \in N_H, j \in N_C, k \in N_S \tag{A.53}$$

Appendix B

This section describes the timesharing procedure for the synthesis of multiperiod HEN.

1. Create an ordered list, in descending order, including all heat exchangers areas for all periods;
2. Select the first area from the ordered list and allocate the corresponding device to the multiperiod HEN;
3. Identify the largest area in each period and assign the corresponding process streams and stage in the superstructure to the device that was allocated in the HEN in Step 2;
4. Eliminate from the ordered list the areas identified in Steps 2 and 3;
5. Check the list. If the list is empty, end the procedure. Otherwise, return to Step 2.

Appendix C. Supplementary material

Supporting Information is provided with equations for calculating the number of variables of MINLP model and main parameters and products outputs for the sugarcane biorefinery. Supplementary data associated with this article can be found, in the online version, at http://dx.doi.org/10.1016/j.apenergy.2017.11.020.

References

[1] Dias MOS, Junqueira TL, Cavalett O, Pavanello LG, Cunha MP, Jesus CDF, et al. Biorefineries for the production of first and second generation ethanol and electricity from sugarcane. Appl Energy 2013;109:72–8. http://dx.doi.org/10.1016/j.apenergy.2013.03.081.

[2] Dantas GA, Legey LFL, Mazzone A. Energy from sugarcane bagasse in Brazil: an assessment of the productivity and cost of different technological routes. Renew Sustain Energy Rev 2013;21:356–64. http://dx.doi.org/10.1016/j.rser.2012.11.080.

[3] Furlan FF, Filho R, Pinto FH, Costa CB, Cruz AJ, Giordano RL, et al. Bioelectricity versus bioethanol from sugarcane bagasse: is it worth being flexible? Biotechnol Biofuels 2013;6:142. http://dx.doi.org/10.1186/1754-6834-6-142.

[4] Jonker JGG, van der Hilst F, Junginger HM, Cavalett O, Chagas MF, Faaij APC. Outlook for ethanol production costs in Brazil up to 2030, for different biomass crops and industrial technologies. Appl Energy 2015;147:593–610. http://dx.doi.org/10.1016/j.apenergy.2015.01.090.

[5] Bechara R, Gomez A, Saint-Antonin V, Schweitzer J-M, Maréchal F. Methodology for the design and comparison of optimal production configurations of first and first and second generation ethanol with power. Appl Energy 2016;184:247–65. http://dx.doi.org/10.1016/j.apenergy.2016.09.100.

[6] Borba CBC, Potrich E, Cruz AJG. Multiobjective optimization of a sugarcane biorefinery involving process and environmental aspects. Renew Energy 2016;96:1142–52. http://dx.doi.org/10.1016/J.RENENE.2015.10.043.

[7] Barbosa Larissa de Souza Noel Simas, Hytönen E, Vainikka P. Carbon mass balance in sugarcane biorefineries in Brazil for evaluating carbon capture and utilization opportunities. Biomass Bioenergy 2017;105:351–63. http://dx.doi.org/10.1016/J.BIOMBIOE.2017.07.015.

[8] Mendes FM, Dias MOS, Ferraz A, Milagres AMF, Santos JC, Bonomi A. Techno-economic impacts of varied compositional profiles of sugarcane experimental hybrids on a biorefinery producing sugar, ethanol and electricity. Chem Eng Res Des 2017;125:72–8. http://dx.doi.org/10.1016/J.CHERD.2017.06.023.

[9] Papoulias SA, Grossmann IE. A structural optimization approach in process synthesis—II. Comput Chem Eng 1983;7:707–21. http://dx.doi.org/10.1016/0098-1354(83)85023-6.

[10] Ravagnani MASS, Caballero Suárez JA. Redes de cambiadores de calor. Publicaciones de la Universidad de Alicante; 2012.

[11] Yee TF, Grossmann IE. Simultaneous optimization models for heat integration—II. Heat exchanger network synthesis. Comput Chem Eng 1990;14:1165–84. http://dx.doi.org/10.1016/0098-1354(90)85010-8.

[12] Lewin DR. A generalized method for HEN synthesis using stochastic optimization—II. The synthesis of cost-optimal networks. Comput Chem Eng 1998;22:1387–405. http://dx.doi.org/10.1016/S0098-1354(98)00221-X.

[13] Martelli E, Mian A, Maréchal F. MINLP model and two-level algorithm for the simultaneous synthesis of heat exchanger networks and utility systems. Comput Aided Chem Eng 2015;37:1979–84. http://dx.doi.org/10.1016/B978-0-444-63576-1.50024-8.

[14] Pavão LV, Costa CBB, da Ravagnani MASS, Jiménez L. Large-scale heat exchanger networks synthesis using simulated annealing and the novel rocket fireworks optimization. AIChE J 2017;63:1582–601. http://dx.doi.org/10.1002/aic.15524.

[15] Yerramsetty KM, Murty CVS. Synthesis of cost-optimal heat exchanger networks using differential evolution. Comput Chem Eng 2008;32:1861–76. http://dx.doi.org/10.1016/j.compchemeng.2007.10.005.

[16] Khorasany RM, Fesanghary M. A novel approach for synthesis of cost-optimal heat exchanger networks. Comput Chem Eng 2009;33:1363–70. http://dx.doi.org/10.1016/j.compchemeng.2008.12.004.

[17] Chen X, Zhaohua L, Yang J, Shao Z, Zhu L. Nested tabu search (TS) and sequential quadratic programming (SQP) method combined with adaptive model reformulation for heat exchanger network synthesis (HENS). Ind Eng Chem Res 2008. http://dx.doi.org/10.1021/IE0712450.

[18] Luo X, Wen Q-Y, Fieg G. A hybrid genetic algorithm for synthesis of heat exchanger networks. Comput Chem Eng 2009;33:1169–81. http://dx.doi.org/10.1016/j.compchemeng.2008.12.003.

[19] Pavão LV, Costa CBB, da Ravagnani MASS. Automated heat exchanger network synthesis by using hybrid natural algorithms and parallel processing. Comput Chem Eng 2016;94:370–86. http://dx.doi.org/10.1016/j.compchemeng.2016.08.009.

[20] Pavão LV, Costa CBB, Ravagnani MASS. Heat exchanger network synthesis without stream splits using parallelized and simplified simulated annealing and particle swarm optimization. Chem Eng Sci 2017;158:96–107. http://dx.doi.org/10.1016/j.ces.2016.09.030.

[21] Tjoe TN, Linnhoff B. Using pinch technology for process retrofit. Chem Eng 1986;93:47–60.

[22] Ravagnani MASS, Módenes AN. Heat exchanger networks with multiple periods of operation. Braz J Chem Eng 1996;13:71–84.

[23] Floudas CA, Grossmann IE. Synthesis of flexible heat exchanger networks for multiperiod operation. Comput Chem Eng 1986;10:153–68. http://dx.doi.org/10.1016/0098-1354(86)85027-X.

[24] Floudas CA, Grossmann IE. Automatic generation of multiperiod heat exchanger network configurations. Comput Chem Eng 1987;11:123–42. http://dx.doi.org/10.1016/0098-1354(87)80013-3.

[25] Floudas CA, Ciric AR, Grossmann IE. Automatic synthesis of optimum heat exchanger network configurations. AIChE J 1986;32:276–90. http://dx.doi.org/10.1002/aic.690320215.

[26] Miranda CB, Costa CBB, Caballero JA, Ravagnani MASS. Optimal synthesis of multiperiod heat exchanger networks: a sequential approach. Appl Therm Eng 2017;115:1187–202. http://dx.doi.org/10.1016/J.APPLTHERMALENG.2016.10.003.

[27] Aaltola J. Simultaneous synthesis of flexible heat exchanger network. Appl Therm Eng 2002;22:907–18. http://dx.doi.org/10.1016/S1359-4311(02)00008-X.

[28] Zhang WVN. Design of flexible heat exchanger network for multi-period operation. Chem Eng Sci 2006;61:7730–53. http://dx.doi.org/10.1016/j.ces.2006.08.043.

[29] Pavão LV, Miranda CB, Costa CBB, Ravagnani MASS. Efficient multiperiod heat exchanger network synthesis using a meta-heuristic approach. Energy 2017. http://dx.doi.org/10.1016/j.energy.2017.09.147.

[30] Jiang D, Chang C-T. A new approach to generate flexible multiperiod heat exchanger network designs with timesharing mechanisms. Ind Eng Chem Res 2013. http://dx.doi.org/10.1021/ie301075v. 130305090342002.

[31] Jiang D, Chang C-T. An algorithmic approach to generate timesharing schemes for multi-period HEN designs. Chem Eng Res Des 2015;93:402–10. http://dx.doi.org/10.1016/j.cherd.2014.04.011.

[32] Miranda CB, Costa CBB, Caballero JA, Ravagnani MASS. Heat exchanger network optimization for multiple period operations. Ind Eng Chem Res 2016;55:10301–15. http://dx.doi.org/10.1021/acs.iecr.6b01117.

[33] Pavão LV, Miranda CB, Costa CBB, Ravagnani MASS. Synthesis of multiperiod heat exchanger networks with timesharing mechanisms using meta-heuristics. Appl Therm Eng 2018;128:637–52. http://dx.doi.org/10.1016/j.applthermaleng.2017.09.002.

[34] Pina EA, Palacios-Bereche R, Chavez-Rodrigues MF, Ensinas AV, Modesto M, Nebra SA. Thermal integration of different plant configurations of sugar and ethanol production from sugarcane. Chem Eng Trans 2014;39:1147–52. http://dx.doi.org/10.3303/CET1439192.

[35] Oliveira CM, Cruz AJG, Costa CBB. Improving second generation bioethanol production in sugarcane biorefineries through energy integration. Appl Therm Eng 2016;109:819–27. http://dx.doi.org/10.1016/j.applthermaleng.2014.11.016.

[36] Pavão LV, Costa CBB, da Ravagnani MASS, Jiménez L. Costs and environmental impacts multi-objective heat exchanger networks synthesis using a meta-heuristic approach. Appl Energy 2017;203:304–20. http://dx.doi.org/10.1016/j.apenergy.2017.06.015.

[37] Kirkpatrick S, Gelatt CD, Vecchi MP. Optimization by simulated annealing. Science (80-) 1983;220.

[38] Kennedy J, Eberhart R. Particle swarm optimization. Proc IEEE Int Conf Neural Networks 1995:1942–8.

[39] Furlan FF, Costa CBB, Cruz AJG, Secchi AR, Soares RP, Giordano RC. Integrated tool for simulation and optimization of a first and second generation ethanol-from-sugarcane production plant. Comput Aided Chem Eng 2012;30:81–5. http://dx.doi.org/10.1016/B978-0-444-59519-5.50017-4.

[40] Costa CBB, Furlan FF, Cruz AJG, de Lima Camargo Giordano R, de Campos Giordano R. Integrated production of 1G–2G bioethanol and bioelectricity from sugarcane: impact of bagasse pretreatment processes. Biofuels in Brazil, Cham: Springer International Publishing; 2014. p. 85–95. http://dx.doi.org/10.1007/978-3-319-05020-1_5.

[41] Ensinas AV. Energy integration and thermo-economic optimization applied to the industrial process of sugar and ethanol production from sugarcane (in Portuguese). PhD Thesis (Chemical Engineering), State University of Campinas; 2008.

[42] US. A best practices steam technical brief: how to calculate the true cost of steam. Washington: Department of Energy; 2003.

[43] FGV. IGPM index. IGPM Index 2017. <http://portalibre.fgv.br/> [accessed January 31, 2017].

[44] Hall SG, Ahmad S, Smith R. Capital cost targets for heat exchanger networks comprising mixed materials of construction, pressure ratings and exchanger types. Comput Chem Eng 1990;14:319–35. http://dx.doi.org/10.1016/0098-1354(90)87069-2.

References

PAVÃO, L. V.; COSTA, C. B. B.; RAVAGNANI, M. A. da S. S.; JIMÉNEZ, L. Large-scale heat exchanger networks synthesis using simulated annealing and the novel rocket fireworks optimization. AIChE Journal, v. 63, n. 5, p. 1582–1601, 2017.

PAVÃO, L. V.; MIRANDA, C. B.; COSTA, C. B. B.; RAVAGNANI, M. A. S. S. Efficient multiperiod heat exchanger network synthesis using a meta-heuristic approach. Energy, v. 142, p. 356–372, 2018a.

PAVÃO, L. V; MIRANDA, C. B.; COSTA, C. B. B.; RAVAGNANI, M. A. S. S. Synthesis of multiperiod heat exchanger networks with timesharing mechanisms using meta-heuristics. Applied Thermal Engineering, v. 128, p. 637–652, 2018b.

Chapter 5

Energy Integration of a Sugarcane Biorefinery using Tabu Search and Particle Swarm Optimization

The results of energy integration presented in the previous chapter demonstrated the potential of this process integration technique in the sugarcane biorefinery, which allows contributing to 1G/2G ethanol production process. However, among proposals of this thesis is the synthesis of heat exchanger networks (HENs) to more than one biorefinery case study, as well as the application of different mathematical methods to solve HEN problems. To meet this objective, a hybrid method composed by Tabu Search (TS) and Particle Swarm Optimization (PSO) was proposed. Both methods, TS and PSO, are simple techniques to be implemented and have already been used by other authors in the HEN synthesis. The Tabu Search was used alone by Lin and Miler (2004) and combining it with SQP method by Chen et al. (2008). The Particle Swarm Optimization has been used alone in the HEN synthesis (SILVA, RAVAGNANI and BISCAIA, 2008; SILVA et al., 2010), as well as combining it with other algorithms (PAVÃO; COSTA; RAVAGNANI, 2016, 2017; PAVÃO et al., 2017a,b,c, 2018a,b). Although those works did not combine TS and PSO, such methods have proven, separately, to be able for HEN synthesis. This chapter presents the HEN synthesis in three industrial case studies of biorefineries using TS and PSO algorithms. The results of this approach are presented in the following text entitled “Synthesis of heat exchanger networks for biorefineries using the hybrid meta-heuristic of Tabu Search and Particle Swarm Optimization”. It was structured into five main topics: introduction; mathematical formulation; biorefinery description and data of case study; results and discussions; and conclusion. To maintain the thesis text more concise, details on description of biorefinery and mathematical model equations are not presented in this chapter, but can be found in Chapters 3 and 4. As will be demonstrated along this chapter, SA-RFO method presented better results than PSO and TS-PSO. A brief comparison of results achieved for Case Study 1 using PSO, SA-RFO and TS-PSO approaches is anticipated in Table 5. Despite the outperformance of SA-RFO, the solutions obtained via SA-RFO and via TS-PSO are very similar (*i.e.*, both methods are good strategies to achieve significant savings and solve large-scale HEN synthesis problems).

Table 5. Compilation of results for Case Study 1 using PSO, SA-RFO and TS-PSO methods.

		PSO			SA-RFO			TS-PSO		
Period	**Process**	**OC (USD/year)**	**CC (USD/year)**	**TAC (USD/year)**	**OC (USD/year)**	**CC (USD/year)**	**TAC (USD/year)**	**OC (USD/year)**	**CC (USD/year)**	**TAC (USD/year)**
P1	**S1**	30,351,067	137,644	30,488,710	30,351,067	137,644	30,488,710	30,351,067	137,644	30,488,710
	S2	22,902,099	144,668	23,046,767	22,902,099	144,668	23,046,767	22,902,099	144,668	23,046,767
	S3	19,427,278	186,540	19,613,818	12,162,587	261,725	12,424,312	12,468,797	279,117	12,747,915
	S4	19,427,278	236,570	19,663,848	12,162,587	489,448	12,652,035	12,468,797	423,534	12,892,331
P2	**S1**	43,926,941	184,932	44,111,874	43,926,941	184,932	44,111,874	43,926,941	184,932	44,111,874
	S2	26,586,353	195,126	26,781,480	26,586,353	195,126	26,781,480	26,586,353	195,126	26,781,480
	S3	25,300,954	217,915	25,518,869	12,562,729	382,785	12,945,514	12,911,180	386,761	13,297,942
	S4	25,300,954	236,570	25,537,524	12,562,729	489,448	13,052,177	12,911,180	423,534	13,334,714
P3	**S1**	57,479,601	205,998	57,685,599	57,479,601	205,998	57,685,599	57,479,601	205,998	57,685,599
	S2	30,246,083	218,640	30,464,722	30,246,083	218,640	30,464,722	30,246,083	218,640	30,464,722
	S3	27,590,386	233,407	27,823,794	13,340,368	489,448	13,829,816	13,963,062	420,427	14,383,489
	S4	27,590,386	236,570	27,826,957	13,340,368	489,448	13,829,816	13,963,062	423,534	14,386,596

Synthesis of heat exchanger networks for biorefineries using the hybrid meta-heuristic of Tabu Search and Particle Swarm Optimization

Oliveira, C. M.[a]; Cruz, A. J. G.[a]; Costa, C. B. B.[b]

[a] Chemical Engineering Department, Federal University of São Carlos, Rodovia Washington Luís, km 235, 13565-905 São Carlos, São Paulo, Brazil

[b] Chemical Engineering Department, State University of Maringá, Av. Colombo 5790, Bloco D-90, 87020-900 Maringá, Paraná, Brazil

Abstract

Energy integration techniques provide improvements to industrial processes in economic and environmental terms. Additionally to mentioned advantages, energy integration in sugarcane biorefineries allows diverting more bagasse for second generation ethanol or electricity production, depending on market demand. Variations in process conditions influence the design of HEN (Heat Exchanger Network). To handle this problem, concepts of synthesis of HEN with multiple operation periods were used. Three industrial case studies of energy integration for sugarcane biorefineries were performed, which differ whether xylose fraction is or is not exploited, to produce ethanol or biogas. In this work, the multiperiod HEN synthesis problem is solved for each period separately, using a Mixed Integer Nonlinear Programming (MINLP) model, and timesharing mechanisms employed in the literature are used to design the HEN that integrates all periods. Each period has a different operating condition and, for solving the MINLP problem, a novel hybrid meta-heuristic approach was used. It combines Tabu Search at upper level and Particle Swarm Optimization at lower level optimization. For all cases, the results showed a notable reduction in Total Annualized Cost (TAC) of HENs proposed in this study compared to processes without any energy integration and with project energy integration (*i.e.*, process existing in Brazilian plants). This decrease in TAC can reach 75% in the process with the multiperiod HEN, when compared to the process without energy integration, and 53% when compared to the process with project energy integration. Moreover, savings in steam demand in the process with the multiperiod HEN can save up to 71% and 47% in relation to processes without energy integration and with project energy integration, respectively. These results demonstrate the potential of energy integration in sugarcane biorefineries, which contributes to 1G/2G ethanol production process.

Keyword: Sugarcane Biorefinery, 1G/2G Ethanol, Multiperiod Heat Exchanger Network, Tabu Search, Particle Swarm Optimization.

5.1 Introduction

Biorefinery can be defined as an installation that integrates bioenergy, biofuel and biochemical production from biomass. Thus, the goal of a biorefinery is to convert a portion of that material into useful products by appropriate processes, which add value to the supply chain. In Brazil, the use of sugarcane biomass has great importance to the industrial sector. The sucro-energetic sector has, as its main products, the sugar and the first generation ethanol (1G) and, as one of its by-products, the biomass, which can be burned in boilers in order to generate electricity in cogeneration systems or hydrolyzed in order to produce second generation ethanol (2G). The development of second generation fuels, such as ethanol, allows increasing the ethanol production per cultivation area and the energy security. However, there are gaps to turn 2G ethanol viable. Some of these challenges are technological developments to help reducing costs of enzymes for co-fermentation or to improve bagasse pretreatments, process optimization, and energy efficiency, among others. In plants, the exchange of thermal energy among process streams, by means of a Heat Exchanger Network (HEN), is an efficient alternative to save energy.

Prices of electricity and ethanol vary according to market demand and even due to environmental policies or technological advances. It implies that operating conditions as well as utilities consumption can vary in the biorefinery. Thus, the heat exchanger network synthesized should be able to meet the different operating conditions. A common practice to deal with seasonal alterations in operating conditions in plants subject to this occurrence is to synthesize a multiperiod HEN. Under that concept, each period represents a different process condition and the multiperiod HEN is able to operate under these established conditions. The different process conditions are represented by variations in temperature, heat capacity, heat transfer convective coefficient or/and number of streams. Although the multiperiod HEN ensures certain flexibility to the process (*i.e.*, the process is not rigid and can meet different operating conditions), the flexibility concept is broader, since this concept includes variations in other process parameters (*e.g.*, the flexible HEN enables alterations in costs of utilities, which are not allowed in the multiperiod HEN). Sequential or simultaneous approaches can be used to solve problems of multiperiod HEN synthesis.

Sequential approach via Mixed Integer Linear Programming (MILP) mathematical formulation for multiperiod HEN synthesis was presented by Floudas and Grossmann (1986). It was based on the Papoulias and Grossmann (1983) model. For each period, the minimum utilities cost is achieved. Then, the MILP model is used to obtain the minimum number of units of the HEN and the stream matches for all periods, subject to the minimum utility consumption for each period. Afterwards, the automatic generation of minimum investment cost for a multiperiod model was developed by Floudas and Grossmann (1987), based on the NLP model for single-period of Floudas, Ciric and Grossmann (1986). In this study, the authors also used the concepts presented in the previous work (1986), so the Linear Programming (LP) model is solved for each period and the number of units of HEN and matches are predicted by the MILP model. More recently, Miranda et al. (2017) modified the approach of Floudas and Grossmann (1987), including a new by-pass stream and changing the NLP model, which allowed better results than those described in the literature.

Aaltola (2002) presented a simultaneous optimization approach using a mathematical programming model to synthesize flexible HEN for multiperiod operations. In that study, a Mixed Integer Nonlinear Programming (MINLP) model based on the stage-wise superstructure (SWS) of Yee and Grossmann (1990) was used. The objective function Total Annualized Costs (TAC) includes operating and capital costs for all periods. The area used in that function is the average of the areas required by the units in all periods. However, in that approach, the capital costs would be slightly underestimated. To attack the mean area problem, Verheyen and Zhang (2006) considered the maximum area required by units in all periods in capital costs calculation. Although the maximal area assumption avoids underestimating the capital costs and is more realistic, some devices can have a large idle area. Ma et al. (2008) divided the problem of the multiperiod HEN synthesis into two stages. In the first stage, a temperature–enthalpy diagram is applied to obtain the utility demand and the multiperiod HEN configuration. In the second stage, an area optimization for all periods is performed.

The authors presented another novelty in that work: the use of a hybrid method for multiperiod HEN synthesis. More recently, Ahmad (2012) presented a simultaneous approach including stream bypass in the mathematical model and solved it using Simulated Annealing (SA). Afterwards, Pavão et al. (2018a) modified a simultaneous approach with the addition of a post-optimization step to improve the TAC.

Simplifications on the stage-wise superstructure and assumptions were often made to simplify the model. Under the assumptions, there were the same duration among all periods (*i.e.*, the total operation time is equally divided among all periods) and the adoption of the maximum area for devices of heat transfer. Besides, the multiperiod HEN model including operating and capital costs for all periods is more complex to solve, since the number of variables is greater than a single-period problem. In that sense, studies attacking some of those relevant challenges in the multiperiod HEN synthesis can be cited. Jiang and Chang (2013) introduced a timesharing mechanism to integrate HENs of all periods into one. According to the researchers, a same device can be used by different pairs of streams throughout the periods, overcoming issues such as overdesign and uncertainty in duration of periods. Although the timesharing strategy uses an MINLP model (*i.e.*, operating and capital costs are minimized simultaneously), it is a sequential strategy, since the optimization problem is solved for each operation condition separately. Recently, Miranda et al. (2016) presented significant improvements to the multiperiod HEN synthesis and corrected inconsistencies in Jiang and Chang (2013 and 2015) scheme. The results showed HEN designs with lower costs than those reported in the literature. Pavão et al. (2018b) used different strategies for the multiperiod HEN synthesis. After that, the timesharing mechanisms and the post-optimization step previously presented in the work of Pavão et al. (2018a) were used to improve the HEN solutions.

Solvers that use deterministic methods and are available in some commercial pieces of software are often used for HEN synthesis. However, studies using two-level optimization via hybrid meta-heuristic approaches have demonstrated improvements to HEN designs when compared to deterministic algorithms. That approach consists in solving the problem at the upper level for integer variables and at the lower level for continuous variables, and has become a good option for the multiperiod HEN synthesis, since the derived optimization model usually comprises a more complex problem. Lewin (1998) introduced a two-level optimization model with the Genetic Algorithm (GA) at both levels of the problem. This strategy was also used with Differential Evolution (DE) and Chaotic Ant Swarm (CAS) algorithm at both levels by Yerramsetty and Murty (2008) and Zhang, Cui and Peng (2016), respectively. Different methods for handling integer and continuous variables, Harmonic Search (HS) and Sequential Quadratic Programming (SQP), were used by Khorasany and Fesanghary (2009). Chen et al. (2008) proposed Tabu Search (TS) for the outer loop and Sequential Quadratic Programming (SQP) for inner loop. According to the authors, adaptations in the model to reduce the number of continuous variables are needed to facilitate the solution in lower level. Recently, Martelli, Mian and Maréchal (2015) used Variable Neighborhood Search (VNS) in the outer loop and the Sequential Quadratic Programming (SQP) in the inner loop. Later, Marteli et al. (2017) presented the HEN synthesis with VNS in the upper level and SNOPT in the lower level, which is a variant of SQP. It is important to comment that SQP method used in the previous works (CHEN et al., 2008; KHORASANY; FESANGHARY, 2009; MARTELLI; MIAN; MARÉCHAL, 2015; MARTELLI et al., 2017) is a deterministic algorithm, thus those methods comprise hybridization of a heuristic and a deterministic method. More recent strategies combine Genetic Algorithm (GA) and Particle Swarm Optimization (PSO) (PAVÃO; COSTA; RAVAGNANI, 2016), Simulated Annealing (SA) and Particle Swarm Optimization (PSO) (PAVÃO; COSTA; RAVAGNANI, 2017), and Simulated Annealing (SA) and Rocket Fireworks Optimization (RFO) (PAVÃO et al., 2017a). This last strategy was also employed in other studies, and showed good results for HEN synthesis in single-period (PAVÃO et al., 2017a) and multiple periods (PAVÃO et al., 2018a,b).

Although energy integration techniques have been developed and improved since the 1970s, there are few studies in the literature that apply those techniques to actual large-scale industrial cases. For biorefineries, Pinch Analysis was used in the works of Pina et al. (2014) and Oliveira, Cruz and Costa (2016). In the previous studies (please, see Chapters 3 and 4), energy integration in a Brazilian biorefinery using multiple operation conditions was performed. It is important to mention that the multiperiod HEN allows achieving more realistic solutions, since process conditions can vary due to several factors. The authors solved the MINLP problems using PSO and SA/RFO, but only one case study was evaluated.

This work includes a comparison among three industrial case studies of energy integration in biorefineries by means of multiperiod HEN synthesis. The case studies differ in the disposal of pentose fraction or the use of this fraction to produce ethanol or biogas. For each case study, three periods were considered. For each period, a different bagasse fraction is diverted to second generation ethanol production. This fraction affects the number of streams involved in energy integration and the flow rates of many of these streams. As commented, the demand and the market prices of ethanol and electricity have great influence on plant operating conditions and on the duration of each period. The timesharing strategy proposed by Jiang and Chang (2013) is an efficient alternative for the HEN synthesis with multiple operating conditions, as presented by Miranda (2016) and Pavão et al. (2018a,b). That scheme does not require the duration of periods to design the multiperiod HEN. It is an important feature for biorefineries, since the duration of a period and the number of transitions from one operating condition to another can be difficult to specify. Thus, timesharing mechanisms were employed. For each period, the MINLP problem was solved using the hybridized method of Tabu Search (TS) and Particle Swarm Optimization (PSO). The combination of TS and PSO algorithms is a new approach and can be used for large-scale HEN synthesis problems. This hybrid method is one of the novelties presented in this study. Another novel consists in designing HENs using mathematical programming for more than one industrial case study of sugarcane biorefinery, which can be in the interest of the scientific community and the industry, leading to new studies and efficient options for the improvement of such plants energetic efficiency. Note that HEN synthesis in biorefineries has as one of the main goals to reduce the steam consumption by the process. Then, less bagasse needs to be burned to generate steam and the surplus can be deviated to 2G ethanol or electricity production, depending on demand. However, other aspects achieved via energy integration, such as the increase of energy security and the decrease of environmental resources consumption and residues generation, are also important. Therefore, all improvements provided by energy integration contribute to catalyze the viability of 2G ethanol production.

5.2 Mathematical formulation

5.2.1 Mathematical model and assumptions

In this work, the problem of HEN synthesis with multiple periods (*i.e.*, the HEN operates under different specified operating conditions) was solved by a sequential approach. In this approach, an MINLP model is solved for each period separately. After, timesharing mechanisms are used to design a HEN that integrates all periods. The nonisothermal mixing stage-wise superstructure (NIM-SWS) based on the superstructure of Yee and Grossmann (1990) was used. Mathematical formulations for HEN synthesis by MINLP models are more complex than other techniques (*e.g.*, Pinch Analysis) and require more computational effort, given their nonlinearities and non-convexities. Thus, several simplifications can be needed to enable solving the problem. Assumptions used in this study are presented as follows.

i. Specific heat capacities are constant;
ii. Latent heat coefficients are equivalent to a large heat capacity over a small temperature difference (equal to 1.0 K);
iii. Heat transfer convective coefficients are constant;
iv. Heat exchangers are in counter-flow arrangement;
v. Nonisothermal mixing;
vi. Minimal and maximal values for heat exchanger areas are equal to 1.0 m^2 and 5,500 m^2, respectively (this assumption aims to make the HEN more practical from a design perspective);
vii. Fouling and pressure drop effects are disregarded;
viii. Piping costs are not included in the TAC.

Since the MINLP model for the HEN synthesis used in this study is well-known in the literature, it will not be presented here. However, its equations and bounds can be found in Chapters 3 and 4.

5.2.2 Tabu Search and Particle Swarm Optimization

Meta-heuristics approaches are a recent trend in heat energy area and have achieved noteworthy solutions. In this work, a hybrid meta-heuristic method was used for solving the MINLP model in each period. This method comprises Tabu Search (TS) for upper level and Particle Swarm Optimization (PSO) for lower level. The mathematical model and the algorithms TS and PSO were written in C++ language. Dev C++ Integrated Development Environment (IDE) and GCC Compiler were used for development and execution of the code, which are free programs. These are interesting features in this work, since several studies use solvers from commercial programs. In addition, C++ language is able to produce faster CPU execution times.

5.2.2.1 Upper level

Tabu Search (TS) is a meta-heuristic method originally developed for combinatorial optimization. This approach was proposed by Glover (1989 and 1990), but some important concepts had already been introduced previously (GLOVER, 1986). It is based on a local search and explores the solution space moving from one solution to another into its neighborhood. An initial solution needs to be specified, which can be generated randomly or from established criteria (*e.g.*, in HEN synthesis problems, this solution can be obtained from Pinch Analysis or a previous literature solution when the problem has already been studied by other authors).

The neighborhood size, N(s), should be defined. The neighborhood elements are generated by modifying the initial solution and each neighbor is a candidate solution. That modification can be provided through one or a sequence of moves. Then, the best neighbor solution is established. This solution, which is called the current solution (s), is the starting point for the next iteration. In addition, if the best neighbor solution is better than the initial solution, it is also the best current solution (s*). It is included on tabu list (TL). The solutions on tabu list are denominated forbidden or tabooed and guide the search by an adaptive memory. The TS approach avoids returning to a recently visited solution and cycling. In next iterations, it is evaluated if the best solution in the neighborhood is tabu (*i.e.*, it is a forbidden solution). If this solution is not present on tabu list, it is accepted as the best neighbor solution; otherwise, the second best solution is evaluated. Thus, the best neighbor solution is inserted on tabu list and the starting point for the next iteration (*i.e.*, it is the current solution). Afterwards, the comparison among those solutions is performed (that is, if the best neighbor solution is better than the best current solution, it replaces the best current solution). However, this exploration procedure can forbid moves leading to unexplored solutions, which could be attractive (GLOVER; TAILLARD; TAILLARD, 1993).

Thus, it is interesting an aspiration criterion for overriding the tabu status and allowing that neighbor to be accepted (LIN; MILLER, 2004). In this work it is used one of the simplest and most commonly aspiration criteria, which consists in accepting the best neighbor solution, even it is tabu, if its objective function value is better than that of the best current solution.

Tabu lists are frequently based on recording attributes, called attributive memory. This memory records information about solution properties, which are the attributes changed from one neighbor to another (GLOVER; MARTI, 2006). Thus, it avoids the evaluation of all attributes of the solution during the search in tabu list, evaluating only one or more attributes. The most common types of attributive memory are short-term memory, intermediate-term memory and long-term memory.

Short-based memory, also called as recency-based memory, maintains attributes that occur in solutions recently visited. These solution attributes are named tabu-active and the solutions that contain them are called tabu. Thus, when the list is full and a new attribute is tabu-active, the oldest tabu-active attribute is excluded from the list. Recency-based memory recoveries only the solutions generated near the search space under analysis. For a tabu list of |TL| size, this memory avoids cycling to |TL| solutions. According to Glover (1989), intermediate-term and long-term memories are used in TS as intensification and diversification strategies, respectively. Intermediate-term memory recovers attributes of the best solutions generated during a specified search period to be used in regional intensification strategies. In this approach, solutions that have attributes of good solutions are favored by limiting or penalizing particular moves during that particular search period. Long-term memory, also called as frequency-based memory, uses lists based on the frequency with which solutions are found. This memory is employed in diversification strategies and aims at diversifying the search process by redirecting to regions still not sufficiently explored on the search space.

5.2.2.2 Lower level

The Particle Swarm Optimization (PSO) is a meta-heuristic method originally developed for continuous optimization. This approach belongs to the group of Evolutionary Computation algorithms. These algorithms are based on natural evolution mechanisms of an initial population to improve the best solution of this population. The evolutionary approach can be subdivided into two subgroups: Evolutionary algorithms and Swarm Intelligence algorithms.

PSO was proposed by Kennedy and Eberhart (1995) and belongs to the Swarm Intelligence algorithms. Its population of individuals is denominated swarm and the elements of the population are particles (that is, each particle of the swarm is a candidate solution). These particles are randomly generated into the search space and have associated a velocity term. Eq. 5.1 calculates the position of particle ($\boldsymbol{x}_p^{k+1}$) for a given iteration (k+1), which depends on the previous position ($\boldsymbol{x}_p^{k}$) and the velocity ($\boldsymbol{v}_p^{k+1}$). The term of velocity is shown in Eq. 5.2, and is determined by weighting the distance between the actual position ($\boldsymbol{x}_p^{k}$) and the best own position ($\boldsymbol{f}_{Bp}$), the distance between the actual position ($\boldsymbol{x}_p^{k}$) and the best position of the swarm ($\boldsymbol{g}_{Bp}$), and the previous own velocity ($\boldsymbol{v}_p^{k}$). The inertia weight (w) controls the impact of previous velocity on the current velocity. A high inertia weight value favors global exploration, while a small inertia weight value favors local exploration. Thus, the satisfactory selection of inertia weight provides a balance between global and local exploration. Often the inertia weight is adjusted dynamically by a function that depends on maximum and minimum inertia weights (w_{max} and w_{min}). Parameters c_1 and c_2 are cognition and social behavior coefficients and, r_1 and r_2 are random number with uniform distribution in the interval [0,1]. Other parameters of the PSO algorithm are number of particles (Npt) and total number of iterations (Iter). The update procedure of particles is performed until the stopping criterion is achieved.

$$\boldsymbol{x}_p^{k+1} = \boldsymbol{x}_p^{k} + \boldsymbol{v}_p^{k+1} \tag{5.1}$$

$$\boldsymbol{v}_p^{k+1} = w \,.\, \boldsymbol{v}_p^{k} + c_1 \,.\, r_1 \,.\, \left(\boldsymbol{f}_{Bp} - \boldsymbol{x}_p^{k}\right) + c_2 \,.\, r_2 \,.\, (\boldsymbol{g}_{Bp} - \boldsymbol{x}_p^{k}) \tag{5.2}$$

5.2.2.3 Algorithm description

In this section, the procedure for solving the HEN synthesis problem using the proposed hybrid method is presented.

Step 1: Initialize tuning parameters of TS and PSO.

Step 2: Generate the initial solution of TS, called current solution (s). This solution indicates the HEN topology and is generated randomly (*i.e.*, the binary variables values are created by TS method).

Step 3: For a given topology, PSO randomly generates heat loads, hot stream fractions and cold stream fractions (*i.e.*, the continuous variables values are created by PSO method). Calculate temperatures, areas and costs.

Step 4: Construct the neighborhood for the initial solution, which is both the current solution (s) and the best current solution (s*). The neighborhood size, N(s), is equal to the superstructure size and only one move is performed for each neighbor during the neighborhood generation. Thus, for each neighbor the topology differs from that of the initial solution by one element (*i.e.*, starting from the initial configuration of the HEN superstructure, each neighbor has one heat exchanger added, if there is no heat exchanger in that given position, or removed, if there is a heat exchanger in that given position).

Step 5: Apply PSO algorithm for each neighbor. Calculate temperatures, areas and costs.

Step 6: Select the best neighbor solution. Judge if this candidate is better than the initial solution. If this solution is better, it is the starting point for the next iteration (*i.e.*, this solution will be the current solution and the best current solution). If no solution in neighborhood is better than the initial solution, the best neighbor solution is chosen for starting the second iteration (*i.e.*, this solution will be the current solution). The best solution in neighborhood is included on tabu list.

Step 7: Construct the neighborhood for the current solution (s).

Step 8: Apply PSO algorithm for each element of neighborhood. Calculate temperatures, areas and costs.

Step 9: Select the best neighbor solution. Judge if this candidate is on tabu list. If it is not present, it assumes the status of current solution (s) and is added on tabu list. Besides that, if this same candidate has objective function value better that the best current solution, it replaces the best current solution (s*). However, if that candidate is tabooed, evaluate the aspiration criteria. If it is satisfied (*i.e.*, the best solution in neighborhood is better than the best current solution), this candidate is accepted and it becomes the current solution and the best current solution. Otherwise, evaluate the second best solution.

Step 10: Judge the stopping criterion (BTmax), which is the number of iterations without any improvement of the best solution. If it is achieved, stop execution; otherwise, return to Step 7.

Table 5.1 presents the tuning parameters for TS and PSO. These values were chosen based on preliminary tests performed to the biorefineries case studies by the present authors.

Table 5.1. Tuning parameters for TS and PSO.

Tabu Search			**Particle Swarm Optimization**					
BTmax	TL	N(s)	Iter	Npt	w_{min}	w_{max}	c_1	c_2
2	35	I·J·K*	100	300	0.4	0.9	1.1	1.1

* The neighborhood has the same size as the superstructure, which is calculated by multiplication of the number of hot streams (I), cold streams (J) and stages (K) of the superstructure. The number of hot and cold streams varies from one case study to another, as well as among the periods.

During the procedure for energy integration of each case study, ten executions of the code for each period were performed. All case studies were run on a 2.50 GHz Intel® Core™ i5-3210 processor with 6.00 GB of RAM. In addition, aiming at maintaining the HEN feasibility and reduce the processing time, four strategies are performed by TS-PSO, as follows.

Strategy 1: In case a hot/cold stream is providing/receiving more heat than the available/required (constraints expressed in Eqs. 3.47 and 3.48 of Chapter 3), that exceeding quantity is removed from a random heat exchanger in that respective stream.

Strategy 2: If stream fractions sum in a stage is greater than one (constraints expressed in Eqs. 3.29 and 3.30 of Chapter 3), the amount that surpass one is removed from a random stream split fraction in that stage. If stream fractions sum in a stage is smaller than one (constraints expressed in Eqs. 3.29 and 3.30 of Chapter 3), the required amount to achieve one is added to a random stream split fraction in that stage. This strategy allows meeting the equality constraints of the HEN model.

Strategy 3: In case the best solution of the swarm is not improved in n iterations for a candidate solution of TS, the next candidate is evaluated. The value n is defined as ten percent of the maximum number of iterations of PSO.

Strategy 4: From one run to another, the best previous solution is the starting point for the next execution (*i.e.*, the best solution of previous execution is introduced as the initial solution of TS and as one of particles in the swarm of PSO). Furthermore, during the evaluation of neighbors, the best solution obtained for the continuous variables (*i.e.*, by the PSO) for the previous neighbor is included as one of particles in the swarm that optimizes the next neighbor.

To handle the other constraints, such as temperature constraints, a penalty function is applied. This function is the sum of all constraint violations multiplied by a constant. In this study, the constant was defined equal to 10^8.

Both methods, TS and PSO, are simple techniques to be implemented, since they use only basic mathematical operators. Studies of energy integration using only TS were performed by Lin and Miler (LIN; MILLER, 2004) and combining it with SQP method by Chen et al. (CHEN et al., 2008). Meanwhile, PSO technique has been widely used in the HEN synthesis by several authors (SILVA, RAVAGNANI; BISCAIA, 2008; SILVA et al., 2010; PAVÃO; COSTA; RAVAGNANI, 2016, 2017, PAVÃO et al., 2017a,b,c, 2018a,b). Although none of those works combined TS and PSO, such methods have proven, separately, to be able for HEN synthesis.

5.2.3 Timesharing strategy

In this study, an MINLP problem is solved separately for each period. Thus, to design the multiperiod HEN, timesharing mechanism (JIANG; CHANG, 2013) was used. This approach is a recent technique that has proven to be efficient and able to reduce investment costs of HEN. It allows the heat exchangers to perform different services throughout the plant operation (*i.e.*, use the same device for different pair of streams matched in different periods). The algorithmic procedure to re-organize the heat exchangers and integrate all HENs into a single one is described in Chapters 3 and 4.

5.3 Biorefineries

In this study, three industrial case studies of energy integration in biorefineries were performed. All of them consist in simulation of processes for 1G/2G anhydrous ethanol and electricity production (FURLAN et al., 2012, 2013). The biorefineries differ whether xylose fraction from bagasse is exploited. Fig. 5.1 presents the diagram of the process. Main parameters, operating conditions and results for biorefinery simulations are presented in Appendix 5.A.

Ethanol and electricity production is a process well-known in the literature. Details about 1G ethanol process production are presented in Chapter 3. The liquid fraction rich in hydrolysis products from hemicellulose (five carbon sugars, notably xylose) coming from the filter (E510) can be discarded, fermented or biodigested. Each one of these routes indicates a biorefinery case study. In Case Study 1, that fraction is discarded. In Case Study 2, the xylose fraction is used to produce 2G ethanol. Thus, operations of concentration (E702) and fermentation (E706) are included. In Case Study 3, that xylose fraction is used to produce biogas, being necessary to add to the process the steps of adjustment of chemical oxygen demand (E801) and biodigestion (E803). It is important to mention that the biogas produced by xylose biodigestion is one more energy source (fuel) to the cogeneration system, allowing more bagasse to be diverted to 2G ethanol production (when compared to simply discarding xylose fraction). Finally, the solid fraction from the filter (E606), which is located after hydrolysis operation, consists mainly of lignin and is sent to the boiler (E403).

The biorefinery represented in Fig. 5.1 corresponds to the process with energy integration, which already has a degree of energy integration. This biorefinery is named in this work process “with project integration “. In biorefineries without any energy integration, every heating and cooling of streams is provided by hot and cold utilities, which is named in this work “without energy integration”. Furthermore, other two terminologies for biorefineries are used in this study. The process with HEN synthesized for each period is named “with the single-period HEN” and the process with the multiperiod HEN is named “with the multiperiod HEN”.

In this work, the assumption of one hot utility and one cold utility for the HEN model was performed. As hot utility, saturated steam at 17.4 bar is selected. Although steam is used at different pressures levels for heating of streams in Brazilian plants, including the vegetable steam produced in the pre-evaporators, in this study only steam at 17.4 bar was considered, since it meets the temperature constraints for all cold streams. Choosing more than one hot utility would make the HEN synthesis problem more complex and difficult to solve, since models with multiple utilities have more variables. Furthermore, case studies in biorefineries are already large-scale problems. As cold utility, cooling water at 298 K is selected. This cold utility is produced in the cooling tower, which cools water from

305 K to 298 K. Costs of hot utility (*chu*) and cold utility (*ccu*) are 96 USD/kW year and 50 USD/kW year, respectively. The coefficients for annual costs of investment on heat exchangers are a = 4,897 USD/ year, b = 33 USD/m$^{1.56}$ year and c = 0.78. Procedure for the calculation of costs of utilities and coefficients for annual costs of investment on heat exchangers is presented in Chapters 3 and 4.

Several assumptions are the same for case studies. One of them refers to the convective heat transfer coefficients of hot streams, cold streams and utilities, which were estimated from the overall heat transfer coefficient given by Ensinas (2008). For estimating them, the hypothesis 'the convective heat transfer coefficients are the same for all streams' was performed. Besides, temperatures of utilities are constants (*i.e.*, possible variations in temperatures of the steam and the cooling water were not considered). In all cases, EMAT was set to 1 K and four stages were used in the superstructure. The total operation time of the plant is 5,760 h/year.

Three periods were considered for each case study. Each period indicates a process condition. In Period 1, no bagasse is deviated for the 2G ethanol production (*i.e.*, this period includes only 1G ethanol and surplus electricity production). In Period 3, the maximum fraction of bagasse is available for 2G ethanol production (*i.e.*, this period includes 1G/2G ethanol and electricity production). The maximum amount of bagasse that could be destined for 2G ethanol production is the maximum value that ensures the maintenance of the energy self-sufficiency of the process. In Period 2, half of that fraction of bagasse is deviated for the 2G ethanol production (*i.e.*, this period includes 1G/2G ethanol and surplus electricity production). This approach of dividing fractions of bagasse among periods is applied to all case studies. In addition, to compare the multiperiod HEN with demands and costs of processes without energy integration, with project energy integration and with the single-period HEN, the multiperiod HEN assumes the utility demand of proposed HEN for each period (that is, for this comparison, the biorefinery would operate throughout the year under the same process condition) and the capital cost estimated by the final device set from the timesharing procedure.

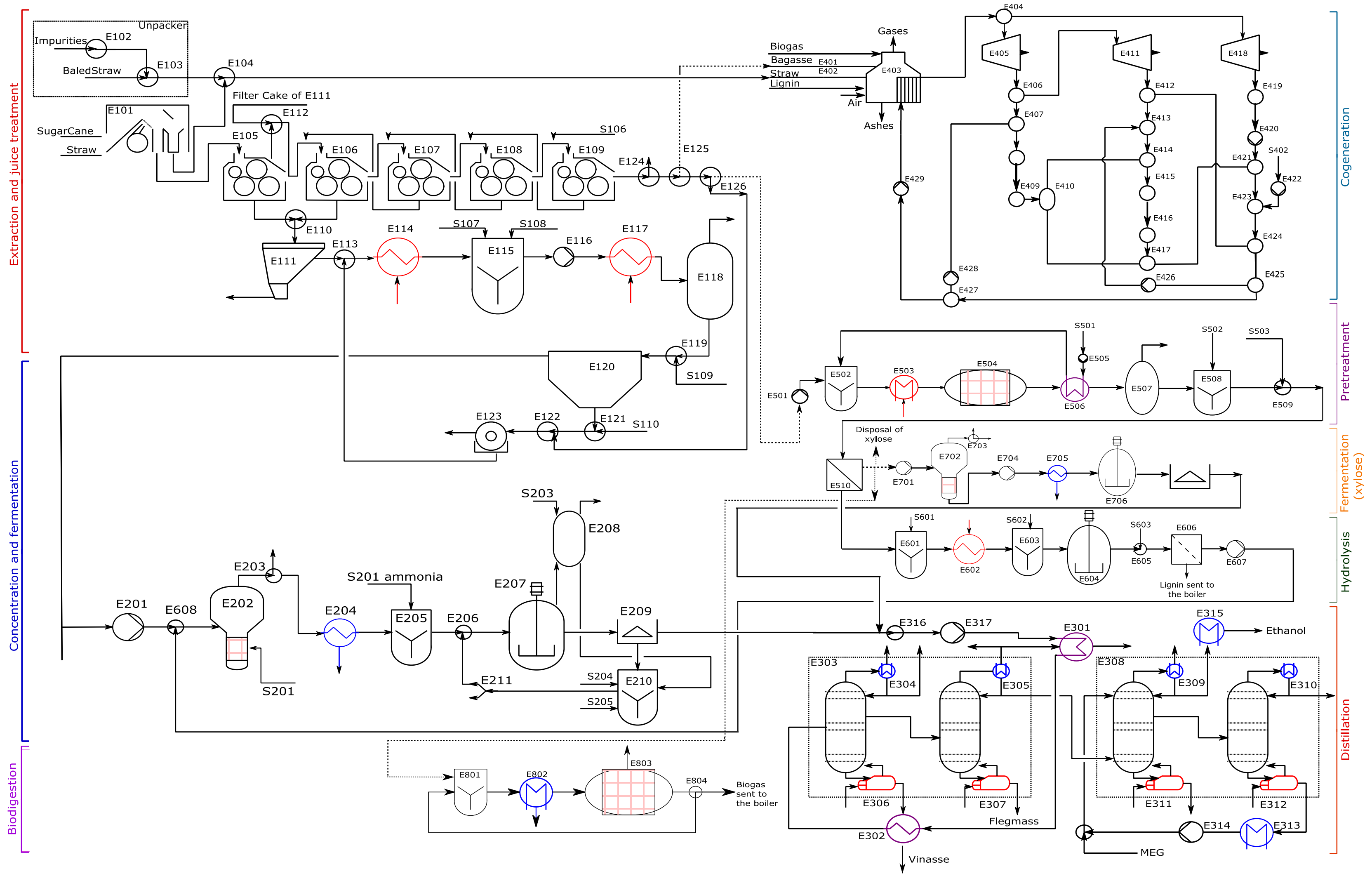

Figure 5.1. Steps of 1G/2G ethanol and eletricity production process.

5.4 Results and discussion

This section presents three industrial case studies of energy integration in biorefineries. Simplified diagrams of multiperiod HENs are presented in each case study, but important design data, such as heat loads, temperatures, bypasses for cold streams in heat exchangers with surplus area, areas and units assigned to each match, are detailed in Appendix 5.B.

5.4.1 Case study 1

Case Study 1 refers to 1G/2G ethanol and electricity production process, with disposal of the fraction of xylose. In Period 1, no bagasse is deviated for 2G ethanol section. In Periods 2 and 3, 33% and 66% of all bagasse is deviated for 2G ethanol production, respectively. Possessing 8 hot streams, 7 cold streams and 4 stages, Period 1 has 896 variables. On the other hand, Periods 2 and 3 have 9 hot streams, 10 cold streams and 4 stages, leading to 1,440 variables. Table 5.2 shows streams data for the three periods. In this table, column 2 designates the label of hot and cold streams. Column 3 indicates the heat exchanger in Table 5.2 that provides the required service (*e.g.*, C4 is the cold stream from the bottom of Column A, which is vaporized in a device called Reboiler A, indicated by E306 in Fig. 5.1).

Table 5.2. Stream data for sugarcane biorefinery of Case Study 1.

	Stream	Device indicated in Fig. 5.1	T^0 (K)	T^{final} (K)	CP (kW/K)	h (kW/m^2 K)
	Period 1					
H1	Concentrated juice	E204	388	306	638	1.38
H2	Vapor from Column D top (Condenser D)	E304	358	357	11,661	1.38
H3	Vapor from Column B top (Condenser B)	E305/E301	355	354	60,307	1.38
H4	Vapor from extractive column top (Condenser DEH1)	E309	351	350	24,592	1.38
H5	Vapor from recovery column top (Condenser DEH2)	E310	333	332	2,074	1.38
H6	Vinasse	E302	385	363	747	1.38
H7	Monoethylene glycol	E313	421	353	33	1.38

H8	Anhydrous ethanol	E315	351	308	43	1.38
C1	Juice	E114	321	343	1,256	1.38
C2	Juice	E117	343	378	1,288	1.38
C3	Wine	E301/E302	303	362	867	1.38
C4	Liquid from Column A bottom (Reboiler A)	E306	384	385	67,968	1.38
C5	Liquid from Column B1 bottom (Reboiler B)	E307	381	382	22,466	1.38
C6	Liquid from extractive column bottom (Reboiler DEH1)	E311	379	407	352	1.38
C7	Liquid from recovery column bottom (Reboiler DEH2)	E312	411	421	335	1.38
	Period 2					
H1	Concentrated juice	E204	388	306	713	1.38
H2	Vapor from Column D top (Condenser D)	E304	358	357	13,086	1.38
H3	Vapor from Column B top (Condenser B)	E305/E301	355	354	66,136	1.38
H4	Vapor from extractive column top (Condenser DEH1)	E309	351	350	26,942	1.38
H5	Vapor from recovery column top (Condenser DEH2)	E310	333	332	2,272	1.38
H6	Vinasse	E302	385	363	862	1.38
H7	Monoethylene glycol	E313	421	353	37	1.38
H8	Anhydrous ethanol	E315	351	308	47	1.38
H9	Pretreated bagasse	E506	468	353	525	1.38
C1	Juice	E114	321	343	1,256	1.38
C2	Juice	E117	343	378	1,288	1.38
C3	Wine	E301/E302	303	362	995	1.38
C4	Liquid from Column A bottom (Reboiler A)	E306	384	385	76,914	1.38
C5	Liquid from Column B1 bottom (Reboiler B)	E307	381	382	23,510	1.38
C6	Liquid from extractive column bottom (Reboiler DEH1)	E311	379	407	386	1.38
C7	Liquid from recovery column bottom (Reboiler DEH2)	E312	411	421	367	1.38
C8	Bagasse + soaking water	E503	439	468	523	1.38
C9	Soaking water	E506	303	458	418	1.38
C10	Solid fraction (cellulose + lignin)	E602	315	323	206	1.38
	Period 3					
H1	Concentrated juice	E204	388	306	788	1.38
H2	Vapor from Column D top (Condenser D)	E304	358	357	14,532	1.38
H3	Vapor from Column B top (Condenser B)	E305/E301	355	354	71,935	1.38
H4	Vapor from extractive column top (Condenser DEH1)	E309	351	350	29,277	1.38
H5	Vapor from recovery column top (Condenser DEH2)	E310	333	332	2,469	1.38
H6	Vinasse	E302	385	363	981	1.38
H7	Monoethylene glycol	E313	421	353	40	1.38
H8	Anhydrous ethanol	E315	351	308	51	1.38
H9	Pretreated bagasse	E506	468	353	1,047	1.38
C1	Juice	E114	321	343	1,256	1.38
C2	Juice	E117	343	378	1,288	1.38
C3	Wine	E301/E302	303	362	1,129	1.38
C4	Liquid from Column A bottom (Reboiler A)	E306	384	385	86,036	1.38
C5	Liquid from Column B1 bottom (Reboiler B)	E307	381	382	24,443	1.38

C6	Liquid from extractive column bottom (Reboiler DEH1)	E311	379	407	419	1.38
C7	Liquid from recovery column bottom (Reboiler DEH2)	E312	411	421	398	1.38
C8	Bagasse + soaking water	E503	439	468	1,042	1.38
C9	Soaking water	E506	303	458	834	1.38
C10	Solid fraction (cellulose + lignin)	E602	315	323	410	1.38

For biorefinery without energy integration (S1), the TAC for Periods 1, 2 and 3 is 30.5, 44.1 and 57.7 million USD/year, respectively. In process with project energy integration (S2), the TAC is 23.0, 26.8 and 30.5 million USD/year for Periods 1, 2 and 3, respectively. Energy integration was performed according to strategies from Section 5.2. For Periods 1, 2 and 3, the average processing time of the algorithm was 25, 63 and 58 minutes, respectively. These values indicate the processing time for one single run for each period. In Periods 1, 2 and 3, the TAC of processes with the single-period HEN (S3) is 12.7, 13.3 and 14.4 million USD/year, respectively. Table 5.3 summarizes the number of heat exchange devices, area and costs for each period of operation.

Table 5.3. Number of heat exchange devices, total area, capital cost (CC), operating cost (OC), and total annualized cost (TAC) for the single-period HEN using TS-PSO in Case Study 1.

	Units	**Total required area (m^2)**	**CC (USD/year)**	**OC (USD/year)**	**Single-period solution TAC (USD/year)**
Period 1	24	25,699.1	279,117	12,468,797	12,747,915
Period 2	32	37,769.0	386,761	12,911,180	13,297,942
Period 3	32	44,639.6	420,427	13,963,062	14,383,489

After applying the timesharing mechanisms to integrate all HENs into a single one, the multiperiod HEN was synthesized (S4). For this HEN, the capital cost estimated is 423,534 USD/year with total area of 45,113.5 m^2 and 32 heat transfer devices. For a hypothetical situation where the three periods have the same operation time, the operating cost and the TAC of the multiperiod HEN are 13,114,347 USD/year and 13,537,881 USD/year, respectively. There is an area overdesign of 75% for Period 1, 19% for Period 2 and 1% for Period 3. Fig. 5.2 shows the multiperiod HEN configuration. In this figure, the labels above heat exchangers indicate the employed device in the multiperiod HEN for each match in Periods 1, 2 and 3, respectively. When a match does not exist in a period, the symbol '-' is used. Note that Periods 1, 2 and 3 have devices with fixed services between H1-C3, H3-C1 and H3-C3 (*i.e.*, these devices perform heat integration between the same pair of streams). The heat exchanger that uses the match H6-C2 has fixed service in Periods 1 and 2, while devices that combine H1-C2, H4-C1 and H6-C5 have fixed services in Periods 1 and 3. Devices assigned to pairs H1-C9, H2-C2, H3-C9, H5-C10, H7-C5, H9-C2 and H9-C4 comprise fixed heat exchanger services in Period 2 and 3. The HENs of Periods 1 and 2 and of Periods 1 and 3 have important differences in theirs configurations, while the HENs of Periods 2 and 3 are more similar. Period 1 has two pairs of streams without any correspondence with other periods. Periods 2 and 3 have four and five pairs of streams that are not matched in other operating conditions, respectively. If the multiperiod HEN were synthesized by merging all HENs into one, this HEN would use all devices from all solutions of periods. For this case study, the multiperiod HEN synthesized by merging would have several devices with idle periods. However, the timesharing strategy proposed by Jiang and Chang (2013) allows a device to be used for different pairs of streams in each period (*i.e.*, a set of heat exchangers is sized to perform different services among operating periods), overcoming overdesign and decreasing investment cost. After using timesharing mechanisms, a set of bypasses must be designed to allocate the correct matching of streams to a device in a given period. In Period 1, five cold streams have more than half of their flow rate bypassing heat exchangers in the designed multiperiod HEN. For Periods 2 and 3, only two and one heat exchanger has bypasses above 50%. When comparing the number of idle devices, Period 1 has 8 idle heat exchangers. In Periods 2 and 3, all devices are being used. Although Period 1 has some devices that are not being used, these heat exchangers present areas lower than 600 m^2 (that is, the economic impact in HEN costs is small, since the area of idle devices is lower than 2% of total area of the multiperiod HEN).

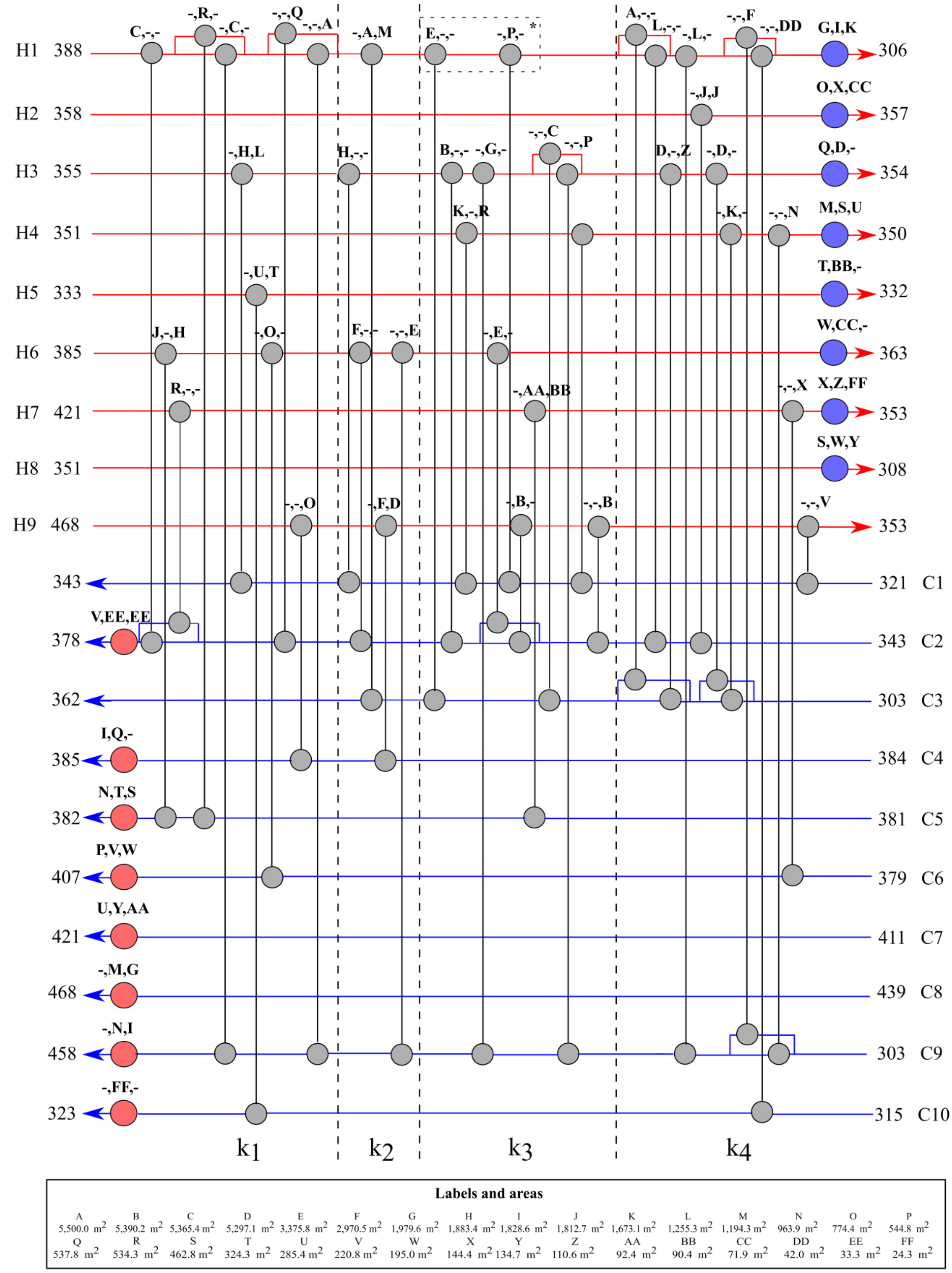

*Note: No splits are represented because these matches never take place in the same period simultaneously.

Figure 5.2. Multiperiod HEN using TS-PSO of Case Study 1.

Table 5.4 shows savings in steam demand and TAC of processes with the single-period and the multiperiod HEN compared to processes without any energy integration and with project energy integration. The saving of steam is the same between processes with the single-period and the multiperiod HEN in each period, because the calculation procedure of operating costs for the multiperiod HEN in a given period assumes that the process operates only in that operating condition. It is important to highlight the savings obtained by the multiperiod HEN, since it allows the biorefinery to operate in different process conditions. The process with the multiperiod HEN presents reduction in TAC of 58%, 70% and 75% when compared to the process without energy integration for Periods 1, 2 and 3, respectively. The process with the multiperiod HEN presents reduction in TAC of 44%, 50% and 53% when compared to the process with project energy integration for Periods 1, 2 and 3, respectively. Furthermore, for those processes, savings of steam reach 54%, 65% and 70% when compared to the process without energy integration and 41%, 45% and 46% when compared to the process with project energy integration for Periods 1, 2 and 3, respectively.

Table 5.4. Saving of steam demand and TAC of the processes with the single-period HEN (S3) and with the multiperiod HEN (S4) using TS-PSO in relation to the processes without energy integration (S1) and with project energy integration (S2) in Case Study 1.

Saving (%)	P1				P2				P3			
	S3/S1	**S3/S2**	**S4/S1**	**S4/S2**	**S3/S1**	**S3/S2**	**S4/S1**	**S4/S2**	**S3/S1**	**S3/S2**	**S4/S1**	**S4/S2**
HU	53.98	40.63	53.98	40.63	64.95	44.97	64.95	44.97	69.77	46.35	69.77	46.35
TAC	58.19	44.69	57.71	44.06	69.85	50.35	69.77	50.21	75.07	52.79	75.06	52.78

Among case studies presented in this work, only Case Study 1 was previously studied. The present authors used PSO and SA-RFO methods to solve this problem (please, see Chapters 3 and 4). When employing adapted PSO for integer and continuous variables, these authors obtained a TAC for the single-period HEN of 19.6, 25.5 and 27.8 million USD/year for Periods 1, 2 and 3, respectively. For the multiperiod HEN, the TAC was 24,342,777 USD/year (that is, for a hypothetical situation where each period operates 1/3 of the total operation time). These results present marginal improvements in TAC when compared to the process with project integration. Since the application PSO algorithm to integer and continuous variables in large-scale problems can present failures, especially in dealing with integer variables, this strategy is not good. Using SA-RFO (OLIVEIRA et al., 2017), these authors achieved a TAC for the single-period HEN of 12.4, 12.9 and 13.8 million USD/year for Periods 1, 2 and 3, respectively. For the multiperiod HEN, the estimated TAC was 12,688,561 USD/year (that is, assuming that each period operates 1/3 of the total operation time). Although, in terms of saving of TAC and steam consumption, the results achieved by SA-RFO are a little better than results obtained in this work, the difference between the TAC solution via SA/RFO and TS/PSO is very small (*i.e.*, for all periods this difference is lower than 2%). Since this case study is a large-scale problem, challenges in mathematical optimization were expected. Chen et al. (CHEN et al., 2008) used TS in upper level and SQP in inner level for the HEN synthesis. These authors detected failures in inner loop, requiring a model reformulation to facilitate the solution with SQP. Later, Pavão et al. (2017a) presented an approach including SA and PSO for lower level, which is called Rocket Fireworks Optimization (RFO). According to the authors, the novel strategy presented better results than those presented using only PSO in lower level. Therefore, there are difficulties in the continuous variables optimization level, which was noticed by those works, as well as in this study.

5.4.2 Case study 2

Case Study 2 refers to 1G/2G ethanol and electricity production process, with the fraction of xylose used to produce 2G ethanol. In Period 1, no bagasse is deviated for the 2G ethanol section. In Periods 2 and 3, 17% and 34% of all bagasse is deviated for the 2G ethanol production, respectively. Period 1 has 8 hot streams, 7 cold streams and 4 stages, so there are 896 variables. The other two periods exhibit 10 hot streams, 10 cold streams and 4 stages, and 1,600 variables. Table 5.5 shows streams data for the three periods.

Table 5.5. Stream data for sugarcane biorefinery of Case Study 2.

	Stream	Device indicated in Fig. 5.1	T^0 (K)	T^{final} (K)	CP (kW/K)	h (kW/m^2 K)
	Period 1					
H1	Concentrated juice	E204	388	306	638	1.38

H2	Vapor from Column D top (Condenser D)	E304	358	357	11,661	1.38
H3	Vapor from Column B top (Condenser B)	E305/E301	355	354	60,307	1.38
H4	Vapor from extractive column top (Condenser DEH1)	E309	351	350	24,592	1.38
H5	Vapor from recovery column top (Condenser DEH2)	E310	333	332	2,074	1.38
H6	Vinasse	E302	385	363	747	1.38
H7	Monoethylene glycol	E313	421	353	33	1.38
H8	Anhydrous ethanol	E315	351	308	43	1.38
C1	Juice	E114	321	343	1,256	1.38
C2	Juice	E117	343	378	1,288	1.38
C3	Wine	E301/E302	303	362	867	1.38
C4	Liquid from Column A bottom (Reboiler A)	E306	384	385	67,968	1.38
C5	Liquid from Column B1 bottom (Reboiler B)	E307	381	382	22,466	1.38
C6	Liquid from extractive column bottom (Reboiler DEH1)	E311	379	407	352	1.38
C7	Liquid from recovery column bottom (Reboiler DEH2)	E312	411	421	335	1.38
	Period 2					
H1	Concentrated juice	E204	388	306	677	1.38
H2	Vapor from Column D top (Condenser D)	E304	358	357	12,943	1.38
H3	Vapor from Column B top (Condenser B)	E305/E301	355	354	64,703	1.38
H4	Vapor from extractive column top (Condenser DEH1)	E309	351	350	26,345	1.38
H5	Vapor from recovery column top (Condenser DEH2)	E310	333	332	2,222	1.38
H6	Vinasse	E302	385	363	876	1.38
H7	Monoethylene glycol	E313	421	353	36	1.38
H8	Anhydrous ethanol	E315	351	308	46	1.38
H9	Pretreated bagasse	E506	468	353	270	1.38
H10	Xylose	E705	388	308	77	
C1	Juice	E114	321	343	1,256	1.38
C2	Juice	E117	343	378	1,288	1.38
C3	Wine	E301/E302	303	362	1,001	1.38
C4	Liquid from Column A bottom (Reboiler A)	E306	384	385	76,318	1.38
C5	Liquid from Column B1 bottom (Reboiler B)	E307	381	382	22,469	1.38
C6	Liquid from extractive column bottom (Reboiler DEH1)	E311	379	407	377	1.38
C7	Liquid from recovery column bottom (Reboiler DEH2)	E312	411	421	359	1.38
C8	Bagasse + soaking water	E503	439	468	269	1.38
C9	Soaking water	E506	303	458	215	1.38
C10	Solid fraction (cellulose + lignin)	E602	315	323	106	1.38
	Period 3					
H1	Concentrated juice	E204	388	306	717	1.38
H2	Vapor from Column D top (Condenser D)	E304	358	357	14,274	1.38
H3	Vapor from Column B top (Condenser B)	E305/E301	355	354	69,257	1.38
H4	Vapor from extractive column top (Condenser DEH1)	E309	351	350	28,162	1.38
H5	Vapor from recovery column top (Condenser DEH2)	E310	333	332	2,375	1.38
H6	Vinasse	E302	385	363	1,010	1.38

H7	Monoethylene glycol	E313	421	353	38	1.38
H8	Anhydrous ethanol	E315	351	308	49	1.38
H9	Pretreated bagasse	E506	468	353	551	1.38
H10	Xylose	E705	388	308	156	
C1	Juice	E114	321	343	1,256	1.38
C2	Juice	E117	343	378	1,288	1.38
C3	Wine	E301/E302	303	362	1,146	1.38
C4	Liquid from Column A bottom (Reboiler A)	E306	384	385	85,032	1.38
C5	Liquid from Column B1 bottom (Reboiler B)	E307	381	382	22,434	1.38
C6	Liquid from extractive column bottom (Reboiler DEH1)	E311	379	407	403	1.38
C7	Liquid from recovery column bottom (Reboiler DEH2)	E312	411	421	383	1.38
C8	Bagasse + soaking water	E503	439	468	548	1.38
C9	Soaking water	E506	303	458	439	1.38
C10	Solid fraction (cellulose + lignin)	E602	315	323	216	1.38

For biorefinery without energy integration (S1), the TAC is 30.5, 38.8 and 47.3 million USD/year for Periods 1, 2 and 3, respectively. For the same periods, in the process with project energy integration (S2), the TAC is 23.0, 25.6 and 28.3 million USD/year. During energy integration, the average processing time of the algorithm was 25, 73 and 62 minutes in Periods 1, 2 and 3, respectively. TAC of the process with the single-period HEN (S3) is 12.7, 13.6 and 14.1 million USD/year, for those same periods. Table 5.6 presents the number of heat exchange devices, area and costs for each period of operation.

Table 5.6. Number of heat exchange devices, total area, capital cost (CC), operating cost (OC), and total annualized cost (TAC) for single-period HEN using TS-PSO in Case Study 2.

	Units	**Total required area (m^2)**	**CC (USD/year)**	**OC (USD/year)**	**Single-period solution TAC (USD/year)**
Period 1	24	25,699.1	279,117	12,468,797	12,747,915
Period 2	39	32,287.5	400,320	13,188,084	13,588,404
Period 3	37	41,598.6	441,626	13,637,792	14,079,418

For the multiperiod HEN (S4), the capital cost estimated is 453,979 USD/year with total area of 42,154.3 m^2 and 39 heat transfer devices. As it was explained in Case Study 1, for a hypothetical situation where the three periods have the same operation time, the operating cost and the TAC of multiperiod HEN are 13,098,225 USD/year and 13,552,204 USD/year, respectively. There is an area overdesign of 64% for Period 1, 31% for Period 2 and 1% for Period 3. Fig. 5.3 shows the multiperiod HEN configuration. Note that Periods 1, 2 and 3 have devices with fixed services between H1-C3, H3-C1, H3-C3 and H6-C2. Devices combining H1-C2 and H7-C2 have fixed services between Periods 1 and 2. Periods 1 and 3 have one device with fixed service between streams H4 and C1. More fixed heat exchanger services are present in Periods 2 and 3 and these services are those related to pairs H1-C6, H1-C9, H2-C2, H2-C3, H2-C9, H3-C10, H4-C2, H4-C9, H5-C10, H7-C5, H9-C2, H9-C4, H9-C5, H10-C3, H10-C6. The HENs of Periods 2 and 3 are very similar (*i.e.*, the devices involve heat transfer among the same pairs of streams). In Period 2, all devices have the same matches of Periods 1 and/or 3. In Period 1, only devices including the streams H3-C2 and H6-C5 do not have services in common with Periods 2 and 3. In Period 3, the devices assigned to pairs H3-C9 and H5-C9 have no fixed services with any other periods. Besides, in Periods 1 and 2, five and ten cold streams have more than half of their flow rate bypassing heat exchangers, respectively. Since the multiperiod HEN uses almost all devices designed for Period 3, in no heat exchanger the required bypasses surpass 50% in this period. When comparing the number of idle devices, Periods 1 and 3 have 15 and 2 idle heat exchangers, respectively. In Period 2, all devices are being used. Those idle heat exchangers in Period 1 present areas that sum up 1,519.4 m^2, which is lower than 4% of the total area of the multiperiod HEN. In Period 3, those idle devices present areas lower than 4 m^2.

Table 5.7. Saving of steam demand and TAC of the processes with the single-period HEN (S3) and with the multiperiod HEN (S4) using TS-PSO in relation to the processes without energy integration (S1) and with project energy integration (S2) in Case Study 2.

Saving (%)	P1				P2				P3			
	S3/S1	**S3/S2**	**S4/S1**	**S4/S2**	**S3/S1**	**S3/S2**	**S4/S1**	**S4/S2**	**S3/S1**	**S3/S2**	**S4/S1**	**S4/S2**
HU	53.98	40.63	53.98	40.63	60.80	42.83	60.80	42.83	66.00	45.54	66.00	45.54
TAC	58.19	44.69	57.61	43.93	64.94	47.00	64.80	46.79	70.26	50.21	70.23	50.16

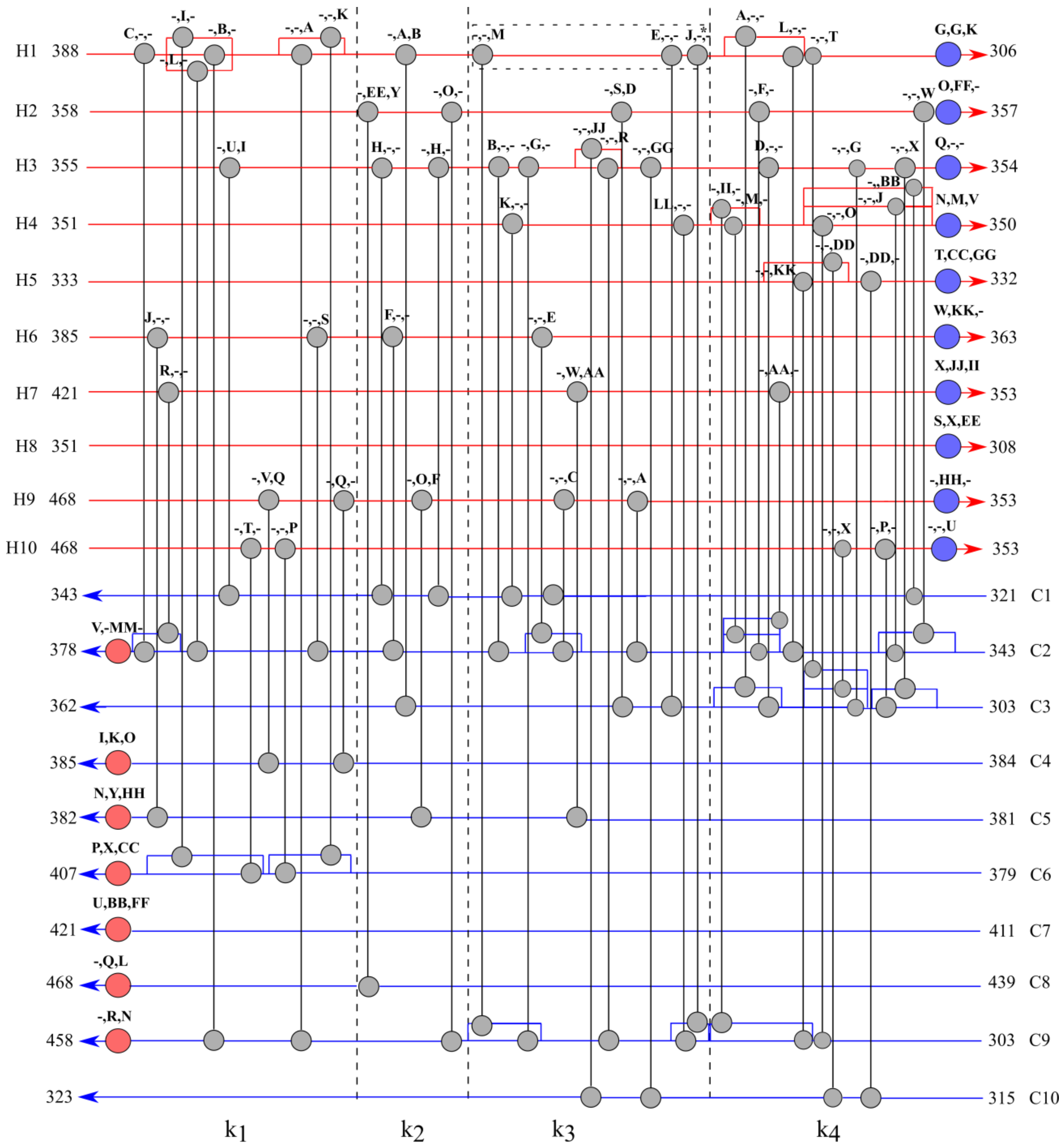

Labels and areas

A	B	C	D	E	F	G	H	I	J	K	L	M	N	O	P
5,500.0 m^2	4,377.2 m^2	3,836.0 m^2	3,672.9 m^2	3,131.8 m^2	2,903.6 m^2	2,473.7 m^2	1,875.0 m^2	1,765.1 m^2	1,501.6 m^2	1,164.8 m^2	1,041.1 m^2	960.6 m^2	950.8 m^2	876.2 m^2	780.7 m^2
Q	R	S	T	U	V	W	X	Y	Z	AA	BB	CC	DD	EE	FF
756.7 m^2	622.7 m^2	581.3 m^2	486.8 m^2	398.8 m^2	378.8 m^2	306.4 m^2	292.3 m^2	274.9 m^2	243.1 m^2	203.4 m^2	164.7 m^2	153.8 m^2	138.9 m^2	129.4 m^2	89.0 m^2
GG	HH	II	JJ	KK	LL	MM									
35.9 m^2	28.6 m^2	24.4 m^2	16.2 m^2	13.3 m^2	2.8 m^2	1.0 m^2									

*Note: No splits are represented because these matches never take place in the same period simultaneously.

Figure 5.3. Multiperiod HEN using TS-PSO for Case Study 2.

Table 5.7 shows savings in steam demand and TAC of processes with the single-period and the multiperiod HEN compared to processes without energy integration and with project energy integration. More attention is given to the savings obtained by the multiperiod HEN. The process with the multiperiod HEN presents reduction in TAC of 58%, 65% and 70% when compared to the process without energy integration for Periods 1, 2 and 3, respectively. The process with multiperiod HEN presents reduction in TAC of 44%, 47% and 50% when compared to the process with project energy integration for Periods 1, 2 and 3, respectively. Still, for those processes, savings of steam reach 54%, 61% and 66% when compared to the process without energy integration for Periods 1, 2 and 3, respectively, and 41%, 43% and 45% when compared to the process with project energy integration for Periods 1, 2 and 3, respectively.

5.4.3 Case study 3

Case Study 3 refers to 1G/2G ethanol and electricity production process. In this case study the fraction of xylose is biodigested to produce biogas. In Period 1, no bagasse is deviated for 2G ethanol section. In Periods 2 and 3, 39% and 78% of all bagasse is deviated for 2G ethanol production, respectively. It is interesting to observe that this case study presents the largest percentages of bagasse that can be deviated to produce 2G ethanol, since the produced biogas serves as complementary fuel in the boiler. Eight hot streams, 7 cold streams and 4 stages are present in Period 1, which implies a mathematical model with 896 variables. The number of variables in the mathematical model is almost doubled (1,600 variables) in Periods 2 and 3, since they have 10 hot streams, 10 cold streams and 4 stages. Table 5.8 shows streams data for the three periods.

Table 5.8. Stream data for sugarcane biorefinery of Case Study 3.

	Stream	**Device indicated in Fig. 5.1**	**T^0 (K)**	**T^{final} (K)**	**CP (kW/K)**	**h (kW/m^2 K)**
	Period 1					
H1	Concentrated juice	E204	388	306	638	1.38
H2	Vapor from Column D top (Condenser D)	E304	358	357	11,661	1.38
H3	Vapor from Column B top (Condenser B)	E305/E301	355	354	60,307	1.38
H4	Vapor from extractive column top (Condenser DEH1)	E309	351	350	24,592	1.38
H5	Vapor from recovery column top (Condenser DEH2)	E310	333	332	2,074	1.38
H6	Vinasse	E302	385	363	747	1.38
H7	Monoethylene glycol	E313	421	353	33	1.38
H8	Anhydrous ethanol	E315	351	308	43	1.38
C1	Juice	E114	321	343	1,256	1.38
C2	Juice	E117	343	378	1,288	1.38

C3	Wine	E301/E302	303	362	867	1.38
C4	Liquid from Column A bottom (Reboiler A)	E306	384	385	67,968	1.38
C5	Liquid from Column B1 bottom (Reboiler B)	E307	381	382	22,466	1.38
C6	Liquid from extractive column bottom (Reboiler DEH1)	E311	379	407	352	1.38
C7	Liquid from recovery column bottom (Reboiler DEH2)	E312	411	421	335	1.38
	Period 2					
H1	Concentrated juice	E204	388	306	724	1.38
H2	Vapor from Column D top (Condenser D)	E304	358	357	13,316	1.38
H3	Vapor from Column B top (Condenser B)	E305/E301	355	354	67,021	1.38
H4	Vapor from extractive column top (Condenser DEH1)	E309	351	350	27,298	1.38
H5	Vapor from recovery column top (Condenser DEH2)	E310	333	332	2,302	1.38
H6	Vinasse	E302	385	363	880	1.38
H7	Monoethylene glycol	E313	421	353	37	1.38
H8	Anhydrous ethanol	E315	351	308	51	1.38
H9	Pretreated bagasse	E506	468	353	604	1.38
H10	Xylose	E705	344	313	674	
C1	Juice	E114	321	343	1,256	1.38
C2	Juice	E117	343	378	1,288	1.38
C3	Wine	E301/E302	303	362	1,010	1.38
C4	Liquid from Column A bottom (Reboiler A)	E306	384	385	78,239	1.38
C5	Liquid from Column B1 bottom (Reboiler B)	E307	381	382	23,622	1.38
C6	Liquid from extractive column bottom (Reboiler DEH1)	E311	379	407	391	1.38
C7	Liquid from recovery column bottom (Reboiler DEH2)	E312	411	421	371	1.38
C8	Bagasse + soaking water	E503	439	468	602	1.38
C9	Soaking water	E506	303	458	481	1.38
C10	Solid fraction (cellulose + lignin)	E602	315	323	237	1.38
	Period 3					
H1	Concentrated juice	E204	388	306	816	1.38
H2	Vapor from Column D top (Condenser D)	E304	358	357	15,094	1.38
H3	Vapor from Column B top (Condenser B)	E305/E301	355	354	74,164	1.38
H4	Vapor from extractive column top (Condenser DEH1)	E309	351	350	30,174	1.38
H5	Vapor from recovery column top (Condenser DEH2)	E310	333	332	2,545	1.38
H6	Vinasse	E302	385	363	1,028	1.38
H7	Monoethylene glycol	E313	421	353	41	1.38
H8	Anhydrous ethanol	E315	351	308	53	1.38
H9	Pretreated bagasse	E506	468	353	1,247	1.38
H10	Xylose	E705	344	313	1,390	
C1	Juice	E114	321	343	1,256	1.38
C2	Juice	E117	343	378	1,288	1.38
C3	Wine	E301/E302	303	362	1,181	1.38
C4	Liquid from Column A bottom (Reboiler A)	E306	384	385	89,594	1.38
C5	Liquid from Column B1 bottom (Reboiler B)	E307	381	382	24,776	1.38
C6	Liquid from extractive column bottom (Reboiler DEH1)	E311	379	407	432	1.38

C7	Liquid from recovery column bottom (Reboiler DEH2)	E312	411	421	411	1.38
C8	Bagasse + soaking water	E503	439	468	1,241	1.38
C9	Soaking water	E506	303	458	993	1.38
C10	Solid fraction (cellulose + lignin)	E602	315	323	488	1.38

For biorefinery without energy integration (S1), the TAC is 30.5, 47.2 and 65.1 million USD/year for Periods 1, 2 and 3, respectively. In the process with project energy integration (S2), the TAC is 23.0, 28.4 and 34.1 million USD/year, respectively. For the energy integration, the average processing time of the algorithm was 25, 84 and 56 minutes in Periods 1, 2 and 3, respectively. TAC of the process with the single-period HEN (S3) is 12.7, 14.2 and 16.8 million of USD/year for those periods. Table 5.9 presents the number of heat exchange devices, area and costs for each period of operation.

Table 5.9. Number of heat exchange devices, total area, capital cost (CC), operating cost (OC), and total annualized cost (TAC) for single-period HEN using TS-PSO in Case Study 3.

	Units	Total required area (m^2)	CC (USD/year)	OC (USD/year)	Single-period solution TAC (USD/year)
Period 1	24	25,699.1	279,117	12,468,797	12,747,915
Period 2	33	42,348.0	424,612	13,737,335	14,161,947
Period 3	31	50,440.1	447,269	16,345,985	16,793,254

For the multiperiod HEN (S4), the estimated capital cost is 468,916 USD/year with total area of 51,976.9 m^2 and 33 heat transfer devices. The operating cost and the TAC of the multiperiod HEN are 14,184,039 USD/year and 14,652,954 USD/year, respectively in the hypothetical situation where the three periods have the same operation time. There is an area overdesign of 102% for Period 1, 23% for Period 2 and 3% for Period 3. Fig. 5.4 shows the multiperiod HEN configuration. Note that Periods 1, 2 and 3 have devices with fixed services between H1-C3, H3-C1, H3-C3 and H6-C2. There is no common service for any one of the heat exchangers in Periods 1 and 2. The device combining H4-C1 has fixed service in Periods 1 and 3. More fixed heat exchanger services are present in Periods 2 and 3, and these services are related to pairs H1-C9, H2-C2, H2-C3, H3-C9, H3-C10, H4-C9, H7-

C5, H9-C2, H9-C4 and H9-C5. Besides that, in Period 1, five cold streams have more than half of their flow rate bypassing heat exchangers. For Periods 2 and 3, two and six heat exchangers have bypasses above 50%. The HENs of Periods 1 and 3 and of Period 1 and 2 have significant differences. However, in Periods 2 and 3 the HENs are similar. Period 1 has four pairs of streams without any correspondence with other periods. Periods 2 and 3 have five and four pairs of streams that are not matched in other operation conditions, respectively. When comparing the number of idle devices, Periods 1 and 3 have 9 and 2 idle heat exchangers, respectively. In Period 2, all devices are being used. Those idle heat exchangers in Period 1 present a total area of 1,184.4 m^2, which is lower than 3% of the total area of the multiperiod HEN. In Period 3, these idle devices present areas lower than 113 m^2.

Table 5.10. Saving of steam demand and TAC of the processes with the single-period HEN (S3) and with the multiperiod HEN (S4) using TS-PSO in relation to the processes without energy integration (S1) and with project energy integration (S2) in Case Study 3.

Saving (%)	P1				P2				P3			
	S3/S1	**S3/S2**	**S4/S1**	**S4/S2**	**S3/S1**	**S3/S2**	**S4/S1**	**S4/S2**	**S3/S1**	**S3/S2**	**S4/S1**	**S4/S2**
HU	53.98	40.63	53.98	40.63	66.61	46.45	66.61	46.45	71.38	47.34	71.38	47.34
TAC	58.19	44.69	57.57	43.86	69.99	50.14	69.89	49.98	74.20	50.73	74.17	50.66

Table 5.10 shows savings in steam demand and TAC of processes with the single-period and with the multiperiod HEN compared to processes without energy integration and with project energy integration. Highlight is given to the savings obtained by the multiperiod HEN. The process with the multiperiod HEN presents reduction in TAC of 58%, 69% and 74% when compared to the process without energy integration for Periods 1, 2 and 3, respectively. The process with the multiperiod HEN presents reduction in TAC of 44%, 50% and 51% when compared to the process with project energy integration for Periods 1, 2 and 3, respectively. Furthermore, for those processes, savings of steam reach 54%, 67% and 71% when compared to the process without energy integration, and 41%, 46% and 47% when compared to the process with project energy integration for Periods 1, 2 and 3, respectively.

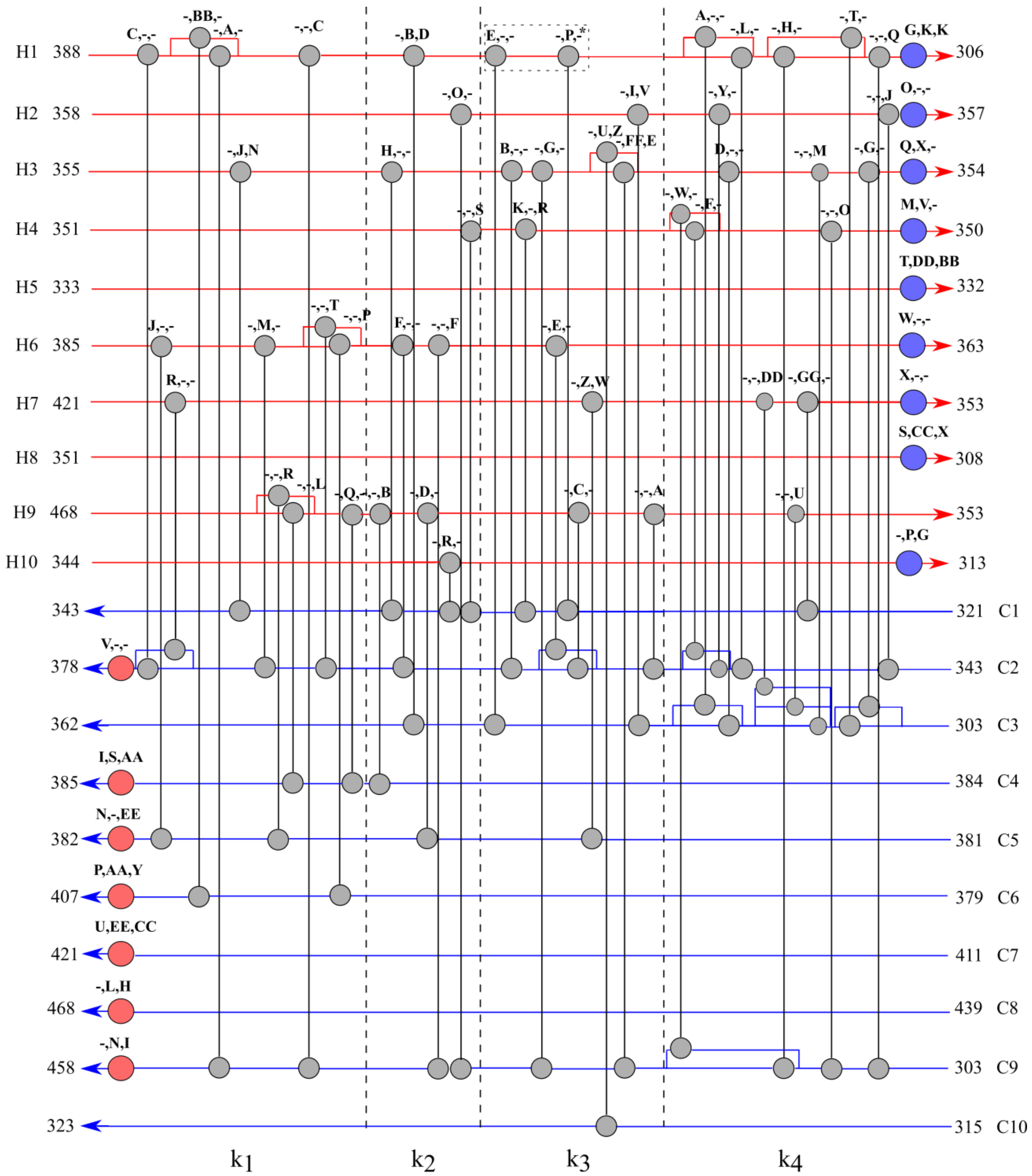

Labels and areas

A	B	C	D	E	F	G	H	I	J	K	L	M	N	O	P
5,500.0 m²	5,498.6 m²	5,494.6 m²	4,419.2 m²	4,380.0 m²	3,114.2m²	12,486.3 m²	2,357.7 m²	2,188.9 m²	2,030.8 m²	1,997 .7m²	1,684.0 m²	1,658.2 m²	1,423.9 m²	1,075.5 m²	946.7 m²
Q	R	S	T	U	V	W	X	Y	Z	AA	BB	CC	DD	EE	FF
774.1 m²	757.7 m²	749.3 m²	748.3 m²	465.1 m²	463.1 m²	293.8 m²	284.8 m²	216.5 m²	198.0 m²	182.1 m²	146.8 m²	134.7 m²	108.0 m²	86.2 m²	77.3 m²
GG															
34.8 m²															

*Note: No splits are represented because these matches never take place in the same period simultaneously.

Figure 5.4. Multiperiod HEN using TS-PSO for Case Study 3.

5.4.4 Remarks

In this section some remarks are presented, which are valid for all case studies. In Appendix 5.B, details about design of HENs are presented. In Tables 5.B.1, 5.B.5 and 5.B.9 of that appendix, note that there are different heat exchangers assigned to the same pair of streams in a given period. For example, in Periods 2 and 3 of Case Study 1, two different heat exchangers are assigned to pair H1-C9 (in stages 1 and 4 of the superstructure); in Period 2 of Case Study 2, two different heat exchangers are assigned to pair H3-C1 (in stages 1 and 2 of the superstructure); in Period 3 of Case Study 3, two different heat exchangers are assigned to pair H6-C2 (in stages 1 and 3 of the superstructure). This HEN configuration, where different devices are assigned to the same pair of streams in different stages of the superstructure in the same period, is obtained due to the maximum area constraint (*i.e.*, area of heat exchanger is limited to 5,500 m^2), which allows designing HENs more feasible from a practical perspective.

Table 5.11. Compilation of results for all case studies for utility demand (CU and HU), total area, operating cost (OC), capital cost (CC), and total annualized cost (TAC) in processes without energy integration (S1), with project integration (S2), with the single-period HEN (S3) and with the multiperiod HEN (S4) using TS-PSO.

Case study (CS)	Period	Process	CU (kW)	HU (kW)	Total required area (m2)	OC (USD/year)	CC (USD/year)	TAC (USD/year)
CS1	P1	S1	171,477	227,505	8,602.4	30,351,067	137,644	30,488,710
		S2	120,324	176,352	9,782.4	22,902,099	144,668	23,046,767
		S3	48,677	104,705	25,699.1	12,468,797	279,117	12,747,915
		S4	48,677	104,705	45,113.5	12,468,797	423,534	12,892,331
	P2	S1	250,778	327,924	12,656.7	43,926,941	184,932	44,111,874
		S2	131,698	208,844	14,722.4	26,586,353	195,126	26,781,480
		S3	37,789	114,935	37,769.0	12,911,180	386,761	13,297,942
		S4	37,789	114,935	45,113.5	12,911,180	423,534	13,334,714
	P3	S1	329,729	428,282	14,623.6	57,479,601	205,998	57,685,599
		S2	142,713	241,266	19,647.7	30,246,083	218,640	30,464,722
		S3	30,892	129,450	44,639.6	13,963,062	420,427	14,383,489
		S4	30,892	129,450	45,113.5	13,963,062	423,534	14,386,596
CS2	P1	S1	171,477	227,505	8,602.4	30,351,067	137,644	30,488,710
		S2	120,324	176,352	9,782.4	22,902,099	144,668	23,046,767
		S3	48,677	104,705	25,699.1	12,468,797	279,117	12,747,915
		S4	48,677	104,705	42,154.3	12,468,797	453,979	12,922,777

	P2	**S1**	222,635	286,678	11,148.9	38,570,441	181,979	38,752,421
		S2	132,526	196,569	12,858.3	25,448,649	191,072	25,639,722
		S3	48,329	112,375	32,287.5	13,188,084	400,320	13,588,404
		S4	48,329	112,375	42,154.3	13,188,084	453,979	13,642,064
	P3	**S1**	275,618	348,571	13,792.1	47,141,522	197,742	47,339,264
		S2	144,639	217,592	16,065.5	28,068,186	208,569	28,276,755
		S3	45,541	118,498	41,598.6	13,637,792	441,626	14,079,418
		S4	45,541	118,498	42,154.3	13,637,792	453,979	14,091,772
CS3	**P1**	**S1**	171,477	227,505	8,602.4	30,351,067	137,644	30,488,710
		S2	120,324	176,352	9,782.4	22,902,099	144,668	23,046,767
		S3	48,677	104,705	25,699.1	12,468,797	279,117	12,747,915
		S4	48,677	104,705	51,976.9	12,468,797	468,916	12,937,713
	P2	**S1**	283,728	342,730	14,477.6	46,982,799	201,589	47,184,388
		S2	154,678	213,680	16,661.9	28,190,367	212,114	28,402,481
		S3	55,431	114,427	42,348.0	13,737,335	424,612	14,161,947
		S4	55,431	114,427	51,976.9	13,737,335	468,916	14,206,250
	P3	**S1**	404,099	466,775	20,792.9	64,864,197	233,625	65,097,823
		S2	191,015	253,691	24,089.6	33,834,622	247,153	34,081,776
		S3	70,917	133,595	50,440.1	16,345,985	447,269	16,793,254
		S4	70,917	133,595	51,976.9	16,345,985	468,916	16,814,900

Table 5.11 compares the values of utilities demand, area and costs among the processes without any energy integration, with project energy integration, with the single-period HEN and with the multiperiod HEN. It is important to recall that operating cost for the multiperiod HEN for each period is the annual operating cost of that given period. However, the operating cost of the multiperiod HEN that operates in multiple conditions depends on the operation time of the plant under each condition. In Table 5.11, note that the operating cost is 100 times greater than the capital cost. Thus, the operating cost has more influence on the total annualized cost. It is worth noticing that, when comparing TAC of processes with the single-period and with the multiperiod HEN, the latter is 1%, 0.3% and 0.02% higher than the former in Case Study 1 for Periods 1, 2 and 3, respectively. For Case Studies 2 and 3, respectively, these numbers are 1%, 0.4% and 0.09%, and 1%, 0.3% and 0.1%. All these numbers represent little increase in TAC of the multiperiod HEN, compared to TAC of the corresponding single-period HENs. Thus, a small additional investment allows the process to operate

in different conditions, ensuring certain flexibility to the process. Furthermore, the uncertainty in values of parameters used to calculate the investment cost does not change significantly the optimal solution, since the TAC is little influenced by the investment cost of HEN. Such uncertainties are generated by assumptions as ‘all convective coefficients are equal’ and ‘constant temperatures of utilities’.

One more important notice refers to HENs costs associated to cold stream 7 in Period 1 and cold streams 7 and 8 in Periods 2 and 3 for all cases studies. These streams could not be integrated to other streams given their high temperatures (that is, only hot utility can be provided for heating cold streams 7 and 8). Thus, there is a built-in cost referring to steam demand and to the area of the heaters that are designed on those streams. In Case Studies 1 and 3, these costs represent 3%, 14% and 23% of TAC for HENs synthesized individually for Periods 1, 2 and 3, respectively. In Case Study 2, these costs represent 3%, 8% and 14% of TAC for HENs synthesized individually for Periods 1, 2 and 3, respectively. Since the steam demand of cold stream 7 and 8 in Case Study 2 is lower than in the other cases, those built-in costs are small. Such results imply important percentage values of TAC are associated to operating and investment costs of streams that cannot be integrated to other process streams. Notably, more relevant fraction of those values is associated to costs of cold stream 8, due to its heat capacity.

When comparing the process with the multiperiod HEN to the process without energy integration, it is inferred that reductions in TAC can reach 75%. This reduction in TAC can reach 53% in the process with multiperiod HEN in relation to the process with project energy integration. For the multiperiod HEN, if comparison is performed in terms of saving of steam, the reduction of steam demand can achieve 71% when compared to the process without energy integration and 47% when compared to the process with project energy integration. These values indicate the maximum saving of TAC and steam demand among all cases and their periods. Although the values differ among case studies and operating conditions, in all cases the saving of TAC represents a very significant cost for the process. However, not all the bagasse saved by energy integration can be used to produce second generation ethanol, because the surplus 2G ethanol will increase heat loads of some streams and, consequently, the steam demand. Therefore, only a fraction of the bagasse saved can be used in 2G ethanol production. Estimating the fraction of the bagasse that can be diverted to 2G ethanol section is not scope of this work, but it can be determined with an iterative procedure. In this procedure, after performing energy integration of the biorefinery, a new fraction of the bagasse is destined to 2G ethanol section and the process is simulated in this new condition. Afterwards, energy integration is applied to this condition in order to attain the current steam demand. This procedure is executed until energy demand does not change significantly. Since the HENs are synthesized to multiple periods, that procedure should be performed to each period. Although this work did not estimate the surplus 2G ethanol production that can be achieved with the multiperiod HEN synthesis, it demonstrates the potential of energy integration to provide improvements in 1G/2G ethanol and electricity production process. Besides that, the synthesis of multiperiod HEN presented in this study is an actual report of energy integration for industrial large scale plants.

It is important to mention that the multiperiod HENs without fixed services require a cleaning step among the transition from one operating condition to another, as well as dead times. The dead times used to shutdown, cleaning, and starting up the plant among changing operating conditions are idle plant periods. However, these periods are commonly rather small than total plant operation time. In this work, these dead times were assumed as negligible and were not included in TAC, similarly to the works conducted by Jiang and Chang (2013, 2015), Miranda et al. (2016), Pavão et al. (2018a,b) and Oliveira et al. (2017). Dead times and their associated costs may be included in the objective function of mathematical model. However, to estimate such costs information about the duration and costs of the plant inactivity periods, and the number of times those transitions occur are required, which are difficult to predict. Additional information about the multiperiod HEN refers to its complexity, since valves, pipes, pumps and control instruments are needed to dislocate some streams to the heat exchangers indicated on the multiperiod HEN, as well as for the design of the bypasses. However, the multiperiod HEN approach allows the biorefinery to operate in multiple process conditions, which is a more realistic hypothesis than supposing that the biorefinery operates with fixed operating conditions.

5.5 Conclusion

The sugarcane industry in Brazil is responsible for putting Brazil in the second place in the rank list of top producers of ethanol in the world. Thus, decreasing costs related to energy demand in ethanol production processes is valuable for the area. Depending on the case study and its period, the saving in TAC can reach 75% in the process with the multiperiod HEN when compared to the process without energy integration and 53% when compared to the process with the project energy integration. Furthermore, the process with the multiperiod HEN can save up to 71% and up to 47% of steam in relation to processes without energy integration and with project energy integration, respectively. The particular reduction in steam demand allows increasing the 2G ethanol production. Besides, the energy integration provides better use of environmental resources and energy security. As a consequence, all those improvements obtained by energy integration in biorefineries contribute to 1G/2G ethanol and electricity production process. In addition, the novel hybrid method TS and PSO presented in this work proved to be efficient to solve large-scale HEN synthesis problems.

Nomenclature

Variables

A	[m^2]	Heat exchanger area
Acu	[m^2]	Cooler area
Ahu	[m^2]	Heater area
C_{total}	[USD/year]	Annualized total cost
Fc	[-]	Fraction of cold stream
Fh	[-]	Fraction of hot stream
LMTD	[K]	Logarithmic mean temperature difference
Q	[kW]	Heat load in a heat exchanger
Qcu	[kW]	Heat load in a cooler
Qhu	[kW]	Heat load in a heater
Qmax	[kW]	Maximum heat load
TAC	[USD/year]	Total annualized cost

Tchuin	[K]	Inlet temperature of the cold stream in a heater
Thcuin	[K]	Inlet temperature of the hot stream in a cooler
Tcin	[K]	Inlet temperature of the cold stream in a heat exchanger
Thin	[K]	Inlet temperature of the hot stream in a heat exchanger
Tcout	[K]	Outlet temperature of the cold stream in a heat exchanger
Thout	[K]	Outlet temperature of the hot stream in a heat exchanger
Tcmix	[K]	Mixture temperature of the cold stream after mixer
Thmix	[K]	Mixture temperature of the hot stream after mixer
U	[kW/(m^2 K)]	Overall coefficient of heat transfer
z	[-]	Binary variable representing existence of a heat exchanger
zcu	[-]	Binary variable representing existence of a cooler
zhu	[-]	Binary variable representing existence of a heater
$\theta^{(1)}$	[K]	Temperature approximation at the hot end of a heat exchanger
$\theta^{(2)}$	[K]	Temperature approximation at the cold end of a heat exchanger
ΔT	[K]	Temperature Difference

Parameters

a	[USD/year]	Annual fixed cost coefficient for heat exchangers
b	[USD/(m^2 year)]	Annual variable cost coefficient for heat exchangers
c	[-]	Area cost exponent
ccu	[USD/(kW year)]	Cost of cold utility
chu	[USD/(kW year)]	Cost of hot utility
CPc	[kW/K]	Heat capacity of the cold stream
CPh	[kW/K]	Heat capacity of the hot stream
C_W	[USD/m^3]	Cost of cooling water
EMAT	[K]	Minimum temperature approximation in the heat exchanger
hc	[kW/(m^2 K)]	Heat transfer convective coefficient of the cold stream

hh	[kW/(m^2 K)]	Heat transfer convective coefficient of the hot stream
h_{IN}	[kJ/kg]	Enthalpy of cooling water at inlet cooler
h_{OUT}	[kJ/kg]	Enthalpy of cooling water at outlet cooler
h_{COND}	[kJ/kg]	Enthalpy of condensation
H_S	[kJ/kg]	Enthalpy of steam
h_W	[kJ/kg]	Enthalpy of boiler feed water
k	[-]	Number of the stage
Tc^0	[K]	Initial temperature of the cold stream
Tc^{final}	[K]	Final (target) temperature of the cold stream
Th^0	[K]	Initial temperature of the hot stream
Th^{final}	[K]	Final (target) temperature of the hot stream

Data set

N_C	[-]	Cold streams
N_H	[-]	Hot streams
N_S	[-]	Stages

Subscripts

i	Cold streams
j	Hot streams
k	Stage superstructure

Text

CSA	Continuous Simulated Annealing
GA	Genetic Algorithm
HS	Harmonic Search
HEN	Heat exchanger network

HENs	Heat exchanger networks
LP	Linear Programming
MILP	Mixed Integer Linear Programming
MINLP	Mixed Integer Nonlinear Programming
NL	Nonlinear Programming
NIM-SWS	Nonisothermal Mixing Stage-Wise Superstructure
SA	Simulated Annealing
SQP	Quadratic Sequential Programming
SWS	Stage-Wise superstructure
PSO	Particle Swarm Optimization
RFO	Rocket Fireworks Optimization
TS	Tabu Search

References

AALTOLA, J. Simultaneous synthesis of flexible heat exchanger network. Applied Thermal Engineering, v. 22, n. 8, p. 907–918, 2002.

AHMAD, M. I.; ZHANG, N.; JOBSON, M.; CHEN, L. Multi-period design of heat exchanger networks. Chemical Engineering Research and Design, v. 90, n. 11, p. 1883–1895, 2012.

CHEN, X.; ZHAOHUA, L.; YANG, J.; SHAO, Z.; ZHU, L. Nested Tabu Search (TS) and Sequential Quadratic Programming (SQP) Method, Combined with Adaptive Model Reformulation for Heat Exchanger Network Synthesis (HENS). 2008.

ENSINAS, A. V. Energy integration and thermo-economic optimization applied to the industrial process of sugar and ethanol production from sugarcane. 2008. PhD Thesis (Chemical Engineering), State University of Campinas, 2008.

FLOUDAS, C. A.; CIRIC, A. R.; GROSSMANN, I. E. Automatic synthesis of optimum heat exchanger network configurations. AIChE Journal, v. 32, n. 2, p. 276–290, 1986.

FLOUDAS, C. A.; GROSSMANN, I. E. Synthesis of flexible heat exchanger networks for multiperiod operation. Computers & Chemical Engineering, v. 10, n. 2, p. 153–168, 1986.

FLOUDAS, C. A.; GROSSMANN, I. E. Automatic generation of multiperiod heat exchanger network configurations. Computers & Chemical Engineering, v. 11, n. 2, p. 123–142, 1987.

FURLAN, F. F.; COSTA, C. B. B.; CRUZ, A. J. G.; SECCHI, A. R.; SOARES, R. P.; GIORDANO, R. C. Integrated tool for simulation and optimization of a first and second generation ethanol-from-sugarcane production plant. Computer Aided Chemical Engineering, v. 30, p. 81–85, 2012.

FURLAN, F. F.; FILHO, R.; PINTO, F. H.; COSTA, C. B.; CRUZ, A. J.; GIORDANO, R. L.; GIORDANO, R. C. Bioelectricity versus bioethanol from sugarcane bagasse: is it worth being flexible? Biotechnology for Biofuels, v. 6, n. 1, p. 142, 2013.

GLOVER, F. Future paths for integer programming and links to artificial intelligence. Computers & Operations Research, v. 13, n. 5, p. 533–549, 1986.

GLOVER, F. Tabu Search-- Part I. ORSA Journal on Computing, v. 1, n. 3, 1989.

GLOVER, F. Tabu Search-Part I1. ORSA Journal on Comput~ng, v. 2, n. I, 1990.

GLOVER, F.; MARTI, R. Tabu Search. In: Metaheuristic Procedures for Training Neutral Networks. [s.l.] Springer US, 2006. p. 53–69.

GLOVER, F.; TAILLARD, E.; TAILLARD, E. A user's guide to tabu search. Annals of Operations Research, v. 41, n. 1, p. 1–28, mar. 1993.

JIANG, D.; CHANG, C.-T. A New Approach to Generate Flexible Multiperiod Heat Exchanger Network Designs with Timesharing Mechanisms. Industrial & Engineering Chemistry Research, v. 52, n. 10, p. 3794–3804, 2013.

JIANG, D.; CHANG, C.-T. An algorithmic approach to generate timesharing schemes for multi-period HEN designs. Chemical Engineering Research and Design, v. 93, p. 402–410, 2015.

KENNEDY, J.; EBERHART, R. Particle Swarm Optimization. Proceedings of IEEE International Conference on Neural Networks, p. 1942–1948, 1995.

KHORASANY, R. M.; FESANGHARY, M. A novel approach for synthesis of cost-optimal heat exchanger networks. Computers & Chemical Engineering, v. 33, n. 8, p. 1363–1370, 2009.

LEWIN, D. R. A generalized method for HEN synthesis using stochastic optimization — II.: The synthesis of cost-optimal networks. Computers & Chemical Engineering, v. 22, n. 10, p. 1387–1405, 1998.

LIN, B.; MILLER, D. C. Solving heat exchanger network synthesis problems with Tabu Search. Computers & Chemical Engineering, v. 28, n. 8, p. 1451–1464, 2004.

MA, X.; YAO, P.; LUO, X.; ROETZEL, W. Synthesis of multi-stream heat exchanger network for multi-period operation with genetic/simulated annealing algorithms. Applied Thermal Engineering, v. 28, n. 8, p. 809–823, 2008.

MARTELLI, E.; ELSIDO, C.; MIAN, A.; MARECHAL, F. MINLP model and two-stage algorithm for the simultaneous synthesis of heat exchanger networks, utility systems and heat recovery cycles. Computers & Chemical Engineering, v. 106, p. 663–689, 2017.

MARTELLI, E.; MIAN, A.; MARÉCHAL, F. MINLP Model and two-level Algorithm for the Simultaneous Synthesis of Heat Exchanger Networks and Utility Systems. Computer Aided Chemical Engineering, v. 37, p. 1979–1984, 2015.

MIRANDA, C. B.; COSTA, C. B. B.; CABALLERO, J. A.; RAVAGNANI, .A.S.S. Optimal synthesis of multiperiod heat exchanger networks: A sequential approach. Applied Thermal Engineering, v. 115, p. 1187–1202, 2017.

MIRANDA, C. B.; COSTA, C. B. B.; CABALLERO, J. A.; RAVAGNANI, M. A. S. S. Heat Exchanger Network Optimization for Multiple Period Operations. Industrial & Engineering Chemistry Research, v. 55, n. 39, p. 10301–10315, 2016.

OLIVEIRA, C. M.; CRUZ, A. J. G.; COSTA, C. B. B. Improving second generation bioethanol production in sugarcane biorefineries through energy integration. Applied Thermal Engineering, v. 109, p. 819–827, 2016.

OLIVEIRA, C. M.; PAVÃO, L. V.; RAVAGNANI, M. A. S. S.; CRUZ, A. J. G.; COSTA, C. B. B. Process integration of a multiperiod sugarcane biorefinery. Applied Energy, 2017.

PAPOULIAS, S. A.; GROSSMANN, I. E. A structural optimization approach in process synthesis—II. Computers & Chemical Engineering, v. 7, n. 6, p. 707–721, 1983.

PAVÃO, L. V.; COSTA, C. B. B.; RAVAGNANI, M. A. da S. S. Automated heat exchanger network synthesis by using hybrid natural algorithms and parallel processing. Computers & Chemical Engineering, v. 94, p. 370–386, 2016.

PAVÃO, L. V.; COSTA, C. B. B.; RAVAGNANI, M. A. S. S. Heat Exchanger Network Synthesis without stream splits using parallelized and simplified Simulated Annealing and Particle Swarm Optimization. Chemical Engineering Science, v. 158, p. 96–107, 2017.

PAVÃO, L. V.; COSTA, C. B. B.; RAVAGNANI, M. A. da S. S.; JIMÉNEZ, L. Large-scale heat exchanger networks synthesis using simulated annealing and the novel rocket fireworks optimization. AIChE Journal, v. 63, n. 5, p. 1582–1601, 2017a.

PAVÃO, L. V.; COSTA, C. B. B.; RAVAGNANI, M. A. da S. S.; JIMÉNEZ, L. Costs and environmental impacts multi-objective heat exchanger networks synthesis using a meta-heuristic approach. Applied Energy, v. 203, p. 304–320, 2017b.

PAVÃO, L. V.; POZO, C.; COSTA, C. B. B.; RAVAGNANI, M. A. S. S.; JIMÉNEZ, L. Financial risks management of heat exchanger networks under uncertain utility costs via multi-objective optimization. Energy, v. 139, p. 98–117, 2017c.

PAVÃO, L. V.; MIRANDA, C. B.; COSTA, C. B. B.; RAVAGNANI, M. A. S. S. Efficient multiperiod heat exchanger network synthesis using a meta-heuristic approach. Energy, v. 142, p. 356–372, 2018a.

PAVÃO, L. V; MIRANDA, C. B.; COSTA, C. B. B.; RAVAGNANI, M. A. S. S. Synthesis of multiperiod heat exchanger networks with timesharing mechanisms using meta-heuristics. Applied Thermal Engineering, v. 128, p. 637–652, 2018b.

PINA, E. A.; PALACIOS-BERECHE, R.; CHAVEZ-RODRIGUES, M. F.; ENSINAS, A. V.; MODESTO, M.; NEBRA, S. A. Thermal integration of different plant configurations of sugar and ethanol production from sugarcane. Chemical Engineering Transactions, v. 39, p. 1147–1152, 2014.

SILVA, A. P.; RAVAGNANI, M. A. S. S.; BISCAIA, E. C. Particle Swarm Optimisation in heat exchanger network synthesis including detailed equipment design. Computer Aided Chemical Engineering, v. 25, p. 713–718, 2008.

SILVA, A. P.; RAVAGNANI, M. A. S. S.; BISCAIA, E. C.; CABALLERO, J. A. Optimal heat exchanger network synthesis using particle swarm optimization. Optimization and Engineering, v. 11, n. 3, p. 459–470, 2010.

YEE, T. F.; GROSSMANN, I. E. Simultaneous optimization models for heat integration—II. Heat exchanger network synthesis. Computers & Chemical Engineering, v. 14, n. 10, p. 1165–1184, out. 1990.

YERRAMSETTY, K. M.; MURTY, C. V. S. Synthesis of cost-optimal heat exchanger networks using differential evolution. Computers & Chemical Engineering, v. 32, n. 8, p. 1861–1876, 2008.

ZHANG, C.; CUI, G.; PENG, F. A novel hybrid chaotic ant swarm algorithm for heat exchanger networks synthesis. Applied Thermal Engineering, v. 104, p. 707–719, 2016.

VERHEYEN, N.; ZHANG, W. Design of flexible heat exchanger network for multi-period operation. Chemical Engineering Science, v. 61, n. 23, p. 7730–7753, 2006.

Appendix 5.A

This section presents parameters, operating conditions and results of simulation of 2G ethanol and electricity production process.

Table 5.B.2. Main data for second generation ethanol production.

	Value	Unit
Pretreatment		
Pressure	1	bar
Temperature	195	°C
Cellulose to glucose yield	8.12	%, w/w
Hemicellulose to xylose yield	46.53	% w/w
Solid/liquid ratio	10	%
Space-time	10	min

Hydrolysis		
Cellulose to glucose yield	75	%, w/w
Solid/liquid ratio	15	%
Enzyme/Cellulose ratio	15	FPU/g
Space-time	48	h
Temperature	50	°C
Fermentation of xylose fraction		
Xylose concentration	50	g/L
Space-time	24-48	h
Temperature	33	°C
Biodigestion		
Chemical Oxygen Demand	20 - 60	kg/m³/day
Temperature	40	°C
Space-time	10.8	h
Sludge humidity	96.5-98.5	%

Table 5.B.3. Main results for 1G/2G anhydrous ethanol and electricity production.

Case study	Period	Bagasse fraction for 2G ethanol	Ethanol production (m^3/day)	Electricity production (MW)	Specific ethanol production (L/tonne of sugarcane)
CS1	1	-	1,779	180	89
	2	0.33	1,949	138	96
	3	0.66	2,118	97	104
CS2	1	-	1,779	180	89
	2	0.17	1,880	149	94
	3	0.34	2,009	117	101
CS3	1	-	1,779	180	89
	2	0.39	2,071	141	104
	3	0.78	2,153	102	108

Appendix 5.B

This section shows details about the single-period HENs and the multiperiod HEN for all case studies.

Table 5.B.1. Single-period HEN for Case Study 1 (Part 1).

Match		**(1,2,1)**	**(1,2,4)**	**(1,3,3)**	**(1,3,4)**	**(3,1,2)**	**(3,2,3)**	**(3,3,4)**	**(4,1,3)**	**(6,2,2)**	**(6,5,1)**	**(7,2,1)**
Period 1												
A_S	m^2	5365.4	1255.3	3375.8	5,500.0	1883.4	5390.2	5297.1	1673.1	2970.5	1812.7	534.3
$A_{i,j,k}$	m^2	2,894.5	515.3	1,877.5	4,580.3	1,344.0	4,377.2	2,824.3	654.9	1,490.0	871.2	154.8
$A_{i,j,k}/A_s$		0.54	0.41	0.56	0.83	0.71	0.81	0.53	0.39	0.50	0.48	0.29
$Q_{i,j,k}$	kW	12,657.2	2,076.1	6,177.6	18,660.6	16,323.5	11,743.3	26,314.8	11,308.5	14,133.2	1,640.5	1,764.5
$Fh_{i,j,k}$		1.00	0.24	1.00	0.76	1.00	1.00	1.00	1.00	1.00	1.00	1.00
$Fc_{i,j,k}$		0.77	1.00	1.00	0.40	1.00	1.00	0.60	1.00	1.00	1.00	0.23
$Thin_{i,j,k}$	K	388.0	358.5	368.2	358.5	355.0	354.7	354.5	351.0	382.8	385.0	421.0
$Thout_{i,j,k}$	K	368.2	344.7	358.5	320.2	354.7	354.5	354.1	350.5	363.9	382.8	367.5
$Tcin_{i,j,k}$	K	364.7	343.0	354.9	303.0	330.0	344.6	303.0	321.0	353.7	381.0	364.7
$Tcout_{i,j,k}$	K	377.5	344.6	362.0	357.3	343.0	353.7	353.3	330.0	364.7	381.1	370.6
LMTD	K	6.3	5.8	4.8	5.9	17.6	3.9	13.5	25.0	13.7	2.7	16.5
Desvio xc	%	36.0	86.8	37.6	1.0	34.4	4.9	2.4	68.2	55.5	97.6	87.9

Match		**(1,1,3)**	**(1,3,2)**	**(1,5,1)**	**(1,9,1)**	**(1,9,4)**	**(2,2,4)**	**(3,1,1)**	**(3,3,4)**	**(3,9,3)**	**(4,3,4)**	**(5,10,1)**	**(6,2,3)**	**(6,6,1)**	**(7,5,3)**	**(9,2,3)**	**(9,4,2)**
Period 2																	
A_S	m^2	544.8	5,500.0	534.3	5,365.4	1,255.3	1,812.7	1,883.4	5,297.1	1,979.6	1,673.1	285.4	3,375.8	774.4	92.4	5,390.2	2,970.5
$A_{i,j,k}$	m^2	544.8	5,416.5	534.3	4,513.2	1,028.0	1,356.8	1,506.5	3,460.0	1,945.1	1,080.7	173.2	2,837.8	774.4	33.3	4,909.4	2,378.6
$A_{i,j,k}/A_s$		1.00	0.98	1.00	0.84	0.82	0.75	0.80	0.65	0.98	0.65	0.61	0.84	1.00	0.36	0.91	0.80
$Q_{i,j,k}$	kW	8,394.6	10,512.1	1,128.8	13,558.1	11,259.5	9,788.0	19,237.4	36,808.0	9,931.4	11,384.9	1,606.0	16,757.1	1,563.6	684.6	18,239.3	42,135.7
$Fh_{i,j,k}$		1.00	1.00	0.27	0.73	1.00	1.00	1.00	1.00	1.00	1.00	1.00	1.00	1.00	1.00	1.00	1.00
$Fc_{i,j,k}$		1.00	1.00	1.00	1.00	1.00	1.00	1.00	0.75	1.00	0.25	1.00	0.47	1.00	1.00	0.53	1.00
$Thin_{i,j,k}$	K	352.7	367.4	388.0	388.0	340.9	358.0	355.0	354.6	354.7	351.0	333.0	383.2	385.0	421.0	387.7	468.0
$Thout_{i,j,k}$	K	340.9	352.7	382.0	362.1	325.1	357.3	354.7	354.0	354.6	350.6	332.3	363.7	383.2	402.5	353.0	387.7
$Tcin_{i,j,k}$	K	321.0	351.4	381.0	353.7	303.0	343.0	327.7	303.0	329.9	303.0	315.0	350.6	379.0	381.0	350.6	384.0
$Tcout_{i,j,k}$	K	327.7	362.0	381.1	386.1	329.9	350.6	343.0	352.4	353.7	348.5	322.8	378.0	383.1	381.0	377.6	384.5

LMTD	K	22.3	2.8	3.1	4.4	15.9	10.5	18.5	15.4	7.4	15.3	13.4	8.6	2.9	29.8	5.4	25.7
Bypass	%	0.2	1.9		2.0	13.1	32.8	24.6	3.5	0.2	4.4	48.0	6.2		99.9	5.1	97.6

Match		**(1,2,1)**	**(1,3,2)**	**(1,9,1)**	**(1,9,4)**	**(1,10,4)**	**(2,2,4)**	**(3,1,1)**	**(3,3,3)**	**(3,3,4)**	**(3,9,3)**	**(4,1,3)**	**(4,9,4)**	**(5,10,1)**	**(6,5,1)**	**(6,9,2)**	**(7,5,3)**	**(7,6,4)**	**(9,1,4)**	**(9,2,3)**	**(9,4,1)**	**(9,4,2)**
Period 3																						
A_S	m^2	537.8	1194.3	5500	2970.5	42	1812.7	1255.3	5365.4	110.6	544.8	534.3	963.9	324.3	1883.4	3375.8	90.4	144.4	220.8	5390.2	774.4	5297.1
$A_{i,j,k}$	m^2	511.3	1,194.3	5,500.0	2,970.5	42.0	1,812.7	1,255.3	5,365.4	110.6	533.2	500.2	963.9	289.7	1,883.4	3,375.8	90.4	144.4	220.8	5,390.2	565.5	5,297.1
$A_{i,j,k}/A_s$		0.95	1.00	1.00	1.00	1.00	1.00	1.00	1.00	1.00	0.98	0.94	1.00	0.89	1.00	1.00	1.00	1.00	1.00	1.00	0.73	1.00
$Q_{i,j,k}$	kW	1,544.4	10,279.4	7,479.9	29,201.5	813.0	11,777.2	14,865.2	52,565.1	3,766.5	737.6	7,830.8	11,879.4	2,467.0	2,819.0	18,763.0	1,263.4	376.6	4,935.9	29,431.0	27,094.4	58,941.6
$Fh_{i,j,k}$		0.16	1.00	0.84	0.97	0.03	1.00	1.00	0.92	1.00	0.08	1.00	1.00	1.00	1.00	1.00	1.00	1.00	1.00	1.00	1.00	1.00
$Fc_{i,j,k}$		1.00	1.00	1.00	0.67	1.00	1.00	1.00	1.00	1.00	1.00	1.00	0.33	1.00	1.00	1.00	1.00	1.00	1.00	1.00	1.00	1.00
$Thin_{i,j,k}$	K	388.0	376.5	388.0	363.5	363.5	358.0	355.0	354.8	354.1	354.8	351.0	350.7	333.0	385.0	382.1	421.0	389.4	357.7	385.8	468.0	442.1
$Thout_{i,j,k}$	K	376.0	363.5	376.7	325.3	330.3	357.2	354.8	354.0	354.0	354.7	350.7	350.3	332.0	382.1	363.0	389.4	380.0	353.0	357.7	442.1	385.8
$Tcin_{i,j,k}$	K	375.0	352.9	375.6	303.0	315.0	343.0	331.2	306.3	303.0	352.3	324.9	303.0	317.0	381.1	353.1	381.0	379.0	321.0	352.1	384.7	384.0
$Tcout_{i,j,k}$	K	376.2	362.0	384.6	355.1	317.0	352.1	343.0	352.9	306.3	353.1	331.2	346.5	323.0	381.2	375.6	381.1	379.9	324.9	375.0	385.0	384.7
LMTD	K	4.4	12.5	2.0	14.2	28.1	9.4	17.2	14.2	49.3	2.0	22.7	17.9	12.3	2.2	8.1	20.2	3.8	32.4	7.9	69.4	16.1
Bypass	%										6.2	28.9		26.8							99.2	

Table 5.B.2. Single-period HEN for Case Study 1 (Part 2).

Match	**(i,j,k)**	**(1,CU,5)**	**(2,CU,5)**	**(3,CU,5)**	**(4,CU,5)**	**(5,CU,5)**	**(6,CU,5)**	**(7,CU,5)**	**(8,CU,5)**	**(9,CU,5)**
Period 1										
A_s	m^2	1979.6	774.4	537.8	1194.3	324.3	195	144.4	462.8	
$A_{i,j,k}$	m^2	1,372.1	302.1	163.7	395.3	97.3	15.5	11.8	113.6	-
$A_{i,j,k}/A_s$	%	0.69	0.39	0.30	0.33	0.30	0.08	0.08	0.25	-
$Q_{i,j,k}$	kW	12,744.5	11,661.0	5,925.4	13,283.5	2,074.0	660.3	479.5	1,849.0	-
$Fh_{i,j,k}$		1.0	1.0	1.0	1.0	1.0	1.0	1.0	1.0	-
$Fc_{i,j,k}$				-	-		-			-
$Thin_{i,j,k}$	K	326.0	358.0	354.1	350.5	333.0	363.9	367.5	351.0	-
$Thout_{i,j,k}$	K	306.0	357.0	354.0	350.0	332.0	363.0	353.0	308.0	-
$Tcin_{i,j,k}$	K	298.0	298.0	298.0	298.0	298.0	298.0	298.0	298.0	-
$Tcout_{i,j,k}$	K	305.0	305.0	305.0	305.0	305.0	305.0	305.0	305.0	-
LMTD	K	13.5	55.9	52.5	48.7	30.9	61.9	58.7	23.6	-
Period 2										
A_s	m^2	1828.6	144.4	42	462.8	90.4	71.9	110.6	195	
$A_{i,j,k}$	m^2	1,502.5	86.0	4.4	462.8	31.6	15.1	35.8	124.2	-
$A_{i,j,k}/A_s$	%	0.82	0.60	0.10	1.00	0.35	0.21	0.32	0.64	-
$Q_{i,j,k}$	kW	13,612.9	3,298.0	159.3	15,557.1	666.0	643.3	1,831.4	2,021.0	-
$Fh_{i,j,k}$		1.0	1.0	-	1.0	1.0	-	1.0	1.0	-
$Fc_{i,j,k}$				-			-			-
$Thin_{i,j,k}$	K	325.1	357.3	354.0	350.6	332.3	363.7	402.5	351.0	-
$Thout_{i,j,k}$	K	306.0	357.0	354.0	350.0	332.0	363.0	353.0	308.0	-
$Tcin_{i,j,k}$	K	298.0	298.0	298.0	298.0	298.0	298.0	298.0	298.0	-
$Tcout_{i,j,k}$	K	305.0	305.0	305.0	305.0	305.0	305.0	305.0	305.0	-
LMTD	K	13.1	55.6	52.4	48.7	30.5	61.8	74.2	23.6	-
Period 3										
A_s	m^2	1673.1	71.9		285.4			24.3	134.7	
$A_{i,j,k}$	m^2	1,673.1	71.9	-	285.4	-	-	24.3	134.7	-
$A_{i,j,k}/A_s$	%	1.00	1.00	-	1.0	-	-	1.0	1.0	-
$Q_{i,j,k}$	kW	15,297.8	2,754.8	-	9,566.8	-	-	1,080.0	2,193.0	-
$Fh_{i,j,k}$		1.0	1.0	-	1.0	-	-	1.0	1.0	-
$Fc_{i,j,k}$		-	-	-		-	-	-		-
$Thin_{i,j,k}$	K	325.4	357.2	-	350.3	-	-	380.0	351.0	-
$Thout_{i,j,k}$	K	306.0	357.0	-	350.0	-	-	353.0	308.0	-
$Tcin_{i,j,k}$	K	298.0	298.0	-	298.0	-	-	298.0	298.0	-
$Tcout_{i,j,k}$	K	305.0	305.0	-	305.0	-	-	305.0	305.0	-
LMTD	K	13.3	55.5	-	48.6	-	-	64.5	23.6	-

Table 5.B.3. Single-period HEN for Case Study 1 (Part 3).

Match	(i,j,k)	(HU,1,0)	(HU,2,0)	(HU,3,0)	(HU,4,0)	(HU,5,0)	(HU,6,0)	(HU,7,0)	(HU,8,0)	(HU,9,0)	(HU,10,0)
Period 1											
A_s	m^2		220.8		1828.6	963.9	544.8	285.4	-	-	-
$A_{i,j,k}$	m^2	-	38.6	-	1,047.9	311.3	168.5	77.8	-	-	-
$A_{i,j,k}/A_s$	%	-	0.17	-	0.57	0.32	0.31	0.27	-	-	-
$Q_{i,j,k}$	kW	-	2,705.7	-	67,968.0	20,825.5	9,856.0	3,350.0	-	-	-
$Fh_{i,j,k}$		-		-					-	-	-
$Fc_{i,j,k}$		-	1.0	-	1.0	1.0	1.0	1.0	-	-	-
$Thin_{i,j,k}$	K	-	479.0	-	479.0	479.0	479.0	486.0	-	-	-
$Thout_{i,j,k}$	K	-	478.0	-	478.0	478.0	478.0	432.0	-	-	-
$Tcin_{i,j,k}$	K	-	375.9	-	384.0	381.1	379.0	411.0	-	-	-
$Tcout_{i,j,k}$	K	-	378.0	-	385.0	382.0	407.0	421.0	-	-	-
LMTD	K	-	101.5	-	94.0	97.0	84.8	62.4	-	-	-
Period 2											
A_s	m^2	-	33.3		537.8	324.3	220.8	134.7	1,194.3	963.9	24.3
$A_{i,j,k}$	m^2	-	4.3	-	537.8	324.3	161.5	85.2	993.6	906.7	1.0
$A_{i,j,k}/A_s$	%	-	0.13	-	1.00	1.00	0.73	0.63	0.83	0.94	0.04
$Q_{i,j,k}$	kW	-	295.6	-	34,778.3	21,696.5	9,244.4	3,670.0	15,167.0	30,041.1	42.0
$Fh_{i,j,k}$		-	-	-	-	-	-	-	-	-	-
$Fc_{i,j,k}$		-	-	-	1.0	1.0	1.0	1.0	1.0	1.0	-
$Thin_{i,j,k}$	K	-	479.0	-	479.0	479.0	479.0	479.0	479.0	479.0	479.0
$Thout_{i,j,k}$	K	-	478.0	-	478.0	478.0	478.0	478.0	478.0	478.0	478.0
$Tcin_{i,j,k}$	K	-	377.8	-	384.5	381.1	383.1	411.0	439.0	386.1	322.8
$Tcout_{i,j,k}$	K	-	378.0	-	385.0	382.0	407.0	421.0	468.0	458.0	323.0
LMTD	K	-	100.6	-	93.7	97.0	82.9	62.4	22.1	48.0	155.6
Period 3											
A_s	m^2		33.3			462.8	195	92.4	1979.6	1828.6	
$A_{i,j,k}$	m^2	-	33.3	-	-	304.5	195.0	92.4	1,979.6	1,828.6	-
$A_{i,j,k}/A_s$	%	-	1.00	-	-	0.66	1.00	1.00	1.00	1.00	-
$Q_{i,j,k}$	kW	-	2,327.4	-	-	20,360.6	11,355.4	3,980.0	30,218.0	61,208.6	-
$Fh_{i,j,k}$		-	-	-	-	-					-
$Fc_{i,j,k}$		-	-	-	-	-	1.0	1.0	1.0	1.0	-
$Thin_{i,j,k}$	K	-	479.0	-	-	479.0	479.0	479.0	479.0	479.0	-
$Thout_{i,j,k}$	K	-	478.0	-	-	478.0	478.0	478.0	478.0	478.0	-
$Tcin_{i,j,k}$	K	-	376.2	-	-	381.2	379.9	411.0	439.0	384.6	-
$Tcout_{i,j,k}$	K	-	378.0	-	-	382.0	407.0	421.0	468.0	458.0	-
LMTD	K	-	101.4	-	-	96.9	84.4	62.4	22.1	48.5	-

Table 5.B.4. Multiperiod HEN for Case Study 1.

Exchanger label	Assigned area (m2)	Period	Match (i,j,k)	Exchanger label	Assigned area (m2)	Period	Match (i,j,k)
A	5500	1	1,3,4	Q	537.8	1	3,CU,4
		2	1,3,2			2	HU,4,0
		3	1,9,1			3	1,2,1
B	5390.2	1	3,2,3	R	534.3	1	7,2,1
		2	9,2,3			2	1,5,1
		3	9,2,3			3	4,1,3
C	5365.4	1	1,2,1	S	462.8	1	8,CU,4
		2	1,9,1			2	4,CU,4
		3	3,3,3			3	HU,5,0
D	5297.1	1	3,3,4	T	324.3	1	5,CU,4
		2	3,3,4			2	HU,5,0
		3	9,4,2			3	5,10,1
E	3375.8	1	1,3,3	U	285.4	1	HU,7,0
		2	6,2,3			2	5,10,1
		3	6,9,2			3	4,CU,4
F	2970.5	1	6,2,2	V	220.8	1	HU,2,0
		2	9,4,2			2	HU,6,0
		3	1,9,4			3	9,1,4
G	1979.6	1	1,CU,4	W	195.0	1	6,CU,4
		2	3,9,3			2	8,CU,4
		3	HU,8,0			3	HU,6,0
H	1883.4	1	3,1,2	X	144.4	1	7,CU,4
		2	3,1,1			2	2,CU,4
		3	6,5,1			3	7,6,4
I	1828.6	1	HU,4,0	Y	134.7	1	-
		2	1,CU,4			2	HU,7,0
		3	HU,9,0			3	8,CU,4
J	1812.7	1	6,5,1	Z	110.6	1	-
		2	2,2,4			2	7,CU,4
		3	2,2,4			3	3,3,4
K	1673.1	1	4,1,3	AA	92.4	1	-
		2	4,3,4			2	7,5,3
		3	1,CU,4			3	HU,7,0
L	1255.3	1	1,2,4	BB	90.4	1	-
		2	1,9,4			2	5,CU,4
		3	3,1,1			3	7,5,3
M	1194.3	1	4,CU,4	CC	71.9	1	-
		2	HU,8,0			2	6,CU,4
		3	1,3,2			3	2,CU,4
N	963.9	1	HU,5,0	DD	42.0	1	-
		2	HU,9,0			2	3,CU,4
		3	4,9,4			3	1,10,4
O	774.4	1	2,CU,4	EE	33.3	1	-
		2	6,6,1			2	HU,2,0
		3	9,4,1			3	HU,2,0
P	544.8	1	HU,6,0	FF	24.3	1	-
		2	1,1,3			2	HU,10,0
		3	3,9,3			3	7,CU,4

Table 5.B.5. Single-period HEN for Case Study 2 (Part 1).

Match		**(1,2,1)**	**(1,2,4)**	**(1,3,3)**	**(1,3,4)**	**(3,1,2)**	**(3,2,3)**	**(3,3,4)**	**(4,1,3)**	**(6,2,2)**	**(6,5,1)**	**(7,2,1)**														
Period 1																										
A_S	m^2	3,836.0	1,041.1	3,131.8	5,500.0	1,875.0	4,377.2	3,672.9	1,164.8	2,903.6	1,501.6	622.7														
$A_{i,j,k}$	m^2	2,894.5	515.3	1,877.5	4,580.3	1,344.0	4,377.2	2,824.3	654.9	1,490.0	871.2	154.8														
$A_{i,j,k}/A_s$		0.75	0.49	0.60	0.83	0.72	1.00	0.77	0.56	0.51	0.58	0.25														
$Q_{i,j,k}$	kW	12,657.2	2,076.1	6,177.6	18,660.6	16,323.5	11,743.3	26,314.8	11,308.5	14,133.2	1,640.5	1,764.5														
$Fh_{i,j,k}$		1.00	0.24	1.00	0.76	1.00	1.00	1.00	1.00	1.00	1.00	1.00														
$Fc_{i,j,k}$		0.77	1.00	1.00	0.40	1.00	1.00	0.60	1.00	1.00	1.00	0.23														
$Thin_{i,j,k}$	K	388.0	358.5	368.2	358.5	355.0	354.7	354.5	351.0	382.8	385.0	421.0														
$Thout_{i,j,k}$	K	368.2	344.7	358.5	320.2	354.7	354.5	354.1	350.5	363.9	382.8	367.5														
$Tcin_{i,j,k}$	K	364.7	343.0	354.9	303.0	330.0	344.6	303.0	321.0	353.7	381.0	364.7														
$Tcout_{i,j,k}$	K	377.5	344.6	362.0	357.3	343.0	353.7	353.3	330.0	364.7	381.1	370.6														
LMTD	K	6.3	5.8	4.8	5.9	17.6	3.9	13.5	25.0	13.7	2.7	16.5														
Bypass	%	23.8	85.3	36.0	1.0	34.0	0.2	1.7	63.5	55.2	97.3	88.4														
Match		**(1,2,1)**	**(1,3,2)**	**(1,6,1)**	**(1,9,1)**	**(1,9,3)**	**(2,2,4)**	**(2,3,3)**	**(2,9,2)**	**(3,1,1)**	**(3,1,2)**	**(3,3,4)**	**(3,10,3)**	**(4,2,4)**	**(4,9,3)**	**(4,9,4)**	**(5,10,4)**	**(6,2,3)**	**(7,2,4)**	**(7,5,3)**	**(9,2,3)**	**(9,4,1)**	**(9,5,2)**	**(10,3,4)**	**(10,6,1)**	
Period 2																										
A_S	m^2	1,041.1	5,500.0	1,765.1	4,377.2	1,501.6	2,903.6	581.3	129.4	398.8	1,875.0	3,131.8	35.9	960.6	2.8	24.4	138.9	3,836.0	203.4	306.4	3,672.9	378.8	876.2	780.7	486.8	
$A_{i,j,k}$	m^2	899.4	4,959.9	1,528.7	3,648.5	1,501.6	1,772.2	401.8	18.7	247.1	1,662.7	2,199.0	8.3	877.2	2.8	4.9	66.2	2,955.8	90.0	157.6	2,576.0	191.4	581.5	519.4	371.6	
$A_{i,j,k}/A_s$		0.86	0.90	0.87	0.83	1.00	0.61	0.69	0.14	0.62	0.89	0.70	0.23	0.91	1.01	0.20	0.48	0.77	0.44	0.51	0.70	0.51	0.66	0.67	0.76	
$Q_{i,j,k}$	kW	2,433.5	13,604.6	1,592.8	8,107.5	9,581.9	9,276.7	3,026.6	117.7	2,188.3	25,443.7	36,883.9	184.8	2,560.4	64.4	161.2	663.2	19,150.9	954.0	1,369.5	10,660.0	8,767.6	11,350.1	5,543.9	616.0	
$Fh_{i,j,k}$		0.33	1.00	0.29	0.38	1.00	1.00	1.00	1.00	1.00	1.00	1.00	1.00	0.95	1.00	0.05	1.00	1.00	1.00	1.00	1.00	1.00	1.00	1.00	1.00	
$Fc_{i,j,k}$		1.00	1.00	0.62	1.00	0.99	0.64	1.00	1.00	1.00	1.00	0.87	1.00	0.33	0.01	1.00	1.00	0.63	0.03	1.00	0.37	1.00	1.00	0.13	0.38	
$Thin_{i,j,k}$	K	388.0	370.1	388.0	388.0	350.0	357.8	358.0	358.0	355.0	355.0	354.6	354.6	351.0	351.0	351.0	333.0	385.0	383.0	421.0	393.5	468.0	435.5	380.0	388.0	
$Thout_{i,j,k}$	K	377.1	350.0	380.0	356.2	335.8	357.0	357.8	358.0	355.0	354.6	354.0	354.6	350.9	351.0	350.9	332.7	363.1	356.5	383.0	354.0	435.5	393.5	308.0	380.0	
$Tcin_{i,j,k}$	K	376.1	348.4	379.0	349.2	303.8	343.0	345.4	348.6	341.3	321.0	303.0	321.3	343.0	303.8	303.0	315.0	352.9	343.0	381.0	352.9	384.0	381.1	303.0	379.0	
$Tcout_{i,j,k}$	K	378.0	362.0	385.9	386.9	348.9	354.3	348.4	349.2	343.0	341.3	345.5	323.0	349.1	328.9	303.8	321.3	376.4	365.5	381.1	375.5	384.1	381.6	344.8	383.3	
LMTD	K	3.9	4.0	1.5	3.2	9.2	7.6	10.9	9.1	12.8	22.2	24.3	32.4	4.2	33.1	47.6	14.5	9.4	15.4	12.6	6.0	66.4	28.3	15.5	2.4	
Bypass	%	51.9	8.7	6.2	1.3		19.3	64.1	94.2	81.9	14.5	12.4	94.7	6.6		98.4	61.4	13.7	39.3	99.8	24.0	99.8	98.2	28.5	29.0	
Match		**132**	**134**	**161**	**191**	**193**	**224**	**233**	**292**	**311**	**334**	**393**	**3103**	**414**	**424**	**494**	**594**	**5104**	**621**	**623**	**753**	**923**	**941**	**952**	**1034**	**1061**

Period 3																										
A_S	m^2	4,377.2	486.8	1,164.8	5,500.0	960.6	306.4	3,672.9	274.9	1,765.1	2,473.7	622.7	16.2	164.7	1,501.6	292.3	13.3	138.9	581.3	3,131.8	203.4	3,836.0	756.7	2,903.6	243.1	780.7
$A_{i,j,k}$	m^2	3,995.4	486.8	1,164.8	5,500.0	960.6	306.4	3,672.9	274.9	1,765.1	2,473.7	622.7	16.2	164.7	1,331.2	292.3	13.3	138.9	581.3	3,131.8	203.4	3,836.0	756.7	2,903.6	243.1	780.7
$A_{i,j,k}/A_s$		0.91	1.00	1.00	1.00	1.00	1.00	1.00	1.00	1.00	1.00	1.00	1.00	1.00	0.89	1.00	1.00	1.00	1.00	1.00	1.00	1.00	1.00	1.00	1.00	1.00
$Q_{i,j,k}$	kW	6,221.9	6,267.5	1,482.9	14,106.2	8,063.6	2,068.0	11,313.2	892.8	24,425.3	38,654.2	5,813.3	363.9	3,206.7	4,779.7	7,457.8	253.6	1,364.1	2,690.7	19,529.3	1,482.0	16,012.3	28,301.0	19,048.3	5,157.3	1,117.6
$Fh_{i,j,k}$		1.00	1.00	0.26	0.74	1.00	1.00	1.00	1.00	1.00	1.00	0.19	0.81	0.11	0.62	0.27	0.35	0.65	1.00	1.00	1.00	1.00	1.00	1.00	1.00	1.00
$Fc_{i,j,k}$		1.00	0.16	0.58	1.00	0.56	0.21	1.00	1.00	1.00	0.76	0.44	1.00	1.00	0.79	0.87	0.13	1.00	1.00	0.52	1.00	0.48	1.00	1.00	0.08	0.42
$Thin_{i,j,k}$	K	366.3	346.3	388.0	388.0	357.6	357.1	357.9	358.0	355.0	354.6	354.6	354.6	351.0	351.0	351.0	333.0	333.0	385.0	382.3	421.0	382.1	468.0	416.6	380.8	388.0
$Thout_{i,j,k}$	K	357.6	337.6	380.2	361.2	346.3	357.0	357.1	357.9	354.6	354.0	354.2	354.6	350.0	350.7	350.0	332.7	332.1	382.3	363.0	382.0	353.0	416.6	382.1	347.8	380.8
$Tcin_{i,j,k}$	K	356.6	303.0	379.0	354.2	320.6	343.0	346.7	352.2	323.6	303.0	320.6	321.3	321.0	343.0	303.0	303.0	315.0	375.9	348.3	381.0	348.3	384.0	381.1	303.0	379.0
$Tcout_{i,j,k}$	K	362.0	337.8	385.3	386.3	353.1	350.6	356.6	354.2	343.0	347.1	351.0	323.0	323.6	347.7	322.5	307.5	321.3	378.0	377.3	381.1	374.4	384.3	381.9	360.8	385.7
LMTD	K	2.3	18.7	1.8	3.7	12.2	9.8	4.5	4.7	20.1	22.6	13.5	32.5	28.2	5.2	37.0	27.6	14.2	6.7	9.0	10.6	6.0	54.2	9.5	30.7	2.1
Bypass	%	1.8													1.1											

Table 5.B.6. Single-period HEN for Case Study 2 (Part 2).

Match		**(1,CU,5)**	**(2,CU,5)**	**(3,CU,5)**	**(4,CU,5)**	**(5,CU,5)**	**(6,CU,5)**	**(7,CU,5)**	**(8,CU,5)**	**(9,CU,5)**	**(10,CU,5)**
Period 1											
A_s	m^2	2,473.7	876.2	756.7	960.6	486.8	306.4	292.3	581.3	-	-
$A_{i,j,k}$	m^2	1,372.1	302.1	163.7	395.3	97.3	15.5	11.8	113.6	-	-
$A_{i,j,k}/A_s$	%	0.55	0.34	0.22	0.41	0.20	0.05	0.04	0.20	-	-
$Q_{i,j,k}$	*kW*	12,744.5	11,661.0	5,925.4	13,283.5	2,074.0	660.3	479.5	1,849.0	-	-
$Fh_{i,j,k}$		1.0	1.0	1.0	1.0	1.0	1.0	1.0	1.0	-	-
$Fc_{i,j,k}$		-	-	-	-	-	-	-	-	-	-
$Thin_{i,j,k}$	*K*	326.0	358.0	354.1	350.5	333.0	363.9	367.5	351.0	-	-
$Thout_{i,j,k}$	*K*	306.0	357.0	354.0	350.0	332.0	363.0	353.0	308.0	-	-
$Tcin_{i,j,k}$	*K*	298.0	298.0	298.0	298.0	298.0	298.0	298.0	298.0	-	-
$Tcout_{i,j,k}$	*K*	305.0	305.0	305.0	305.0	305.0	305.0	305.0	305.0	-	-
LMTD	*K*	13.5	55.9	52.5	48.7	30.9	61.9	58.7	23.6	-	-
Period 2											
A_s	m^2	2,473.7	89.0		950.8	153.8	13.3	16.2	243.1	28.6	-
$A_{i,j,k}$	m^2	1,729.4	13.6	-	698.5	73.5	2.9	3.4	121.5	7.6	-
$A_{i,j,k}/A_s$	%	0.70	0.15	-	0.73	0.48	0.21	0.21	0.50	0.27	-
$Q_{i,j,k}$	*kW*	20,193.7	522.0	-	23,559.0	1,558.8	121.1	124.5	1,978.0	272.4	-
$Fh_{i,j,k}$		1.0	-	-	1.0	1.0	-	-	1.0	-	-
$Fc_{i,j,k}$		-	-	-	-	-	-	-	-	-	-
$Thin_{i,j,k}$	*K*	335.8	357.0	-	350.9	332.7	363.1	356.5	351.0	354.0	-
$Thout_{i,j,k}$	*K*	306.0	357.0	-	350.0	332.0	363.0	353.0	308.0	353.0	-
$Tcin_{i,j,k}$	*K*	298.0	298.0	-	298.0	298.0	298.0	298.0	298.0	298.0	-
$Tcout_{i,j,k}$	*K*	305.0	305.0	-	305.0	305.0	305.0	305.0	305.0	305.0	-
LMTD	*K*	16.9	55.4	-	48.9	30.7	61.5	53.2	23.6	51.9	-
Period 3											
A_s	m^2	1,875.0			378.8	35.9		24.4	129.4		398.8
$A_{i,j,k}$	m^2	1,875.1	-	-	378.8	35.9	-	24.4	129.4	-	398.8
$A_{i,j,k}/A_s$	%	1.00	-	-	1.00	1.00	-	1.00	1.00	-	1.00
$Q_{i,j,k}$	*kW*	22,652.0	-	-	12,717.9	757.3	-	1,102.0	2,107.0	-	6,205.1
$Fh_{i,j,k}$		1.0	-	-	1.0	1.0	-	-	1.0	-	1.0
$Fc_{i,j,k}$		-	-	-	-	-	-	-	-	-	-
$Thin_{i,j,k}$	*K*	337.6	-	-	350.5	332.3	-	382.0	351.0	-	347.8
$Thout_{i,j,k}$	*K*	306.0	-	-	350.0	332.0	-	353.0	308.0	-	308.0
$Tcin_{i,j,k}$	*K*	298.0	-	-	298.0	298.0	-	298.0	298.0	-	298.0
$Tcout_{i,j,k}$	*K*	305.0	-	-	305.0	305.0	-	305.0	305.0	-	305.0
LMTD	*K*	17.5	-	-	48.7	30.5	-	65.4	23.6	-	22.6

Table 5.B.7. Single-period HEN for Case Study 2 (Part 3).

Match		**(HU,1,0)**	**(HU,2,0)**	**(HU,3,0)**	**(HU,4,0)**	**(HU,5,0)**	**(HU,6,0)**	**(HU,7,0)**	**(HU,8,0)**	**(HU,9,0)**	**(HU,10,0)**
Period 1											
A_s	m^2		378.8		1,765.1	950.8	780.7	398.8	-	-	-
$A_{i,j,k}$	m^2	-	38.6	-	1,047.9	311.3	168.5	77.8	-	-	-
$A_{i,j,k}/A_s$	%	-	0.10	-	0.59	0.33	0.22	0.20	-	-	-
$Q_{i,j,k}$	kW	-	2,705.7	-	67,968.0	20,825.5	9,856.0	3,350.0	-	-	-
$Fh_{i,j,k}$		-	-	-	-	-	-	-	-	-	-
$Fc_{i,j,k}$		-	1.0	-	1.0	1.0	1.0	1.0	-	-	-
$Thin_{i,j,k}$	K	-	479.0	-	479.0	479.0	479.0	486.0	-	-	-
$Thout_{i,j,k}$	K	-	478.0	-	478.0	478.0	478.0	432.0	-	-	-
$Tcin_{i,j,k}$	K	-	375.9	-	384.0	381.1	379.0	411.0	-	-	-
$Tcout_{i,j,k}$	K	-	378.0	-	385.0	382.0	407.0	421.0	-	-	-
LMTD	K	-	101.5	-	94.0	97.0	84.8	62.4	-	-	-
Period 2											
A_s	m^2	-	1.0		1,164.8	274.9	292.3	164.7	756.7	622.7	-
$A_{i,j,k}$	m^2	-	1.0	-	1,042.1	146.1	147.3	83.4	511.0	463.9	-
$A_{i,j,k}/A_s$	%	-	1.00	-	0.89	0.53	0.50	0.51	0.68	0.74	-
$Q_{i,j,k}$	kW	-	44.5	-	67,550.4	9,749.4	8,347.2	3,590.0	7801	15,292.5	-
$Fh_{i,j,k}$		-	-	-	-	-	-	-	-	-	-
$Fc_{i,j,k}$		-	1.0	-	1.0	1.0	1.0	1.0	1.0	1.0	-
$Thin_{i,j,k}$	K	-	479.0	-	479.0	479.0	479.0	479.0	479	479.0	-
$Thout_{i,j,k}$	K	-	478.0	-	478.0	478.0	478.0	478.0	478	478.0	-
$Tcin_{i,j,k}$	K	-	378.0	-	384.1	381.6	384.9	411.0	439	386.9	-
$Tcout_{i,j,k}$	K	-	378.0	-	385.0	382.0	407.0	421.0	468	458.0	-
LMTD	K	-	100.5	-	93.9	96.7	82.1	62.4	22.1	47.8	-
Period 3											
A_s	m^2	-	-	-	876.2	28.6	153.8	89.0	1,041.1	950.8	-
$A_{i,j,k}$	m^2	-	-	-	876.2	28.6	153.8	89.0	1,041.1	950.8	-
$A_{i,j,k}/A_s$	%	-	-	-	1.0	1.0	1.0	1.0	1.0	1.0	-
$Q_{i,j,k}$	kW	-	-	-	56,731.0	1,903.7	8,683.5	3,830.0	15,892.0	31,457.7	-
$Fh_{i,j,k}$		-	-	-	-	-	-	-	-	-	-
$Fc_{i,j,k}$		-	-	-	1.0	1.0	1.0	1.0	1.0	1.0	-
$Thin_{i,j,k}$	K	-	-	-	479.0	479.0	479.0	479.0	479.0	479.0	-
$Thout_{i,j,k}$	K	-	-	-	478.0	478.0	478.0	478.0	478.0	478.0	-
$Tcin_{i,j,k}$	K	-	-	-	384.3	381.9	385.5	411.0	439.0	386.3	-
$Tcout_{i,j,k}$	K	-	-	-	385.0	382.0	407.0	421.0	468.0	458.0	-
LMTD	K	-	-	-	93.8	96.5	81.8	62.4	22.1	48.0	-

Table 5.B.8. Multiperiod HEN for Case Study 2.

Exchanger label	Assigned area (m2)	Period	Match (i,j,k)	Exchanger label	Assigned area (m2)	Period	Match (i,j,k)
		1	1,3,4			1	HU,7,0
A	5500.0	2	1,3,2	U	398.8	2	3,1,1
		3	1,9,1			3	10,CU,4
		1	3,2,3			1	HU,2,0
B	4377.2	2	1,9,1	V	378.8	2	9,4,1
		3	1,3,2			3	4,CU,4
		1	1,2,1			1	6,CU,4
C	3836.0	2	6,2,3	W	306.4	2	7,5,3
		3	9,2,3			3	2,2,4
		1	3,3,4			1	7,CU,4
D	3672.9	2	9,2,3	X	292.3	2	HU,6,0
		3	2,3,3			3	4,9,4
		1	1,3,3			1	-
E	3131.8	2	3,3,4	Y	274.9	2	HU,5,0
		3	6,2,3			3	2,9,2
		1	6,2,2			1	-
F	2903.6	2	2,2,4	Z	243.1	2	8,CU,4
		3	9,5,2			3	10,3,4
		1	1,CU,4			1	-
G	2473.7	2	1,CU,4	AA	203.4	2	7,2,4
		3	3,3,4			3	7,5,3
		1	3,1,2			1	-
H	1875.0	2	3,1,2	BB	164.7	2	HU,7,0
		3	1,CU,4			3	4,1,4
		1	HU,4,0			1	-
I	1765.1	2	1,6,1	CC	153.8	2	5,CU,4
		3	3,1,1			3	HU,6,0
		1	6,5,1			1	-
J	1501.6	2	1,9,3	DD	138.9	2	5,10,4
		3	4,2,4			3	5,10,4
		1	4,1,3			1	-
K	1164.8	2	HU,4,0	EE	129.4	2	2,9,2
		3	1,6,1			3	8,CU,4
		1	1,2,4			1	-
L	1041.1	2	1,2,1	FF	89.0	2	2,CU,4
		3	HU,8,0			3	HU,7,0
		1	4,CU,4			1	-
M	960.6	2	4,2,4	GG	35.9	2	3,10,3
		3	1,9,3			3	5,CU,4
		1	HU,5,0			1	-
N	950.8	2	4,CU,4	HH	28.6	2	9,CU,4
		3	HU,9,0			3	HU,5,0
		1	2,CU,4			1	-
O	876.2	2	9,5,2	II	24.4	2	4,9,4
		3	HU,4,0			3	7,CU,4
		1	HU,6,0			1	-
P	780.7	2	10,3,4	JJ	16.2	2	7,CU,4
		3	10,6,1			3	3,10,3
Q	756.7	1	3,CU,4	KK	13.3	1	-
		2	HU,8,0			2	6,CU,4

		3	9,4,1			3	5,9,4
R	622.7	1	7,2,1	LL	2.8	1	-
		2	HU,9,0			2	4,9,3
		3	3,9,3			3	-
S	581.3	1	8,CU,4	MM	1.0	1	-
		2	2,3,3			2	HU,2,0
		3	6,2,1			3	-
T	486.8	1	5,CU,4				
		2	10,6,1				
		3	1,3,4				

Table 5.B.9. Single-period HEN for Case Study 3 (Part 1).

Match		**(1,2,1)**	**(1,2,4)**	**(1,3,3)**	**(1,3,4)**	**(3,1,2)**	**(3,2,3)**	**(3,3,4)**	**(4,1,3)**	**(6,2,2)**	**(6,5,1)**	**(7,2,1)**
Period 1												
A_S		5494.6	1684	4380	5,500.0	2357.7	5498.6	4419.2	1997.7	3114.2	2030.8	757.7
$A_{i,j,k}$		2,894.5	515.3	1,877.5	4,580.3	1,344.0	4,377.2	2,824.3	654.9	1,490.0	871.2	154.8
$A_{i,j,k}/A_s$		0.53	0.31	0.43	0.83	0.57	0.80	0.64	0.33	0.48	0.43	0.20
$Q_{i,j,k}$		12,657.2	2,076.1	6,177.6	18,660.6	16,323.5	11,743.3	26,314.8	11,308.5	14,133.2	1,640.5	1,764.5
$Fh_{i,j,k}$		1.00	0.24	1.00	0.76	1.00	1.00	1.00	1.00	1.00	1.00	1.00
$Fc_{i,j,k}$		0.77	1.00	1.00	0.40	1.00	1.00	0.60	1.00	1.00	1.00	0.23
$Thin_{i,j,k}$		388.0	358.5	368.2	358.5	355.0	354.7	354.5	351.0	382.8	385.0	421.0
$Thout_{i,j,k}$		368.2	344.7	358.5	320.2	354.7	354.5	354.1	350.5	363.9	382.8	367.5
$Tcin_{i,j,k}$		364.7	343.0	354.9	303.0	330.0	344.6	303.0	321.0	353.7	381.0	364.7
$Tcout_{i,j,k}$		377.5	344.6	362.0	357.3	343.0	353.7	353.3	330.0	364.7	381.1	370.6
LMTD		6.3	5.8	4.8	5.9	17.6	3.9	13.5	25.0	13.7	2.7	16.5
Bupass	%	36.3	88.2	42.2	1.0	41.4	5.4	2.2	69.1	56.2	97.8	88.7

Match		**(1,3,2)**	**(1,3,4)**	**(1,6,1)**	**(1,9,1)**	**(1,9,4)**	**(2,2,4)**	**(2,3,3)**	**(2,9,2)**	**(3,1,1)**	**(3,3,4)**	**(3,9,3)**	**(3,10,3)**	**(4,2,4)**	**(4,9,4)**	**(6,2,1)**	**(6,2,3)**	**(7,1,4)**	**(7,5,3)**	**(9,2,3)**	**(9,4,1)**	**(9,5,2)**	**(10,1,2)**
Period 2																							
A_S		5,498.6	748.3	146.8	5,500.0	2,357.7	216.5	2,188.9	1,075.5	2,030.8	2,486.3	465.1	77.3	3,114.2	293.8	1,658.2	4,380.0	34.8	198.0	5,494.6	774.1	4,419.2	757.7
$A_{i,j,k}$		5,185.7	748.3	146.8	5,500.0	1,682.1	216.5	1,539.0	988.1	1,512.5	1,927.1	465.1	77.3	2,363.3	293.8	1,096.7	2,518.6	34.9	198.0	4,555.4	774.1	3,238.2	757.7
$A_{i,j,k}/A_s$	%	0.94	1.00	1.00	1.00	0.71	1.00	0.70	0.92	0.74	0.78	1.00	1.00	0.76	1.00	0.66	0.58	1.00	1.00	0.83	1.00	0.73	1.00
$Q_{i,j,k}$		9,321.4	8,249.5	344.4	14,975.5	15,114.7	1,239.0	8,966.5	3,110.5	19,353.0	33,052.6	2,400.9	1,896.0	6,928.3	4,802.4	4,636.9	14,723.1	1,072.8	1,443.0	17,552.7	29,734.4	22,172.7	7,206.2
$Fh_{i,j,k}$		1.00	0.35	0.06	0.94	0.65	1.00	1.00	1.00	1.00	1.00	0.27	0.73	0.82	0.18	1.00	1.00	1.00	1.00	1.00	1.00	1.00	1.00
$Fc_{i,j,k}$		1.00	0.22	1.00	1.00	0.74	0.10	1.00	1.00	1.00	0.78	1.00	1.00	0.90	0.26	1.00	0.45	1.00	1.00	0.55	1.00	1.00	1.00
$Thin_{i,j,k}$		366.8	354.0	388.0	388.0	354.0	357.1	357.8	358.0	355.0	354.6	354.7	354.7	351.0	351.0	385.0	379.7	382.0	421.0	382.1	468.0	418.8	344.0
$Thout_{i,j,k}$		354.0	321.1	380.0	366.0	322.0	357.0	357.1	357.8	354.7	354.2	354.6	354.7	350.7	350.0	379.7	363.0	353.0	382.0	353.0	418.8	382.1	333.3
$Tcin_{i,j,k}$		352.8	303.0	379.0	355.9	303.0	343.0	343.9	349.4	327.6	303.0	344.4	315.0	343.0	303.0	374.4	349.3	321.0	381.0	349.3	384.0	381.1	321.9
$Tcout_{i,j,k}$		362.0	339.9	379.9	387.0	345.5	352.7	352.8	355.9	343.0	345.0	349.4	323.0	349.0	341.2	378.0	374.9	321.9	381.1	374.0	384.4	382.0	327.6
LMTD		2.6	16.0	3.4	3.9	13.0	8.3	8.4	4.6	18.5	24.9	7.5	35.5	4.2	23.7	6.1	8.5	44.6	10.6	5.6	55.7	9.9	13.8
Bypass	%	5.1				10.1		25.4	5.6	28.7	10.8			15.3		52.6	12.8			8.5		93.0	

Match	**(1,3,2)**	**(1,9,1)**	**(1,9,4)**	**(2,2,4)**	**(2,3,3)**	**(3,1,1)**	**(3,3,4)**	**(3,9,3)**	**(3,10,3)**	**(4,1,2)**	**(4,9,4)**	**(6,2,1)**	**(6,6,1)**	**(6,9,2)**	**(7,3,4)**	**(7,5,3)**	**(9,2,3)**	**(9,3,4)**	**(9,4,1)**	**(9,4,2)**	**(9,5,1)**
Period 3																					
A_S	4419.2	5494.6	774.1	2031	463.1	1423.9	1658.2	4380	198	749.3	1075.5	748.3	946.7	3114.2	108	293.8	5500	465	1684	5498.6	757.7
$A_{i,j,k}$	4,419.2	5,494.7	733.2	2,030.8	231.5	1,423.9	1,658.2	4,380.0	159.5	557.0	1,075.5	485.8	903.7	3,114.3	40.1	219.4	5,499.3	408.9	1,684.0	5,498.6	646.1
$A_{i,j,k}/A_s$	1.00	1.00	0.95	1.00	0.50	1.00	1.00	1.00	0.81	0.74	1.00	0.65	0.95	1.00	0.37	0.75	1.00	0.88	1.00	1.00	0.85
$Q_{i,j,k}$	23,243.9	10,727.4	10,970.1	12,426.1	2,667.6	17,747.5	33,366.6	19,145.5	3,904.0	9,884.5	20,289.5	1,810.3	1,665.1	19,140.6	1,188.8	1,599.0	30,843.6	9,212.0	53,877.0	27,109.6	22,361.0
$Fh_{i,j,k}$	1.00	1.00	1.00	1.00	1.00	1.00	1.00	0.82	0.18	1.00	1.00	0.41	0.59	1.00	1.00	1.00	1.00	1.00	0.71	1.00	0.29
$Fc_{i,j,k}$	1.00	1.00	0.39	1.00	1.00	1.00	0.77	1.00	1.00	1.00	0.61	1.00	1.00	1.00	0.02	1.00	1.00	0.21	1.00	1.00	1.00
$Thin_{i,j,k}$	374.9	388.0	346.4	357.8	358.0	355.0	354.5	354.8	354.8	351.0	350.7	385.0	385.0	381.6	382.0	421.0	385.1	360.4	468.0	406.9	468.0
$Thout_{i,j,k}$	346.4	374.9	332.9	357.0	357.8	354.8	354.0	354.4	354.5	350.7	350.0	380.7	382.3	363.0	353.0	382.0	360.4	353.0	406.8	385.1	407.0
$Tcin_{i,j,k}$	342.3	373.0	303.0	343.0	340.1	328.9	303.0	334.5	315.0	321.0	303.0	376.6	379.0	353.8	303.0	381.0	352.6	303.0	384.3	384.0	381.1
$Tcout_{i,j,k}$	362.0	383.8	331.3	352.6	342.3	343.0	339.8	353.8	323.0	328.9	336.6	378.0	382.9	373.0	345.3	381.1	376.6	340.5	384.9	384.3	382.0
LMTD	7.6	2.8	21.7	8.9	16.7	18.1	29.2	6.3	35.5	25.7	27.3	5.4	2.7	8.9	43.0	10.6	8.1	32.7	46.4	7.1	50.2
Bypass %			5.8		84.9				59.6	57.7		74.0	3.7		44.7	99.5		12.3			95.8

Table 5.B.10. Single-period HEN for Case Study 3 (Part 2).

Match	***(i,j,k)***	**(1,CU,5)**	**(2,CU,5)**	**(3,CU,5)**	**(4,CU,5)**	**(5,CU,5)**	**(6,CU,5)**	**(7,CU,5)**	**(8,CU,5)**	**(9,CU,5)**	**(10,CU,5)**
Period 1											
A_s	m^2	2486.3	1075.5	774.1	1658.2	748.3	293.8	284.8	749.3	-	-
$A_{i,j,k}$	m^2	1,372.1	302.1	163.7	395.3	97.3	15.5	11.8	113.6	-	-
$A_{i,j,k}/A_s$	%	0.55	0.28	0.21	0.24	0.13	0.05	0.04	0.15	-	-
$Q_{i,j,k}$	kW	12,744.5	11,661.0	5,925.4	13,283.5	2,074.0	660.3	479.5	1,849.0	-	-
$Fh_{i,j,k}$		1.0	1.0	1.0	1.0	1.0	1.0	1.0	1.0	-	-
$Fc_{i,j,k}$				-	-		-			-	-
$Thin_{i,j,k}$	K	326.0	358.0	354.1	350.5	333.0	363.9	367.5	351.0	-	-
$Thout_{i,j,k}$	K	306.0	357.0	354.0	350.0	332.0	363.0	353.0	308.0	-	-
$Tcin_{i,j,k}$	K	298.0	298.0	298.0	298.0	298.0	298.0	298.0	298.0	-	-
$Tcout_{i,j,k}$	K	305.0	305.0	305.0	305.0	305.0	305.0	305.0	305.0	-	-
LMTD	K	13.5	55.9	52.5	48.7	30.9	61.9	58.7	23.6	-	-
Period 2											
A_s	m^2	1997.7		284.8	463.1	108			134.7		946.7
$A_{i,j,k}$	m^2	1,393.3	-	284.8	463.1	108.0	-	-	134.7	-	946.7
$A_{i,j,k}/A_s$	%	0.70	-	1.00	1.00	0.80	-	-	1.00	-	1.00
$Q_{i,j,k}$	kW	11,362.5	-	10,318.5	15,567.3	2,302.0	-	-	2,193.0	-	13,687.8
$Fh_{i,j,k}$		1.0	-	-	1.0	1.0	-	-	1.0	-	
$Fc_{i,j,k}$			-	-			-	-		-	
$Thin_{i,j,k}$	K	321.7	-	354.2	350.6	333.0	-	-	351.0	-	333.3
$Thout_{i,j,k}$	K	306.0	-	354.0	350.0	332.0	-	-	308.0	-	313.0
$Tcin_{i,j,k}$	K	298.0	-	298.0	298.0	298.0	-	-	298.0	-	298.0
$Tcout_{i,j,k}$	K	305.0	-	305.0	305.0	305.0	-	-	305.0	-	305.0
LMTD	K	11.8	-	52.5	48.7	30.9	-	-	23.6	-	21.0
Period 3											
A_s	m^2	1997.7				146.8			284.8		2486.3
$A_{i,j,k}$	m^2	1,997.7	-	-	-	119.4	-	-	203.4	-	2,486.3
$A_{i,j,k}/A_s$	%	1.00	-	-	-	0.81	-	-	0.71	-	1.00
$Q_{i,j,k}$	kW	21,970.6	-	-	-	2,545.0	-	-	3,311.0	-	43,090.0
$Fh_{i,j,k}$		1.0	-	-	-	1.0	-	-	1.0	-	
$Fc_{i,j,k}$		-	-	-	-	-	-	-		-	
$Thin_{i,j,k}$	K	332.9	-	-	-	333.0	-	-	351.0	-	344.0
$Thout_{i,j,k}$	K	306.0	-	-	-	332.0	-	-	308.0	-	313.0
$Tcin_{i,j,k}$	K	298.0	-	-	-	298.0	-	-	298.0	-	298.0
$Tcout_{i,j,k}$	K	305.0	-	-	-	305.0	-	-	305.0	-	305.0
LMTD	K	15.9	-	-	-	30.9	-	-	23.6	-	25.1

Table 5.B.11. Single-period HEN for Case Study 3 (Part 3).

Match	***(i,j,k)***	(HU,1,0)	(HU,2,0)	(HU,3,0)	(HU,4,0)	(HU,5,0)	(HU,6,0)	(HU,7,0)	(HU,8,0)	(HU,9,0)	(HU,10,0)
Period 1											
A_s	m^2	-	463.1		2188.9	1423.9	946.7	465.1	-	-	-
$A_{i,j,k}$	m^2	-	38.6	-	1,047.9	311.3	168.5	77.8	-	-	-
$A_{i,j,k}/A_s$	%	-	0.08	-	0.48	0.22	0.18	0.17	-	-	-
$Q_{i,j,k}$	kW	-	2,705.7	-	67,968.0	20,825.5	9,856.0	3,350.0	-	-	-
$Fh_{i,j,k}$		-		-					-	-	-
$Fc_{i,j,k}$		-	1.0	-	1.0	1.0	1.0	1.0	-	-	-
$Thin_{i,j,k}$	K	-	479.0	-	479.0	479.0	479.0	486.0	-	-	-
$Thout_{i,j,k}$	K	-	478.0	-	478.0	478.0	478.0	432.0	-	-	-
$Tcin_{i,j,k}$	K	-	375.9	-	384.0	381.1	379.0	411.0	-	-	-
$Tcout_{i,j,k}$	K	-	378.0	-	385.0	382.0	407.0	421.0	-	-	-
LMTD	K	-	101.5	-	94.0	97.0	84.8	62.4	-	-	-
Period 2	m^2										
A_s	%	-	-	-	749.3		182.1	86.2	1,684.0	1,423.9	-
$A_{i,j,k}$	kW	-	-	-	749.4	-	182.1	86.2	1,143.7	1,036.8	-
$A_{i,j,k}/A_s$		-	-	-	1.00	-	1.00	1.00	0.68	0.73	-
$Q_{i,j,k}$		-	-	-	48,504.6	-	10,603.6	3,710.0	17,458.0	34,151.0	-
$Fh_{i,j,k}$	K	-	-	-	-	-	-	-	-	-	-
$Fc_{i,j,k}$	K	-	-	-	1.0	-	1.0	1.0	1.0	1.0	-
$Thin_{i,j,k}$	K	-	-	-	479.0	-	479.0	479.0	479.0	479.0	-
$Thout_{i,j,k}$	K	-	-	-	478.0	-	478.0	478.0	478.0	478.0	-
$Tcin_{i,j,k}$	K	-	-	-	384.4	-	379.9	411.0	439.0	387.0	-
$Tcout_{i,j,k}$		-	-	-	385.0	-	407.0	421.0	468.0	458.0	-
LMTD	m^2	-	-	-	93.8	-	84.4	62.4	22.1	47.7	-
Period 3	kW										
A_s		-	-	-	182.1	86.2	216.5	134.7	2357.7	2188.9	-
$A_{i,j,k}$		-	-	-	133.4	12.3	182.1	95.5	2,357.7	2,188.9	-
$A_{i,j,k}/A_s$	K	-	-	-	0.73	0.14	0.84	0.71	1.00	1.00	-
$Q_{i,j,k}$	K	-	-	-	8,607.4	816.0	10,430.9	4,110.0	35,989.0	73,641.9	-
$Fh_{i,j,k}$	K	-	-	-	-	-	-	-	-	-	-
$Fc_{i,j,k}$	K	-	-	-	1.0	1.0	1.0	1.0	1.0	1.0	-
$Thin_{i,j,k}$	K	-	-	-	479.0	479.0	479.0	479.0	479.0	479.0	-
$Thout_{i,j,k}$		-	-	-	478.0	478.0	478.0	478.0	478.0	478.0	-
$Tcin_{i,j,k}$		-	-	-	384.9	382.0	382.9	411.0	439.0	383.8	-
$Tcout_{i,j,k}$		-	-	-	385.0	382.0	407.0	421.0	468.0	458.0	-
LMTD		-	-	-	93.5	96.5	83.0	62.4	22.1	48.8	-

Table 5.B.12. Multiperiod HEN for Case Study 3.

Exchanger label	Assigned area (m2)	Period	Match (i,j,k)	Exchanger label	Assigned area (m2)	Period	Match (i,j,k)
		1	1,3,4			1	7,2,1
A	5500	2	1,9,1	R	757.7	2	10,1,2
		3	9,2,3			3	9,5,1
		1	3,2,3			1	8,CU,4
B	5498.6	2	1,3,2	S	749.3	2	HU,4,0
		3	9,4,2			3	4,1,2
		1	1,2,1			1	5,CU,4
C	5494.6	2	9,2,3	T	748.3	2	1,3,4
		3	1,9,1			3	6,2,1
		1	3,3,4			1	HU,7,0
D	4419.2	2	9,5,2	U	465.1	2	3,9,3
		3	1,3,2			3	9,3,4
		1	1,3,3			1	HU,2,0
E	4380	2	6,2,3	V	463.1	2	4,CU,4
		3	3,9,3			3	2,3,3
		1	6,2,2			1	6,CU,4
F	3114.2	2	4,2,4	W	293.8	2	4,9,4
		3	6,9,2			3	7,5,3
		1	1,CU,4			1	7,CU,4
G	2486.3	2	3,3,4	X	284.8	2	3,CU,4
		3	10,CU,4			3	8,CU,4
		1	3,1,2			1	-
H	2357.7	2	1,9,4	Y	216.5	2	2,2,4
		3	HU,8,0			3	HU,6,0
		1	HU,4,0			1	-
I	2188.9	2	2,3,3	Z	198	2	7,5,3
		3	HU,9,0			3	3,10,3
		1	6,5,1			1	-
J	2030.8	2	3,1,1	AA	182.1	2	HU,6,0
		3	2,2,4			3	HU,4,0
		1	4,1,3			1	-
K	1997.7	2	1,CU,4	BB	146.8	2	1,6,1
		3	1,CU,4			3	5,CU,4
		1	1,2,4			1	-
L	1684	2	HU,8,0	CC	134.7	2	8,CU,4
		3	9,4,1			3	HU,7,0
		1	4,CU,4			1	-
M	1658.2	2	6,2,1	DD	108	2	5,CU,4
		3	3,3,4			3	7,3,4
		1	HU,5,0			1	-
N	1423.9	2	HU,9,0	EE	86.2	2	HU,7,0
		3	3,1,1			3	HU,5,0
		1	2,CU,4			1	-
O	1075.5	2	2,9,2	FF	77.3	2	3,10,3
		3	4,9,4			3	-
		1	HU,6,0			1	-
P	946.7	2	10,CU,4	GG	34.8	2	7,1,4
		3	6,6,1			3	-
		1	3,CU,4				
Q	774.1	2	9,4,1				
		3	1,9,4				

Chapter 6

Conclusions and Recommendations to Future Work

This work presents the industrial case studies of energy integration in sugarcane biorefineries. Mixed Integer Nonlinear Programming with multiple periods was used to synthesize HENs that operate under more than one operating condition, such as changes in the number of streams and their flow rates. Three mathematical methods were used to solve MINLP problems.

The first method applied was an adapted Particle Swarm Optimization (PSO) algorithm in a case study in which pentoses fraction is disposed (CS1). Using this strategy, for CS1, in the process with the multiperiod HEN, the saving in TAC can reach 52% when compared to the process without energy integration and 15% when compared to the process with project energy integration. Moreover, the process with the multiperiod HEN can save up to 48% and 14% of steam in relation to processes without energy integration and with project energy integration, respectively. These results represent marginal improvements when compared to the process already existing in Brazilian plants (*i.e.*, the process with project integration).

In the second mathematical strategy, a hybrid meta-heuristic method, composed by Simulated Annealing (SA) and Rocket Fireworks Optimization (RFO), was used to solve optimization problems. The same case study, CS1, was solved. For CS1, in the process with the multiperiod HEN, the saving in TAC can reach 76% when compared to the process without energy integration and 55% when compared to the process with the typical project energy integration. Furthermore, the process with the multiperiod HEN can save up to 71% and 48% of steam in relation to process without energy integration and with project energy integration, respectively.

In the third mathematical strategy, a novel hybrid meta-heuristic approach was applied to three case studies. This approach consists of Tabu Search (TS) and Particle Swarm Optimization (PSO) algorithms. For CS1, the process with the multiperiod HEN presents reductions in TAC of up to 75% when compared to the process without energy integration and 53% when compared to the process with project energy integration. Besides, for that process, saving of steam reaches 70% when compared to the process without energy integration and 46% when compared to the process with project energy integration. For CS2, a case study in which pentose fraction is fermented to 2G ethanol, the process with the multiperiod HEN presents reduction in TAC and steam demand of up to 70% and 66%, respectively, when compared to the process without energy integration. Improvements in TAC and steam demand for that case study can reach 50% and 45%, respectively, when compared to the process with project energy integration. For the last case study, CS3, in which pentose fraction is biodigested to biogas, a complementary fuel to the boiler, the process with the multiperiod HEN presents reduction in TAC and steam demand of up to 74% and 71%, respectively, when compared to the process without energy integration. When compared to the process with project energy integration, these numbers reach 51% and 47%, respectively.

SA-RFO method presented better results than PSO and TS-PSO. However, the difference in TAC of the solution obtained via SA-RFO and via TS-PSO is very small, and both methods were able to achieve significant savings, demonstrating that both methods are good strategies to solve large-scale HEN synthesis problems. As noticed in other works, there are challenges in inner loop optimization due to the number of variables to be estimated. Therefore, modifications in mathematical method used in lower level can allow improving the solution. as verified in the literature with RFO method, which is composed by two algorithms in inner level, SA and PSO, and which was able to achieve better results in benchmarking problems than using only PSO in inner level. Furthermore, in this study, the adapted PSO presented poor solutions when compared to the other applied methods. Besides the difficulties already mentioned in lower optimization level (continuous variables), PSO algorithm has failures when dealing with integer variables (*i.e.*, the variables of upper level) in large-scale problems.

Other important comparison among meta-heuristics methods used in this study refers to the computational effort. SA-RFO method is more efficient, since the execution time and the number of objective function evaluations are lower than PSO and TS-PSO. Tabu Search algorithm explores each element of the neighborhood. Thus, the execution time and the number of objective function evaluations are higher, because the size of the neighborhood is equal to the number of elements of it. However, TS-PSO approach can be improved through strategies, such as the evaluation of only some elements of the neighborhood, modifications in attributive memory or inclusion of other method along with PSO in inner level. The stand-alone PSO approach is not adequate to large scale problems of HEN synthesis, since the execution time and the number of objective function evaluations are higher and solutions are not good. Among methods used in this study, stand-alone PSO is the least efficient one.

Although the results differ among mathematical methods used for energy integration in biorefineries, they demonstrate that it is possible to reduce the steam consumption in process, and so more bagasse can be diverted to produce 2G ethanol or electricity, depending on the market demand. Besides that, it can help increasing energy security and decreasing environmental resources consumption, as well reducing waste generation. In that manner, with all the improvements provided by energy integration, it is expected to contribute with viability of 2G ethanol production process.

Recommendations to future works

In this thesis, industrial case studies of energy integration in sugarcane biorefineries were performed, but some topics were not approached since they are out of the scope of this work. They can be explored, nonetheless, in future works, in order to provide efficient options for energetic efficiency. Some suggestions for future works are presented below.

1. Estimate the fraction of the bagasse that can be diverted to 2G ethanol section from energy integration, and so surplus ethanol 2G production;

2. Simulate the process of 1G/2G ethanol production using the HENs synthesized in this work;

3. Synthesize HENs under variations in flow rates.

4. Synthesize HENs including the operation time in the objective function.

5. Assess the controllability and security issues of multiperiod HEN.

References

AALTOLA, J. Simultaneous synthesis of flexible heat exchanger network. Applied Thermal Engineering, v. 22, n. 8, p. 907–918, 2002.

AHMAD, M. I.; ZHANG, N.; JOBSON, M.; CHEN, L. Multi-period design of heat exchanger networks. Chemical Engineering Research and Design, v. 90, n. 11, p. 1883–1895, 2012.

ANANTHARAMAN, R.; GUNDERSEN, T. The Sequential Framework For Heat Exchanger Network Synthesis – Network Generation And Optimization. Computer Aided Process Engineering, v. 21, p. 725–730, 2006.

BEHERA, S.; SAHOO, S.; PATI, B. B. A review on optimization algorithms and application to wind energy integration to grid. Renewable and Sustainable Energy Reviews, v. 48, p. 214–227, 2015.

BOCHENEK, R.; JEŻOWSKI, J. M. Genetic algorithms approach for retrofitting heat exchanger network with standard heat exchangers. v. 21, p. 871–876, 2006.

BOUKOUVALA, F.; MISENER, R.; FLOUDAS, C. A. Global optimization advances in Mixed-Integer Nonlinear Programming, MINLP, and Constrained Derivative-Free Optimization, CDFO. European Journal of Operational Research, v. 252, n. 3, p. 701–727, 2016.

CHEN, C.-L.; HUNG, P.-S. Simultaneous Synthesis of Flexible Heat-Exchange Networks with Uncertain Source-Stream Temperatures and Flow Rates. 2004.

CHEN, X.; ZHAOHUA, L.; YANG, J.; SHAO, Z.; ZHU, L. Nested Tabu Search (TS) and Sequential Quadratic Programming (SQP) Method, Combined with Adaptive Model Reformulation for Heat Exchanger Network Synthesis (HENS). 2008.

DURAN, M. A.; GROSSMANN, I. E. An outer-approximation algorithm for a class of mixed-integer nonlinear programs. Mathematical Programming, v. 36, n. 3, p. 307–339, 1986.

EL-TEMTAMY, S. A.; GABR, E. M. Design of optimum flexible heat exchanger networks for multiperiod process. Egyptian Journal of Petroleum, v. 21, n. 2, p. 109–117, 2012.

FLOUDAS, C. A.; CIRIC, A. R.; GROSSMANN, I. E. Automatic synthesis of optimum heat exchanger network configurations. AIChE Journal, v. 32, n. 2, p. 276–290, 1986.

FLOUDAS, C. A.; GROSSMANN, I. E. Synthesis of flexible heat exchanger networks for multiperiod operation. Computers & Chemical Engineering, v. 10, n. 2, p. 153–168, 1986.

FLOUDAS, C. A.; GROSSMANN, I. E. Automatic generation of multiperiod heat exchanger network configurations. Computers & Chemical Engineering, v. 11, n. 2, p. 123–142, 1987.

FURMAN, K. C.; SAHINIDIS, N. V. A Critical Review and Annotated Bibliography for Heat Exchanger Network Synthesis in the 20th Century. 2002.

GEOFFRION, A. M. Generalized Benders decomposition. Journal of Optimization Theory and Applications, v. 10, n. 4, p. 237–260, 1972.

GROSSMANN, I. E. Review of Nonlinear Mixed-Integer and Disjunctive Programming Techniques. Optimization and Engineering, v. 3, n. 3, p. 227–252, 2002.

GROSSMANN, I. E.; CABALLERO, J. A.; YEOMANS, H. Advances in mathematical programming for the synthesis of process systems. Latin American Applied Research, v. 30, n. 4, p. 263–284, 2000.

GROSSMANN, I. E.; KRAVANJA, Z. Mixed-Integer Nonlinear Programming: A Survey of Algorithms and Applications. In: [s.l.] Springer New York, 1997. p. 73–100.

GUNDEPSEN, T.; NAESS, L. The synthesis of cost optimal heat exchanger networks: An industrial review of the state of the art. Computers & Chemical Engineering, v. 12, n. 6, p. 503–530, 1988.

GUNDERSEN, T.; TRAEDAL, P.; AHMADY, A. H. Improved sequential strategy for the synthesis of near-optimal heat exchanger networks. Computers & Chemical Engineering, v. 21, p. S59–S64, 1997.

ISAFIADE, A.; BOGATAJ, M.; FRASER, D.; KRAVANJA, Z. Optimal synthesis of heat exchanger networks for multi-period operations involving single and multiple utilities. Chemical Engineering Science, v. 127, p. 175–188, 2015.

ISAFIADE, A. J.; FRASER, D. M. Interval based MINLP superstructure synthesis of heat exchanger networks for multi-period operations. Chemical Engineering Research and Design, v. 88, n. 10, p. 1329–1341, 2010.

ISAFIADE, A. J.; SHORT, M. Simultaneous synthesis of flexible heat exchanger networks for unequal multi-period operations. Process Safety and Environmental Protection, v. 103, p. 377–390, 2016a.

ISAFIADE, A. J.; SHORT, M. Multi-Period Heat Exchanger Network Synthesis Involving Multiple Sources of Utilities and Environmental Impact. Computer Aided Chemical Engineering, v. 38, p. 2067–2072, 2016b.

JIANG, D.; CHANG, C.-T. A New Approach to Generate Flexible Multiperiod Heat Exchanger Network Designs with Timesharing Mechanisms. Industrial & Engineering Chemistry Research, v. 52, n. 10, p. 3794–3804, 2013.

JIANG, D.; CHANG, C.-T. An algorithmic approach to generate timesharing schemes for multi-period HEN designs. Chemical Engineering Research and Design, v. 93, p. 402–410, 2015.

KANG, L.; LIU, Y. Retrofit of Heat Exchanger Networks for Multiperiod Operations by Matching Heat Transfer Areas in Reverse Order. Industrial & Engineering Chemistry Research, v. 53, n. 12, p. 4792–4804, 2014.

KANG, L.; LIU, Y. Minimizing investment cost for multi-period heat exchanger network retrofit by matching heat transfer areas with different strategies. Chinese Journal of Chemical Engineering, v. 23,

n. 7, p. 1153–1160, 2015.

KANG, L.; LIU, Y.; WU, L. Synthesis of multi-period heat exchanger networks based on features of sub-period durations. Energy, v. 116, p. 1302–1311, 2016.

KHORASANY, R. M.; FESANGHARY, M. A novel approach for synthesis of cost-optimal heat exchanger networks. Computers & Chemical Engineering, v. 33, n. 8, p. 1363–1370, 2009.

KLEMEŠ, J. J.; KRAVANJA, Z. Forty years of Heat Integration: Pinch Analysis (PA) and Mathematical Programming (MP). Current Opinion in Chemical Engineering, v. 2, n. 4, p. 461–474, 2013.

KLEMEŠ, J. J.; VARBANOVA, P. S.; KRAVANJA, Z. Recent developments in Process Integration. Chemical Engineering Research and Design, v. 91, n. 10, p. 2037–2053, 2013.

KONUKMAN, A. E. S.; ÇAMURDAN, M. C.; AKMAN, U. Simultaneous flexibility targeting and synthesis of minimum-utility heat-exchanger networks with superstructure-based MILP formulation. Chemical Engineering and Processing: Process Intensification, v. 41, n. 6, p. 501–518, 2002.

LAND, A. H.; DOIG, A. G. An Automatic Method of Solving Discrete Programming Problems. Econometrica, v. 28, n. 3, p. 497, 1960.

LEWIN, D. R. A generalized method for HEN synthesis using stochastic optimization — II.: The synthesis of cost-optimal networks. Computers & Chemical Engineering, v. 22, n. 10, p. 1387–1405, 1998.

LIN, B.; MILLER, D. C. Solving heat exchanger network synthesis problems with Tabu Search. Computers & Chemical Engineering, v. 28, n. 8, p. 1451–1464, 2004.

MA, X.; YAO, P.; LUO, X.; ROETZEL, W. Synthesis of multi-stream heat exchanger network for multi-period operation with genetic/simulated annealing algorithms. Applied Thermal Engineering, v. 28, n. 8, p. 809–823, 2008.

MARECHAL, F.; KALITVENTZEFF, B. Targeting the integration of multi-period utility systems for site scale process integration. Applied Thermal Engineering, v. 23, n. 14, p. 1763–1784, 1 out. 2003.

MARTELLI, E.; MIAN, A.; MARÉCHAL, F. MINLP Model and two-level Algorithm for the Simultaneous Synthesis of Heat Exchanger Networks and Utility Systems. Computer Aided Chemical Engineering, v. 37, p. 1979–1984, 2015.

MIAN, A.; MARTELLI, E.; MARÉCHAL, F. Framework for the Multiperiod Sequential Synthesis of Heat Exchanger Networks with Selection, Design, and Scheduling of Multiple Utilities. Industrial & Engineering Chemistry Research, v. 55, n. 1, p. 168–186, 2016a.

MIAN, A.; MARTELLI, E.; MARÉCHAL, F. Multiperiod Sequential Synthesis of Heat Exchanger Networks and Utility Systems including storages. Computer Aided Process Engineering, v. 38, p. 967–972, 2016b.

MIRANDA, C. B.; COSTA, C. B. B.; CABALLERO, J. A.; RAVAGNANI, .A.S.S. Optimal synthesis of multiperiod heat exchanger networks: A sequential approach. Applied Thermal Engineering, v. 115, p. 1187–1202, 2017.

MIRANDA, C. B.; COSTA, C. B. B.; CABALLERO, J. A.; RAVAGNANI, M. A. S. S. Heat Exchanger Network Optimization for Multiple Period Operations. Industrial & Engineering Chemistry Research, v. 55, n. 39, p. 10301–10315, 2016.

MORAR, M.; AGACHI, P. S. Review: Important contributions in development and improvement of the heat integration techniques. Computers & Chemical Engineering, v. 34, n. 8, p. 1171–1179, 2010.

PAPOULIAS, S. A.; GROSSMANN, I. E. A structural optimization approach in process synthesis—II. Computers & Chemical Engineering, v. 7, n. 6, p. 707–721, 1983.

PARDALOS, P. M.; DU, D.-Z. Handbook of combinatorial optimization. 1. ed. [s.l.] Kluwer Academic Publishers, 1998.

PAVÃO, L. V.; COSTA, C. B. B.; RAVAGNANI, M. A. da S. S. Automated heat exchanger network synthesis by using hybrid natural algorithms and parallel processing. Computers & Chemical Engineering, v. 94, p. 370–386, 2016.

PAVÃO, L. V.; COSTA, C. B. B.; RAVAGNANI, M. A. S. S. Heat Exchanger Network Synthesis without stream splits using parallelized and simplified Simulated Annealing and Particle Swarm Optimization. Chemical Engineering Science, v. 158, p. 96–107, 2017.

PAVÃO, L. V.; COSTA, C. B. B.; RAVAGNANI, M. A. da S. S.; JIMÉNEZ, L. Large-scale heat exchanger networks synthesis using simulated annealing and the novel rocket fireworks optimization. AIChE Journal, v. 63, n. 5, p. 1582–1601, 2017.

PAVÃO, L. V.; MIRANDA, C. B.; COSTA, C. B. B.; RAVAGNANI, M. A. S. S. Efficient multiperiod heat exchanger network synthesis using a meta-heuristic approach. Energy, v. 142, p. 356–372, 2018a.

PAVÃO, L. V; MIRANDA, C. B.; COSTA, C. B. B.; RAVAGNANI, M. A. S. S. Synthesis of multiperiod heat exchanger networks with timesharing mechanisms using meta-heuristics. Applied Thermal Engineering, v. 128, p. 637–652, 2018b.

PINTARIČ, Z. N.; KASAŠ, M.; KRAVANJA, Z. Sensitivity analyses for scenario reduction in flexible flow sheet design with a large number of uncertain parameters. AIChE Journal, v. 59, n. 8, p. 2862–2871, 2013.

PINTARIČ, Z. N.; KRAVANJA, Z. Identification of critical points for the design and synthesis of flexible processes. Computers & Chemical Engineering, v. 32, n. 7, p. 1603–1624, 2008.

RAVAGNANI, M. A. S. S.; CABALLERO SUÁREZ, J. A. Redes de cambiadores de calor. [s.l.] Publicaciones de la Universidad de Alicante, 2012.

RAVAGNANI, M. A. S. S.; MÓDENES, A. N. Heat exchanger networks with multiple periods of operation. Brazilian Journal of Chemical Engineering, v. 13, n. 2, p. 71–84, 1996.

SABOO, A. K.; MORARI, M.; WOODCOCK, D. C. Design of resilient processing plants—VIII. A resilience index for heat exchanger networks. Chemical Engineering Science, v. 40, n. 8, p. 1553–

1565, 1985.

SADELI, E.; CHANG, C.-T. Heuristic Approach to Incorporate Timesharing Schemes in Multiperiod Heat Exchanger Network Designs. Industrial & Engineering Chemistry Research, v. 51, n. 23, p. 7967–7987, 2012.

SHORT, M.; ISAFIADE, A. J.; FRASER, D. M.; KRAVANJA, Z. Two-step hybrid approach for the synthesis of multi-period heat exchanger networks with detailed exchanger design. Applied Thermal Engineering, v. 105, p. 807–821, 2016.

SIENIUTYCZ, S.; JEŻOWSKI, J. Energy optimization in process systems and fuel cells. [s.l.] Elsevier Science, 2013.

SILVA, A. P.; RAVAGNANI, M. A. S. S.; BISCAIA, E. C. Particle Swarm Optimisation in heat exchanger network synthesis including detailed equipment design. Computer Aided Chemical Engineering, v. 25, p. 713–718, 2008.

SILVA, A. P.; RAVAGNANI, M. A. S. S.; BISCAIA, E. C.; CABALLERO, J. A. Optimal heat exchanger network synthesis using particle swarm optimization. Optimization and Engineering, v. 11, n. 3, p. 459–470, 2010.

SILVA, M. L. Descrição: Aplicação da analise pinch na sintese de redes de trocadores de calor flexiveis. 1995. State University of Campinas, 1995.

SMITH, R. Chemical Process: Design and Integration. [s.l.] Wiley, 2014.

SWANEY, R. E.; GROSSMANN, I. E. An index for operational flexibility in chemical process design. Part I: Formulation and theory. AIChE Journal, v. 31, n. 4, p. 621–630, 1985.

TOIMIL, D.; GÓMEZ, A. Review of metaheuristics applied to heat exchanger network design. International Transactions in Operational Research, v. 24, n. 1–2, p. 7–26, 2017.

VERHEYEN, N.; ZHANG, W. Design of flexible heat exchanger network for multi-period operation. Chemical Engineering Science, v. 61, n. 23, p. 7730–7753, 2006.

WESTERLUND, T.; PETTERSSON, F. An extended cutting plane method for solving convex MINLP problems. Computers & Chemical Engineering, v. 19, p. 131–136, 1995.

YEE, T. F.; GROSSMANN, I. E. Simultaneous optimization models for heat integration—II. Heat exchanger network synthesis. Computers & Chemical Engineering, v. 14, n. 10, p. 1165–1184, 1990.

YERRAMSETTY, K. M.; MURTY, C. V. S. Synthesis of cost-optimal heat exchanger networks using differential evolution. Computers & Chemical Engineering, v. 32, n. 8, p. 1861–1876, 2008.

ZHANG, C.; CUI, G.; PENG, F. A novel hybrid chaotic ant swarm algorithm for heat exchanger networks synthesis. Applied Thermal Engineering, v. 104, p. 707–719, 2016.